Aus dem Zentrum für Innere Medizin der Universität zu Köln

Klinik und Poliklinik für Innere Medizin I

Hämatologie und Onkologie

Direktor: Universitätsprofessor Dr. med. M. Hallek

Histogenetische und funktionelle Charakterisierung der malignen T-Zelle der T-Prolymphozytenleukämie

Inaugural-Dissertation zur Erlangung der Würde eines

doctor rerum medicinalium

der Hohen Medizinischen Fakultät

der Universität zu Köln

vorgelegt von

Nicole Yvonne Weit

aus Langenau

promoviert am 04. Juni 2014

Dekan: Universitätsprofessor Dr. med. Dr. h. c. Th. Krieg

1. Berichterstatter: Universitätsprofessor Dr. med. M. Hallek
2. Berichterstatter: Universitätsprofessor Dr. med. R. Thomas

Erklärung

Ich erkläre hiermit, dass ich die vorliegende Dissertationsschrift ohne unzulässige Hilfe Dritter und ohne Benutzung anderer als der angegebenen Hilfsmittel angefertigt habe; die aus fremden Quellen direkt oder indirekt übernommenen Gedanken sind als solche kenntlich gemacht.

Bei der Auswahl und Auswertung des Materials sowie bei der Herstellung des Manuskriptes habe ich keine Unterstützungsleistungen erhalten.

Weitere Personen waren an der geistigen Herstellung der vorliegenden Arbeit nicht beteiligt. Insbesondere habe ich nicht die Hilfe einer Promotionsberaterin / eines Promotionsberaters in Anspruch genommen. Dritte haben von mir weder unmittelbar noch mittelbar geldwerte Leistungen für Arbeiten erhalten, die im Zusammenhang mit dem Inhalt der vorgelegten Dissertationsschrift stehen.

Die Dissertationsschrift wurde von mir bisher weder im Inland noch im Ausland in gleicher oder ähnlicher Form einer anderen Prüfungsbehörde vorgelegt.

Nicole Weit

Köln, den 01.09.2013

Die dieser Arbeit zugrunde liegenden Immunphänotypisierungen sowie sämtliche Zellkulturexperimente wurden von mir selbst geplant, durchgeführt und ausgewertet.

Die Konzeption der TPLL1 Studie, die Sammlung der klinischen Daten sowie die statistische Auswertung geschah durch die Deutsche CLL Studiengruppe. Von mir wurde in diesem Zusammenhang die Western Blot Analyse der TCL1 Proteinexpression durchgeführt. Die Patientenproben hierfür wurden freundlicherweise von Herrn Prof. Stilgenbauer cryokonserviert und mir zur Verfügung gestellt.

Die Heatmap Darstellung der Korrelation der immunphänotypischen Daten wurde von Giuliano Crispatzu erstellt.

Die Bereitstellung der übrigen Patientenproben geschah durch die Deutsche CLL Studiengruppe bzw. die einsendenden Ärzte. Die Diagnosestellung oblag den einsendenden Ärzten bzw. Dr. Herling.

Acknowledgements

Above all, many thanks go to Prof. Hallek for agreeing to supervise this work, his support and making a project like this possible.

I thank Dr. Herling for providing the idea, the funding, and helpful discussions.

Many thanks go to all current and former members of the Herling lab for helpful discussions. Special thanks go to Dr. Alexandra Schrader and Giuliano Crispatzu for designing the heatmaps. Petra Mayer, Alexandra Breuer and Lisa Ulbrich helped out with sample preparation in my absence. I'm very thankful to Rodica Maniu for all her help and sharing her expertise in immunohistochemistry. Hannes Beckert was a great source of motivation and made the trips to San Francisco and Berlin memorable. Dr. Nils Lilienthal, Dr. Wagma Popal, Cornelia Gleim and Dr. Marius Stiefelhagen deserve many thanks for discussions, scientific and otherwise. Dr. Nina Reinart and Dr. Katrin Reiners were always there to discuss data, science in general and of course flow cytometry.

Without Dr. Georg Hopfinger the completion of my thesis would not have been possible. Thank you for helping me with blood samples, for answering all my questions and providing me with the clinical perspective and the faith to try the impossible.

Many thanks also go to Dr. Natali Pflug and the German CLL study group.

Dr. Michael Kapinsky provided me with the necessary tools to perform and illustrate a principal component analysis on flow cytometric data.

Dr. Andreas Böhmler's patience to answer every last question was crucial in the completion of this work. Thank you for designing the best Kaluza analysis protocol and helping me to get „R"esults.

None of this would have been possible without the unwavering support and believe of my parents, family, and friends. Anja, Christian and Stephanie, thank you for all your corrections and suggestions for my thesis. Tanja and Christian never stopped believing I could finish what I started. Over the years I found many „phriends" who were there for the good times and the bad. I could not have done it without you.

„Abenteuer-

Eine waghalsige Unternehmung aus Gründen des Forschungsdrangs oder des Übermuts,

mit lebensbedrohlichen Aspekten, unberechenbaren Gefahren und manchmal fatalem

Ausgang."

Walter Moers

Table of contents

Glossary

A-T	ataxia teleangiectasia
AF	Alexa Fluor
AICD	activation-induced cell death
AITL	angioimmunoblastic T-cell lymphoma
ALCL	anaplastic large cell lymphoma
ALK	anaplastic large cell lymphoma kinase
ALL	acute lymphoblastic leukemia
AP-1	activator protein 1
APC	allophycocyanine
ATLL	adult T-cell leukemia/lymphoma
ATM	ataxia teleangiectasia mutated
BCL2	B-cell lymphoma 2
BCR	B-cell receptor
BPDCN	blastic plasmacytoid dendritic cell neoplasm
BSA	bovine serum albumine
Ca	calcium
CD	cluster of differentiation
CLL	chronic lymphocytic leukemia
CR	complete remission
CREB	cAMP response element-binding protein
CTCL	cutaneous T-cell lymphoma
DAG	diacylglycerol
DC	dendritic cell
DMSO	dimethylsulfoxide
DSB	double strand break
DTT	dithiothreitol
ECD	electron-coupled dye, PE-Texas Red
EDTA	ethylenediaminetetraacetate
ELISA	enzyme linked immunosorbent assay
ERK	extracellular signal-regulated kinase
FBS	fetal bovine serum
FITC	fluorescein isothiocyanate

FMC	fludarabine, mitoxanthrone, cyclophosphamide
FSC	forward scatter
Foxo3a	forkhead box O3a
GCLLSG	German CLL Study Group
G-protein	guanine nucleotide-binding protein
H$_2$DCFDA	2',7'-dichlorodihydrofluorescein diacetate
HRP	horseradish peroxidase
HSTL	hepatosplenic T-cell lymphoma
IFN	interferon
Ig	immunoglobulin
IkB	inhibitor of kappa B
IL	interleukin
iono	Ionomycin
IP3	inositol-1,4,5-trisphosphate
ITAM	immunoreceptor tyrosine-activation motif
LAT	linker of activated T-cells
LBL	lymphoblastic lymphoma
Lck	lymphocyte specific protein kinase
MAPK	mitogen-activated protein kinase
MF	mycosis fungoides
MFI	mean fluorescence intensity
MHC	major histocompatibility complex
MRD	minimal residual disease
MTCP1	mature T-cell proliferation 1
NF-kB	nuclear factor kappa B
NFAT	nuclear factor of activated T-cells
ORR	overall response rate
OS	overall survival
PAGE	polyacrylamide gel electrophoresis
PBMC	peripheral blood mononuclear cells
PC5	PE-Cy5
PC5.5	PerCP-Cy5.5
PC7	PE-Cy7

13

PCA	Principal Component Analysis
PE	phycoerythrin
PerCP	perinidin-chlorophyll-protein
PFS	progression free survival
PHA	phytohemagglutinin
PI	propidium iodide
PIP2	phosphatidylinositol-4,5-bisphosphate
PKC	protein kinase C
PLC	phospholipase C
PMA	phorbol-myristyl-acetate
PR	partial remission
PTCL/L	peripheral T-/NK-cell lymphoma/leukemia
PTCL-nos	peripheral T-cell lymphoma not otherwise specified
R	receptor
ras-GEF	rat sarcoma-guanosine nucleotide exchange factor
ROS	reactive oxygen species
RPMI	Rosswell Park Memorial Institute medium
RT	room temperature
S1P	sphingosine 1-phosphate
SCT	stem cell transplantation
SDF-1	stromal cell-derived factor-1
SDS	sodium dodecylsulfate
SLP76	SH2 domain containing leukocyte protein of 76kDa
SS	Sézary syndrome
SSC	side scatter
T-PLL	T-cell prolymphocytic leukemia
TCL1	T-cell leukemia 1
T_{CM}	central memory T-cell
TCR	T-cell receptor
T_{EM}	effector memory T-cell
TGF	transforming growth factor
T-LGL	T-cell large granular leukemia
TML1	TCL1/MTCP1-like 1

TNF	tumor necrosis factor
vs.	versus
ZAP70	zeta chain associated protein kinase 70

I. Introduction

I.1. Mature T-cell malignancies

T-lymphocytes (T-cells) form an essential part of the adaptive immune system. In order to be able to mount an effective immune response T-cells have to undergo major chromosomal rearrangements to generate a functional antigen receptor and also undergo phases of strong proliferation [18] (for details see I.5). These factors, however, also contribute to the inherent risk of T-cells for malignant transformation due to their reduced susceptibility to cell death at certain developmental stages.

Despite this, T-cell malignancies have a much lower incidence than leukemias and lymphomas derived from B-lymphocytes [172]. While our concept of B-cell malignancies was greatly advanced by correlating B-cell leukemia and lymphoma entities to certain stages of normal B-cell development [126, 118], the pathobiology of most peripheral T-cell lymphoma entities is only poorly understood due to their rareness and a profound lack of appropriate experimental models [220]. Correlating T-cell malignancies with "normal" T-cell subsets has proven difficult because T-cell differentiation at least in the periphery shows much greater variability and plasticity [86].

The most clear-cut distinction can be made between immature, developing T-cells or thymocytes and mature T-cells in the periphery. Accordingly, T-cell malignancies can be divided into two groups corresponding to the maturation state of the underlying T-cell population [198]: Acute lymphoblastic leukemias (ALL) and their tissue-based counterpart, lymphoblastic lymphomas (LBL), are derived from immature T-cells [1]. The second group, T-cell malignancies derived from phenotypically mature T-cells, shows a much lower incidence but is far more aggressive than immature T-cell leukemias/lymphomas. Of note, it is still possible that the initiating oncogenic event leading to mature T-cell malignanices might occur at an immature differentiation state. Aberrations causally involved in the development of ALL often introduce a block in T-cell differentiation. This is not the case for their mature counterparts, therefore the term "mature T-cell malignancy" refers to the description of the final phenotype much more stringently than it implies the cell of origin. These so-called peripheral T-/NK-cell lymphomas/leukemias (PTCL/L) comprise a heterogeneous group of T-cell and NK-cell derived hematopoietic tumors and reflect the extensive functional variability of mature T-cell subsets [177, 86]. With few exceptions, PTCL/L mainly affect adults in the

second half of life. Generally, the prognosis for PTCL/L is worse than for lymphoblastoid malignancies and B-cell non-Hodgkin lymphoma. An overview over the entities distinguished at the moment is given in Table I.1-1.

Table I.1-1: The 2008 WHO classification of mature T- and NK-cell malignancies [198]

Primarily leukemic T/NK-cell tumors		T/NK-cell tumors of extranodal sites
T-cell prolymphocytic leukemia (T-PLL)		Extranodal NK/T-cell lymphoma, nasal type (NK/TCL)
T-cell large granular lymphocytic leukemia (T-LGL)		Enteropathy-associated T-cell lymphoma (EATL)
Chronic lymphoproliferative disorders of NK-cells		
Aggressive NK-cell leukemia		Hepatosplenic T-cell lymphoma (HSTL)
Adult T-cell leukemia/lymphoma (ATLL)		Subcutaneous panniculitis-like T-cell lymphoma (SPTCL)
Primarily cutaneous T-cell tumors		Primarily nodal T-cell tumors
Mycosis fungoides (MF)		Peripheral T-cell lymphoma, not otherwise specified (PTCL,nos)
Sézary syndrome (SS)		
Primary cutaneous CD30-positive T-cell lymphoproliferative disorders		Angioimmunoblastic T-cell lymphoma (AITL)
	Primary cutaneous anaplastic large cell lymphoma (c-ALCL)	Anaplastic large cell lymphoma (ALCL), ALK+
	Lymphomatoid papulosis	Anaplastic large cell lymphoma (ALCL), ALK-
Primary cutaneous peripheral T-cell lymphomas, rare subtypes		EBV+ T-cell lymphoproliferative disorders of childhood
	Primary cutaneous γδ T-cell lymphoma	
	Primary cutaneous CD8+ aggressive epidermotropic cytotoxic T-cell lymphoma	Systemic and hydroa vacciniforme-like lymphoma
	Primary cutaneous CD4+ small / medium T cell lymphoma	

For most T-cell neoplasias no diagnosis-defining genetic events have been described. Taken together with the often unspecific clinical presentation, finding the correct diagnosis is often challenging [77]. An exemplary algorithm for the classification of mature, leukemic T-cell malignancies is presented below (Figure I.1.1-1).

Given their rarity and heterogeneous nature, the first attempts to classify T-cell malignancies and to set them apart from other lymphoid diseases have only been made

as late as 1994 with the Revised European American Lymphoma (REAL) classification proposal. Prior classification schemes such as the Kiel classification and the Working Formula were mainly based on clinical and morphological/immunological characteristics [84]. The REAL classification and the following WHO classification from 2005 and its updated version from 2008 integrated also refined immunophenotyping and molecular genetic features [135, 198].
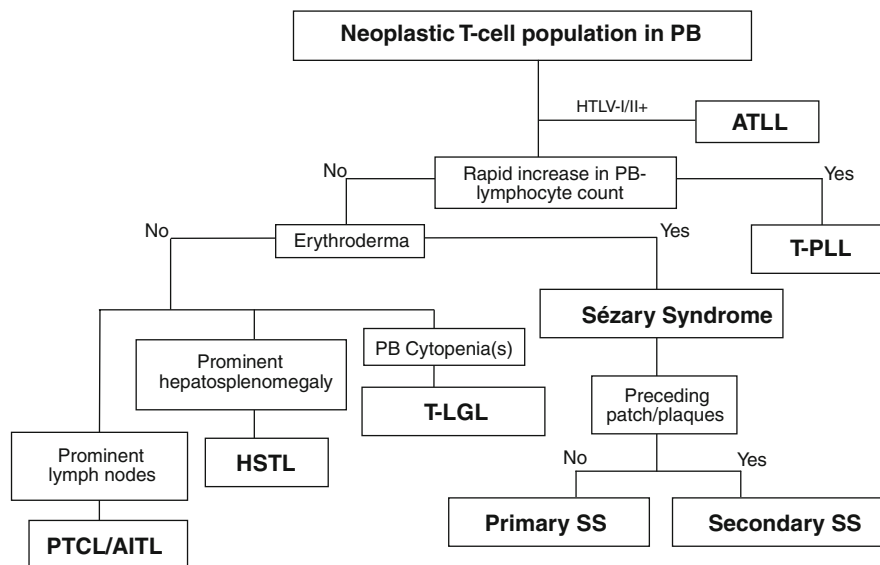
Figure I.2.1-1: Algorithm for the classification of T-cell neoplasms involving peripheral blood (PB). Leukemic PTCL/L were assigned to a WHO category based on the sequential application of the dominant presenting clinico-pathologic feature. Modified from Herling et al. [71]. HTLV = human T lymphotropic virus, ATLL = adult T- cell leukemia/lymphoma, T-PLL = T-cell prolymphocytic leukemia, T-LGL = T large granular lymphocytic leukemia, HSTL = hepatosplenic T-cell lymphoma, PTCL = peripheral T-cell lymphoma, AITL = angioimmunoblastic T-cell lymphoma, SS = Sézary syndrome.

Due to a lack of unequivocal molecular disease-defining markers and the marked plasticity of mature T-cell subsets, presentation at extranodal sites is still a major factor in the classification of PTCL/L. There are two exceptions from this rule, T-cell prolymphocytic leukemia (T-PLL) and anaplastic large cell lymphoma kinase (ALK) positive anaplastic large cell lymphoma (ALCL). ALK-positive systemic ALCL is characterized by the recurrent chromosomal aberration t(2;5)(p23;q35) which leads to the aberrant generation and expression of the NPM-ALK fusion protein. NPM-ALK is detected in 60-80% of all systemic ALCL cases and was repeatedly shown to have transforming and oncogenic properties in *in vitro* studies and mouse models [30]. The molecular hallmark of T-PLL is an aberrant expression of the T-cell leukemia 1 (TCL1)

oncogene as the result of a chromosomal inversion inv(14) or translocation t(14;14) [216].

I.2. T-cell prolymphocytic leukemia

I.2.1. Incidence

T-cell prolymphocytic leukemia (T-PLL) belongs to the group of mature T-cell leukemias. With an incidence in the USA and the UK estimated to be around 0.5-0.6 per million, T-PLL is a rare disease. Initially T-PLL was described as T-cell chronic lymphocytic leukemia (T-CLL), the T-cell counterpart to chronic lymphocytic leukemia (CLL) of B-cells [21]. It became quickly apparent that in contrast to the much more indolent course of most CLL cases, T-PLL shows a much faster progression. Even with targeted immunotherapeutics and stem cell transplantation (SCT) becoming more and more established, the median overall survival is only around 24 months, proving T-PLL to be an aggressive and fatal malignancy [221]. Of note, a subset of patients suffers from a much more indolent disease that still might be called T-CLL and be distinguished from T-PLL [109, 79].

I.2.2. Clinical aspects and therapy

The median age at presentation of T-PLL patients is 62 years (range 46-83) [135]. As with many lymphoid malignancies, the clinical presentation of T-PLL is often unspecific with fever, fatigue, weight loss, and night sweats being the initial complaints. The first indication of a hematologic disease constitutes of swollen lymph nodes and increased white blood cell counts, requiring establishment of a rigorous medical history and diligent clinical examination [77]. White blood cell counts are often extremely elevated and median pre-treatment lymphocyte doubling time was shown to be as short as 8 months in a monocentric study including 86 patients [72]. The accumulation of small to medium sized prolymphocytes in the peripheral blood is often accompanied by lymphadenopathy and hepatosplenomegaly [135]. A further characteristic clinical feature is the involvement of extramedullary sites, eg. in serous effusions and skin efflorescences, which might also facilitate diagnosis. Clinically prominent skin manifestations occur in approx. 20% of patients making the skin one of the most frequently affected sites [209]. Skin lesions in T-PLL show a wide range of diversity and include edema, rashes, and macular/papular lesions and often show a perivascular

infiltration pattern [70]. Anemia and thrombocytopenia are also frequently observed [42].

T-PLL usually shows a rapid progression and does not respond well to standard multi-agent chemotherapy. Due to the low incidence, T-PLL has remained understudied for a long time and only few clinical trials have been conducted so far. Currently, the sole available cure is allogeneic SCT, although this is not an applicable option for many of the typically elderly T-PLL patients [54].

Conventional combination chemotherapies like CHOP (cyclophosphamide, doxorubicin, vincristine, prednisone) only induce transient responses (3 months) in one third of patients while the majority of patients remain unresponsive [135]. The first compound to show efficacy and comparatively high response rates in T-PLL was the purine analog 2´deoxycoformycin (pentostatin) [140].

The monoclonal therapeutic cluster of differentiation (CD) 52 antibody alemtuzumab is the only targeted agent that achieves high remission rates in T-PLL [26]. CD52 is mostly highly expressed in T-PLL, making T-PLL cells the ideal target for anti-CD52 directed therapy [87]. Over 75% of patients which were often resistant to previous therapy respond to alemtuzumab treatment, among them 60% of patients achieving a complete remission (CR) [26]. Clearance of T-PLL cells from peripheral blood is extremely rapid, while alemtuzumab is less effective in serous effusions and pronounced bulky disease. Nevertheless, alemtuzumab significantly prolongs overall survival (OS) in responding patients. Disease free intervals are durable, opening up the possibility for allogeneic stem cell transplantation [221]. The main complications under alemtuzumab therapy are infections and viral reactivation due to the prolonged leukopenia/T-cell suppression. The combination of alemtuzumab with pentostatin shows a favorable outcome compared to either substance alone in a small patient cohort reported by Ravandi and coauthors. A response was elicited in 69% of patients with a median duration of 20 months and a median OS of 10.2 months [169]. In a recent study we could show the efficacy of FMC (fludarabine, mitoxanthrone, cyclophosphamide) followed by alemtuzumab treatment in previously untreated patients (1st line) [78]. Recently, Krishnan et al. reported on the outcome of stem cell transplantation after alemtuzumab treatment [105]. The control group consisted of patients in complete remission after alemtuzumab with a minimum survival of 6 months after treatment. The median survival of all allogenic or autologous SCT patients was 48 months compared to

20 months in the control group not undergoing SCT [105]. A recent retrospective study including 41 patientes provides further support for allogeneic SCT in the treatment of T-PLL by showing a median overall survival of 21% after 3 years [221].

In a current trial (T-PLL2) by the German CLL Study Group (GCLLSG) the effectiveness of adding alemtuzumab to FMC already in the induction phase is under investigation (http://www.dcllsg.de/studie/tpll2/index.php).

I.2.3. T-PLL cells are morphologically similar to prolymphocytes

Morphological analysis of a peripheral blood smear of a T-PLL patient typically shows a predominance of small to medium sized cells with basophilic cytoplasm and the occurence of cytoplasmic blebs (Figure I.2.3-1). At least one nucleolus is always visible [209]. Of note, in many cases only few typical prolymphocytes are observed, while the remaining T-PLL cells show a variable morphology. In the latter cases nuclear morphology ranges from round or oval to markedly irregular shaped or cerebriform nuclei [137]. On a cytomorphological level one can distinguish a small-cell variant, which anecdotal reports assign a less aggressive clinical course [82]. T-PLL cells in the skin vary from classic nucleolated prolymphocytes, to medium-sized cells with regular nuclei and inconspicuous nucleoli, to small cells with cerebriform or Sézary cell-like nuclear contours [20]. According to previous work clinically obvious skin involvement does not possess prognostic relevance [70].
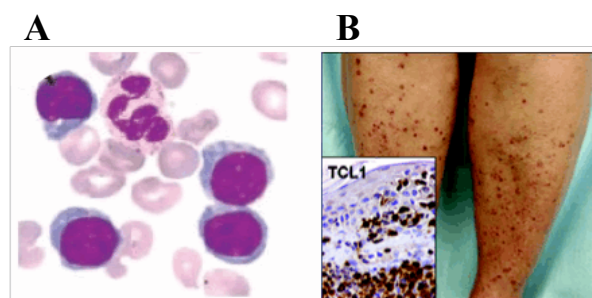
Figure I.2.3-1: Mophology and dermal infiltration of T-PLL cells. (A) A blood smear reveals pro-lymphocytes with basophilic cytoplasm. **[170] (B)** The T-PLL cells infiltrating the skin stain highly positive for T-cell leukemia 1 (TCL1) (inset) [71].

I.2.4. T-PLL cells carry a characteristic immunophenotype

Immunophenotyping of peripheral blood cells from T-PLL patients identifies the malignant T-cells as mature, post-thymic T-lymphocytes lacking expression of TdT, CD1a and HLA-DR, the classical marker for immature T-cell populations. In more than

half of the cases, all pan-T-cell antigens (CD2, CD3, CD5, CD7) are expressed, albeit with occasionally reduced intensity for CD3. CD7 expression is characteristically higher in T-PLL cells compared to healthy T-cells [60]. In addition, CD7 is the pan T-cell marker least likely to be lost by T-PLL cells. Analysis of T-cell receptor (TCR) gene rearrangement reveals the monoclonal derivation of T-PLL and rearrangement of the TCRβ and γ chains [50]. Even though surface expression of the TCR complex including CD3 is sometimes not detectable, these molecules are always expressed in the cytoplasm. The malignant clone can be further described by analysis of CD4 and CD8 expression, with the majority of cases showing CD4+ expression (CD4+ CD8- 62%). CD4+CD8+ and CD4- CD8+ cases are reported with a frequency of 35% and 4%, respectively [99, 71].

An important aspect of T-cell biology is the distinction between naïve and antigen-experienced or memory T-cells. The classical markers assigned to these phenotypes are the RA and RO isoforms of CD45 for naïve and memory cells, respectively [186]. In a previously published patient collective, only 20% of cases showed a naïve phenotype whereas in over 60% CD45RO was expressed. Detection of this memory phenotype shows a trend towards inferior outcome [170]. The prevalence of cases with antigen experienced T-PLL cells argues against the long held believe that T-PLL cells present at an intermediate stage of differentiation between thymic and mature T-cell. So far, T-PLL cells have only been poorly characterized regarding their cell type of origin and their functional features.

Technical advances over the last decade that made the flow cytometric analysis of over 10 markers at the same time feasible allowing for an even more detailed analysis of the immunophenotype of T-cells cells [10, 38]. Applying this technology to the analysis of T-PLL will facilitate diagnosis and reveal more about the biological properties of T-PLL cells.

I.2.5. Recurrent cytogenetic aberrations implicate a central role for TCL1 in T-PLL

Classic karyotyping is still of great importance for the diagnosis of T-PLL. T-PLL patients often display a complex karyotype pointing towards defective DNA damage repair mechanisms involved in disease development [33]. Recurrent alterations in T-PLL include the chromosomes 14, 11, and 8. The frequently observed isochromosome 8

and trisomy 8 have been linked to increased expression of c-myc in T-PLL [133]. C-myc has long been known to have transforming properties *in vivo* and may play a role in the development of overt leukemia [164]. More recent comparative genomic hybridization analysis with increased resolution revealed the frequent loss of 8p in >75% of the analyzed T-PLL cases [44]. The often deleted region 11q22-23 harbors the ataxia teleangiectasia mutated (ATM) gene. ATM acts as a master regulator of DNA double-strand break (DSB) repair which is especially crucial during lymphocyte development. Physiologically occurring DSBs during TCR gene rearrangement cannot be properly repaired in absence of ATM and might lead to either lymphocyte death or transformation. Due to the loss of ATM activity in 60% of T-PLL patients, ATM was previously implicated to act as a tumor suppressor in T-PLL [194]. In sporadic T-PLL a true loss of heterozygosity is sometimes observed when one ATM allele is deleted and the second one is affected by a loss of function mutation.

Patients constitutionally homozygous for ATM mutations and an accompanying loss of ATM function suffer from a condition called ataxia teleangiectasia (A-T). One hallmark of A-T is the high incidence of lymphoid malignancies particularly resembling sporadic T-PLL, further arguing for the central role of ATM deficiency in T-PLL [218, 115]. In A-T patients the occurence of the hallmark aberration of T-PLL involving chromosome 14 precedes TCR rearrangement and the clonal evolution of both malignant and non-malignant T-cells carrying t(14;14) and t(X;14) is observed [188].

The most characteristic chromosomal rearrangements in T-PLL, namely inv(14)(q11;q32) and t(14;14)(q11;q32) involve the proto-onocogene TCL1 [19]. Resulting from the recurrent inv14/t(14;14), TCRα regulatory elements induce the strong aberrant expression of the TCL1 gene in T-PLL cells [216].

I.3. The lymphoid proto-oncogene TCL1

I.3.1. The role of TCL1 in T-PLL

Overexpression of TCL1 at the protein level can be detected in 80% of T-PLL cases and is of both diagnostic and prognostic significance. High protein levels of TCL1 are associated with increased presenting white blood cell counts and shorter lymphocyte doubling time [72]. Also, an inverse correlation of TCL1 expression levels with OS could be shown [72]. In T-cell neoplasias TCL1 expression is specific for T-PLL.

However, as not all T-PLL cases can be identified based on TCL1 expression due to the 20% of TCL1 protein negative cases, the diagnostic sensitivity is limited [209].

A transgenic mouse model shows a causative role of TCL1 in the development of a mature T-cell malignancy. These mice carry a TCL1 transgene that is expressed specifically in T-cells under the control of an lck promoter. After a long latency period (>12 months) T-cell leukemias occur that resemble the course and biologic features of T-PLL [217]. The long time necessary for the development of overt leukemia in this model hints at a necessity for secondary events for full transformation and disease progression (Figure I.3.1-1).
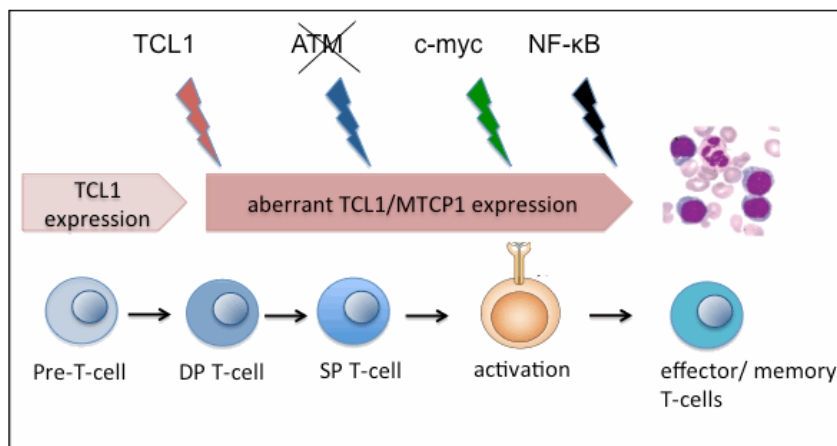
Figure I.3.1-1: Model of accumulation of recurrent aberrations during T-PLL development and progression. DP = double positive; SP = single positive

Physiologic TCL1 expression is shut down during the early pre-T-cell stage. Chromosomal aberrations presumably occuring during V(D)J-recombination in the thymus induce the up-regulation of TCL1. As TCL1 expression does not induce a developmental arrest, additional aberrations including ATM loss, and activation of c-myc and the nuclear factor kappa B (NF-kB) pathway can occur during further T-cell differentiation and contribute to full leukemic transformation. Recently, coexpression of ATM and TCL1 in CLL and a direct interaction between them was shown, further hinting at a leukemia-promoting cooperation of these proteins [55], [57].

In a transplantation model TCL1 expression in hematopoietic progenitor cells induces leukemia after a characteristically long latency period. Mature T-cells, however, are resistant towards TCL1-induced transformation [150]. This is presumably due to homeostatic mechanisms in mature T-cells that prevent the outgrowth of single clones

and warrants further investigation of this phenomenon. In functional studies, TCL1 high T-PLL cells display increased protein kinase B (PKB, also known as AKT) activity and a hyperproliferative phenotype [72].

There is anecdotal evidence of T-PLL cases carrying aberrations of the TCL1 locus in the absence of detectable TCL1 gene expression. As other genes neighboring the TCL1 locus have been shown not to be affected by rearrangements inducing TCL1 overexpression, the involvement of any of these genes seems unlikely [158]. It is conceivable that upon disease progression and the accumulation of additional aberrations, the need for TCL1 expression is lost. Discrepancies between the presence of the chromosomal aberrations inv14/t(14;14) and TCL1 on the protein level might also be caused by the involvement of neighboring genes such as TCL1/MTCP1-like 1 (TML1) [195], rearrangements of the TCRα locus and the B-cell receptor immunoglobulin variable heavy chain IgVH segment at 14q32 which constitute so called empty rearrangements that do not involve TCL1 gene family members. Among the approx. 20% of cases that do not show chromosomal dysregulation of TCL1, a small number of T-PLL cases display the up-regulation of another member of the TCL1 family, mature T-cell proliferation 1 (MTCP1), due to the chromosomal translocation t(X;14) [193]. T-cell specific transgenic expression of MTCP1 causes the development of monoclonal transplantable lymphoproliferations in mice that are phenotypically similar to human T-PLL [62].

Given the occurence of T-PLL late in life and the long latency period observed in the relevant mouse models, as well as anectodal evidence from T-PLL cases that were diagnosed incidentally at still low WBC and could be followed over an extended period, the cooperating genetic events in T-PLL seem to accumulate over time (Figure I.2.5-1).

I.3.2. TCL1 is important in embryogenesis and lymphocyte development

TCL1 was first discovered by breakpoint analysis of the recurrent chromosomal rearrangements of chromosome 14 in a T-PLL-like lymphoma of an A-T patient [218]. It became the namesake of the TCL1 protein family that in humans also includes TML1 and MTCP1. While it is well established that the X chromosomal p13 splice variant of the MTCP1 protein is also involved in T-PLL in the rare cases carrying the t(14;X), only little is known about the relevance of TML1 [206]. With regard to TCL1, it was demonstrated that physiological expression is restricted to early CD4-CD8- progenitor

subsets of T-cells, naïve B-cells, and embryonic stem cells [80]. In more mature T-cells, TCL1 expression is shut down by promoter hyper-methylation [52]. The knockout of TCL1 in the murine system leads to impaired lymphocyte development and function of both T and B cell lineages, interferes with embryonic cleavage and causes defects in hair germ cell differentiation [149, 95]. The described expression pattern and the phenotype of TCL1 knockout mice suggest a role for TCL1 in normal embryogenesis as well as in lymphoid development and function.

I.3.3. TCL1 is aberrantly expressed in multiple hematological malignancies

The distinctive chromosomal alterations involving TCL1 are reiterated in mature T-cell neoplasias arising in patients suffering from A-T, further pointing towards a cooperation of TCL1 with ATM in the initiation of T-cell malignancies (see I.2.5). Other malignancies showing aberrant expression of TCL1 are for example blastic plasmacytoid dendritic cell neoplasms (BPDCN) [74] and CLL, where recently an association of high TCL1 expression with adverse outcome was shown [69, 73].

I.3.4. TCL1 influences major intracellular signal transduction pathways

Structural data show that TCL1 is a 14kDa β-barrel shaped protein with a hydrophobic binding domain [76]. Due to its lack of enzymatic activity, for a long time little has been known about TCL1 function. In 2000, however, two publications showed TCL1 to bind to and enhance the activity of AKT [159, 110]. Initially defined in a yeast two-hybrid screen and by co-immunoprecipitation experiments, the direct protein-protein interaction between TCL1 and AKT has been widely studied by us and others (reviewed by Teitell [206]). It is now thought, that the interaction of the kinase AKT with its modulator TCL1 facilitates membrane recruitment of the kinase complex and strengthens kinase activity by enabling more efficient AKT transphosphorylation [72, 73].

Only recently, TCL1 was shown to inhibit transcription promoted by activator protein 1 (AP-1) by directly binding to AP-1 family members in interaction studies and reporter gene assays. In the same study an influence of TCL1 on the nuclear factor (NF)-kappa B signaling cascade was demonstrated. Binding of the NF-kB co-activator p300/cAMP response element-binding protein (CREB) by TCL1 augmented NF-kB activity [160]. Further proof of a TCL1-mediated NF-kB activation was found when inhibitor of kappa

B (IkB), the inhibitor of the NF-kB transcription factors, was identified as another binding partner of TCL1 [175].

I.4.   The role of T-cell receptor signaling in T-PLL

How TCL1 transforms the T-PLL precursor and which pathways the overt tumor cell relies on is not well understood. The TCL1-high subset of T-PLL was shown to be responsive to TCR ligation and differs from TCL1-negative T-PLL cases in an accelerated AKT activation and enhanced proliferation in response to stimulation. The response to TCR cross-linking increases in proportion to TCL1 expression levels. Among the subset of surface-TCR expressing T-PLL, the proliferative response to TCR engagement in T-PLL cases that are strongly positive for TCL1 surpassed that of TCL1-low / negative tumor cells. Faster kinase phosphorylation following TCR stimulation in correlation with TCL1 expression is also observed [72].

TCL1 is recruited to membrane associated activation complexes upon TCR stimulation as shown in co-localization studies [72]. These clusters also contain pAKT and the TCR-proximal Src-family kinase Lck. Prolonged stimulation leads to organization of these complexes into discrete foci. Constitution and temporo-spacial dynamics of these activation-dependent aggregates led to the proposition that TCL1 expression not only influences TCR dependent AKT activation but also regulates TCR proximal signaling events more directly. Accordingly, TCL1 enhances the activation of intracellular signaling pathways downstream of TCR activation [73, 72].

Within the B-cell compartment, the growth-stimulatory effects of B-cell receptor (BCR) engagement in CLL cultures correlate strongly with the levels of TCL1 and the kinetics of TCL1-AKT recruitment to BCR membrane complexes. TCL1 expression enhances BCR-induced activation of AKT in a dose-dependent manner. The extent of AKT activation after BCR cross-linking correlates also with the outcome of BCR stimulation [73]. Taken together, these results point strongly towards an involvement of TCL1 in antigen receptor signaling with modulatory effects on its outcome.

I.5. T-cell biology

I.5.1. T-cell development and differentiation

T-cells develop from bone marrow-derived lymphoblastoid precursor cells and undergo maturation in the thymus, the central organ of T-cell development. A schematic overview over T-cell development and differentiation is provided in Figure I.5.1-1.

Thymic T-cell populations can be classified according to their differential expression of surface proteins. These include the T-cell receptor (TCR) complex, co-receptors as well as signaling- and adhesion molecules [191]. The earliest thymic differentiation stage is characterized by the absence of both CD4 and CD8 co-receptors and accordingly these cells are called „double negative". The double negative stage can be further subdivided according to the expression of the interleukin (IL) 2 receptor (IL-2R) alpha chain CD25 and the adhesion molecule CD44 (Figure I.5.1-2). These thymocytes also physiologically express TCL1.
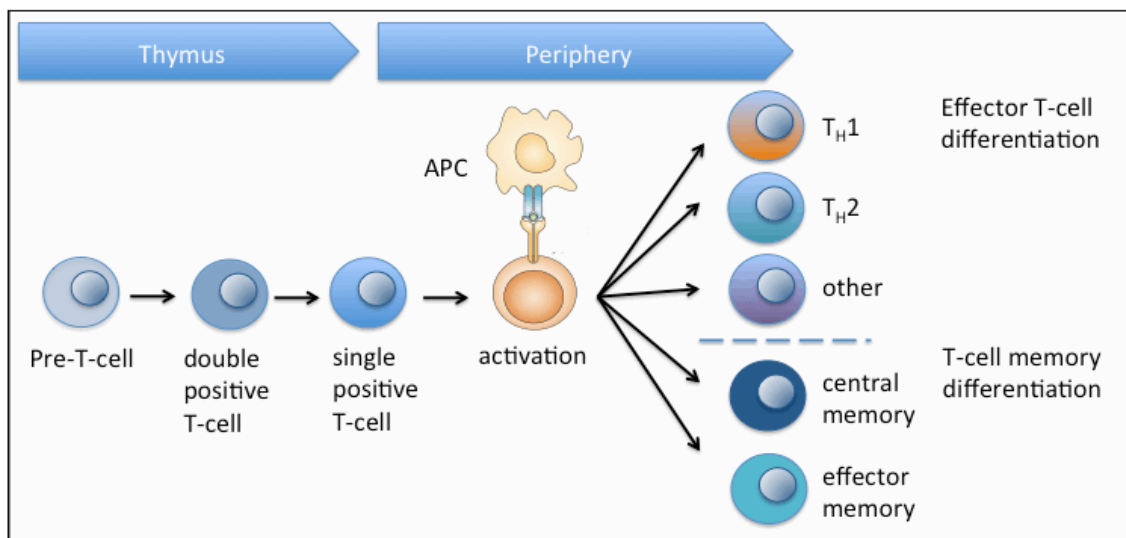
Figure I.5.1-1: T-cells develop through distinct stages and can be subdivided into several effector and memory subpopulations in the periphery. APC = antigen presenting cell.

At the double negative stage, rearrangement of the TCRβ gene segments takes place and the pre-TCR is expressed. Once the pre-TCR is assembled and enters a complex with CD3, a phase of proliferative expansion is induced, further TCRβ gene rearrangements are suppressed and the expression of both CD4 and CD8 starts. At this point, TCL1 expression is silenced. These cells have progressed to the „double positive" stage and account for the majority of thymocytes. When proliferation has stopped, the size of

these cells decreases and they continue to rearrange the TCRα gene segments until a functional TCR is generated and expressed on double positive cells [68] (for a detailed description of the TCR and its function refer to I.6).
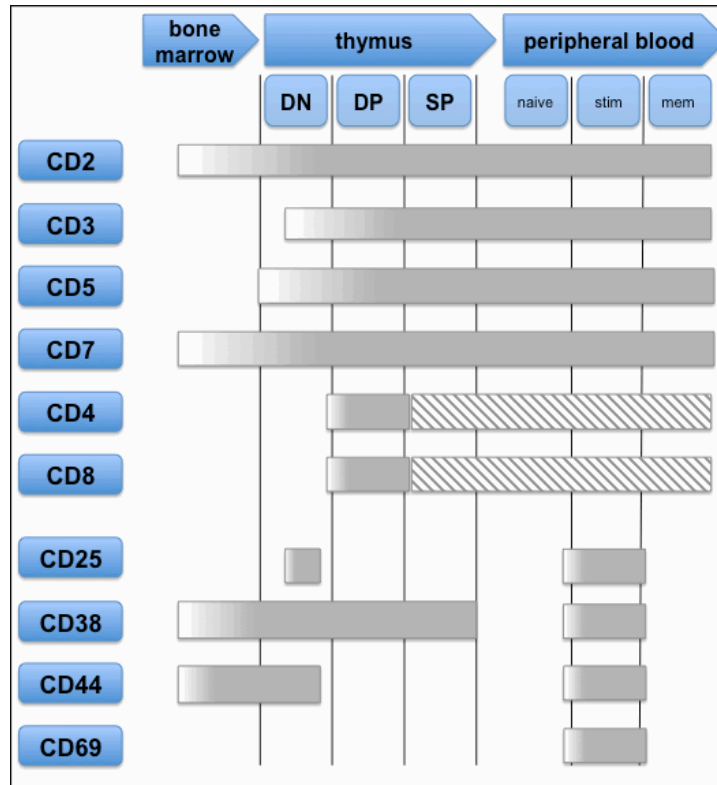
Figure I.5.1-2: Expression patterns of T-cell and activation markers during T-cell differentiation. DN = double negative thymocytes. DP = double positive thymocytes, SP = single positive thymocytes, stim = stimulated, acivated effector T-cells, mem = memory T-cells.

The generation of the T-cell receptor repertoire by V(D)J rearrangement is a completely random process. Therefore, thymic selection checkpoints are in place to ensure the functionality of the expressed TCR. Negative selection eliminates all T-cells that react strongly to auto-antigens and confers a large part of the central tolerance mechanism that prevents autoimmune reactions by eliminating T-lymphocytes with a high affinity towards self [27]. A certain degree of self-reactivity, however, is required for the immune system to function. Therefore, positive selection ensures that all T-cells leaving the thymus are capable of interacting with peptide - self- major histocompatibility complexes (MHC) and transducing a functional signal. Only T-cells retaining some self-reactivity receive survival signals, whereas T-cells that do not recognize self-MHC molecules die by neglect [56]. Both positive and negative selection, depend on and are

controlled by TCR-associated signaling events. About 98% of all double positive thymocytes are selected against and only the remaining 2% develop into single positive thymocytes that express either CD4 or CD8 and finally leave the thymus as mature T-cells.

Naïve mature T-cells are characterized by expression of the CD45RA isoform, low levels of CD44 and co-expression of the homing molecules CD62L and CCR7, and undergo further differentiation in the periphery (Figure I.5.1-1). Upon egress from the thymus mature naïve T-cells circulate in the peripheral blood and enter the T-cell zones of secondary lymphoid organs via high endothelial venules. This homing to lymph nodes is mediated by the expression of CD62L (L-selectin) and the chemokine receptor CCR7 [4]. The T-cell is guided into the underlying tissue along chemokine gradients, eg. by the CCR7 ligands CCL19 and CCL21 that are expressed in the T-cell zones of peripheral lymphoid organs [201]. Within the T-cell zone, T-cells can establish contact with antigen presenting dendritic cells (DCs) and scan them for specific peptide:MHC complexes. When a naïve T-cells encounters its specific antigen in this context, clonal expansion and differentiation are induced. If the encountered stimulus is sufficiently strong, the T-cells first undergo a proliferative phase and after 4 to 5 days start to differentiate into effector cells [92].
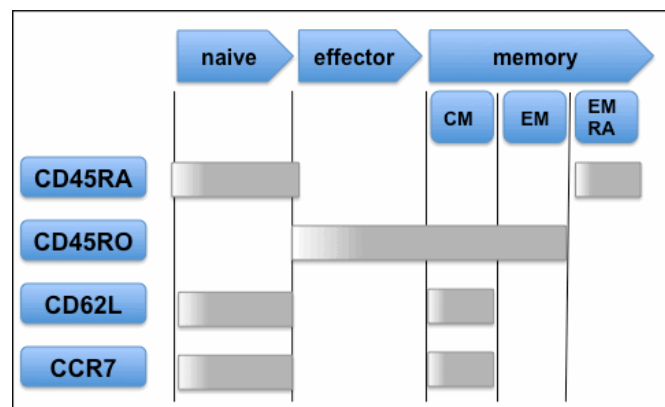
Figure I.5.1-3: CD45 isoforms and lymph node homing markers are expressed in characteristic patterns during different stages of T-cell differentiation. Assessment of effector molecules such as cytokines (and their receptors) or cytotoxic molecules is necessary to unambiguously identify short-lived effector T-cells. CM = central memory T-cells T_{CM}, EM = effector memory T-cells T_{EM}, EMRA = T_{EMRA}.

Effector T-cells characteristically lose the expression of CD45RA and up-regulate CD45RO instead, and the number of CD44 molecules on the cell surface increases

[141]. With respect to lymph node homing receptors, CCR7 expression is lost while the expression of CD62L is highly variable [181]. While most of the newly generated effector T-cells will die by neglect once the antigen is cleared from the system, some will persist as effector memory T-cells (T$_{EM}$). Under conditions of low antigen concentration the initial stimulation of a T-cell might not be sufficient to induce differentiation. These cells are thought to proliferate as non-effector T-cells that express both CCR7 and CD62L and can further differentiate into central memory T-cells (T$_{CM}$) under the influence of homeostatic cytokines [114] (Figure I.5.1-3).

With increasing age, T-cells accumulate which are immunophenotypically similar to memory T-cells but their TCR repertoire does not correlate with previously experienced infections. These so-called memory phenotype T-cells are generated after cytokine and self-peptide-mediated TCR signaling induced homeostatic proliferation. Due to their lower requirements for activation than naïve T-cells, these cells mediate protection against antigens that are only encountered late in life [192].

I.5.2.   Effector T-cell subsets

In general, effector T-cell function involves the interaction of an effector T-cell with an antigen-presenting cell. This is especially obvious for CD8+ effector T-cells. These so-called killer T-cells mediate a cytotoxic effect by the release of toxic molecules into the target cell and produce interferon (IFN)-γ which inhibits viral replication [5]. The effector population of CD4+ T-cells consists of the so-called helper T-cells (T$_H$ cells) that can be further classified into subsets according to their cytokine profile [161] (Figure I.5.2-1).

The first CD4+ effector T-cell subsets to be described were T$_H$1 and T$_H$2 cells. T$_H$1 cells activate the microbicidal properties of macrophages by the production of the cytokines IFN-γ and tumor necrosis factor (TNF)-α. The chemokine receptors CCR5 and CXCR3 are enriched on T$_H$1 cells [124, 200]. T$_H$2 cells produce copious amounts of IL-4 and IL-5 to provide help for the activation of antigen-specific B-cells [165]. Other cytokines produced by T$_H$2 cells include the immunosuppressive IL-10 [49]. Chemokine receptors predominantly expressed on T$_H$2 cells include CCR3 and CCR4 [180, 200]. Differentiation towards the T$_H$1 or T$_H$2 lineage largely depends on the cytokine milieu present at the time of T-cell stimulation and in part on the strength of the TCR signal [17]. T$_H$1 differentiation is driven by the induction of the expression of the transcription

31

factor T-bet by IL-18 and the signature T_H1 cytokines IL-12 and IFN-γ. At the same time, IFN-γ inhibits T_H2 differentiation, which is driven by an IL-4 mediated up-regulation of GATA-3. The T_H2-typical cytokines IL-10 and IL-4 in turn negatively regulate T_H1 differentiation [228] (Figure I.5.2-1).
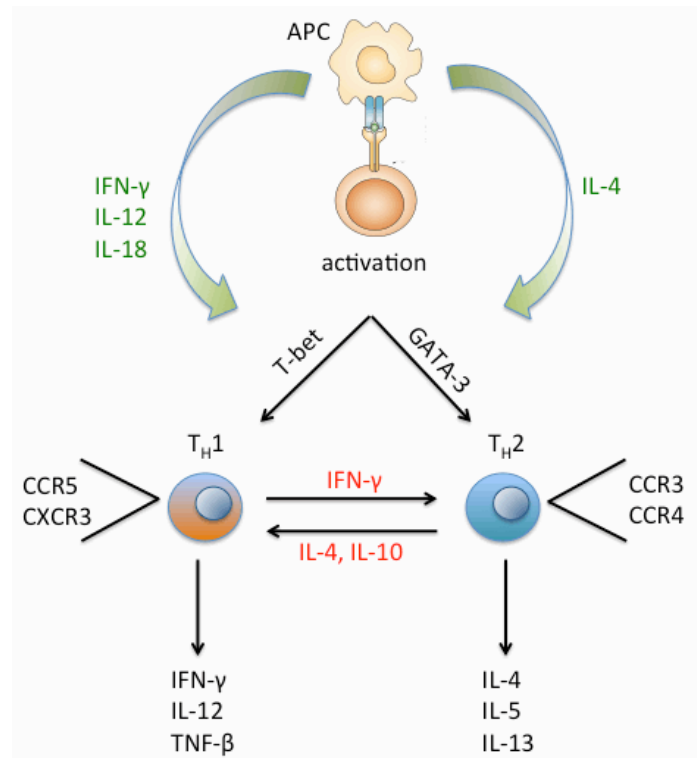
Figure I.5.2-1: Effector T-cell differentiation is controlled by the cytokine milieu and the resulting T_H1 and T_H2 cells differ with respect to cytokine production and chemokine receptor expression. Green: positive regulation, red: negative regulation

A considerable number of additional T-cell subsets with varying degrees of plasticity has been described. The best studied helper T-cells in this regard are presumably regulatory T-cells (T_{reg}). T_{reg} cells mediate peripheral tolerance by releasing immunosuppressive cytokines like IL-10 and transforming growth factor (TGF)-β and are identified by CD25 positivity, low levels of CD127 and the expression of the transcription factor FoxP3 [48]. The two other main functional CD4+ effector cell subsets are follicular helper T-cells (T_{FH}) and T_H17 cells. T_{FH} are located in the B-cell zone of lymph follicles and provide help for stepwise B-cell development. Their development is induced by IL-6 and IL-21 and mediated by Bcl-6. Production of IL-17 and IL-21 is critical for their effector function [45]. T_H17 on the other hand develop under the influence of IL-6, TGF-β and IL-23, which induce the up-regulation of RORγt. Besides their signature cytokines IL-17 and IL-17F, these cells produce IL-21

and IL-22 and play a major role in inflammatory reactions via the recruitment of neutrophils [41]. While especially T_H1 and T_H2 have long been considered to be terminal differentiation states, considerable plasticity has been observed for T_H17 and T_{reg} so that effector T-cell differentiation is no longer viewed as a strictly unidirectional process [147].

I.5.3.   T-cell memory

Memory T-cells confer protection against previously encountered antigens and ensure an efficient immune reaction even before the onset of symptoms of an infection. Two types of memory T-cells can be distinguished based on their generation, functional features, and their surface receptor expression [182] (Table I.5-1). The generation of T_{EM} and T_{CM} was briefly outlined in paragraph I.5.1. In the following the functional differences between the two memory subsets will be described in detail. T_{EM} have largely lost their ability to home to peripheral lymphoid organs in favor of chemokine receptors and adhesion molecules that direct the homing to inflamed tissue [29, 24]. These cells are predominantly CD8+ and are capable of very rapid effector function and have a low stimulation threshold [182]. CD8+ T_{EM} carry a high amount of cytotoxic effector molecules like granzyme B and perforin and all T_{EM} have the propensity to secret cytokines within hours after stimulation [214]. With respect to their chemokine receptor profile, CD4+ T_{EM} primed towards T_H1 predominantly express CCR5 and CXCR6 whereas cells primed towards a T_H2 effector type are generally positive for CCR3 and CRTh2 [13, 148]. The cytokine profile produced by CD4+ T_{EM} when stimulated under neutral conditions recapitulates the helper phenotype that was imprinted before their memory differentiation (Table I.5-2). Nevertheless, stimulation under opposite polarizing conditions induces a conversion of the helper phenotype as a certain degree of cytokine flexibility is retained in these cells [142]. For example, if a T-cell primed towards a T_H1 phenotype is stimulated in the presence of IL-4, a cytokine inducing T_H2 polarization, the CD4+ T_{EM} cell is able to acquire a T_H2 phenotype and produce IL-4. The proliferative potential of T_{EM} is lower than that of T_{CM} owing to the shorter telomeres in T_{EM} cells and their higher likelihood to undergo apoptosis [129, 183, 190]. This deficit, however, can be overcome by survival signaling induced by CD28 costimulation [12]. Interestingly, the expression of the co-receptor CD28 is lower in CD8+ T_{EM} than in CD4+ T_{EM} and T_{CM}. The subset with the lowest proliferative

potential and the lowest percentage of CD28 positive cells is the so-called T_{EMRA} [58]. This population comprises CD8+ effector memory cells that instead of CD45RO express CD45RA [181].

Within the T_{CM} subset CD4+ T-cells predominate. These cells are either still uncommited or commited non-effector cells. The latter can be subdivided into pre-T_H1 according to CXCR3 expression and pre-T_H2 by CCR4 positivity . Like $T_{EM,}$ T_{CM} have a very low activation threshold. In contrast to T_{EM}, T_{CM} require a period of several days after stimulation to further differentiate and acquire adequate effector function, which is especially true for cytokine production [179].

Table I.5-1: Characterization of T-cell differentiation stages according to surface marker expression.

		CD45 RA	CD45 RO	CCR7	CD62L	CD44
	naive	+	-	+	+	(+)
	effector	-	+	-	-	++
memory	EM	-	+	-	-	++
memory	CM	-	+	+	+	++
memory	EMRA	+	-	-	-	++

CM = central memory T-cells T_{CM}, EM = effector memory T-cells T_{EM4}, EMRA = T_{EMRA}.

Table I.5-2: Functional subsets of effector and memory T-cells are characterized by transcription factors, chemokine receptors and cytokine prodution.

	transcription factor	chemokine R	other markers	cytokines
T_H1	T-bet	CCR5, CXCR3		IFNγ
T_H2	GATA-3	CCR3, CCR4		IL-4
T_H17	RORγt	CCR6	IL-23R	IL-17
T_{FH}	BCL6	CXCR5	ICOS	IL-10
T_{reg}	FoxP3		CD25	IL-10

I.6.   The T-cell antigen receptor

I.6.1.   T-cell receptor proximal signaling

The TCR complex is one of the main tools for a T-cell to gather information about its surroundings. Signals mediated by the TCR will ultimately define cell fate (see section I.5). The TCR recognizes antigen presented by MHC molecules [40, 178]. The actual T-cell receptor is a heterodimer that in the majority of cases consists of an α- and a β-chain, only about 5% of T-cells carry a γδ-heterodimer. The majority of PTCL/L is derived from αβ-T-cells. The T-cell receptor repertoire has to be able to recognize an extraordinary number of different antigens. The diversity necessary for this is generated in part by thymic somatic genomic recombination processes [153]. The four TCR gene loci (α, β, γ and δ) each consist of several V (variable) segments, short D (diversity) segments (β and γ only), J (joining) segments and one or two C (constant) regions. The Vβ locus contains 65 different Vβ segments that can be grouped into 25 subfamilies based on sequence and 22 subfamilies based on function [176]. During TCR rearrangement, randomly chosen V, (D) and J segments are combined to give rise to a unique TCR. The process of allelic exclusion ensures the rearrangement of the TCR gene loci is stopped as soon as a functional TCR chain is expressed. This ensures that every T-cell expresses TCRs of only a single specificity. The expression of a distinct Vβ chain on a subpopulation of T-lymphocytes is indicative of a possible underlying clonal expansion. Analysis of the TCR repertoire based on Vβ chain expression is an important experimental tool to distinguish polyclonal from oligoclonal or monoclonal T-cell proliferations [113].

The TCR heterodimer is a transmembrane protein with a relatively small intracellular domain. By itself, it lacks the ability to transduce signals over the cell membrane. Therefore, the TCR heterodimer associates with the CD3 complex consisting of a CD3 gamma chain, a CD3 delta chain, two CD3 epsilon chains, and two zeta-chains, the latter being the most important for signal transduction [15]. The so-called immunoreceptor tyrosine-activation motif (ITAM) is present in the intracellular domains of the CD3 chains and crucial for the initiation of TCR signaling [171]. Upon recognition of antigen by the TCR, ITAMS are phosphorylated starting the TCR proximal signaling cascade.
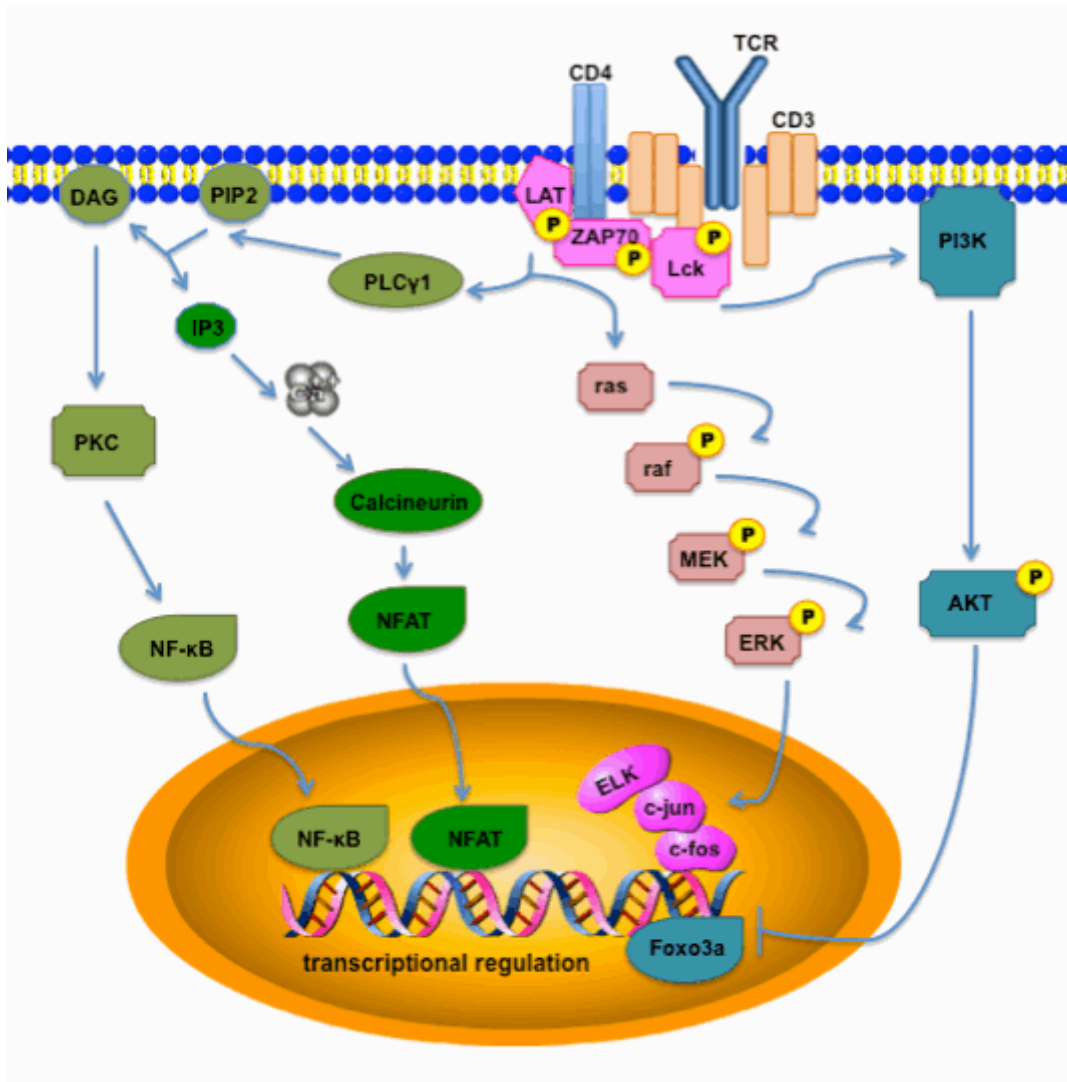
Figure I.6.1-1: The T-cell receptor signaling cascade. The clonotypic TCR heterodimer associates with the CD3 complex for the recruitment of the ζ-chain-associated protein kinase 70 (ZAP70), which in turn is activated by lymphocyte specific protein tyrosine kinase (Lck). The CD4 and CD8 co-recepetors bring Lck into close proximity to the TCR complex. Activated ZAP70 recruits and phosphorylates adaptor proteins like linker of activated T-cells (LAT), which in turn recruit and allow for the activation of phospholipase C,γ1 (PLCγ1). PLCγ1 hydrolyses phosphatidylinositolbisphosphate (PIP2) into diacylglycerol (DAG) and inositol trisphosphate (IP3), which activate protein kinase C (PKC) and induce an increase in intracellular Ca^{2+} levels, respectively. Active PKC ultimately leads to the nuclear translocation of nuclear factor κ B (NF-κB). Lck also mediates the activation of the phosphatidylinositol 3-kinase (PI3K) and thereby activation of the AKT signaling pathway. AKT phosphorylates and thereby inhibits Forkhead box O3a (Foxo3a). Increased Ca^{2+} levels activate the transcription factor nuclear factor of activated T-cells (NFAT) in a calcineurin dependent manner. The mitogen-activated protein kinase (MAPK) cascade is activated in response to TCR ligation by adaptor protein mediated recruitment of rat sarcoma-guanosine nucleotide exchange factors (ras-GEFs).

The phosphorylated ITAMS are in turn able to recruit kinases like zeta-chain-associated protein kinase 70 (ZAP70), leading to their activation [28]. Adapter proteins such as

linker of activated T-cells (LAT) [227] and SH2 domain containing leukocyte protein of 76kDa (SLP76) [108] are phosphorylated and become platforms for the further recruitment and activation of kinases and other enzymes like eg. phospholipase Cγ (PLCγ) [11]. Activation of PLCγ eventually results in the generation of two crucial second messengers, Ca^{2+} [215] and reactive oxygen species (ROS) [65] (Figure I.6.1-1). ROS are oxygen-containing chemically reactive molecules. A description of their biological role in the context of TCR signaling can be found in I.6.3.

I.6.2. Ca^{2+} as second messenger

At the resting state, the concentration of free intracellular Ca^{2+} is tightly regulated at about 100-200nM. In response to TCR cross-linking, activated PLCγ breaks down phosphatidylinositol-4,5-bisphosphate (PIP2) into inositol-1,4,5-trisphosphate (Ins(1,4,5)P3) (IP3) and diacylglycerol (DAG). Ligation of receptors on the endoplasmatic reticulum by IP3 induces the depletion of internal Ca^{2+} stores by the release of Ca^{2+} into the cytoplasm. This in turn activates store-operated Ca^{2+} channels in the plasma membrane allowing for an influx of Ca^{2+} from the extracellular space. The stimulation-induced increase in intracellular Ca^{2+} activates a number of signaling proteins [152]. Most prominent among them is the Ca^{2+} dependent phosphatase calcineurin and its target nuclear factor of activated T-cells (NFAT) [134]. It has been shown that the pattern of Ca^{2+} oscillations (amplitude and frequency) contains information that regulates cell survival and programmed cell death [151].

The patterns of Ca^{2+} signaling differ between the various functional T-cell subsets and presumably reflect the differential sensitivities of these groups towards TCR activation and the differences in the outcome of stimulation [208]. Memory T-cells display an increase in the magnitude of the Ca^{2+} rise compared to naïve T-cells [6]. In general, CD8 positive T-cells are thought to give a lower Ca^{2+} response than CD4 positive T-cells [167]. In addition, store operated Ca^{2+} channels have been shown to play a crucial role in the modulation of naïve T-cell survival [152].

I.6.3. Reactive oxygen species as a second signaling messenger

Oxidative signaling that is induced in response to TCR and CD28 co-receptor cross-linking influences a number of stimulation outcomes in T-cells including proliferation, survival and cytokine production [94]. Activation induced cell death depends at least in

part on oxidative signals for the efficient transcriptional up-regulation of CD95L [65]. Enhanced H_2O_2 production after T-cell stimulation leads to NF-κB activation. In addition, mitochondrial ROS act synergistically with Ca^{2+} signaling to up-regulate IL-2 and IL-4 transcription in an NF-κB and AP-1 dependent manner [93].

I.6.4. Distal T-cell receptor signaling

Downstream of the TCR proximal signaling cascade major intracellular signaling pathways are activated, namely the mitogen-activated protein (MAP) kinases extracellular signal-regulated kinase (ERK) and p38, the transcription NF-kB and NFAT and, especially in the context of costimulation, the AKT axis ([189] and references therein) (Figure I.6.1-1).

I.6.5. The outcome of T-cell receptor signaling

The functional outcome of TCR stimulation is variable and strongly affected by the context in which antigen-recognition occurs. This includes a dependence on differentiation and activation state of the cell, co-receptor and cytokine receptor signaling. In addition, the affinity and abundance of the encountered antigen as well as the time point have an influence [199]. In general, antigen-recognition via the TCR leads to activation of the T-cell. In the following the possible outcomes of TCR signaling are outlined in the context of the stage of differentiation.

I.6.5.1. Proliferation

In naïve T-cells, two types of TCR signals are important for survival and proliferation. Homeostasis of the naïve T-cell pool depends largely on "tonic" TCR signaling mediated by interaction with self-peptide-MHC complexes [16]. Together with IL-7R signaling, this has been shown to prolong the survival of naïve T-cells in the periphery and to induce homeostatic proliferation especially under lymphopenic conditions [196]. Recent work also identified the interaction between T-cells and steady-state dendritic cells (DC) as crucial for the maintenance of T-cell responsiveness [120]. Interestingly, TCR-mediated signals are dispensable for homeostatic proliferation of memory T-cell subsets [58].

To fully activate a T-cell in order to induce clonal expansion and effector functions, TCR engagement by itself is not sufficient. Recognition of a foreign-peptide-self-MHC complex provides the initiating TCR-mediated signal for the induction of an immune

response. This first activation step leads to the up-regulation of cytokine- and chemokine receptors eg. the high affinity IL-2Rα chain, which in turn makes the T-cells more susceptible to co-stimulatory signals that allow for full activation of the cell [119].

I.6.5.2. Cytokine production

Cytokines are small secreted proteins that have a multitude of functions in the regulation of the immune system including the control of proliferation, migration and effector functions. The so-called type I cytokines share four α-helical bundles as a structural feature. An important subset of this cytokine family is the common cytokine receptor gamma-chain (Υ_c) family including IL-2, IL-4, IL-7, IL-9, IL-15 and IL-21. The receptors of these cytokines all share Υ_c [174].

IL-2 is one of the best studied cytokines involved in T-cell biology and an important T-cell growth factor. It mediates both pro-survival and pro-apoptotic effects depending on the context of T-cell stimulation. IL-2 is crucial for proliferation, survival and differentiation of activated T-cells. The production of IL-2 is tightly regulated on the molecular level. A large number of transcription factors have to bind to the multiple regulatory elements controlling the IL-2 promoter, some of them, like Oct1, are produced constitutively, but gene expression is only switched on when also the 3 major transcriptions factors downstream of the TCR are activated, namely NFAT, AP-1 and NF-kappa B [35].

There are three IL-2 receptor chains that can act in different combinations. The IL-2R β chain (CD122) forms an heterodimeric receptor complex of intermediate affinity with Υ_c, while the IL-2R α chain (CD25) can act as a monomeric low affinity IL-2 receptor. Both IL-2R α and β are up-regulated in response to TCR stimulation and together with Υ_c form the heterotrimeric high affinity IL-2 receptor [132]. On naïve T-cells only low levels of CD122 are detectable and CD25 expression is absent. Similarly most memory T-cells express neither molecule with the exeption of a CD122 high CD8+ subset [174].

IL-4 is the signature T_H2 cytokine as it determines both differentiation and function of these T-cells and is also produced predominantly by this cell type. Similar to CD122, expression of the IL-4R α chain (CD124) is absent on naïve T-cells and up-regulated in response to TCR stimulation [14].

IL-7 plays a crucial role both during T-cell development and for homeostasis of the mature T-cell compartment. It mediates survival of resting naïve and memory T-cells and induces the proliferation of both subsets under lymphopenic conditions. Under

normal physiologic conditions the proliferation-promoting effect of IL-7 is only exerted on memory T-cells [130]. Accordingly, the IL-7Rα chain is expressed on naïve T-cells and is especially high on resting memory T-cells but is rapidly down-regulated in response to TCR stimulation [2].

I.6.5.3. Activation-induced cell death

Clonal expansion of activated T-cells is a prerequisite for efficient clearance of antigen from the system. In order to retain homeostasis of the immune system, however, most of the newly generated antigen-specific T-cells need to be eliminated again at the end of an immune response. This is achieved by a process termed activation-induced cell death (AICD) [104]. During AICD, apoptosis is induced in expanded T-cells that are re-stimulated by TCR engagement in the absence of protective co-receptor signals. This effect is mimicked in an *in vitro* model by repeated stimulation of T-cells on day 1 and day 6 by either an unspecific stimulus such as phytohemagglutinin (PHA) or direct cross-linking of the TCR complex in the presence of IL-2.

Cell death induction in this case occurs via the so-called extrinsic pathway. Stimulated T-cells up-regulate CD95L and thus are able to cross-link the death receptor CD95 on neighboring T-cells [103]. While freshly activated T-cells are largely resistant towards CD95 cross-linking, during the expansion phase T-cells become highly susceptible to apoptosis induction, allowing for down-regulation of the immune response [100] (Figure I.6.5-1). Defects in the CD95/CD95L system can lead to autoimmune manifestations due to impaired T-cell homeostasis [204].
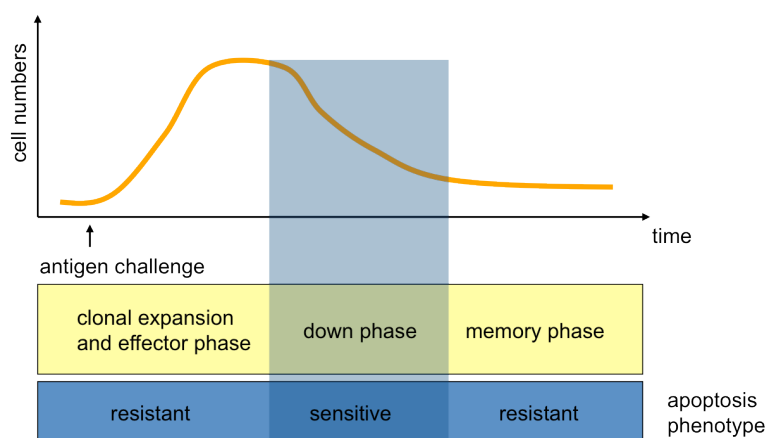
Figure I.6.5-1: T-cells show differential sensitivity to apoptosis induction over the course of an immune response. Adapted from Kramer et al. [103].

I.7. The role of chemokines and their receptors in T-cell biology

Chemokines are cytokines with a chemoattractive function. By definition, chemokines are low-molecular weight chemotactic proteins. They are classified according to the configuration of cysteine residues near their N-terminus [8]: CXC-chemokines or α-chemokines (X denominates the aminoacid separating two cysteine residues.) CC- or β-chemokines, C- or gamma-chemokines with only one cysteine residue and CX_3C- or δ-chemokines, that show 3 aminoacids between the two cytokine residues. The most important chemokine family with respect to their influence on lymphocyte homing and migration are CXC chemokines (Table I.7-1). One prominent example of this group is stromal cell-derived factor-1 (SDF-1). First described in 1993 as a chemotactic substance for lymphocytes produced by bone marrow stroma cells [203], SDF-1 was also shown to be produced by stroma cells in other organs and influence the migration of a number of cell types including granulocytes, DCs, endothelial cells and microglia [97]. SDF-1 mediates its effects via the chemokine receptor CXCR4 (CD184) that was initially described as leukocyte-derived seven transmembrane domain receptor (LESTR) [123] and is also known as Fusin on the basis of its function as a co-receptor for the human immunodeficiency virus on CD4 T-cells [47]. CXCR4, like all chemokine receptors, is a seven transmembrane receptor coupled to pertussis toxin-sensitive inhibitory guanine nucleotide-binding proteins (G_i-proteins). Conformational changes of the receptor induced by ligand binding lead to the activation of the heterotrimeric G-protein and in the case of chemokine receptors in turn inhibit the activity of adenylate cyclase, thus reducing the amount of the 2nd messenger cAMP [157]. CXCR4 plays an important role during the migration of hematopoietic progenitor cells and the maturation of thymic progenitors to immature T-cells [197]. In the mature T-cell compartment CXCR4 shows a trend towards preferential expression on T_H2 cells but is widely found on T-cells in lymphoid tissues [91]. Surface expression of CXCR4 is subject to regulation in response to T-cell costimulation via CD28 [185]. In recent years, in addition to its role as a chemotactic factor, CXCR4 was shown to associate with the TCR complex upon stimulation and to act as a co-stimulator for CD4 T-cell activation [107].

Another receptor for α-chemokines that has been implicated in T-cell biology is CXCR3. The CXCR3-A isoform is expressed on T_H1 cells and mediates survival and

chemotaxis in response to one of its three ligands CXCL9 (Mig), CXCL10 (IP-10), and CXCL11 (I-TAC) [63].

Beta-chemokine receptors that are of importance in T-cell physiology include CCR4 and CCR5 (Table I.7-1). CCR4 binds both CCL22 (macrophage-derived chemokine (MDC)) and CCL17 (thymus and activation-regulated chemokine (TARC)). It is uniformly expressed on *in vitro* polarized T_H2 lymphocytes. In addition, CCR4 is also preferentially found on single-positive CD4+ thymocytes and on a major fraction of non-intestinal CD4+ memory T-cells in the peripheral blood, including skin-homing T-cells. Interestingly, these circulating CCR4+ memory T-cells co-express the T_H1-associated receptors CXCR3 and CCR5, indicating a higher complexity of chemokine receptor expression patterns *in vivo* [3].

Table I.7-1 Chemokine receptors expressed on defined T-cell subsets and their ligands.

name	ligand (examples)	expressed by (examples)
CCR3	eotaxin	T_H2 cells
CCR4	MDC, TARC	T_H2 cells
CCR5	RANTES	T_H1 cells
CCR7	CCL19	lymph node homing T-cells
CXCR3	Mig, IP-10	T_H1 cells
CXCR4	SDF-1	lymphocytes, stem cells

MDC = macrophage derived chemokine/CCL22, TARC = thymus and activation regulated cytokine/CCL17, RANTES = regulated upon activation normal T-cell express sequence/CCL5, Mig = monokine-induced by Interferon-γ/CXCL9, IP-10 = γ-Interferon inducible protein 10/CXCL10, SDF-1 = stromal cell derived factor-1/CXCL12

The chemokine receptor CCR5 is mainly known for its role as a co-receptor in human immuno deficiency virus infection. Physiologically, however, CCR5 mediates aspects of the inflammatory response after binding of its ligands CCL3 (MIP-1α), CCL4 (MIP-1β), CCL5 (RANTES) and CCL8 (MCP-2) [90]. In the T-cell compartment CCR5 is mainly found on circulating memory T cells and T_H1 effector cells [124].

CCR3 has been implicated in the directed migration of eosinophiles through its ligand eotaxin. Recently, however, CCR3 expression on T_H2 cells has been shown to be crucial in the modulation of the skin microenvironment in CTCL [145].

The interaction between chemokines and their cognate receptors is the major factor that controls migration of immune cells and thus is indispensable for an efficient immune response [128]. As outlined above, T-cell precursors migrate from the bone marrow to the thymus where they undergo a number of differentiation steps that are orchestrated by chemokine receptor signaling. Mature T-cells recirculate in a strongly chemokine-dependent manner through secondary lymphoid organs to maximize the probability of antigen encounter. Changes in chemokine receptor expression mediate the capacity of effector T-cells to migrate to any tissue where pathogens may be present [8].

I.8.   Goal of the present work

The pathobiology of T-PLL is only incompletely understood. T-PLL is rare and sizable sample collections are the exception. By using comprehensive immunophenotyping of a large cohort of T-PLL, the **1st aim** of the presented work was to identify a „normal T-cell counterpart" for the T-PLL tumor cell. Multi-colour flow cytometric analysis of leukemic T-PLL samples allowed the identification and characterization of T-PLL tumor cells and potential clonal subsets, which differ for example in memory marker expression. Special emphasis was placed on identifying a prototypic T-PLL immunoprofile. We asked whether T-PLL cells displayed a physiolgic „T-cell signature" based on an unequivocal asignment to established (immunophenotypically defined) functional subsets of normal T-cells or if there are non-conventional expression patterns to be found in T-PLL. Besides a potential diagnotsic use, defining subsets of T-PLL cases characterized by activation or memory marker expression was expected to be important in drawing conclusions about the biology of T-PLL and the characteristics of its clinical (e.g. homing to particular sites, specific symptoms) presentations.

The **2nd aim** was to investigate the functionality of the TCR signaling cascade and the outcome of TCR activation in T-PLL cells to better characterize this potential pathogenic force in T-PLL. This might also reveal rationales towards potential therapeutic targets. The **3rd aim** was to interrogate the functional relevance of the characteristic oncogene TCL1 in primary T-PLL cells. To that end the response of primary T-PLL cells to TCR-dependent stimuli had been tested in order to correlate the cellular response to the TCL1 expression level [72].

Overall, by better defining characteristic features of the T-PLL tumor cell, novel therapeutic targets in this poor prognostic disease might be revealed.

II. Material and Methods

II.1. Reagents

II.1.1. Chemicals

All chemicals were purchased from the following companies, if not indicated otherwise: Sigma (Munich, Germany), Carl Roth (Karlsruhe, Germany), and Merck (Darmstadt, Germany).

II.1.2. Kits and special reagents

Reagent	Manufacturer
7-AAD	BD Biosciences (Heidelberg, Germany)
Annexin V – Phycoerythrin	BD Biosciences
Annexin V binding buffer	BD Biosciences
Anti murine IgG sepharose	Sigma Aldrich (Steinheim, Germany)
Brefeldin A Solution	Biolegend (Fell, Germany)
Complete mini	Roche (Grenzach-Wyhlen, Germany)
Dynal T-cell Expander	Life Technologies (Darmstadt, Germany)
Fluo-4 AM	Life Technologies
H_2DCFDA	Life Technologies
Human Basic Kit Flowcytomix	Bender MedSystems GmbH, (Vienna, Austria)
Human T Cell Nucleofector® Kit	Lonza (Cologne, Germany)
IOTest Beta Mark	Beckman Coulter (Krefeld, Germany)
Nitrocellulose transfer membrane	Santa Cruz Biotechnology (Heidelberg, Germany)
Pacific Blue Monoclonal Antibody Labeling Kit	Life Technologies
PhosStop	Roche
Pierce ECL	Thermo Scientific (Braunschweig, Germany)
Protein A/G sepharose	Life Technologies
SuperSignal West Pico	Thermo Scientific
X-ray films	Santa Cruz Biotechnology

II.1.3. Analytical antibodies

II.1.3.1. Antibodies for flow cytometry

If not indicated otherwise antibodies for flow cytometry were purchased from Biolegend (Fell, Germany) .

Antigen	Clone	Conjugate	Manufacturer
CD2	TS1/8	PC7	Biolegend
CD3	Hit3a	Pacific Blue	Biolegend
CD3	Hit3a	APC Cy7	Biolegend
CD4	OKT4	APC AF750	Biolegend
CD5	BL1a	ECD	Beckman Coulter (Krefeld, Germany)
CD5	UCHT2	PC7	Biolegend
CD7	CD7-6B7	AF488	Biolegend
CD8	Hit8a	AF488	Biolegend
CD19	J3-119	ECD	Beckman Coulter
CD25	BC96	PE	Biolegend
CD38	HIT2	PE	Biolegend
CD40L	24-31	APC eFluor780	eBiosciences (Frankfurt, Germany)
CD44	IM7	PC7	Biolegend
CD45	HI30	BD Horizon V500	BD Biosciences (Heidelberg, Germany)
CD45RA	HI100	PE	Biolegend
CD45RO	UCHL1	AF700	Biolegend
CD62L	DREG-56	APC AF750	Biolegend
CD69	FN50	PC5.5	Biolegend
CD95	DX2	PC7	Biolegend
CD95L	NOK-1	PE	Biolegend
CD122	TU27	APC	Biolegend
CD124	hIL4R-M57	PE	Biolegend
CD127	HCD127	AF488	Biolegend
CCR3	5E8	AF647	Biolegend
CCR4	TG6/CCR4	PC5.5	Biolegend
CCR5	HEK1/85a	FITC	Biolegend
CCR7	TG8/CCR7	PC5.5	Biolegend

Antigen	Clone	Conjugate	Manufacturer
CXCR3	TG1/CXCR3	Pacific Blue	Biolegend
CXCR4	12G5	PC7	Biolegend
BCL2	BCl/10C4	AF647	Biolegend
GATA3	L50-823	PC7	BD
T-bet	4B10	PC5.5	eBioscience
IFN gamma	4S.B3	PE	Biolegend
IL-2	MQ1-17H12	APC	Miltenyi Biotech (Bergisch Gladbach, Germany)
IL-4	MP4-25D2	PC5.5	Miltenyi
Ki67	SP6	FITC	Upstate (Millipore, Schwalbach, Germany)
pAKT	D9E	AF647	CST (Danvers, MA, USA)
pERK	D13.14.4E	AF488	CST

II.1.3.2. Antibodies for Western blot

antigen	Clone	source	manufacturer
β-actin	AC-15	Mouse monoclonal	Sigma Aldrich
TCL1A	1-21	Mouse monoclonal	Herling et al., 2006

II.1.3.3. Stimulatory antibodies

antigen	Clone	source	manufacturer
CD3	OKT3	Mouse monoclonal	lab owned hybridomas
CD28	15E8	Mouse monoclonal	lab owned hybridomas
IgG		Goat polyclonal	Jackson Immunoresearch (Newmarket, UK)

II.1.4. Cytokines and chemokines

Reagent	Manufacturer
Recombinant human IL-2	Peprotech (Hamburg, Germany)
Recombinant human IL-4	Peprotech
Recombinant human IL-7	Peprotech

II.1.5. Media and sera

Reagent	Manufacturer
Roswell Park Memorial Institute medium (RPMI) 1640	PAA Laboratories GmbH, Pasching, Austria
X-vivo15 with Gentamycin	Lonza (Cologne, Germany)
Chemically defined (CD) hybridome mediuam	Life Technologies (Darmstadt, Germany)
FBS standard quality	PAA
FBS Gold	PAA
L-Glutamine 200mM (100x), liquid	Life Technologies
GlutaMAX	Life Technologies
Penicilin-Streptomycin, liquid	Life Technologies
Cholesterol lipid concentrate (250x)	Life Technologies

II.2. Consumables

All cell culture consumables were purchased from Sarstedt (Nümbrecht, Germany), if not indicated otherwise.

Material	Manufacturer
Cell strainer 40µm	BD Falcon (Heidelberg, Germany)
Cell strainer 70µm	BD Falcon
Vacuum filtration units, PES, .45µM	VWR International (Darmstadt, Germany)
IsoFlow™ Sheath Fluid	Beckman Coulter (Krefeld, Germany)
FlowCheck Pro Beads	Beckman Coulter
Flow Clean Cleaning Agent	Beckman Coulter
BD FACSFlow Sheath Fluid	BD Biosciences (Heidelberg, Germany)
BD FACSRinse	BD Biosciences
BD FACSClean	BD Biosciences
Lymphocyte Separation Medium 1077	PAA (Cölbe, Germany)

II.3. Instruments

Instrument	Type	Manufacturer
Scale	Acculab Vicon	Sartorius (Göttingen, Germany)
Scale	MC1AnalyticAC2105	Sartorius
Centrifuge	centrifuge 5415R	eppendorf (Hamburg, Germany)
Centrifuge	Allegra X-23R	Beckman Coulter (Krefeld, Germany)
Centrifuge	J-6B	Beckman Coulter
Centrifuge	Biofuge pico	Heraeus (Hanau, Germany)
Centrifuge	5810R	eppendorf
Centrifuge rotor - Allegra	SX4250	Beckman Coulter
Centrifuge rotor - Allegra	S2096	Beckman Coulter
Centrifuge rotor – J-6B	JS5.2	Beckman Coulter
Electrophoresis system	mini-PROTEAN 3	Biorad (Munich, Germany)
Laminar flow hood	SterilGuard III advance	Baker (Sanford, USA)
Laminar flow hood	HA2448	Heraeus
Refrigerator/freezer -20°C	cofort	Liebherr (Biberach, Germany)
Refrigerator	SANTO1905TK	AEG (Nürnberg, Germany)
Freezer -20°C	Arctis 60110	AEG
Freezer -80°C	AV073P	Labotect (Göttingen, Germany)
Freezer -80°C	MDF U74V	Sanyo (Munich, Germany)
Heating block	Thermomixer 5436	eppendorf
Hemocytometer	Neubauer chamber	Karl Roth (Karlsruhe, Germany)
Incubator	C200	Labotect
Magnetic stirrer	IKAMAG NEO REO	IKA Labortechnik (Staufen, Germany)
Microscope	Axiovert25	Karl Zeiss (Oberkochen, Germany)
Magnetic cell separator	MidiMACS	Miltenyi Biotech (Bergisch Gladbach, Germany)
Magnetic cell separator	MPC-S	Life Technologies (Darmstadt, Germany)
Magnetic cell separator	MPC-1	Life Technologies

Instrument	Type	Manufacturer
Liquid phase N2 tank	MVE cryosystem 4000	Princetoncryo (Flemington, NJ, USA)
Spectral photometer	nanodrop	Peqlab (Erlangen, Germany)
Nucleofector	Nucleofector II	Amaxa (Lonza, Cologne, Germany)
O_2 sensor	MSA O2	ALTAIR (Böblingen, Germany)
pH meter	LAB850	Schott (Mainz, Germany)
Pipette aid	accu-jet pro	BRAND (Wertheim, Germany)
Pipette aid	macro	BRAND
Microliter pipette	Research variable 100-1000μL	eppendorf
Microliter pipette	Research variable 20-200μl	eppendorf
Microliter pipette	Research variable 2-20μL	eppendorf
Microliter pipette	Research variable 1-10μL	eppendorf
Microliter pipette	Research variable 0,5-2,5μl	eppendorf
Protein blotting cell	Trans Blot SD	Biorad
Power supply	Power Pac HC	Biorad
Rocking platform	Rocking Platform	VWR (Darmstadt, Germany)
Sample roller	coulter mixer	Beckman Coulter
Scanner	EPSON Perfection V100 Photo	EPSON (Meerbusch, Germany)
Vacuum gas pump	PM20405-80	VWR
Vortex mixer	Genie 2	Bender & Hobein (Bruchsal, Germany)
Vortex mixer	lab dancer vario	IKA Labortechnik
Water bath	JB Aqua 2	Grant Instruments (Shepreth, UK)
X-ray developing machine	Curix 60	Agfa (Cologne, Germany)

II.4. Solutions

II.4.1. Media for cell culture

RPMI standard medium for lymphoid cells:

88% (v/v)	RPMI 1640
10% (v/v)	FBS Gold
1% (v/v)	L-Glutamine
1% (v/v)	Penicillin-Streptomycin

X-vivo15 for primary T- and T-PLL cells

X-vivo15 was purchased complete with L-glutamine, gentamycin, recombinant transferrin, and phenol red. It was developed to sustain the proliferation of T-cells under serum-free conditions, therefore no further supplementation was necessary.

CD medium for hybridoma cell lines:

95% (v/v)	CD
1% (v/v)	GlutaMAX
4% (v/v)	cholesterol

Standard freezing medium

90% (v/v)	FBS Standard quality
10% (v/v)	DMSO

Freezing medium for hybridoma cells

50% (v/v)	conditioned medium from exponentially growing hybridoma cell cultures
40% (v/v)	FBS standard quality
10% (v/v)	DMSO

II.4.2. Buffers

Joe's protein lysis buffer

25mM	Hepes
400mM	NaCl
1.5mM	$MgCl_2$
2mM	EDTA
0.5% (v/v)	Triton X-100
1x	Complete mini
1x	PhosSTOP

Sample loading buffer (reducing) (5x)

50 % (v/v)	glycerol
10 % (w/v)	sodiumdodecylsulfat
50 mM	tris/HCl, pH 6,8
25 % (v/v)	β-mercaptoethanol
0.25 mg/ml	bromphenolblue

PBS

137 mM	NaCl
8.1 mM	Na_2HPO_4, pH 7,4
2.7 mM	KCl
1.5 mM	KH_2PO_4

PBS-T

PBS
0.05 % (w/v) Tween-20

Running buffer (SDS-PAGE)

25 mM	tris/HCl
0.19 M	glycin
1 %	SDS

Transfer-buffer (Western blot, semi-dry)

25 mM	tris/HCl
0.19 M	glycin
20 % (v/v)	methanol
0.037 % (w/v)	SDS

Fix-solution for flow cytometry

92% (v/v)	PBS
8% (v/v)	formaldehyde

Permeabilization solution for flow cytometry

99.77% (v/v)	PBS
0.23% (v/v)	Triton X-100

Erythrocyte lysis solution

8.29g	ammonium chloride
1.0g	potassium bicarbonate
0.037g	EDTA
ad 1L	bi-destilled (dd) H_2O

Propidium iodide staining solution

0.1% (v/v)   Triton X-100
0.2mg/mL   RNAse A
0.02mg/mL   propidium iodide
in   PBS

II.5.   Methods of protein biochemistry

II.5.1.   Preparation of eukaryotic whole cell lysates

Cells were transfered to 1.5mL reaction tubes and pelleted at 250xg for 5min, subsequently they were washed once with chilled PBS and resuspended in an appropriate volume of Joe's lysis buffer. Typically, $5x10^6$ cells were lysed in 250μL ice-cold Joe's lysis buffer. The lysates were incubated on ice for 20 min. Remaining debris and DNA were pelleted by centrifugation at 10000xg for 30min at 4°C. The supernatant was used for subsequent analyses.

II.5.2.   Determination of protein content

II.5.2.1.   Protein determination according to Bradford

The Bradford protein assay is a quantitative detection method for proteins. It is based on the ability of the dye Coomassie-Brilliant-Blue G-250 to form complexes with cationic as well as with non-polar hydrophobic protein side-chains under acidic conditions. This stabilizes the dye in its deprotonated anionic form as sulfate, which in turn shifts the absorption maximum of the dye from 470nm to 595nm wave length. The increasing absorption at 595nm correlates with the protein concentration of the solution.

To determine the protein concentration of whole cell lysates 1 volume Rotiquant was diluted with 4 volumes of ddH$_2$O. 1mL diluted Rotiquant was mixed with 2μL whole cell lysate. A standard curve was prepared by adding 2, 4, 6, 8, and 10μg bovine serum albumin to 1mL Rotiquant working solution. 200μL of the standard and test conditions were transferred to a 96-well microtiter plate in duplicate and absorption at $\lambda = 595$nm was measured. Blank values were substracted from all measurements. The arithmetic mean was calculated for all duplicate values. The measurements for the standard dilution were used to determine the formula describing the partial regression line. According to this formula protein concentration of the whole cell lysates was calculated.

II.5.2.2. Protein determination by absorption at λ = 280nm

The protein content of a solution can be determined by measuring the absorbance of the solution in the near UV range at 280nm. The absorption at this wavelength depends on the content of aromatic amino acids (Tyrosine, Tryptophane and Phenylalanine). Therefore the absorption coefficient at 280nm depends strongly on the protein sequence. To determine the protein concentration of purified antibodies the absorption at 280nm was measured using a nanodrop device and the protein concentration was calculated using an approximate coefficient for a 10mg/mL IgG solution of 13.7.

II.5.3. Separation of protein by SDS-polyacrylamide gel electrophoresis

Denaturating sodium dodecyl sulfate polyacrylamide gel electrophoresis (SDS-PAGE) is a method to separate proteins according to their electrophoretic mobility, which is mainly determined by the molecular weight. To prepare the samples whole cell lysates were boiled in a sample buffer containing dithiothreitole (DTT) to reduce disulfide bonds and SDS to denature proteins. The main function of SDS in this context was, however, to mask the endogenous charge of the proteins by adding a substantial negative charge so that they will migrate through a gel in response to voltage according to the lenght of the polypeptide chain only.

As separation matrix two polyacrylamide gels layered on top of each other are required. The top gel, the so-called stacking gel, contains a lower percentage of polyacrylamide than the lower gel, the so-called resolving gel. This leads to a larger pore size and faster migration speed in the stacking gel. The two gels also differ in pH, with the stacking gel having a lower pH of 6.8. The purpose of the stacking gel is to focus the sample loaded onto the gel. This depends on the presence of „fast" leading ions like for example chloride ions, that due to their charge and low size could migrate through the gel at a higher speed than the „slower" trailing ions like glycine. The pH of the stacking gel is close to the isoelectric point of glycine (5.97), so that only a part of the glycine dissociates and only a part is present in the mobile ionic form. The mobility coefficient of the proteins contained in the samples lies between those of leading and trailing ions.

To start the electrophoresis voltage was applied to the gel. This induced the migration of the ions towards the anode. The field intensity is higher in the area of the faster chloride ions, whereas it is lower in the area of the trailing ions, as the conductivity increases with increasing mobility of the ions and decreases with increasing electrostatic

potential. This leads to the development of a potential gradient that focuses the specific ion species. The higher pH value within the resolving gel causes the glycin to deprotonate and gain a higher mobility, therefore it will overtake the larger proteins and migrate faster leading to more defined protein bands. The gels were prepared according to the formulations given in Table II.5-1.

Table II.5-1: Gel composition for SDS-PAGE

[mL]	Stacking gel	Resolving gel 6%	Resolving gel 10%	Resolving gel 12%	Resolving gel 15%
H_2O	5.5	10.6	7.9	6.6	4.1
30% acrylamide mix	1.3	4.0	6.7	8.0	10.05
1M Tris pH 6.8	1.0				
1.5 M Tris pH 8.8		5.0	5.0	5.0	5.0
10% (w/v) SDS	0.08	0.2	0.2	0.2	0.2
10% (w/v) APS	0.08	0.2	0.2	0.2	0.2
TEMED	0.010	0.016	0.016	0.016	0.016

Due to the higher polyacrylamide concentration and the associated smaller pore size of the resolving gel the migration speed of proteins depends strongly on their molecular weight. The higher the molecular weight of the proteins to be analyzed the lower the percentage of the resolving gel has to be.

II.5.4. Visualization of proteins by Western blot

Western blotting allows the visualization of proteins separated by SDS-PAGE using specific antibodies recognizing the protein of interest. For this, the proteins have to be transferred from the polyacrylamide gel onto a membrane (polyvinylidene difluoride (PVDF) or nitrocellulose). The membrane is then incubated with the primary antibody and an enzyme labelled secondary antibody is used to visualize the protein.

II.5.4.1. Semi-dry blot

In a semi-dry blot chamber the so-called blotting sandwich was assembled. From bottom to top 3 layers of Whatman paper soaked in blotting buffer, the pre-wetted and in case of PVDF methanol acitvated membrane, the resolving gel and another 3 layers

of wet Whatman paper were pressed together to get rid of air bubbles. Current was applied at 0.8mA per cm^2 membrane for 2 hours (h).

II.5.4.2. Antibody staining and ECL-based detection

After sucsessful transfer of the proteins the membrane was washed quickly with PBS-T and unspecific binding sites for the antibodies were saturated by incubation with 5% non-fat milk powder in PBS-T for 1h at room temperature (RT) under constant agitation. After blocking the membrane was incubated with the primary antibody diluted in 2% milk in PBS-T and sodium azide over night at 4°C under constant agitation. For detection of TCL1 in whole cell lysates of samples with expected low expression of TCL1, sterile filtered hybridoma supernatant of 1-21-clone hybridoma cells was diluted 1:1000 in PBS without the addition of any other protein.

Following incubation with the primary antibody the membrane was washed three times for 5min with PBS-T and incubated with a horseradish peroxidase (HRP)-coupled secondary antibody diluted 1:10000 in 2% milk in PBS-T for 1h at RT. Subsequently, the membrane was washed 3 times for 10min with PBS-T. Finally, a peroxidase substrate for enhanced chemiluminescence was added as per manufacturer's instruction. Under alkaline conditions the cyclic diacylhydrazide luminol is oxidized in a peroxidase/H$_2$O$_2$ catalyzed reaction. A sheet of X-ray film was exposed to the resulting luminescence.

II.5.5. Antibody purification from hybridoma supernatants

To produce large amount of antibodies of known specificity *in vitro* so-called hybridoma cell lines can be generated. For this, single antibody-producing cells are isolated typically from a mouse mounting a polyclonal immune response against the antigen of interest. These single cells are then fused with immortalized myeloma cells to form a hybridoma that is able to proliferate and generate the immunoglobulin of the original cell. Limiting dilution procedures allow for the establishment of hybridoma cell lines that derive from a single cell clone and therefore produce an unlimited amount of a monoclonal antibody [226].

Hybridoma cells secrete the antibody into the culture medium. For certain applications, eg. flow cytometry or immunoprecipitation, it is desirable to purify the antibody in order to eliminate contaminations by other proteins. Purification of antibodies is achieved by specific binding of the antibody heavy chain to either Protein A or G

coupled to an insoluble matrix. Protein A and G are derived from the cell wall of the bacterium Staphylococcus aureus. Physiologically, binding of the F_C part of the antibody heavy chain to Protein A or G abolishes the opsonizing function of antibodies and protects the pathogen from recognition by the immune system [51]. Using Protein A/G for antibody purification has the disadvantage that serum immunoglobulins are co-purified. This can be circumvented by using sepharose coupled antibodies specific for the constant region of the species the antibody of interest is derived from, for example α-murine IgG immunoglobulins to purify a murine antibody [122]. The binding of the antibody to both Protein A/G or α-IgG can be reversed by low pH or high salt concentrations. Antibody purification was performed in a cold room at 4°C.

II.5.5.1. Purification of anti (α)-TCL1 clone 1-21

The monoclonal antibody 1-21 was established by standard immunization of a BALB/c mouse with a specific 14–amino acid peptide epitope that maps to the outer AKT binding loop region of TCL1 and fusion of spleen cells with the myeloma line NS1 followed by screening of hybridomas with the immunizing peptide (Antibody Shared Resource; Cold Spring Harbor Laboratory, Cold Spring, NY) by Herling et al. as described previously [69]. Western blots using this antibody detected a strong single 13.5kDa band in cells transfected with a TCL1-expressing construct [69].

1-21 hybridoma cells were cultured in CD medium supplemented with Glutamax and cholesterol. For production of antibody containing supernatant 1-21 cells were seeded at a density of $1x10^6$ cells per mL and the supernatant was harvested after 48h by centrifugation at 1000xg for 10min and filtration through a 0.45μm membrane. Supernatants were stored at -20°C until purification.

To prepare the column 4mL of resuspended ProteinG-Sepharose slurry were poured into BioRad Polyprep column to give a final column volume of 2mL matrix. Tubing was attached to the column via a three-way syringe. After the matrix had settled the column was washed with 10 column volumes 1xPBS and 5 column volumes 2xPBS. The hybridoma supernatants were thawed in a waterbath at 37°C, diluted with an equal volume of 4xPBS and sterile filtered over a .45μm membrane. Per run 250-300mL of pre-diluted supernatant were applied onto the column, the flow through was directly re-applied to the column. After antibody binding 10 column volumes of 2xPBS were used to wash the column. The bound antibody was eluted with 5 column volumes of 0.1M

glycin pH 2.5 into 12 reaction tubes pre-loaded with 500µL 1M Tris pH8. The pooled fractions were diluted with an equal volume of 2xPBS and applied to an Amicon 50 Spin Column MWC 50000. After centrifugation as per manufacturer's instructions, the top-chamber remnant was resuspended in 2xPBS and centrifuged again. This procedure was repeated once to achieve a buffer exchange. The antibody concentration was determined by measuring absorbance at 280nm using a nanodrop instrument. The concentrated antibody was aliquoted and stored at -20°C until use.

The column was regenerated by running 5 column volumes of 0.1 M glycine pH 2.5 followed by 25 column volumes of sodium acetate pH5 containing 0.5M sodium chloride. The column was stored at 4°C in 2xPBS with sodium azide to prevent microbial contamination and was re-used up to 5 times.

II.5.5.2.   Purification of α-CD3 clone OKT3 and α-CD28 clone 15E8

OKT3 and 15E8 hybridoma cells were cultured in RPMI 1640 supplemented with 10% FBSGold, 1% L-glutamin and 1% penicilin/streptomycin. For production of antibody containing supernatant hybridoma cells were seeded at a density of $1x10^6$ cells per mL and the supernatant was harvested after 48h by centrifugation at 1000xg for 10min and filtration through a 0.45µm membrane. Supernatants were stored at -20°C until purification.

To prepare the column 5mL of resuspended α-murine IgG agarose slurry were poured into a C10 10 column to give a final column volume of 2.5mL matrix. The column was connected to a P500 pump and 10 column volumes of PBS were run over the column to help settle and compact the matrix. The hybridoma supernatants were thawed in a waterbath at 37°C and centrifuged twice at 6000xg to pellet any remaining particles that might clog the column (5min and 1h, respectively, at 4°C). After centrifugation the supernatants were sterile filtered over a 0.45µm membrane. Per run, 1.5 to 2L of supernatant were applied onto the column per run and the flow through retained for a second round of purification. After antibody-binding the column was washed with 2 column volumes of PBS. The bound antibody was eluted with 10 column volumes of freshly prepared 0.1M glycine pH 1.8 into reaction tubes containing 100µL 10x PBS.

After elution the column was washed with PBS until the pH of the flow through was back to pH7. Consequently the column was stored in 0.1% Sodium azide in PBS at 4°C and re-used up to 10 times. The elution fractions were pooled and dialyzed against 2L PBS over night. The dialyzed antibody solution was concentrated using Vivaspin

columns according to manufactureres instructions. Finally, the protein concentration was determined by measuring the absorbance at 280nm. The antibody was aliquoted into PP screw top vials and stored at -20°C until use.

II.6. Cells and Cell Lines

II.6.1. General culture conditions

All cell cultures, primary cells as well as cell lines, were incubated at 37°C and 5% CO_2 in an atmosphere saturated with water vapor. All cell lines were passaged twice a week as described below (II.6.3.2).

II.6.2. Cell Lines

Line	Phenotype	Source	Reference
OKT3	CD3 hybridoma	ATCC	
15E8	CD28 hybridoma	ATCC	
1-21	TCL1 hybridoma	lab owned	Herling et al., 2006 [69]

II.6.3. Primary cell cultures

This study included patients with T-PLL who were diagnosed at the University Hospital of Cologne and cooperating centres that were enrolled in the TPLL1 and TPLL2 studies of the German CLL Study Group and who had available tumor material and sufficient clinical information. The diagnosis of T-PLL was established based on the revised World Health Organization criteria and a previously published algorithm for diagnosis of T-cell leukemias that includes clinical, morphologic, immunophenotypic, and karyotypic features [198].

Peripheral blood mononuclear cells (PBMC) from healthy donors were obtained from buffy coat material provided by the Department of Transfusion Medicine according to the ethic vote 03-143. Tumor samples and buffy coat material from healthy donors were acquired in accordance with a protocol approved by the University Hospital of Cologne institutional review board and in accordance with the Declaration of Helsinki.

II.6.3.1. Isolation of PBMC from T-PLL samples and buffy coat

Buffy coat material from healthy volunteers was provided by the Department of Transfusion Medicine. For isolation of PBMC, the buffy coat material was poured over

a cell strainer to filter out clumps, diluted with the same volume of PBS and layered over lymphocyte separation medium (LSM 1077).

EDTA-anti coagulated peripheral blood or bone marrow samples from T-PLL patients were obtained after written informed consent. The samples were diluted with an equal volume of PBS and carefully layered over lymphocyte separation medium.

LSM 1077 contains a hydrophilic polysaccharide and has a density higher than lymphocytes, monocytes and platelets but lower than erythrocytes and most granulocytes. These differences in density resulted in a separation into distinct phases upon centrifugation (800xg for 20min at RT without brake to preserve the gradient). Due to their lower density, erythorocytes pelleted at the bottom of the tube under a layer of the separation medium. The mononuclear cells formed an interphase between the separation medium and the blood plasma. The diluted plasma was stored at -20°C for further analysis. The interphase was carefully transferred to a fresh tube and washed twice with PBS (1st wash, 800xg 5min, 2nd wash 200xg 10min to remove a possible platelet contamination).

II.6.3.2. Subculturing and medium change

To passage cells growing in suspension, an aliquot of an exponentially growing culture was transferred to a fresh culture vessel and diluted to a 2- to 10- times higher final volume depending on proliferative activity.

II.6.3.3. Cryo-storage of viable cells

Cells were frozen at $5\text{-}10\text{x}10^7$ cells per vial for primary cells or $5\text{-}10\text{x}10^6$ cells per vial for cell lines in 1mL of freezing medium. The cells to be frozen were pelleted by centrifugation and resuspended in 1mL freezing medium per vial. The cell suspension was pipetted into cryo tubes and transferred to -80°C in an isopropanol-filled freezing box. This results in a constant temperature decrease of about 1°C per minute. After a minimum of 24h the vials were transferred into liquid nitrogen (-196°C) for long-term storage.

Frozen cells were taken in culture by thawing them in a 37°C water bath under constant agitation and transferring them into 10mL culture medium in an appropriate culture vessel. The medium was exchanged on the following day.

II.6.3.4.   Stimulation with plate-bound antibodies

Cell culture plates were coated with the stimulating antibodies OKT3 (αCD3) and 15E8 (αCD28) by adding the desired amount of antibody to a volume of PBS sufficient to cover the bottom of the cell culture vessel completely (typically 500µL per well in a 6-well plate). Plates were incubated for at least 30min at 37°C. After the incubation period the antibody dilution was removed and the well was gently washed 3 times with fresh PBS. Cells were added at a density of 5×10^6/mL in a sufficient amount of culture medium (typically 2mL per well in a 6 well plate) and incubated at 37°C for the desired time. For short term stimulations the cells were centrifuged onto the plates at 250xg for 3min at RT to ensure contact with the antibodies.

II.7.   Immunophenotyping using flow cytometry

II.7.1.   Principle

In a flow cytometer cells or particles are transported by a jet of liquid in single suspension through monochromatic laser beams of defined wave length. The resulting scattered light and excited fluorescence is detected and makes it possible to analyze physical and indirectly also biological properties of the particle.

The directions of the light scatter contains information on size and granularity of a cell, with the amount of light scattered to the front correlating with cell size and the side scatter measured at a 90° angle increasing with higher granularity.

The expression pattern of antigens displayed on the cell surface can be assessed by using fluorochrome-coupled antibodies. Intracellular proteins can be evaluated after permeabilization of the cell membrane. Fluorescent probes can be used to analyze a number of cellular functions in real time, for example changes in intracellular levels of Ca^{2+} or ROS.

The availability of a multitude of different fluorochromes with specific emission wavelengths allows for the staining of different epitopes in parallel and makes co-expression studies possible (multi-color stainings). The instrument used for multi-color analyses for this work was a Gallios flow cytometer by Beckman Coulter equipped with 3 solid-state lasers with emission maxima of 405, 488 and 638nm, respectively. The available detectors allow for the assessment of forward and side scatter, and 10 different fluorescence channels. An overview over the utilized fluorochromes is given in Table II.7-1.

Table II.7-1: Utilized fluorochromes and their properties

Fluorochrome	Laser [nm]	Emission [nm]	Filter (Gallios ^{TM})
FITC (Fluorescein isothiocyanate)	488	518	525 BP 40
Alexa Fluor (AF) 488	488	519	525 BP 40
Phycoerythrin (PE)	488	575	575 BP 30
PE/Texas Red (ECD)	488	615	620 BP 30
Perinidin-Chlorophyll-Protein (PerCP)	488	675	765 BP 20
PE-Cy5 (PC5)	488	667	765 BP 20
PerCP-Cy5.5 (PC5.5)	488	690	695 BP 30
PE-Cy7 (PC7)	488	785	755 LP
Allophycocyanine (APC)	638	660	660 BP 20
AF647	638	668	660 BP 20
AF700	638	723	725 BP 20
APC AF750	638	775	755 LP
APC-Cy7	638	760	755 LP
Pacific Blue	405	455	450 BP 40
BD Horizon V500	405	500	550 BP 40

Laser: laser wave length used for excitation; 488nm blue solid state laser; 638nm: red solid state laser; 405nm: violet solid state laser; Emission: wavelength of maximum emission; Filter: filter configuration for detection at a Gallios flow cytometer; DC: dichroic; BP: band pass; SP: short pass; LP: long pass.

II.7.2. Titration of fluorochrome coupled antibodies

In order to determine the optimal concentration for every antibody that resulted in the best resolution between specifically stained cells and background noise, every fluorochrome coupled antibody for flow cytometry was titrated on whole blood samples from healthy donors. Initially, for every antibody 2 different volumes per test were tested. Generally, if the recomended volume per test was 20μL, the second volume tested was 5μL per test. If 10μL were recomended, 2μL were used and for a recomended volume of 2μL, this was compared to 0.5μL per test. The mean fluorescence intensity (MFI) was determined for negative and positive populations, respectively. The relative increase in staining intensity was determined according to the

formula below and conditions leading to a higher relative increase in MFI were given preference:

$$\text{relative increase in MFI} = (\text{MFI}_{positive}-\text{MFI}_{negative})/\text{MFI}_{negative}$$

II.7.3. Immunophenotyping of T-PLL samples

II.7.3.1. Staining procedure for whole blood samples

As a standard 100μL of EDTA- anti-coagulated peripheral blood were used per test in 5mL polystyrole tubes. Only in cases with known white blood cell counts above 50.000 cells per μL the sample volume was reduced to 50μL to avoid antigen excess. Antibodies directed against surface epitopes were added as previously determined by titration for optimal staining results. The samples were vortexed and incubated for 20min in the dark at RT. To fix the cells 110μL of a 8% phosphate buffered formaldehyde solution were added and incubated for another 10 min in the dark at RT. To permeabilize the cell membranes and lyse erythrocytes 2mL of pre-warmed lysis buffer were added and incubated for 15min at RT protected from light. After washing the cells twice with PBS (350xg, 3min) and decanting the supernatant, cells were resuspended in the residual PBS volume and antibodies for intracellular staining were added. Cells were washed after a 20min incubation in the dark at RT and resuspended in 500μL of PBS prior to measuring on a Gallios flow cytometer.

To immunophenotypically characterize the T-PLL samples, 5 multi-color panels were developed.

II.7.3.2. Panel 1: TCL1 expression in lymphocyte subsets

II.7.3.2.1. Rationale for and design of panel 1

The purpose of panel 1 (Table II.7-2) was to determine the TCL1 status of different lymphocyte subpopulations, especially in T-PLL peripheral blood samples. The highest priority was given to the TCL1 antibody. The APC conjugated 1-21 TCL1 antibody (eBioscience) was chosen because it gave superior resolution of the negative and positive populations in comparison to the other conjugates commercially available at the beginning of this study (AF488 from upstate and PE from eBioscience), showing more than a one log step shift for positively staining cells. To discriminate the T-PLL clone the 2nd priority was assigned to the markers for T-helper cells and cytotoxic T-cells, CD4 and CD8, respectively. The conjugates were chosen so they would be excited by

different lasers to minimize spectral overlap. The dimmer AF488 was chosen for the usually highly expressed CD8 and the brighter APC-AF750 tandem conjugate was used for CD4. Staining for the T-cell associated markers CD3 and CD5 were included to reliably identify T-cells. Because the (partial) loss of T-cell markers is characteristic for T-cell malignancies, both CD3 and CD5 were used. In addition, CD3 surface staining was important to determine whether or not the T-PLL cells could be stimulated by CD3 cross-linking for further experiments. Again, the markers were put onto different excitation wavelengths to avoid artefacts by compensation. The co-receptor CD28 was analzyed to gain insight on the differentiation state of the T-PLL clone. In addition, CD28 staining showed whether or not the cells could be stimulated by CD28 cross-linking for further experiments. AF700 was chosen because it is a fluorochrome with a high staining index useful for rather dimly expressed markers like CD28.

Table II.7-2: Markers used in panel 1

Specificity	Fluorochrome	Function
TCL1	APC	protein of interest
CD4	APC AF750	cytotoxic T-cells
CD8	AF488	T-helper cells
CD5	PC5.5	T-cell lineage
CD3	Pacific blue	T-cell lineage
CD28	AF700	co-receptor
CD25	PE	IL-2Rα
CD69	PC7	early activation
CD19	ECD	B-cell lineage
CD45	BD Horizon V500	pan-leukocyte marker

The B-cell marker CD19 was included for the identification of B-cells that could serve as an intrinsic positive control for the TCL1 staining, because over 50% of B-cells of healthy donors stained positive for TCL1. TCL1 positivity was usually preserved in at least a subset of residual naïve B-cells within a T-PLL patient sample. An ECD coupled CD19 antibody was used, because this caused the least spectral overlap with the already set fluorophores while leaving more common fluorophores available for use with less common markers. CD45 is the most commonly used pan-leukocyte marker to discriminate between lymphocytes and other subsets of PBMC in flow cytometry.

CD45 is therefore available conjugated to virtually all fluorochromes. A CD45 BD Horizon V500 conjugate was chosen for this study because only minor spectral overlap was expected with markers of higher priority and at the time of panel design only very few antibodies were available for detection in fluorescence channel FL10. The activation markers CD25 and CD69 were so-called luxury markers [131], they were stained to assess the activation state of the T-PLL clone. The combination of CD25 PE conjugate with CD8 AF488, however, might lead to an underestimation of CD25 expression. Due to the high spillover from FL1 (CD8 AF488) into FL2 (CD25 PE) high compensation values are required, and CD25 dim populations might be lost.
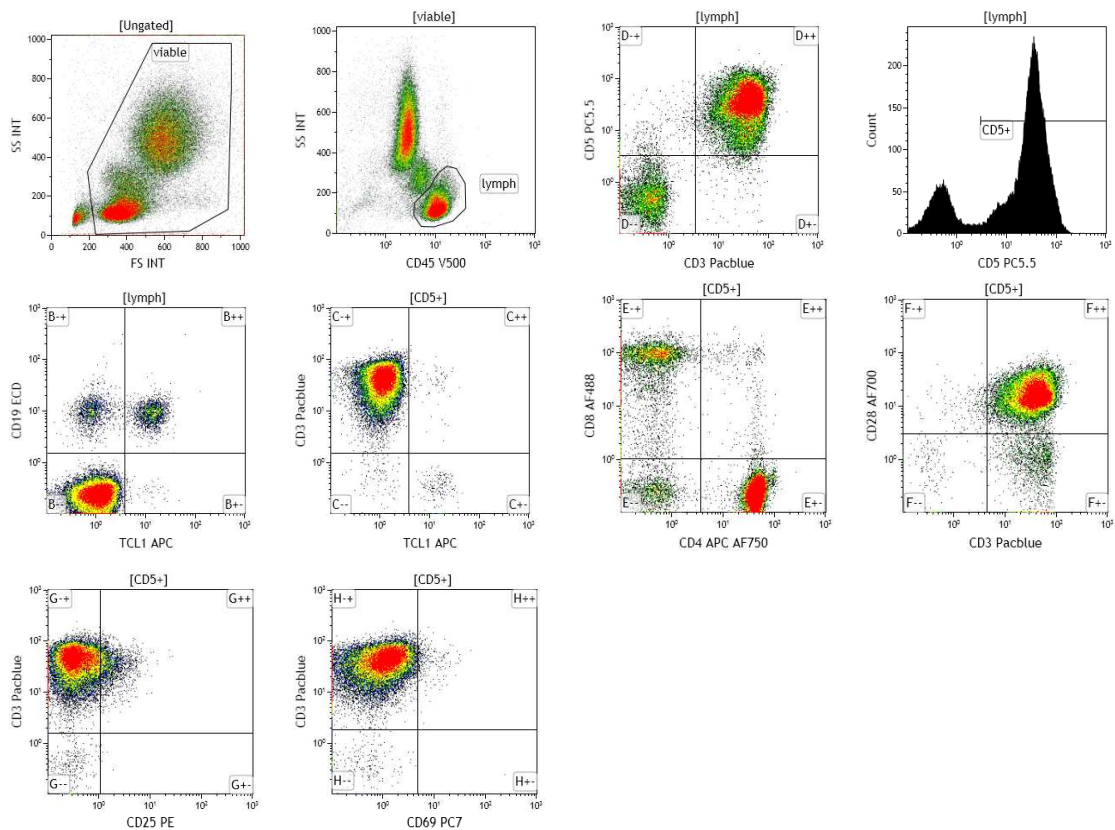
Figure II.7.3-1: Gating strategy to determine the pattern of TCL1 expression of lymphoctes in whole peripheral blood of a healthy donor. Viable cells were gated based on FSC/SSC characteristics. By comparing SSC and CD45 expression the lymphoid population (lymph) was determined. The expression of the T-cell associated markers CD3 and CD5 was plotted and a CD5 positive gate defined for further analysis. TCL1 expression on all lymphocytes was compared to CD19 expression and the TCL1 cut off set according to TCL1+ CD19+ B-cells. TCL1 expression in the T-cell compartment was analyzed by comparing CD3 and TCL1 expression on CD5+ cells. CD4 and CD8 expression was determined on CD5+ cells to define T-cell lineages. Comparison on CD3 and CD28 expression revealed whether the CD5+ cells could be stimulated by CD3 and CD28 cross-linking. The activation markers CD25 and CD69 were compared to CD3 expression for the CD5+ population.

II.7.3.2.2.   Gating strategy

To detfine the lymphocyte population and to rule out a loss of CD45 staining on T-PLL cells, plots showing forward scatter (FSC) vs. side scatter (SSC) and CD45 vs. SSC were compared. Subsequently, a lymphocyte gate was drawn around the CD45 bright SSC low population. For this population the TCL1 expression of B-cells was determined by comparing CD19 and TCL1 expression. The T-cell population was defined using a density plot for CD3 vs. CD5. In the next step TCL1 expression was analyzed in comparison to CD3, usually by gating on the CD5 positive T-cell population. In addition, the distribution of CD4 and CD8 expression was determined for CD5 postive cells. To assess whether the cells can be stimulated by targeting antibodies, CD3 was plotted against CD28 for CD5 positive cells. In TCL1 positive cases, CD25 and CD69 expression were depicted in density plots against TCL1 (Figure II.7.3-1). In TCL1 negative cases activation marker expression was compared to CD3, or in CD3 negative cases to CD5.

II.7.3.3.   Panel 2: Memory status

Table II.7-3: Markers included in panel 2

Specificity	Fluorochrome	Function
CD45RO	AF700	memory T-cells
CD45RA	PE	naïve T-cells
CD62L	APC AF750	selectin
CCR7	PC5.5	memory/homing
CD44	PC7	memory/homing
TCL1	APC	T-PLL cells
CD7	FITC	T-cell subset
CD5	ECD	T-cell lineage
CD3	Pacific blue	TCR complex component
CD45	BD Horizon V500	pan-leukocyte marker

II.7.3.3.1.   Rationale for and design of the memory status panel

Panel 2 (Table II.7-3) was designed in order to determine the memory status of the malignant population in the peripheral blood of T-PLL patients. Again, CD45 was stained to aid in the distinction of the lymphocyte population from monocytes and

granulocytes. No single unambiguous marker for T-PLL cells has been identified, therefore the combination of CD3 and CD5 was used along with TCL1 to bias the analysis towards T-PLL cells. CD3, CD5, and CD45 conjugates were asigned a low priority and fluorochromes were chosen that did not interfere with analysis of other markers. Again, the TCL1-APC conjugate was used for its bright staining over a wide expression range. CD7 expression was assessed because T-PLL cells are known to highly express this molecule. CD7 is present on most T-cell subsets and is missing only from certain memory T-cell populations [168].
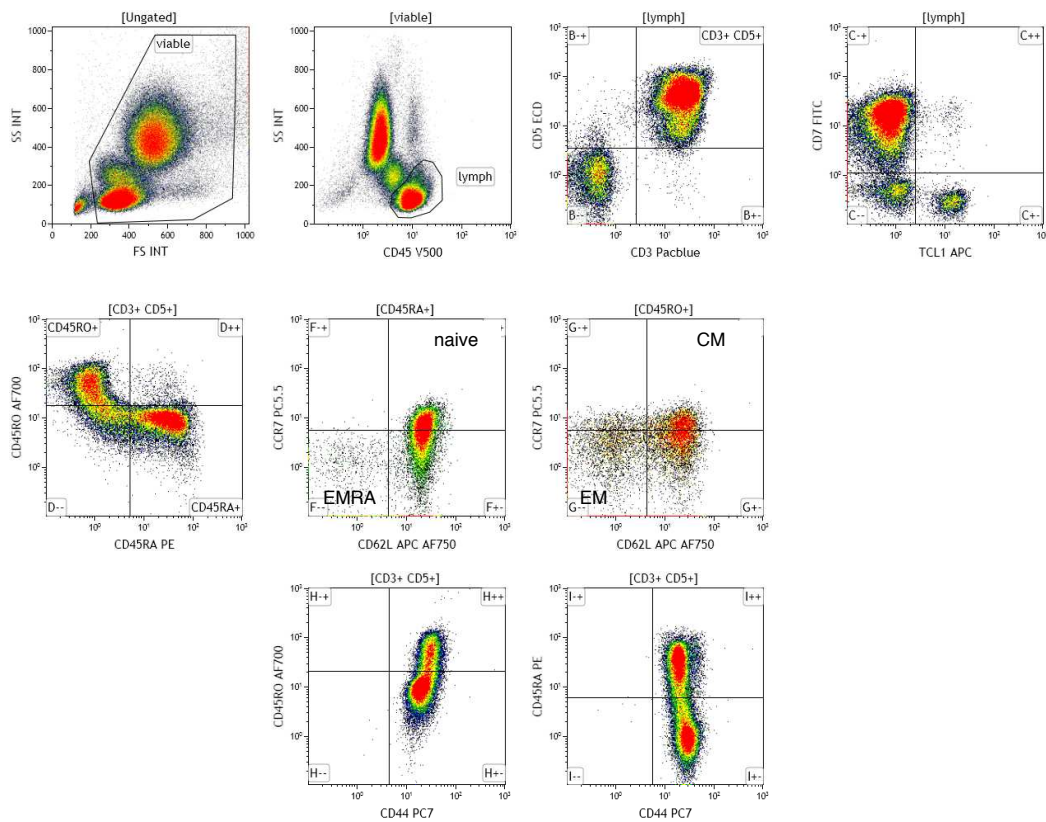
Figure II.7.3-2: Gating strategy to determine the memory status of T-lymphocytes in whole peripheral blood of a healthy donor. Viable cells were gated based on FSC/SSC characteristics. By comparing SSC and CD45 expression the lymphoid population (lymph) was determined. The expression of the T-cell associated markers CD3 and CD5 was plotted and a CD3+ CD5+ gate defined for further analysis. TCL1 expression on all lymphocytes was compared to CD7 expression. The distribution of CD45RA and CD45RO was shown for CD3+ CD5+ T-cells. Naïve T-cells were defined as CD45RA+ CD62L+ CCR7+ and T_{EMRA} (EMRA) as CD45RA+ CD62L- CCR7-. Central memory T-cells (CM) were gated based on CD45RO+ CD62L+ CCR7+ and effector memory T-cells (EM) as CD45RO+ CD62L variable and CCR7-. CD44 expression was compared to CD45RA and CD45RO on T-cells.

The CD45 isoforms RA and RO have long been used as markers for naïve and memory T-cells, respectively. These markers were used in combination with fluorochromes that

are excited by different lasers to minimize spectral overlap and achieve optimal resultion. The combination of CD62L, CCR7, and CD44 expression was used to further define memory T-cell subpopulations. These markers were distributed on channels that allowed for the use of bright fluorochromes because expression of chemokine recptors like CCR7 is characteristically dim. CD44 has recently been described as marker of a memory T-cell type with stem cell like properties, it was also used to evaluate the activation status [7].

II.7.3.3.2.   Gating strategy

As outlined above, CD45 expression was used to define the lymphocyte population and T-cells were defined by CD3 and CD5 positivity. TCL1 expression was analyzed regarding two aspects. On the one hand, TCL1 positivity was used to identify the T-PLL population. On the other hand, TCL1 expression levels were compared to the expression of memory markers in order to detect possible correlations. To define the memory phenotype CD45RA was plotted against CD45RO (Figure II.7.3-2). In cases that showed single positivity for either one marker, the memory phenotype was defined according to homing marker expression as follows in Table II.7-4 [181]:

Table II.7-4: Immunophenotypic characteristics of naïve and memory T-cell subpopulations

	CD45RA	CD45RO	CCR7	CD62L
naïve	+	-	+	+
T_{EMRA}	+	-	-	-
effector memory	-	+	-	variable
central memory	-	+	+	+

An analysis of CD44 expression intensity was challenging, as often no healthy T-cell population remained that could have been used as a reference. Because no standardization procedure of the cytometer settings was performed as part of the experiment setup, absolute fluorescence intensities for CD44 could not be compared across samples over a prolonged time. Therefore, CD44 expression intensity was not taken into account for the assignment of a memory phenotype to T-PLL samples.

II.7.3.4.   Panel 3: Chemokine receptor expression in T-PLL

II.7.3.4.1.   Rationale for and design of panel 3:

CD45 expression was used to define the lymphocyte population and T-cells were identified by CD5 positivity. TCL1 was stained to identify T-PLL cells in TCL1 positive cases. In this panel a TCL1 antibody conjugated with PE was used. This introduced an additional level of control of the accuracy of the flow cytometric determination of the TCL1 status in T-PLL samples. By using a different antibody conjugate it could be ruled out that weakly positive stainings for the conjugates are due to incorrect compensation and spectral overlap. When chosing fluorochrome coupled antibodies for the staining of chemokine receptors the most severe limitation was limited availability of the antibodies conjugated to less common fluorochromes. Care was taken to avoid excessive spectral overlap by using PC5.5 instead of PC5 and omitting FL7 (AF700). See Table II.7-5 for a list of markers and fluorochromes used in this panel.

Table II.7-5: Markers included in panel 3:

Specificity	Fluorochrome	Function
CXCR4	PC7	chemokine-R, homing
CXCR3	Pacific blue	chemokine-R, T_H1
CCR3	AF647	chemokine-R, T_H2
CCR4	PC5.5	chemokine-R, T_H2
CCR5	FITC	chemokine-R, T_H1
CD40L	APC eFluor780	TNF family member
TCL1	PE	T-PLL marker
CD5	ECD	T-cell lineage
CD45	BD Horizon V500	pan-leukocyte marker

II.7.3.4.2.   Gating strategy

T-cells and T-PLL cells were identified as outlined above.

TCL1 expression levels were compared to the expression of the chemokine receptors in order to detect correlations. In addition, chemokine receptor expression was plotted against CD5 expression in all cases (Figure II.7.3-3).
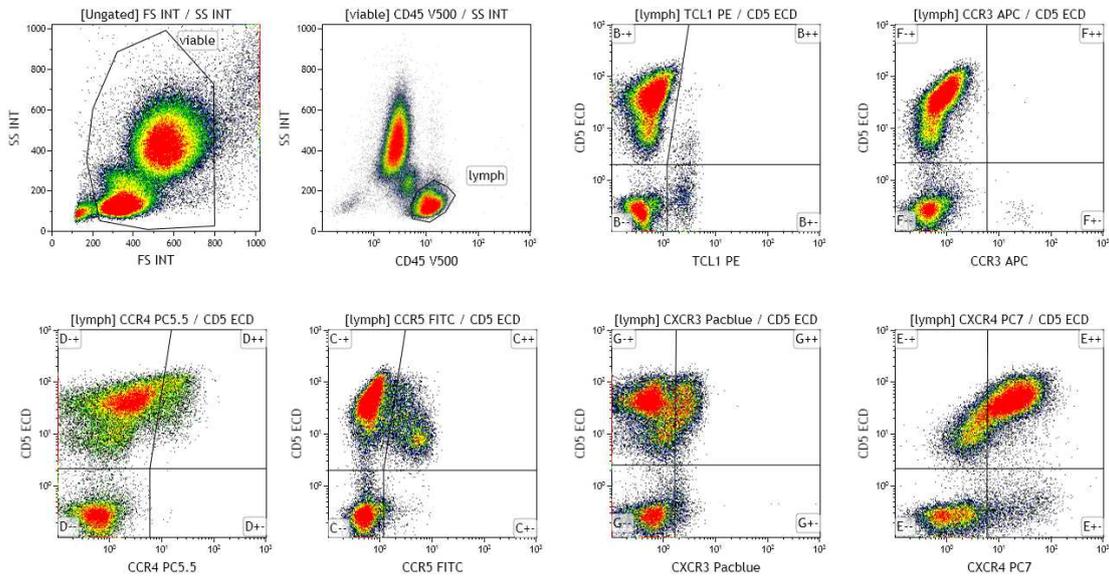
Figure II.7.3-3: **Gating strategy to determine the chemokine receptor expression pattern on T-lymphocytes in whole peripheral blood of a healthy donor.** Viable cells were gated based on FSC/SSC characteristics. By comparing SSC and CD45 expression the lymphoid population (lymph) was determined. TCL1 expression on all lymphocytes was compared to CD5 expression. Chemokine receptor expression was compared to CD5.

II.7.3.5.   Panel 4: Cytokine receptor expression and T-helper phenotype

II.7.3.5.1.   Rationale for and design of panel 4:

Table II.7-6: Markers included in panel 4.

Specificity	Fluorochrome	Function
CD122	APC	IL-2 R β chain
CD124	PE	IL-4 R β chain
CD127	AF488	IL-7 R α chain
T-bet	PC5.5	T_H1 transcription factor
GATA3	PC7	T_H2 transcription factor
TCL1	Pacific blue	T-PLL marker
CD5	ECD	T-cell lineage
CD45	BD Horizon V500	pan-leukocyte marker

CD45, CD5 and TCL1 were included into the panel as outlined above (II.7.3.4.1). When choosing fluorochrome coupled antibodies for the staining of cytokine receptors the most severe limitation was the limited availability of the antibodies conjugated to less common fluorochromes such as APC tandem conjugates or Pacific Blue. At the time the panel was designed the only possible combination for the two intracellular markers of T helper cell fate, T-bet and GATA-3, was in FL4 and FL5, respectively. In addition, the intracellular staining procedure required excessive optimization and up to now failed to yield satisfactory results as part of this antibody panel. See Table II.7-6 for a list of markers and fluorochromes used in this panel.

II.7.3.5.2. Gating strategy

T-cells and T-PLL cells were determined as outlined above. Measuring of TCL1 expression levels using a 1-21 Pacific blue conjugate using Life Technologies's Pacific Blue Monoclonal Antibody Labeling Kit had to be discontinued because efficient conjugation could not be achieved. Instead the expression of cytokine receptors was compared to CD5 expression in order to detect possible correlations.
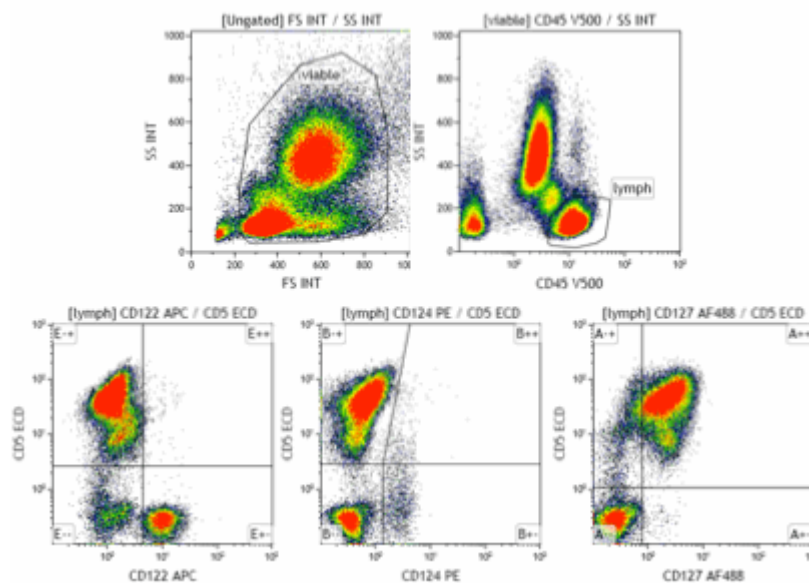
Figure II.7.3-4: Gating strategy to determine the cytokine receptor expression pattern on T-lymphocytes in whole peripheral blood of a healthy donor. Viable cells were gated based on FSC/SSC characteristics. By comparing SSC and CD45 expression the lymphoid population was determined (lymph). Cytokine receptor expression was plotted vs. CD5.

To define a T-helper phenotype GATA3 was plotted against T-bet. As neither GATA3 nor T-bet staining could be verified these results were omitted for the anlysis of the T-

cell immunophenotype. T-cells and T-PLL cells were determined as outlined above. Cytokine receptor expression was compared to CD5 in all cases (Figure II.7.3-4).

II.7.3.6. Panel 5: Proliferation and cell death

II.7.3.6.1.   Rationale for and design of panel 5

CD45, CD5 and TCL1 were included into the panel as outlined above. Ki67 staining had been previously established and optimized in the lab and was therefore continued using the Ki67-FITC conjugate. BCL2 was chosen as AF647 conjugate as this is both a bright fluorochrome and well suited for intracellular staining. For CD95 and CD95L bright fluorochromes were chosen from the available combinations. See Table II.7-7 for a list of markers and fluorochromes used in this panel. CD1a was also assessed as part of this panel in a reduced number of T-PLL cases. Unfortunately, staining of viably frozen PBMC of known T-PLL samples (TPLL1 trial patients) revealed an unspecific positive staining. Therefore, CD1a was not taken into account in the following analyses.

Table II.7-7: Markers included in panel 5:

Specificity	Fluorochrome	Function
Ki67	FITC	proliferation
CD69	PC5.5	early activation
BCL2	AF647	survival
CD95	PC7	cell death induction
CD95L	PE	cell death induction
TCL1	Pacific blue	T-PLL marker
CD5	ECD	T-cell lineage
CD45	BD Horizon V500	pan-leukocyte marker

II.7.3.6.2.   Gating strategy

T-cells and T-PLL cells were determined as outlined above. As outlined above reliable TCL1 Pacific blue conjugation could not be achieved. Therefore, expression levels of the markers analyzed were compared to CD5 (Figure II.7.3-5).
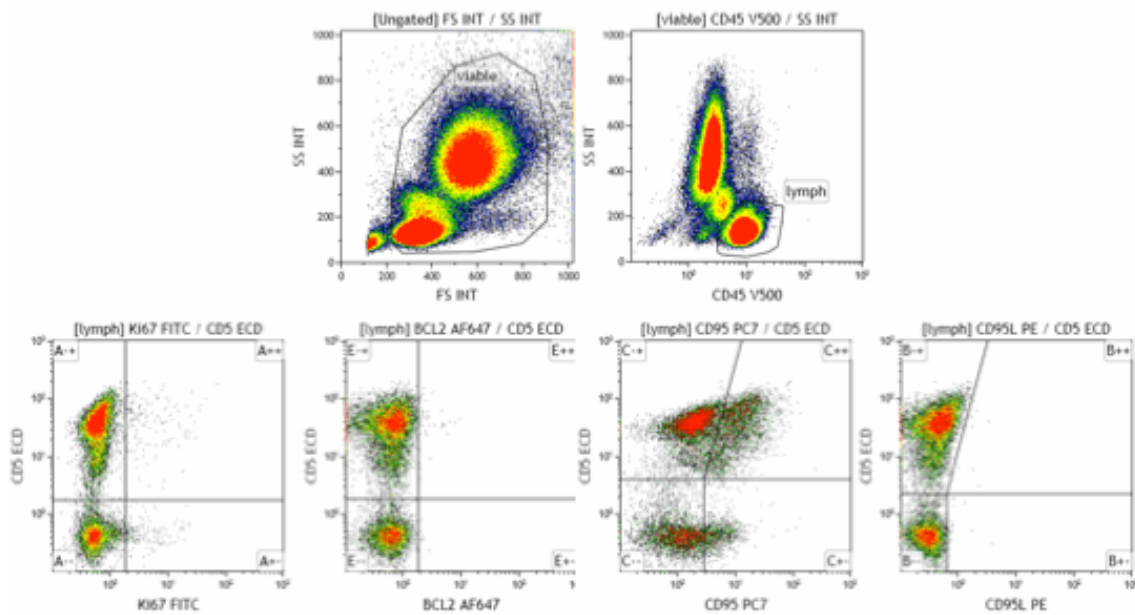
Figure II.7.3-5: Gating strategy to characterize expression pattern of pro- and anti-apoptotic molecules and proliferation markers on T-lymphocytes in whole peripheral blood of a healthy donor. Viable cells were gated based on FSC/SSC characteristics. By comparing SSC and CD45 expression the lymphoid population was determined. The expression of single markers was compared to CD5 expression.

II.7.4. TCR Vβ repertoire analysis

TCR Vβ repertoire analysis was performed using a collection of TCR Vβ antibody cocktails. Each antibody cocktail contained antibodies against 3 different Vβ chains families labelled with either FITC or PE or both FITC and PE, thereby combining a staining for 3 different TCR Vβ using only two colours (Table II.7-9). The TCR Vβ staining was combined with staining for markers of T-cell differentiation and memory status (Table II.7-8).

II.7.4.1. Rationale and design of a TCR Vβ panel backbone

The purpose of the panel backbone was to facilitate identification of the T-PLL population in peripheral blood samples or isolated and viably frozen PBMC from T-PLL patients. CD45 was included to discriminate lymphocytes from monocytes and granulocytes. CD5 was used as a surrogate T-cell marker. Due to the limited amount of markers that could be stained in parallel, CD5 was used instead of CD3 to make the backbone applicable for both surface CD3 positive and negative cases. TCL1 was used as a specific marker for T-PLL cells in TCL1-positive T-PLL cases. In order to analyze the clonality with respect to subpopulations within the T-PLL cell populations

CD45RO, CD62L and CCR7 were stained in order to assign a memory phenotype and define possible subpopulations (for details see II.7.3.3.1).

Table II.7-8: Markers included in the Vβ repertoire analysis:

Specificity	Fluorochrome	Function
CD5	PC7	T-cell lineage
CD4	APC AF750	T-helper cell lineage
CD45	Krome Orange	pan-leukocyte marker
TCL1	APC	T-PLL marker
CD45RO	AF700	memory
CD62L	Pacific blue	lymph node homing
CCR7	PC5.5	exravasation

Table II.7-9: TCR Vβ reagent composition

Tube	Vβ	Fluorochrome	Clone	Isotype murine unless indicated otherwise
A	Vβ 5.3	PE	3D11	IgG1
	Vβ 7.1	PE+FITC	ZOE	IgG2a
	Vβ 3	FITC	CH92	IgM
B	Vβ 9	PE	FIN9	IgG2a
	Vβ 17	PE+FITC	E17.5F3	IgG1
	Vβ16	FITC	TAMAYA1.2	IgG1
C	Vβ18	PE	BA62.6	IgG1
	Vβ5.1	PE+FITC	IMMU157	IgG2a
	Vβ 20	FITC	ELL1.4	IgG
D	Vβ 13.1	PE	IMMU222	IgG2b
	Vβ 13.6	PE+FITC	JU74.3	IgG1
	Vβ 8	FITC	56C5.2	IgG2a
E	Vβ 5.2	PE	36213	IgG1
	Vβ 2	PE+FITC	MPB2D5	IgG1
	Vβ 12	FITC	VER2.23	IgG2a
F	Vβ 23	PE	AF23	IgG1
	Vβ 1	PE+FITC	BL37.2	IgG1 (rat)
	Vβ21.3	FITC	IG125	IgG2a
G	Vβ 11	PE	C21	IgG2a
	Vβ 22	PE+FITC	IMMU546	IgG1
	Vβ 14	FITC	CAS1.13	IgG1
H	Vβ 13.2	PE	H132	IgG1
	Vβ 4	PE+FITC	WJF24	IgM (rat)
	Vβ 7.2	FITC	ZIZOU4	IgG2a

II.7.4.2. Staining procedure for TCR Vβ repertoire analysis

Peripheral blood or density gradient isolated and viably frozen PBMC of T-PLL patients were incubated with TCR Vβ chain antibody cocktails and the backbone panel of T-cell lineage and memory markers. After staining for 30min at RT, the cells were fixed with a final concentration of 2% formaldehyde diluted in PBS for 10 min followed by permeabilization with PBS + Triton for 15min. Due to the presence of TCR Vβ chain antibodies during this step, an intracellular staining of TCR Vβ chains cannot be ruled out. After washing the cells once the samples were incubated for 20min with anti-TCL1 for intracellular staining. After an additional washing step the samples were analyzed by flow cytometry according to the manufacturers instructions.

II.7.4.3. Gating strategy for TCR Vβ repertoire analysis

As the TCR Vβ analysis was performed in 8 single tubes, list mode data of all measurments was combined into a multi-file analysis and the gates used to identify lymphocytes, CD5 positive cells and T-cell subpopulations were linked across all data sets analyzed. Lymphocytes were identified in a plot depicting CD45 expression vs. side scatter. CD5 positive cells were identified in a plot of CD5 vs. side scatter gated on lymphocytes. TCL1 and CD4 expression were shown for all CD5 positive lymphocytes and the T-PLL population was defined within this plot. For the T-PLL population, fluorescence channel 1 and 2 were shown and TCR Vβ populations gated based on the fluorochrome combination given in Table II.7-9. Unfortunately, further analysis of memory subpopulations was not feasible due to reduced signal resolution on thawed PBMC and the fact that all analyzed peripheral blood samples only showed homogenous expression of the memory markers used.

A representative measurement is shown in Figure II.7.4-1. The percentage of TCR Vβ chain expressing T-PLL cells was analyzed for clonality. In keeping with previously published studies using similar reagents, TCR clonality was categorized as shown in Table II.7-10 [46]. A T-PLL population was considered clonal if either 50% of T-PLL cells stained positive for one specific TCR Vβ chain or >70% of T-PLL cells failed to react with the TCR Vβ antibody repertoire used. An example of a TCR Vβ clonogram is shown in Figure II.7.4-2.

Table II.7-10: Criteria for TCR clonality categorization

clonality	criterium
proven clonality	single TCR Vβ expressed 10-fold above normal maximum
	single TCR Vβ expressed on >50% of T-cells in any subpopulation of interest
suspected clonality	single TCR Vβ expressed on 40-49% of cells in an T-cell population of interest
	>70% of cells failed to react with any TCR Vβ antibodies tested*
non-clonality	none of the above criteria were met

* for viably frozen samples a percentage of at least 65% of cells not reactive with any TCR Vβ antibody was considered sufficient for clonality, as the high autofluorescence caused higher variability
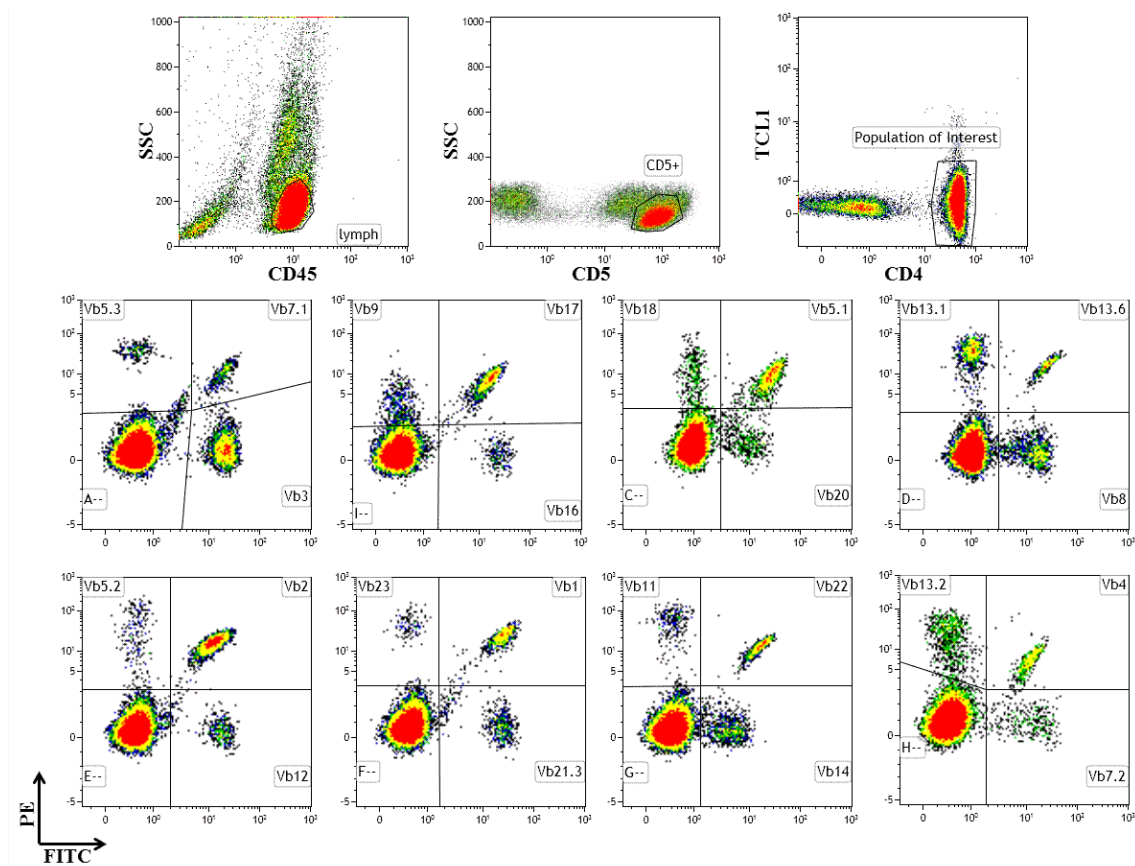
Figure II.7.4-1: Representative staining of TCR Vβ expression on T-cells. Viably frozen PBMC of a healthy donor were thawed, stained and analyzed as outlined above.
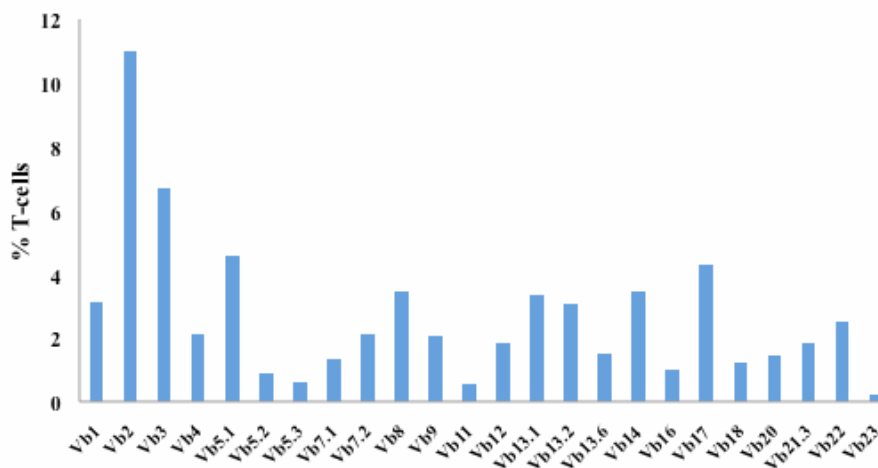
Figure II.7.4-2: TCR Vβ expression in a healthy adult. A peripheral blood sample of a healthy donor was stained for TCR Vβ chain expression as described above. Shown is a representative clonogram.

II.7.5. Immunostaining of isolated lymphocytes and cell lines

Per test $1x10^6$ cells were resuspended in 100μL of PBS. Antibodies against surface markers were added and incubated for 20min at RT, protected from light. If no intracellular proteins were analyzed, cells were washed once, resuspended in 500μL of PBS and measured. For detection of intracellular markers, cells were fixed directly after the incubation with surface antibodies using 100μL of a 4% phosphate buffered formaldehyde solution. To avoid excessive cell loss, the samples were not vortexed at this point and the incubation was performed at 4°C for 10min. Permeabilization of the cell membrane and intracellular staining were performed as described above (II.7.3.1).

II.7.6. Flow cytometric measurements and data analysis

Multi-color measurements were performed on a Beckman Coulter Gallios flow cytometer. The instrument was serviced regularly. To control for optimal instrument conditions, FlowCheck Pro Fluropheres were used daily to check stability of the fluidic systems as well as laser performance and alignment.

Instrument settings for the immunophenytping of leukemia samples were adjusted using whole blood samples from healthy volunteers and cut offs for positive and negative controls set accordingly. For the determination of TCL1 expression the residual B-cell population in blood samples from T-PLL patients was used as intrinsic control.

To quantify the expression of TCL1 and cell surface markers, the mean fluorescence intensity was compared to that of fluorochrome-labeled unspecific antibodies of the

same isotype. To calculate the percentage of positive cells a fraction of <2% false-positive cells was tolerated in the negative controls.

When measuring homogeneous cell populations approximately 10.000 events were acquired and analyzed. For immunophenotyping of leukemia samples 100.000 events were measured within the lymphocyte gate as judged by forward/side scatter.

To display single- or double-positive events density plots were used. The MFI was shown as histogram. Because the MFI is not an absolute value and strongly depends on instrument settings and to a lesser extent also on the properties of the antibody used (age, correct storage, conjugation efficiency), MFI values were always normalized to the MFI of isotype controls or biological controls.

II.7.7.   Flow cytometric determination of intracellular Ca^{2+} release

II.7.7.1.   Principle

Receptor-mediated quantitative changes in intracellular Ca^{2+} levels ([Ca2+]i) in response to stimulation were analyzed using an optimized flow cytometric method similar to the one first described by Vandenberghe et al. [213]. For the work presented here the derivative fluo-4 AM was used instead of the classical fluo-3 Ca^{2+} indicator described by Tsien et al. [143]. In comparison to fluo-3, the absorption maximum of fluo-4 is shifted towards the blue spectrum by approx. 12nm, resulting in increased fluorescence intensity when excited at 488nm, the standard wavelength used in flow cytometers. Fluo-4 is a membrane permeable acetomethylester that diffuses into the cytoplasm where it is hydrolysed by unspecific esterases and loses its ability to cross the membrane („loading" of cells [96]). Hydrolysed fluo-4 binds cytosolic Ca^{2+} which results in a strong increase in fluorescence. Due to the low dissociation constant (K_d=345nM) fluo-4 allows for a very sensitive detection of low levels of Ca^{2+}.

II.7.7.2.   Loading of cells and measurement

Freshly isolated primary cells were incubated for at least 2h at a density of $1x10^7$ cells per mL in RPMI complete medium supplemented with 50U/mL IL-2 under cell culture conditions. After 2h fluo-4 was added to a final concentration of 10μM, dye loading was performed for 20min at 37°C. Excessive dye was washed away with 10mL RPMI + IL-2 by centrifugation at 250xg for 5min. The fluo-4 loaded cells were resuspended at a

density of $2x10^6$ cells per mL and aliquots of 500µL were dispensed into 5mL polypropylene tubes.

The measurement was performed on a FACSCalibur flow cytometer (Beckton Dickinson). The fluorescence emitted by fluo-4 was detected in the FITC-channel and measured over time. It was visualized in a dot plot of fluo-4 fluorescence on the y-axis against time on the x-axis. For every sample the baseline fluorescence was measured for 75s, then acquisition was paused, the stimulus diluted in 100µL RPMI + IL-2 was pipetted into the tube, vortexed once and the measurement continued for another 425s.

II.7.7.3. Analysis

To allow for better comparison of the measurements the relative change in MFI of fluo-4 was plotted against time. The MFI was determined for 21 periods of 25s each. The arithmetic mean was calculated for the first 3 time segments and defined as baseline. The relative proportional change in MFI was subsequently calculated according to the following formula:

$$\text{relative increase in fluo-4 MFI [\%]} = (\text{MFI} - \text{MFI}_{baseline}) / \text{MFI}_{baseline} \times 100$$

II.7.8. Flow cytometric determination of intracellular ROS levels

II.7.8.1. Principle

The amount of ROS in response to TCR and co-receptor stimulation was determined according to a method commonly used to detect reactive oxygen intermediates in neutrophils and macrophages (Yuan et al., 1993). This method relies on the use of 2',7'-dichlorodihydrofluorescein diacetate (H_2DCFDA), a membrane-permeable dye that is converted to its fluorescent form by cleavage of the acetate groups by intracellular esterases and oxidation by ROS.

II.7.8.2. Loading of cells and measurement

Dye loading was performed in PBS, as primary and secondary amines in the medium can lead to extracellular hydrolysis of the acetate ester. Cells were resuspended in PBS at a density of $5x0^6$ cells/mL and H_2DCFDA was added at a final concentration of 5µM. After a 30min incubation at 37°C the now loaded cells were washed once with PBS, resuspended in RPMI complete medium supplemented with 50U/mL IL-2 and stimulated as described above for 30min. At the end of the stimulation period, fluorescence of the cells was measured either in the FITC channel of a FACSCalibur or

in FL1 on the Beckman Coulter Gallios flow cytometer. The relative increase in ROS levels after stimulation was calculated according to the following formula as published previously [65]:

$$\text{relative increase MFI [\%]} = (\text{MFI}_{stim}-\text{MFI}_{ctrl})/ \text{MFI}_{ctrl}\text{x00}$$

II.7.9.   Intracellular staining of cytokines

II.7.9.1.   Principle

Cytokine production is usually measured in the cell culture supernatants of stimulated cells by methods like eg. enzyme-linked immuno-sorbent assay (ELISA). This has the clear disadvantage that only a batch analysis of whole cell populations are possible. To detect the production of cytokines on the single cell level, intracellular stainings and their read-out using flow cytometry have been developed. To this end, cells are stimulated in the presence of substances that prevent the exocytosis of freshly generated cytokines. The cytokines accumulate within the cell and can be measured by standard methods of intracellular staining for flow cytometry.

II.7.9.2.   Stimulation, staining and analysis

PBMC were isolated from the peripheral blood of patients with T-PLL by density gradient centrifugation. The isolated cells were cultured at a density of $5\text{x}10^6$ cells/mL in RPMI supplemented with 10% FBS Gold, 5% PenStrep, 5% L-Glutamin and 10U/mL IL-2. Stimulation was performed by adding PMA (phorbolmyristylacetate) and ionomycin to the cultures at a final concentration of 100ng/mL and 1mM, respectively, and incubating the cells for the desired period of time at 37°C. For the last 4h of time in culture Brefeldin A was added according to manufacturer's instructions to block secretion of cytokines. At the end of the culture period cells were fixed and permeabilized as described above (II.7.3.1) and the cytokines stained and analyzed by flow cytometry.

II.8.   Measurement of programmed cell death

II.8.1.   Principle

Programmed cell death or apoptosis is characterized on the cellular level by shrinking of the cell, blebbing of the cell membrane and ultimately the loss of membrane integrity. Most of these phenomena can be observed microscopically. On the molecular level,

apoptotic cells show the degradation of their DNA, which can be visualized after electrophoresis as „DNA-ladder". Another hallmark of apopotosis is the „flip-flop" of phosphatidylserine from the inner leaflet of the cell membrane to the outside [222]. This is a comparatively early event in cells undergoing apoptosis that is widely used experimentally to measure cell death induction. Phosphatidylserine is specificall bound by Annexin V. By adding fluorochrome labelled Annexin V to a cell suspension, apoptotic cells can be stained and visualized for example by flow cytometry [211]. This staining is usually combined with either propidium iodide or 7-AAD. Both are essentially colorless molecules that are unable to cross an intact cell membrane. If membrane integrity is lost, these molecules enter the cell or, more specifically, the nucleus and intercalate with DNA [187]. This causes a change in their fluorescence properties that can be monitored by flow cytometry. Both the 7-AAD and Annexin V stainings taken together allow for the discrimination of 4 populations. Double negative cells are viable, Annexin V single positive cells are at an early apoptotic stage, double positive cells are considered to be apoptotic and 7-AAD single positive cells are considered necrotic.

In general, at least two hallmarks of apoptosis need to be assessed to clearly identify the mode of programmed cell death as apoptosis. As the definition of the mode of cell death induction was beyond the scope of this work, Annexin V – 7AAD negativity was deemed sufficient as a measurement of viability.

II.8.2. Annexin V-PE – 7-AAD co-staining of lymphoid cells

For the measurement of viability cells were pelleted after the desired treatment, washed once with PBS (3min at 300xg) and resuspended in 200μL Annexin V-PE and 7-AAD diluted in Annexin V binding buffer according to manufacturer's instructions. After a 20min incubation period at RT in the dark 300μL Annexin V binding buffer were added per sample. The cells were analyzed for AnnexinV/7AAD positivity by flow cytometry. Viability was defined as the percentage of Annexin V/7AAD double negative cells of all cells measured and the rate of programmed cell death induced by the treatment was calculated as follows:

$$\text{Specific cell death [\%]} = (\text{viability}_{baseline} - \text{viability}_{treated}) / \text{viability}_{baseline} \times 100$$

II.9. Cell cycle analysis

II.9.1. Principle

Before dividing into two daughter cells all of the genetic information available within a cell has to be duplicated. This process makes it possible to distinguish the different phases of the cell cycle based on the DNA content of a single cell. Quiescent cells or cells just entering the cell cycle in the first gap phase (G1) contain 2 sets of each chromosomes, they are diploid or „2C". During the so-called S phase new DNA is synthesized to replicate to chromosomes and the DNA content doubles to 4C or tetraploidy and stays that way during the second gap phase, G2, and throughout mitosis. The DNA content of cells can be visualized using stochiometric dyes that change their fluorescence pattern upon DNA binding. One of the most commonly used dyes in flow cytometry for this purpose is propidium iodide (PI). PI intercalates between bases of double-stranded DNA and RNA molecules. It can easily be exited using a standard 488nm blue laser. The hydrophobic environment the dye encounters upon intercalation induces a shift in its absorption spectrum and also increases its fluorescence quantum efficiency. Accordingly, a dye molecule bound to DNA emits 20-30 times as much fluorescence than a molecule in solution. The fluorescence emitted by a cell stained with PI increases in proportion with the DNA content. Therefore, cells in different cell cycle phases can be visualized as a series of distinct peaks in a histogram display of PI fluorescence [36].

PI carries 2 positive charges and can therefore be considered incapable of permeating the cell membrane. Thus, cell cycle analysis using PI is only possible on previously fixed and permeabilized cells.

II.9.2. Staining of cells and flow cytometric measurement

Per sample $1x10^6$ cells were washed once with cold PBS and thoroughly resuspended in 500µL PBS. Care was taken to disrupt all aggregates as these would interfere with downstream analysis. While vortexing the sample for 30s 4mL of ice cold 70% ethanol were added drop wise. The samples were fixed for at least 2h or over night at -20°C. The fixed cells were pelleted at 350xg for 5min and the ethanol thoroughly decanted. Cells were resuspended in 4mL PBS and incubated for 1min at RT before washing. The cells were then resuspended in 500µL PI staining solution, incubated for 30min at RT and analyzed immediately.

Cell cycle analysis was performed on a FACSCalibur flow cytometer at low flow velocity measuring 100-200 events/s. Doublettes were excluded from the analysis based on their pattern in a plot of signal height versus the area under the curve. For single cells both signal height and the area under the curve of the signal increase proportionately to cell size. For two cells sticking together to form a doublette the signal height will stay the same as for a single cell while the area under the curve doubles.

II.10. *In vitro* modelling of AICD
II.10.1. Assay procedure

In order to mimick restimulation events occuring *in vivo* resulting in a termination of an immune response by AICD, PBMC were isolated from peripheral blood samples of T-PLL patients or Buffy coats from healthy donors on day 1. The isolated cells were cultured in RPMI standard medium supplemented with 10U/mL IL-2. T-cell stimulation was performed over night with 1µg/mL PHA. On day 2 the stimulus was removed by washing the cells with cold PBS. The cells were cultured in RPMI standard medium + IL-2 until day 6 when PHA was added again to restimulate the T-cells [184]. Apoptosis induction was determined on day 7 by flow cytometric analysis of Annexin V and 7AAD staining (II.8). As controls, viability was also determined for unstimulated cells on day 2 and day 7. For cells stimulated once on day 1 and day 6 viability was measured on day 2 and day7 as well. A schematic overview is given in Figure II.10.1-1.
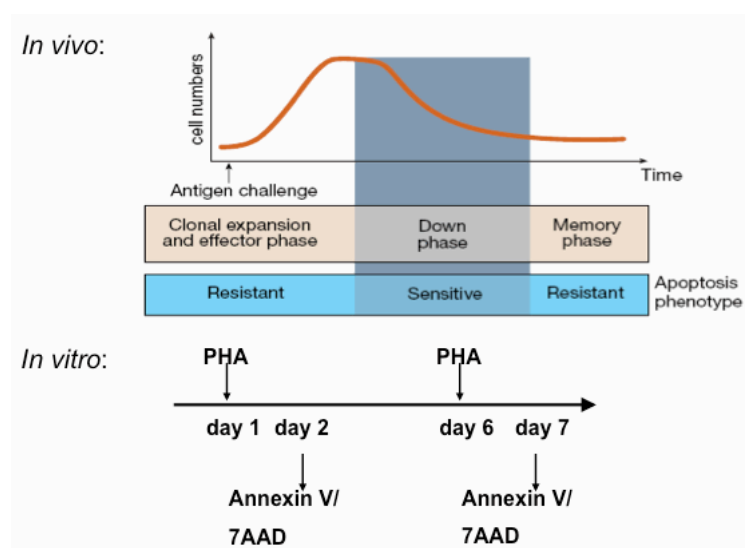
Figure II.10.1-1: Comparison between the *in vivo* occurence of AICD in T-cells and the experimental setup *in vitro*. Adapted from [103].

II.11. Determination of chemokine and cytokine levels in patient plasma samples

II.11.1. Principle of the fluorescence based immunoassay

The assay applied as part of the present work is based on the use of beads coated with antibody specific for a certain chemokine or cytokine (in the following referred to as analyte). In order to assess a number of different analytes within one measurement bead populations differing in size and spectral properties were used (Table II.11-1). After binding of the analyte to the antibody bound to a specific bead population a biotin-conjugated secondary antibody specific for the analyte is added. In the last step beads that have the analyte bound to their surface and accordingly are also recognized by secondary antibody are visualized by streptavidin conjugated PE. In contrast to traditional ELISAs, only minimal sample volumes are required for the analysis of up to 30 analytes in a single run.

Table II.11-1: Chemokines and cytokines analyzed in the plasma of T-PLL patients

Analyte
IL-2
IL-4
IL-10
IL-1RA
IFN-γ
PDGF-BB
RANTES
TNF-α

II.11.2. Assay procedure and panel of analyzed chemokines and cytokines

Assay buffers, bead and streptavidin mixtures as well as the standard mixture were prepared according to manufacturers instructions. The filter plate was pre-wetted with 50μL assay buffer and the liquid removed using a vacuum filtration manifold. 25μL of the standard mixture were added to the designated wells. 50μL assay buffer (1x) were added to the filter plate to pre-wet the wells. 25μL of the quick-thawed and centrifuged samples were added to the remaining wells. To all wells 25μL of bead mixture were added followed by 50μL biotin-conjugate mixture. The plate was covered with adhesive film and incubated protected from light for 2h at room temperature on a microplate

shaker at 500 rpm. The wells were emptied using the vacuum filtration manifold and washed twice with 100µL assay buffer per well per wash. 100µL assay buffer were added followed by 50µL streptavidin-PE solution and incubated again for 1h as before. The wells were washed again as described above and the contents resuspended in 200µL assay buffer and transfered to individual tubes. Cytometer setup and data acqusition were performed according to manufacturer's instructions. Data analysis including generation of standard curves was performed using the FlowCytomixPro Software version 2.4.

II.12. SiRNA-based knockdown of TCL1

II.12.1. Principle

In contrast to the knockout of a gene by deleting it from the germline, knockdown refers to a method of post-transcriptional down-regulation of a protein of interest. The method utilizes the machinery used by the cell for RNA interference, a cellular defense mechanism against viruses with a double stranded RNA genome. The double stranded RNA serves as a template and all mRNAs with a corresponding sequence are degraded leading to an abrogation in protein expression. This phenomenon is utilized experimentally by introducing small interfering RNAs (siRNAs) corresponding to the mRNA encoding the protein of interest. These RNA molecules can be supplied either as single or double strand and usually consist of 21 nucleotides [139].

One step limiting the use of this method is the need to bring exogenous nucleic acids into the cell. Lymphocytes are hard to transfect, especially in the resting state. Nucleofection is a method that combines electroporation and lipid-mediated transfection and has been shown to be very efficient for lymphocytes.

II.12.2. Nucleofection of primary T-PLL lymphocytes

Isolated PBMC from patients with T-PLL were cultured for at least 6h in X-vivo15 supplemented with 10U/mL IL-2. siRNA duplexes were prepared and diluted according to manufacturer's instructions. Nucleofection reagent (Human T-cell nucleofector solution, Lonza) was prepared according to manufacturer's instructions and mixed with either 5µg vector DNA (pMAX-GFP (Lonza)) as control for transfection efficiency or 30µL of the respective siRNA duplex solution. 5×10^6 cells were pelleted by centrifugation at 200xg for 10min, the conditioned medium was collected and the cells

resuspended in the solution/nucleic acid dilution and transferred into a cuvette. Nucleofection was performed using a Nucleofector-2 device (Lonza). The electroporated cells were transferred back into conditioned medium and cultured for 24h. TCL1 expression was assessed by flow cytometry to evaluate the knockdown efficiency after 24h and further functional studies were initiated at that point. For primary T-PLL cells the optimal protocol for TCL1 knockdown with respect to siRNA sequence and nucleofection program was found to be strongly donor dependent.

II.12.3. Nucleic acids used to target TCL1 for knockdown experiments

siTCL1-1	TCL1A Validated Stealth RNAi DuoPak Duplex 1
sense sequence	GGGCCUGGGAGAAGUUCGUGUAUUU
anti-sense sequence	CCCGGACCCUCUUCAAGCACAUAAA

siTCL1-2	TCL1A Validated Stealth RNAi DuoPak Duplex 2
sense sequence	GGCUGCCCUUAACCAUCGAGAUAAA
anti-sense sequence	CCGACGGGAAUUGGUAGCUCUAUUU

siTCL1-3	siGENOME SMARTpool duplex(3)
sense sequence	CCAAGCCUGCUGCCUAUCAUU
anti-sense sequence	5'P-UGAUAGGCAGCAGGCUUGGUU

II.13. Statistical analysis

If not otherwise indicated results are given as mean ± standard deviation based on at least 3 independent experiments or the indicated number of patient samples.

The statistical analysis of data was performed using Prism 6 for Macintosh (GraphPad Software, Inc.). For the determination of statistic significance of normal distributed values a Student's t test was performed. For the direct comparison of treated and untreated populations a paired t test was used. For cases where the distribution of results differed from a normal distribution, the Man-Whitney U test was performed.

If more than two groups were compared a One-way Anova test was performed for normally distributed results. Tukey's multiple comparisons test was used to correct for the repeated testing necessary. Assessment of correlations was done using the Spearman test. For values that did not follow a normal distribution, a Kruskal-Wallis test followed by Dunn's multiple comparisons test was performed.

In general, a probability of „chance" error with $P \leq 0.05$ was considered significant.

The heatmap display of a data matrix was generated using Heatplus (Alexander Ploner (2012). Heatplus: Heatmaps with row and/or column covariates and colored clusters [163]. R package version 2.6.0 http://www.R-project.org [205]). The matrix was organized based on hierarchical clustering using Eukledian distances and complete linkage. The analysis of flow cytometric data was performed similar to other published studies [219].

Agglomerative hierarchical clustering and principal component analysis were performed using XLStat Version 2013.

III. Results

III.1. Immunophenotypic analysis of T-PLL revealed novel disease-defining aspects

III.1.1. Intertumoral heterogeneity of surface marker expression in primary T-PLL samples

Flow cytometry is an important part of the diagositc work-up for hematologic malignancies as peripheral blood samples can be easily obtained and results can be generated within 2 hours [32]. For the diagnosis of T-PLL it is possible to analyze TCL1 by flow cytometry, however, the staining procedure is more laborious and not done routinely. Therefore, defining a surface phenotype specific for T-PLL would greatly facilitate the diagnostic work-up. In this part of the study, the expression of T-cell markers on T-PLL cells in the peripheral blood was assessed by 10-colour flow cytometry to ascertain the „T-PLL phenotype" previously described (CD7+ CD5+ CD3+/- CD4+ CD8- TCL1+) and to evaluate if this phenotype is uniform for most patients and if all T-PLL cells from one donor show the same marker expression.

Patient samples were only considered as part of the following analysis if immunophenotypic data was obtained for all five marker panels by flow cytometric analysis. Also, only samples analyzed between March 2008 and March 2012 were included. This left n=53 T-PLL samples for analysis. For 19 of these samples, staining and flow cytometric analysis was performed on whole blood, the remaining 34 samples were analyzed after isolation of PBMC and cryo-storage. Due to the limited nature of the available material especially for cryo-preserved material, not all markers were analyzed for every T-PLL case. For one T-PLL patient of the TPLL1 trial cohort, the number of cryo-preserved PBMC was not sufficient to perform the whole staining panel for flow cytometry. In this case priority was given to the memory makers over T-cell (subset) markers. This explains deviations in total case numbers in some sub-analyses.

The immunophenotype of the T-PLL samples was first assessed with respect to the pan-leukocyte marker CD45 and the T-cell lineage markers CD3, CD5, and CD7, the TCR co-receptor CD28, as well as markers for cytotoxic and helper T-cell populations CD8 and CD4, respectively.

87

III.1.2. Expression of the pan-leukocyte marker CD45 was reduced in a subset of T-PLL cases

CD45 was initially included in the analysis of T-PLL cells in the peripheral blood in order to facilitate identification of lymphoid cells. For the 19 T-PLL samples stained directly in whole blood a comparison of CD45 expression intensity between (malignant) lymphocytes and other leukocytic populations (monocytes, granulocytes) was possible. CD45 expression showed the typical intensity and homogeneity expected in a lymphoid cell population in only 13 of the 19 (68%) peripheral blood samples analyzed.

The remaining 6 cases displayed a loss of CD45, either generally from all T-lymphoid cells or a partial loss from a subpopulation of the malignant lymphocytes as defined by the expression pattern of T-cell markers assessed in parallel (Figure III.1.2-1).
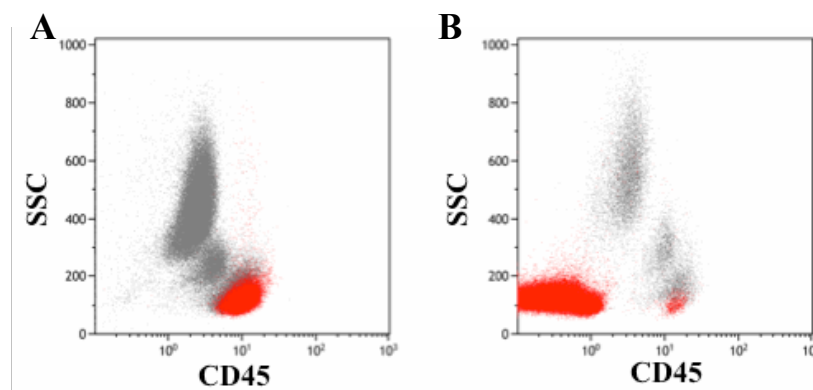
Figure III.1.2-1: CD45 expression was lost in a subset of T-PLL cases. Shown are colour dot plots for CD45 expression vs. SSC gated on viable cells. T-lymphocytes are shown in red. **(A)** Shown is a peripheral blood sample of a healthy donor. **(B)** Shown is a peripheral blood sample of a T-PLL patient. The T-lymphoid population (red) shows a distinct loss in CD45 expression.

III.1.3. T-PLL cells showed variability in pan-T-cell marker expression

T-cells are characterized by the co-expression of certain CD molecules, some of which are occasionally lost in mature T-cell malignancies. Expression of the pan-T-cell markers CD3, CD5, and CD7 was analyzed by flow cytometry in the peripheral blood of patients suffering from T-PLL and results are shown in Table III.1-1. The pan-T marker CD2 was not part of the panel analyzed in the present work. It has been demonstrated already to show low variability in other T-PLL series [72].

Table III.1-1: T-cell lineage marker expression on T-PLL clones of peripheral blood

marker	positive		negative	
CD3	41/51	80%	10/51	20%
CD5	49/51	96%	2/51	4%
CD7	41/44	93%	3/44	7%

T-PLL cases were classified as positive or negative for a marker based on a cutoff of 50% marker expressing lymphocytes.

Surface CD3 (sCD3) expression was found to be absent in one fifth of T-PLL cases. In 20% (10/51) of cases, sCD3 expression was undectable on virtually all T-lymphoid cells, while in 10% (5/51) an additional sCD3 positive T-cell population remained. In contrast, CD5 expression was never lost completely but reduced in 7% (2/51). CD7 expression was mostly high (93%, 41/44). The co-receptor CD28 was expressed in 47 out of 53 T-PLL cases (87%). High frequency of CD28 positive T-PLL cells correlated strongly with an increased occurence of CD127 positive T-PLL cells as well as a higher number of CD25 and CD95 positive cells (Table III.7-1). The frequency of CD7 expression was inversely correlated with CD45RO expression (rho=-0.28, *P*=0.039), which means that T-PLL with loss of CD7 in the majority of their tumor cells showed a tendency to express CD45RO more strongly. T-PLL cases with fewer CD7 positive T-PLL cells also contained CD124 positive cells with increased frequency (rho=-0.38, *P*=0.007). A similar inverse correlation was observed between the frequency of CD7 positive cells and CCR3 expression (rho=-0.33, *P*=0.017).

III.1.4. A number of T-PLL samples displayed aberrant expression of CD4 and CD8 TCR coreceptors as T-cell subset markers

In Table III.1-2, a summary of the observed T-helper and cytotoxic T-cell phenotypes from n=52 T-PLL cases as judged by the expression patterns of CD4 and CD8 is shown. For one T-PLL case expression data on CD4 and CD8 was not available. The largest group of samples displayed a phenotype comparable to that of a CD4 single positive T-helper cell (65%, 34/52). A cytotoxic CD8 single positive phenotype was prevalent in

15% of T-PLL samples (8/52). In the remaining 20% (10/52) a subpopulation coexpressing both CD4 and CD8 dominated.

Table III.1-2: T-helper lineage marker expression in T-PLL clones in the peripheral blood

marker	positive	
CD4+ CD8-	34/52	65%
CD4- CD8+	8/52	15%
CD4+ CD8+	10/52	20%

52 T-PLL cases were classified as positve for a marker if >50% of T-cells (defined by their CD3 and CD5 expression pattern) stained positive.

In summary of III.1.2-4, the patient cohort analyzed in the present study showed expression of CD7 in 93% of T-PLL cases and 20% sCD3 negative T-PLL peripheral blood samples. In addtion, CD45 expression was diminished in 32% of cases. CD5 expression was lost in 4% of T-PLL cases analyzed. Similar heterogeneity was observed for CD4 and CD8 expression with 65% of T-PLL cases showing CD4 single positivity, 20% of all T-PLL cases showing double positivity, and 15% being CD8 single positive. Overall, the observed heterogeneity with respect to basic immunophenotypic features of T-PLL cells in the peripheral blood samples analyzed here fits well with other analyzed T-PLL patient collectives [72, 135]. This is, however, the first study to show the loss of CD45 as a commonality of 32% of T-PLL cases (for more details, see discussion).

III.1.5. All surface CD3 negative T-PLL cases expressed CD4

The most distinct subgroup of T-PLL cases was defined by either the complete absence of sCD3 expression on the malignant T-cell population or the presence of a sCD3 negative subpopulation (20% of all T-PLL cases analyzed).

Cytoplasmic CD3 was not analyzed as part of this work. The remaining healthy T-cells per sample retained physiologic sCD3 expression. Negativity for CD3 on the T-PLL cell surface showed a highly significant correlation with the presence of sCD4 expression (for the correlation between CD3 positivity and CD4 positivity: rho=-0.44, P=0.0012) (Table III.7-1). CD4 was expressed in all sCD3 negative cases (10/51) and all cases with a sCD3 negative subpopulation (5/51). Co-expression of CD8 was

observed in one CD3-negative case and in one case with a sCD3 negative subpopulation (Figure III.1.5-1).
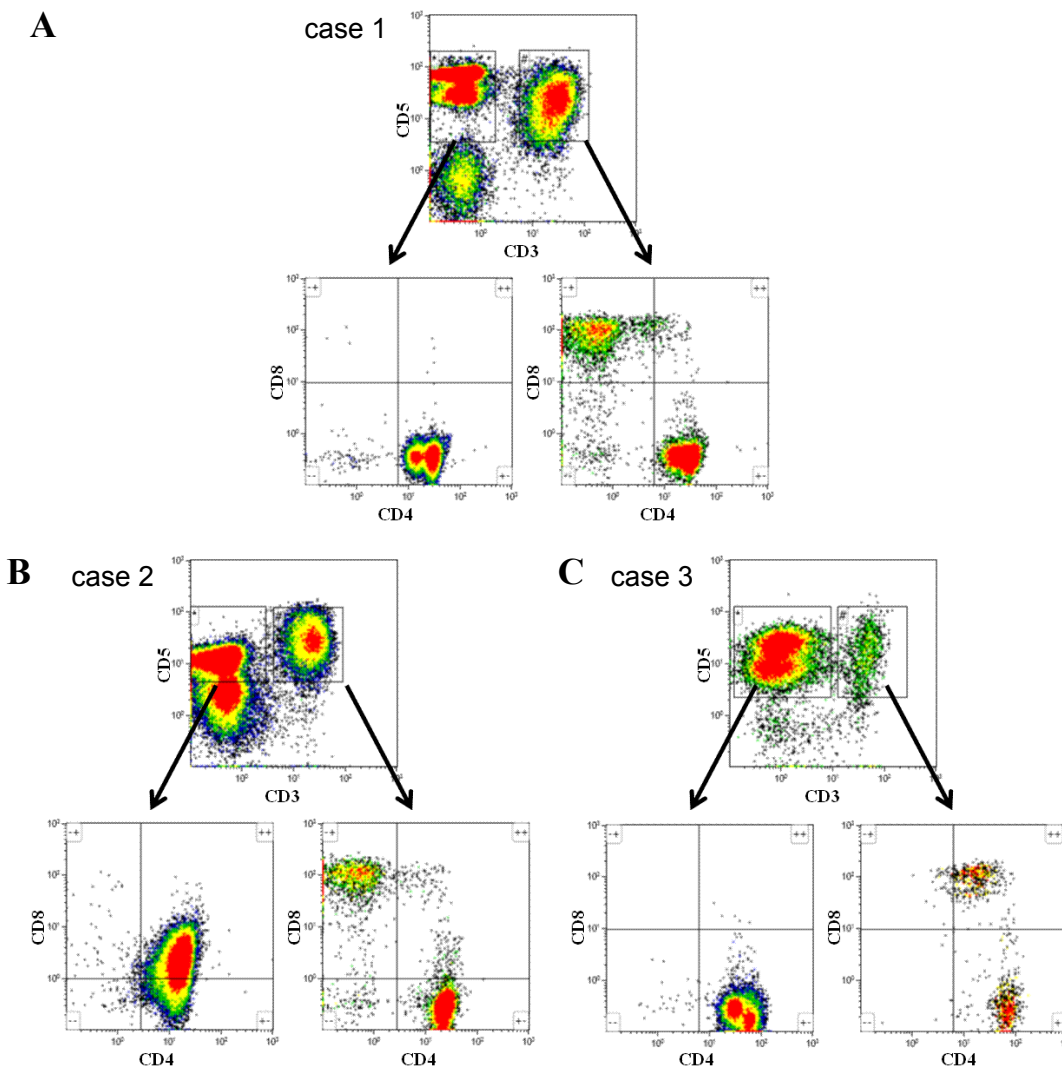
Figure III.1.5-1: **All CD3-negative T-PLL cells expressed CD4.** Shown are density plots for CD3 and CD5 expression gated on lymphocytes and CD4 vs. CD8 gated on CD5+CD3- or CD5+CD3+ populations, respectively. **(A)** Shown is a case with a prominent CD5+CD3- population comprising 60% of lymphocytes, these cells are CD4 single positive. A minor CD5+CD3+ population contains both CD4+ likely T-PLL cells as judged by a reduction in CD4 fluorescence intensity that is also seen in the CD5+CD3- cells and a CD8 single positive population that might contain residual healthy T-cells. **(B)** In this case the CD5+CD3- population (60% of lymphocytes) also shows a decrease in CD5 fluorescence intensity. These cells are CD4 positive and also show a low expression of CD8. The CD5+CD3+ population contains most likely residual healthy T-cells that are single positive for either CD4 or CD8. The intensity of CD4 expression seems slightly diminished in the CD4 single positive population as compared to the CD5+CD3- T-PLL cells. **(C)** Here the most prominent population (approx. 90% of lymphocytes) is CD5+CD3-. These cells are CD4 single positive. The CD5+ population retaining CD3 expression also contains cells double positive for CD4 and CD8 (4% of lymphocytes).

III.2. Characteristics of TCL1 expression in T-PLL and clinical relevance

III.2.1. Flow cytometric analysis of TCL1 expression in peripheral blood samples from patients with T-PLL

Thus far TCL1 had been routinely detected by immunohistochemistry. Flow cytometric determination of TCL1 expression was applied as part of this work because it allows for analysis of higher cell numbers and has higher sensitivity. For the first time, the expression of TCL1 and up to 9 additional markers per cell could be analyzed in parallel and also differences in TCL1 expression could be assessed on a single cell level.

III.2.1.1. TCL1 expression levels varied also between TCL1 positive T-PLL cases

Unequivocal positivity of malignant T-cells for the expression of TCL1 was identified in 67% of T-PLL cases analyzed (Table III.2-1).

TCL1 expression levels were assessed in three independent stainings per sample using two different fluorochrome conjugates (PE and APC) of the α-TCL1 antibody clone 1-21. The resolution of positive and negative populations was higher when using the APC conjugate, however, unspecific background staining was also increased. For the exemplary staining shown below, the relative increase in MFI of the positive population over the negative subpopulation was 4.98-fold for APC as compared to 2.74-fold for PE (Figure III.2.1-1).
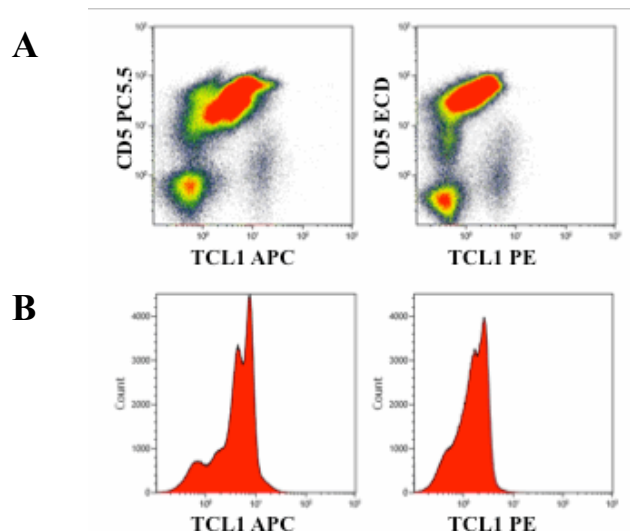
Figure III.2.1-1: Comparison of TCL1 staining in one exemplary T-PLL sample using APC and PE conjugates. All plots shown are gated on lymphocytes. **(A)** Density depiction of CD5 vs. TCL1 expression. **(B)** Histogram plot of TCL1 expression.

Identification of TCL1 positive T-PLL T-lymphocytes was aided in most cases by a remaining (physiologically) TCL1 expressing B-cell population. The latter cells were used to adjust the threshold for TCL1 positivity. Figure III.2.1-2 shows examples of one TCL1 negative T-PLL case and two clearly positive cases. In comparison to B-lymphocytes, expression intensity in T-PLL T-lymphocytes was decreased.
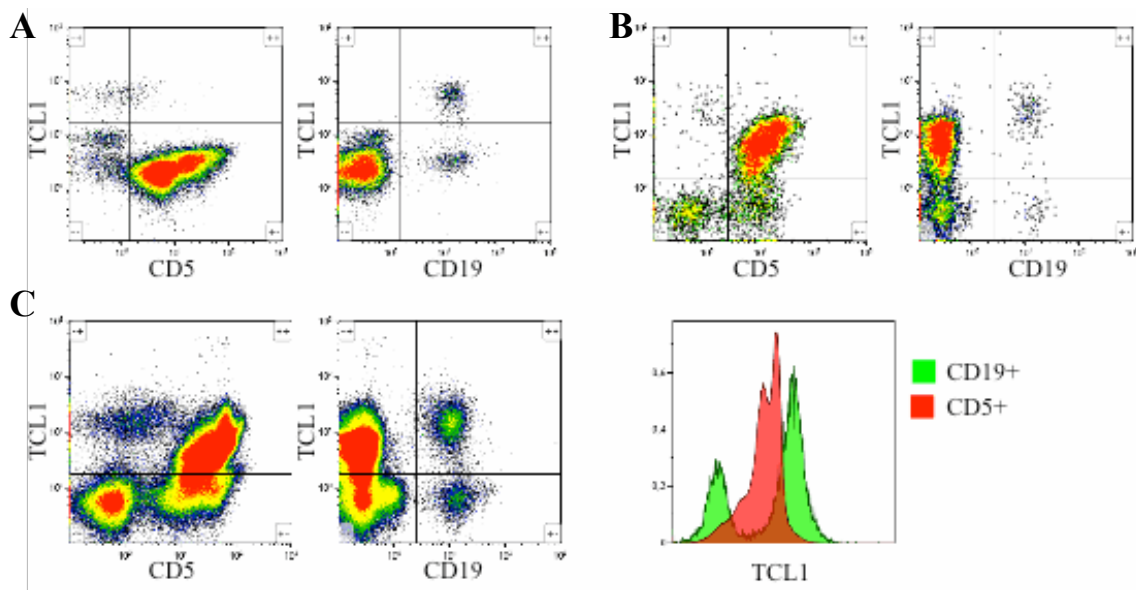
Figure III.2.1-2: **Intertumoral heterogeneity of TCL1 expression intensity in T-PLL. (A-C)** Shown is the TCL1 expression as measured with α-TCL1 APC against the T-cell marker CD5 and the B-cell marker CD19. **(A)** TCL1 expression is absent in T-cells while a distinct TCL1+ B-cell population can be identified. **(B)** A distinct TCL1+ CD5+ population can be determined in addition to a small remaining TCL1+ B-cell population. **(C)** The T-lymphoid cells show a continuous up-regulation of TCL1 in contrast to the TCL1+ B-cells that can be clearly distinguished from the TCL1- B-cells. An overlay depiction of TCL1 staining intensity of B-cells (green, CD19+) and T-PLL cells (red, CD5+) of the case show in **(C)** shows a lower intensity of TCL1 expression in the T-lymphocytes.

In summary, clear TCL1 positivity in T-PLL cases could be determined reliably by flow cytometry. For T-PLL cases that showed only low expression levels or very few TCL1 positive cells, unequivocal assessment is often difficult by flow-cytometry alone. This problem was minimized by the use of fluorochromes such as APC, which is small with a high quantum yield and based on the laser and filter setup used less likely to be influenced by sprectral overlap from other fluorochromes.

Table III.2-1 TCL1 expression analysis by flow cytometry in T-PLL cells

TCL1		
positive	35/52	67%
negative	17/52	33%

TCL1 expression as part of the complete immunophenotyping panel was assessed in 52 T-PLL cases. Only T-PLL cases where TCL1 staining was performed using an APC conjugated TCL1 antibody were taken into account. In 33% of cases (17/52) TCL1 could not be detected in the overall T-cell population or the percentage of TCL1 positive T-cells was below 5% as the set cut-off. These cases were categorized as TCL1 protein negative. In 67% of samples (35/52) TCL1 expression was detected in at least 6% of T-cells, ranging up to 99% of T-cells, with a median of 58% TCL1 positive T-cells (Table III.2-1). A higher number of TCL1 expressing T-PLL cells correlated strongly with an increased frequency of T-PLL cells positive for the activation marker CD25 (rho=0.43, *P*=0.002) (Table III.7-1). Other markers showing a correlation with the expression frequency of TCL1, meaning that they were more frequently expressed in T-PLL samples with higher numbers of TCL1 positive cells, were the IL-7 receptor α chain CD127 (rho=0.32, *P*=0.027), which is highly expressed on naive but quickly down-regulated after stimulation and the chemokine and homing receptor CCR7 (rho=0.31 , *P*=0.016), which is also expressed on naive and central memory T-cells.

III.2.1.2. Variability of TCL1 expression within individual T-PLL blood samples

In order to assess, whether or not TCL1 expression was actually homogeneous within the T-PLL cell population, TCL1 expression was analyzed flow cytometrically in peripheral blood samples as this allows assessment at the single cell level. The flow cytometric analysis of whole blood samples as compared to viably frozen PBMC results in a higher resolution of cell subpopulations. This leads to a higher sensitivity for the detection of small differences in protein expression levels. Therefore, only T-PLL cases that had whole blood samples available for TCL1 staining were taken into account to assess intra-tumoral variability in TCL1 expression. Out of 19 available of such (fresh) T-PLL peripheral blood samples there were 12 TCL1 protein positive samples that

allowed the comparison of TCL1 expression levels in subpopulations within individual cases.
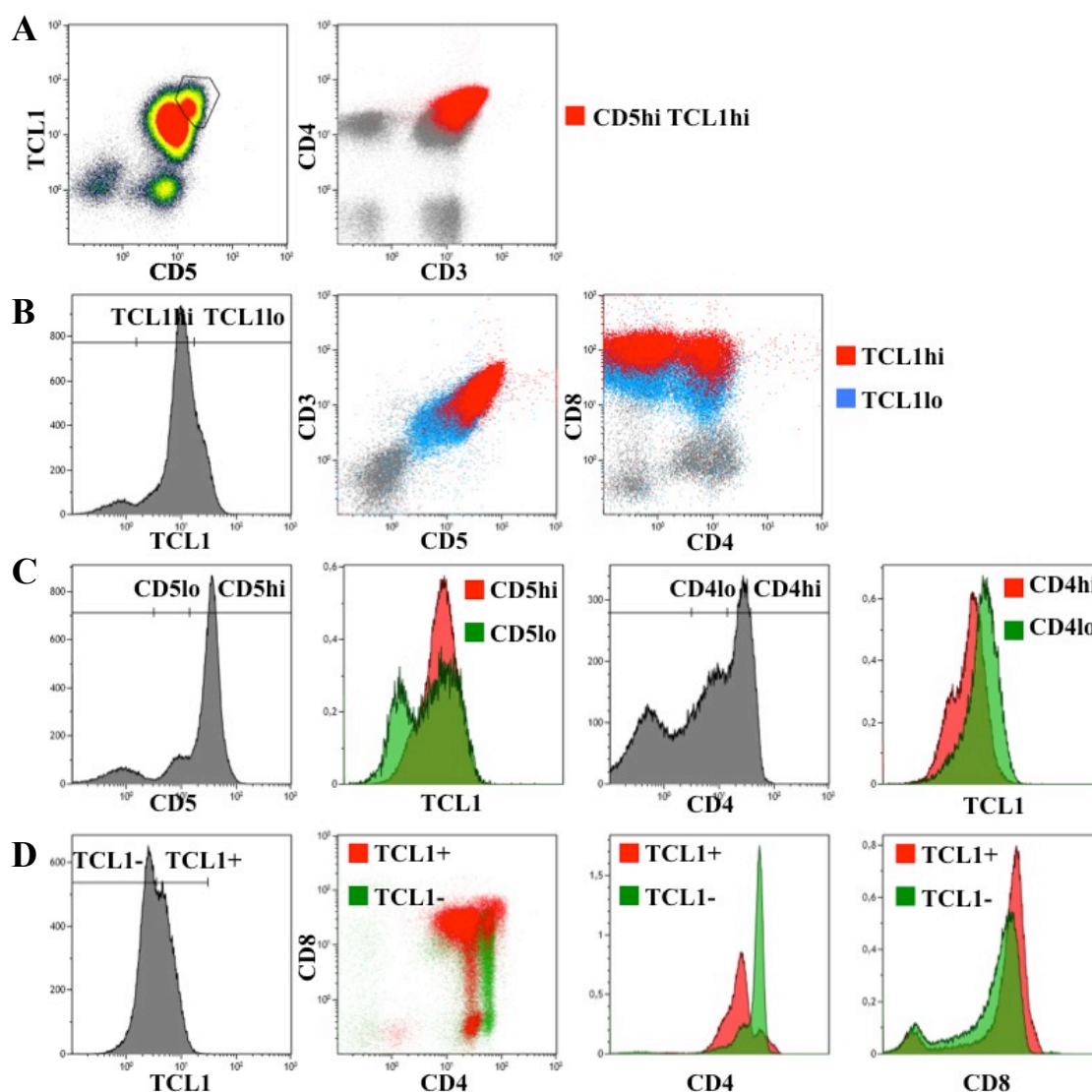
Figure III.2.1-3: TCL1 expression levels showed complex correlations with T-cell associated markers. Shown are immunostainings of TCL1 APC, CD5 PC7, CD3 Pacific Blue, CD4 APC AF750 and CD8 AF488 on 4 peripheral blood samples of patients with T-PLL. Plots were gated on lymphocytes as judged by CD45 vs. SSC unless indicated otherwise. **(A)** A CD5hi TCL1 hi population was defined in a a density plot of CD5 vs. TCL1 expression and visualized in red in a dot plot comparing CD3 and CD4 expression. **(B)** TCL1lo and TCL1hi populations were defined in a histogram displaying TCL1 expression and visualized in blue or red, respectively, in dot plots depicting CD5 vs. CD3 and CD4 vs. CD8 expression. **(C)** In histograms of CD5 and CD4 expression intensity lo and hi populations were defined and TCL1 expression was compared for lo (green) and hi (red) populations in overlay presentations of histograms. **(D)** TCL1lo and TCL1hi populations were defined in a histogram displaying TCL1 expression and visulized in green or red, respectively, in dot plots depicting CD4 vs. CD8 and overlay depiction of histograms of CD4 and CD8 expression.

95

T-PLL cells even within individual T-PLL blood samples showed varibility with regard to TCL1 expression levels, in contrast to naïve B-cells that show a high and homegeneous TCL1 expression. T-PLL subpopulations differing in TCL1 expression were detectable within 6 out of 12 individual TCL1 positive T-PLL blood samples (50%). These populations were not clearly distinct from each other but rather showed an expression continuum ranging from low to high cellular TCL1 protein levels (Figure III.2.1-3).
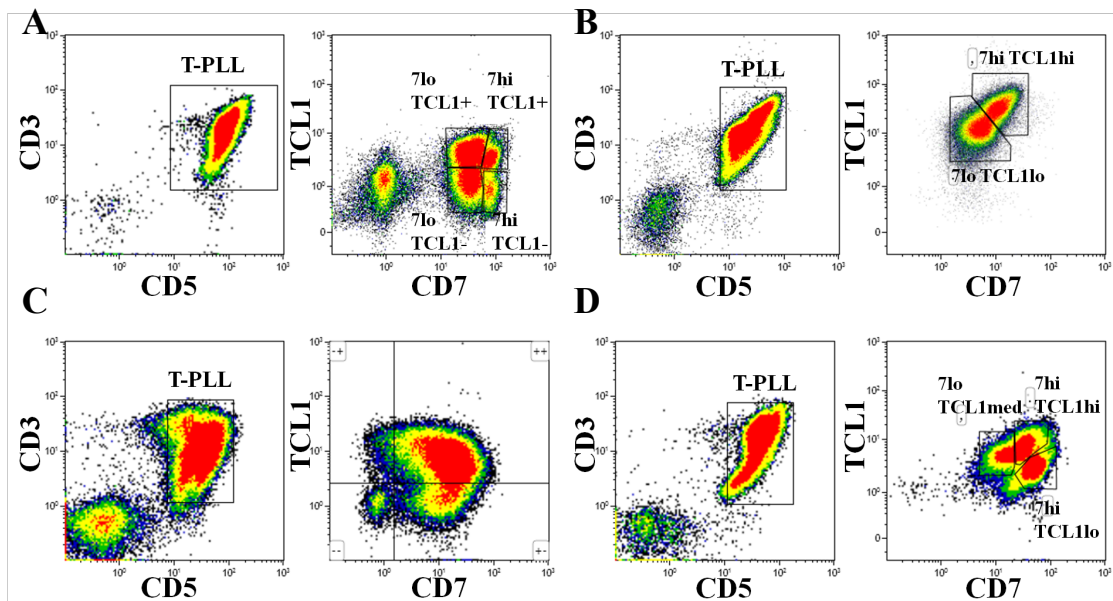
Figure III.2.1-4: Intratumoral heterogeneity of TCL1 expression. Shown are density plots for CD5 vs. CD3 to delineate the T-PLL T-cells and CD7 vs. TCL1 gated on CD3+CD5+ T-PLL T-cells. Panels **A** to **D** represent blood samples from 4 different T-PLL patientes. For a description of the respective expression patterns see III.2.1.2. „T-PLL": marks the T-lymphoid population containing T-PLL cells. „hi": populations with high marker expresssion. „lo": populations with lo marker expression. „med": populations with intermediate marker expression. „7": CD7.

Subpopulations high in TCL1 expression also showed a higher expression of at least one T-cell lineage marker. In 5 out of the 6 T-PLL cases this marker was CD7. Only in few T-PLL cases these subpopulations could be clearly distinguished and gated for quantification. Therefore, only a descriptive qualitative analysis was possible. For example, increased TCL1 expression was detected in a CD3 high, CD4 high, CD5 high subpopulation (Figure III.2.1-3, panel A). In a corresponding case, higher TCL1 expression was observed in the CD3 high, CD5 high, CD8 high subpopulation (panel B). In a CD4/CD8 double positive case, higher TCL1 levels were seen in CD4 low CD5 high cells (panel C). In one case where TCL1 expression was observed in 46% of

CD4/CD8 double positive T-lymphocytes, higher TCL1 levels were measured in parallel to increasing CD8 and decreasing CD4 levels (panel D).

Figure III.2.1-4 shows 4 exemplary cases for the relationship between CD7 and TCL1. Panel A shows 4 unusually distinct subpopulations covering all 4 combinatorial possibilities (CD7 low TCL1 negative, CD7 high TCL1 negative, CD7 low TCL1 positive, CD7 high TCL1 positive). Panel B shows CD7 high TCL1 high vs. CD7 low TCL1 low populations, a pattern observed in 2/7 cases. In C a case showing no subpopulations that can be clearly distinguished based on TCL1 and CD7 expression intensity is depicted. Panel D shows 3 populations that lack a positive correlation of TCL1 and CD7 expression intensity.

In summary of III.2.1, TCL1 expression was detected by flow cytometry in 35 out of 52 (67%) peripheral blood samples from T-PLL patients. In the TCL1 positive T-PLL cases, the aberrant TCL1 expression reached generally lower expression levels than in physiologically TCL1 positive B-cells. The median fluorescence intensitiy of TCL1 in the B-cell compartment was increased 2-3-fold over TCL1 expression in T-PLL cells (P=0.0018). In most TCL1 positive cases intra-tumoral subpopulations differing from each other in the expression intensity of TCL1 and often of at least one T-cell associated marker could be identified. Associations of general TCL1-levels or -status of a given tumor with the expression of differentiation or activation markers is indicated above (III.2.1.1). Most noteworthy, TCL1 expression showed a positive correlation with surface CD25, CD127, and CCR7 expression.

III.2.2. High TCL1 expression was associated with shorter progression free survival in T-PLL

The TPLL1 trial conducted by the German CLL Study Group (GCLLSG) was designed to investigate the efficacy and safety of a novel therapeutic concept consisting of induction treatment with fludarabine, mitoxantrone, and cyclophosphamide (FMC, up to four cycles) followed by alemtuzumab consolidation (12 weeks, 30 mg IV 3 times per week) [78]. From 11/2001 to 2/2007, 25 patients were entered in the study. The overall response rate (ORR) after alemtuzumab consolidation reached 94 % (10 CR; 10 partial remission (PR)). Median OS was 17.1 months and median progression free survival (PFS) 11.9 months. To compare TCL1 levels between T-PLL patients in this study,

TCL1 protein levels were determined by Western blot and categorized according to a densitometric cutoff of >0.5 TCL to β-actin ration for positive cases. TCL1 was found to be expressed in 12/20 (60%) of samples (Figure III.2.2-1).
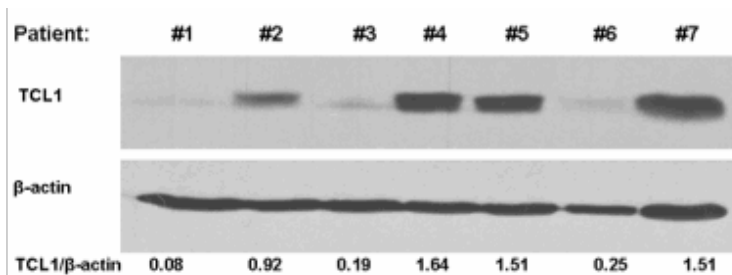
Figure III.2.2-1: **Western blot analysis revealed differences in TCL1 protein expression across peripheral blood samples isolated from T-PLL patients.** Whole cell lysates were prepared from isolated PBMC, separated by SDS-PAGE and protein expression visualized by Western blot.
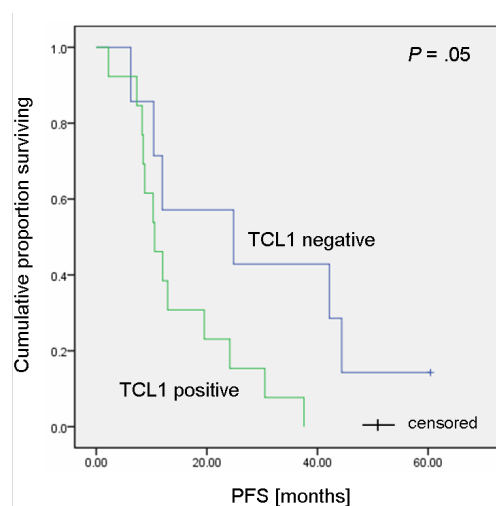
Figure III.2.2-2: **TCL1 expression was associated with shorter progression free survival in T-PLL.** The Kaplan-Meier curve of progression-free survival (PFS) after FMC-A of the entire 25-patient trial cohort shows an inverse correlation with TCL1 protein expression graded on immunoblots following normalization to β-Actin levels (cut-off >0.5 TCL1/β-Actin ratio). Median PFS for the TCL1-positive group was 10.6 months as opposed to 24.8 months for the TCL1-negative subset (Hopfinger et al., Cancer 2013 **[78]**).

TCL1 levels did not show a significant correlation with presenting features or treatment response in the present patient cohort. TCL1 positivity was associated with shorter PFS in response to FMC-alemtuzumab (10.6 vs. 24.8 months median in TCL1-negative cases, P=0.05) (III.2.2-2).

III.3.   Analysis of tumor clonality in T-PLL

III.3.1.   In 64% of T-PLL cases a clonal Vβ expansion was observed

The existence of subpopulations differing in TCL1 expression intensity raised the question whether there might be more than one T-PLL clone present in the peripheral blood of a patient. Therefore clonality was assessed by analyzing the TCR Vβ spectrum. Out of 46 T-PLL samples stained with the TCR Vβ antibody panel, 44 samples were available for final analysis. The remaining cases did not yield enough cells per tube for a reliable quantification of TCR Vβ families. In 15 T-PLL cases clonality was proven by their specific staining with one TCR Vβ antibody (>50% of the T-PLL T-cell population stained positive). Vβ2 and Vβ12 were detected in 3 T-PLL patients, respectively (for an exemplary staining see Figure III.3.1-3). Vβ17 in two T-PLL patients, Vβ familes detected in individual T-PLL cases include Vβ3, Vβ4, Vβ5.1, Vβ5.3, Vβ11, Vβ13.1, Vβ16, Vβ18 and Vβ21.3 (Figure III.3.1-1).
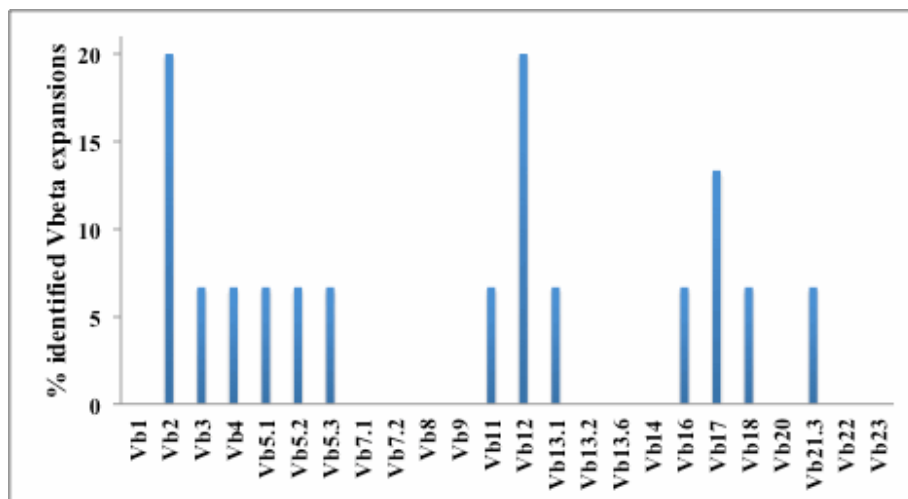
Figure III.3.1-1: Incidence of expansion of TCR Vβ families in n=44 T-PLL samples.

No correlation could be detected between the usage of certain Vβ chains and other markers assessed by flow cytometry. However, all Vβ chains expressed showed a strong correlation with CD3 positivity, thus serving as a proof of principle for the analysis method applied (data not shown). As the transport of the TCR to the cell surface is dependent on the expression of surface CD3, surface CD3 negative T-PLL cases were expected to also be negative for the expression of all TCR Vβ families. In 15 T-PLL cases, more than 70% of the T-PLL T-cells cells failed to react with the TCR Vβ antibody panel. This implicates besides gaps of coverages of the available Vβ antibody reagents (the antibodies used in this work covered about 70% of the normal human TCR

Vβ repertoire of CD3+ lymphocytes) the existence of dynamic clonal evolutions (retractions / expansions / coexistences) in T-PLL and requires additional PCR-based analyses (Figure III.3.1-2).
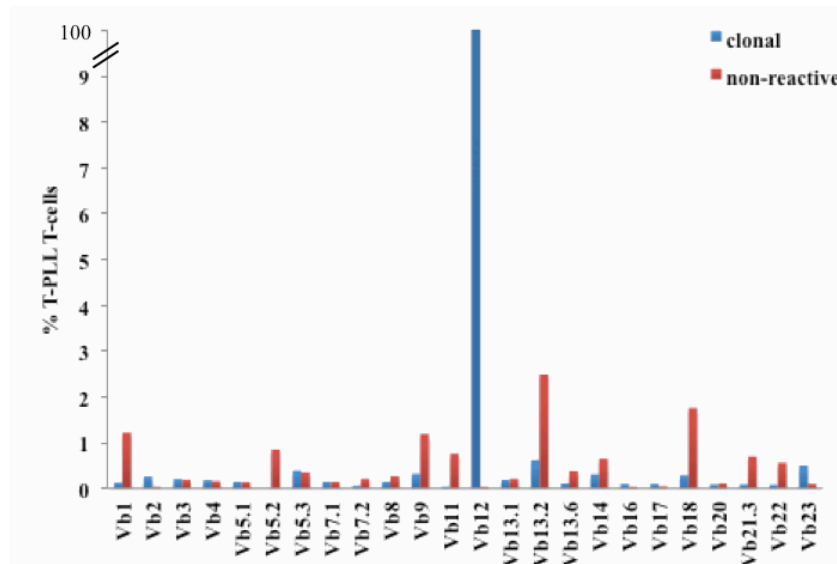
Figure III.3.1-2: Exemplary clonograms proving clonality in one T-PLL case (blue) and showing multiple clones in the cell gate of suspected neoplastic nature (non-reactive T-cells) in another T-PLL (red). The T-PLL cells in the case in red were recognized by several but none predominant of the Vβ antibodies used.
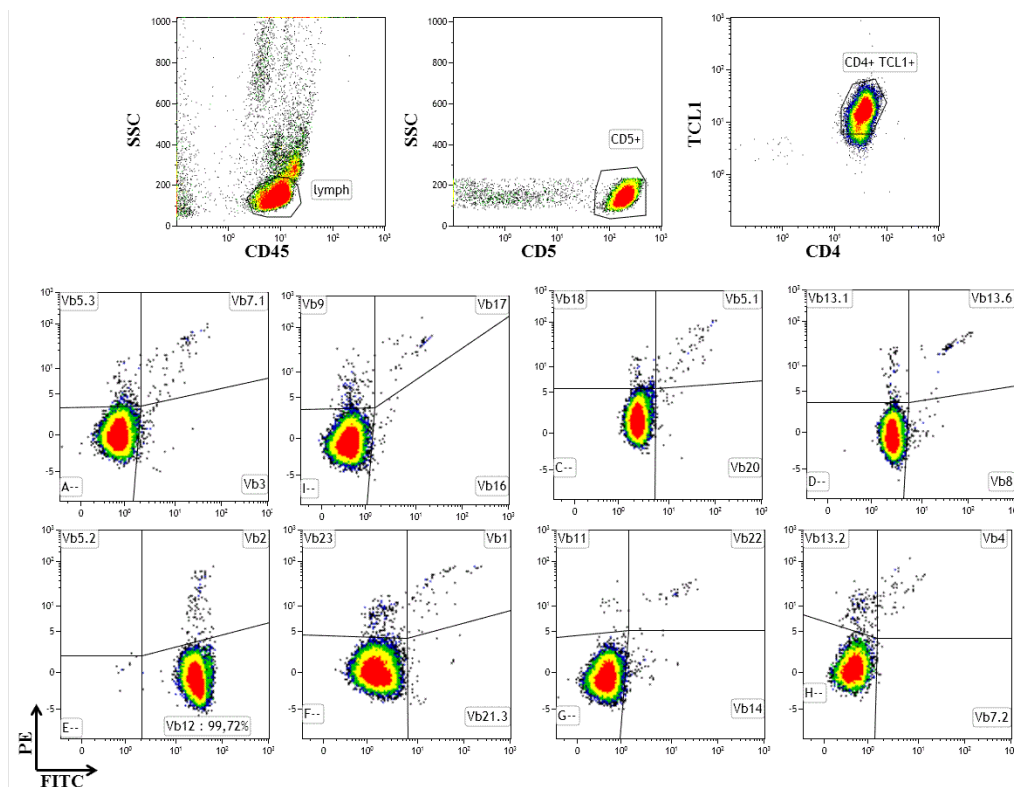
Figure III.3.1-3: CD4+ TCL1+ T-PLL clone expressing Vβ12. Peripheral blood of a T-PLL patient was analyzed for TCR Vβ chain expression and monoclonality was established based on an expression of Vβ12 on 99% of T-PLL cells (CD4+ TCL1+).

III.3.2. Oligoclonal and dual TCR Vβ usage was observed in T-PLL

In 12 T-PLL cases, no clonal population could be stained positive for with the available TCR Vβ antibodies. These cases also contained more than 30% of T-PLL T-cells that stained with the antibody panel (median 61%, range from 31% to 100%). Based on the available data no conclusive statement regarding clonality can be made in these cases. For one patient determination of clonality based on flow cytometry alone was not feasible. In this case, the T-PLL cells stained positive for two TCR Vβ families (Figure III.3.2-1).
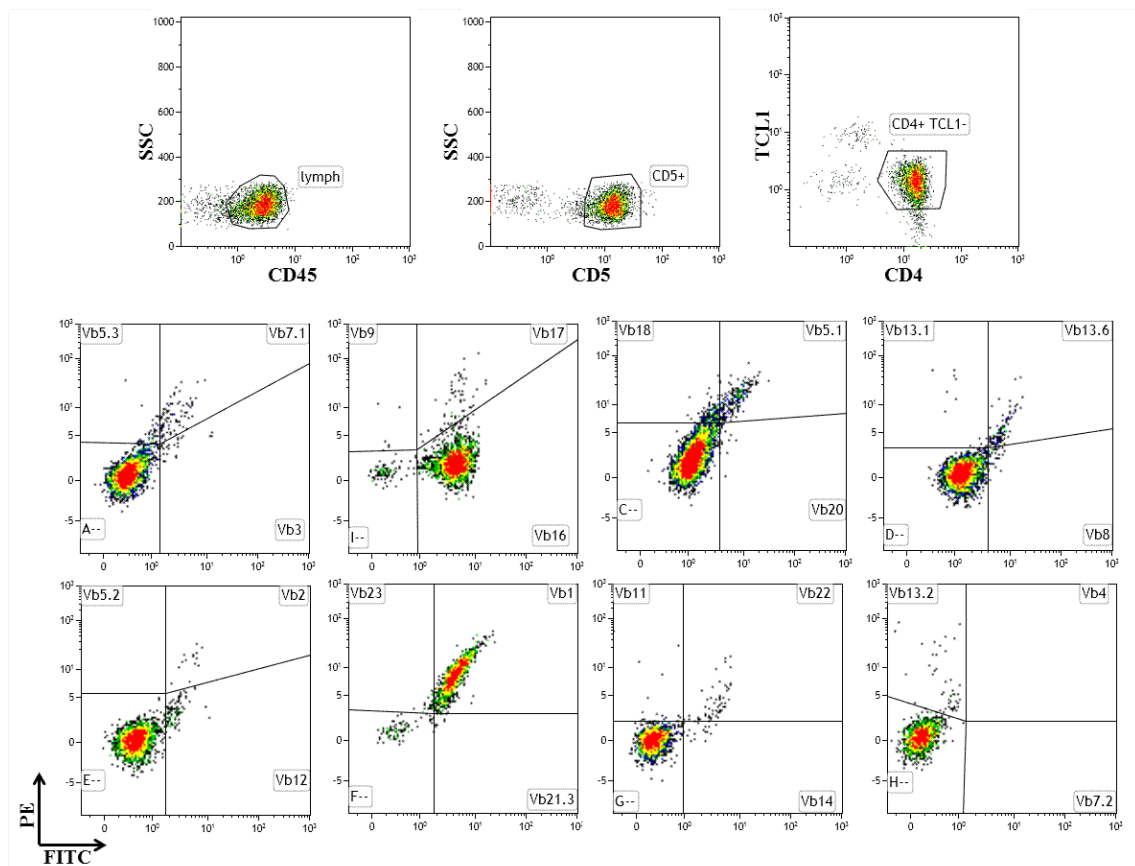
Figure III.3.2-1: T-PLL cells reacting with two TCR Vβ chain antibodies, Vβ1 and Vβ16.
Viably frozen PBMC from a T-PLL patient were thawed stained and analyzed as described previously. Due to low viability after thawing, the gating strategy was based on viable cells as judged by scatter characteristics.

Immunophenotyping and Vβ chain analysis of the T-PLL patient shown in Figure III.3.2-2 and Figure III.3.2-3 revealed the existence of several subpopulations. TCL1 was not expressed in the T-PLL cells, therefore unequivocal identification of the malignant cells was not possible. The dominating T-cell population expressed CD8 while being negative for CD4. These cells showed a decreased intensity when staining

for CD5. This population was considered clonal, as 50% of the CD4 negative T-cells stained positive for Vβ8. The physiological frequency of Vβ8 positive T-cells is 4.7% +/-3%. A more than 10-fold increase in frequency is a criterium for clonality.
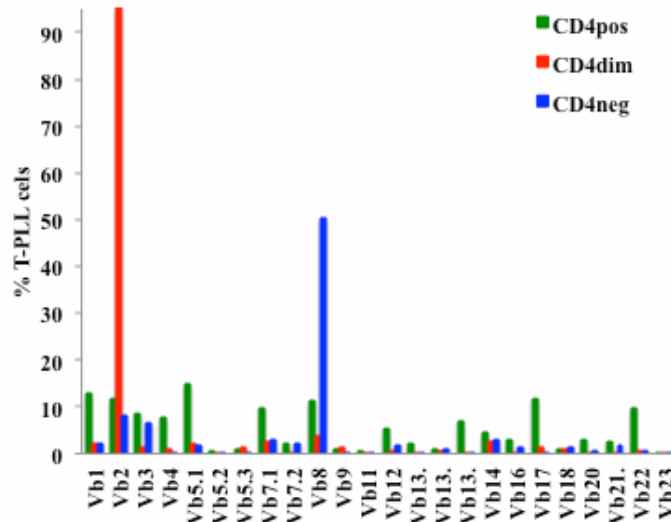
Figure III.3.2-2: Clonogram of T-PLL subpopulations in the peripheral blood of one T-PLL patient. The CD4 dim population showed clonal staining of Vβ2 (red). The CD4 negative T-cell population can be considered clonal based on 50% of cells staining positive for Vβ8 (blue).

A small T-cell subpopultaion also expressed CD8 but dimly co-expressed CD4. These cells were also CD5 dim. This population was clonal and expressed Vβ2. The CD4 brightly expressing subpopulation of T-cells contains a proportion of CD4/CD8 double positive cells. However, CD8 was not stained in parallel to the Vβ chains, therefore clonality analysis was not possible for the CD4bright CD8 positive T-PLL subpopulation. In total, the CD4 bright T-cell population showed no signs of clonality. Based on the loss in CD5 expression intensity and the aberrant co-expression pattern of CD4, both the CD5 dim CD8 positive and the CD5 dim CD4 dim CD8 positive populations were considered to be of T-PLL origin. The fact that these populations show expression of different Vβ families, namely Vβ8 and Vβ2 indicates an oligoclonal character of the T-PLL cells in this case.
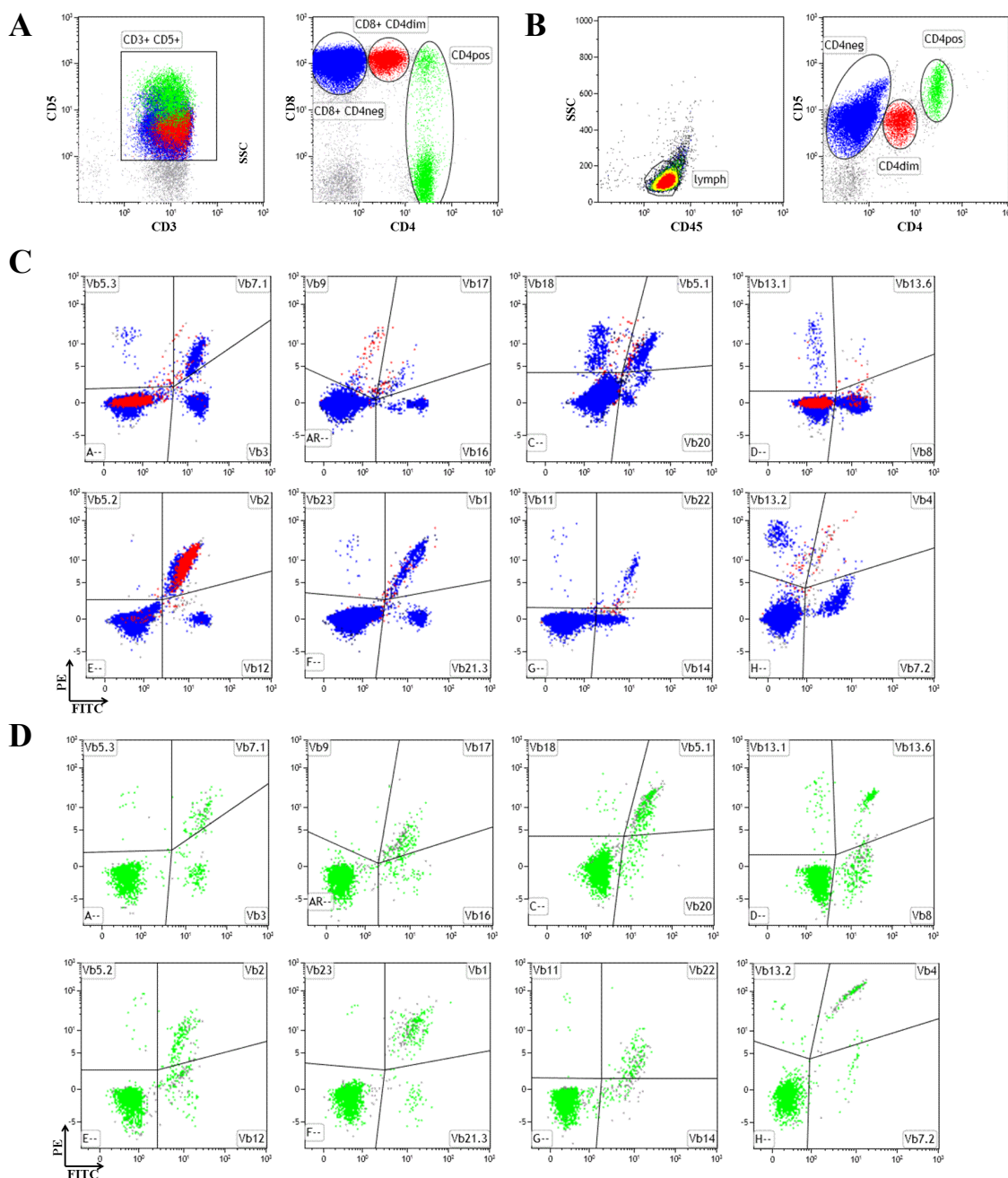
Figure III.3.2-3: T-PLL subpopulations characterized by differences in CD4 expression levels express TCRs belonging to different Vβ families. (A) Immunophenotyping of PBMC of a T-PLL patient reveals 3 subpopulations that differ in CD5 expression levels and CD4 expression (CD4 positive – green, CD4 dim – red, CD4 negative – blue). **(B)** Gating of the three T-PLL populations for TCR Vβ analysis shown in **(C)** and **(D)** after staining and flow cytometric analysis of PBMC of a T-PLL patient. **(C)** Shown is the TCR Vβ chain expression on CD4 negative T-cells (blue) and CD4 dim T-cells (red). The CD4 negative population contains a clonal population expressing Vβ8, while the CD4 dim cells express Vβ2. **(D)** TCR Vβ expression of CD4 positive T-cells (green) shows no indications of clonality.

In summary of chapter III.3, clonality could be proven directly by flow cytometric staining for the relevant TCR Vβ chain antibody in 34% of T-PLL cases. For another 34% of T-PLL patients, the T-PLL cells failed to react with any of the TCR Vβ chain

antibodies available. This constitutes an indirect proof of clonality, since the antibody collection used covers about 70% of the normal human TCR Vβ repertoire of CD3+ lymphocytes. Therefore, if none of the T-cells in a sample were stained, they either all expressed TCR Vβ chains the kit missed to detect or they expressed no Vβ chains at all. Either way, the T-PLL tumor cells differed from healthy T-cells and showed a homogenous phenotype which was in this context indicative of monoclonality. For the remaining 32% of T-PLL cases, no conclusion on clonality could be reached by flow cytometry. Of note, in one patient the T-PLL cells reacted with two TCR Vβ antibodies. Most interestingly, in one T-PLL case an oligoclonal character of the disease could be shown by Vβ8 and Vβ2 expression in different T-PLL subpopulations within the sample.

III.4. Memory phenotype distribution in T-PLL peripheral blood samples

If a specific memory phenotype can be assigned to a malignant T-cell entity, this often provides a biological explanation for the clinical behavior. Therefore, the expression of T-cell memory markers such as the CD45 isoforms RA and RO and the homing receptors CCR7 and CD62L were assessed on cryoconserved PBMC and peripheral blood samples of 53 T-PLL patients.

III.4.1. CD45 isoform expression in peripheral blood derived T-PLL cells showed aberrant patterns

Usually, analysis of T-cell memory is based on CD45 isoform expression. Normal T-cells express either CD45RA or CD45RO, with CD45RA single positivity being a marker for naive T-cells and certain memory subsets and CD45RO single positivity for memory T-cells and CD45RA/RO double positivity for transitional T-cells. For the majority of T-PLL cases analyzed here, CD45RA and CD45RO expression did not fall into the conventional categories (Figure III.4.1-1).

In 15 of the analyzed T-PLL a CD45RA positive CD45RO negative phenotype (definitions, see Figure III.4.1-1 legend) was observed and in 9% of the cases a CD45RO positive CD45RA negative profile could be detected. In 54% of the T-PLL samples analyzed here, the T-PLL population expressed neither CD45RA nor CD45RO. The absence of this CD45RA/RO expression conincided with a loss of general CD45 expression, and accounts for the absence of both CD45RA and CD45RO in 32% of T-

PLL cases. This leaves 22% of the T-PLL cases that are CD45 positive but which do not express the CD45RA and CD45RO isoform. In the remaining 20% of the cases assessed as part of this work, a mix of different subpopulations was detected within the T-PLL population.
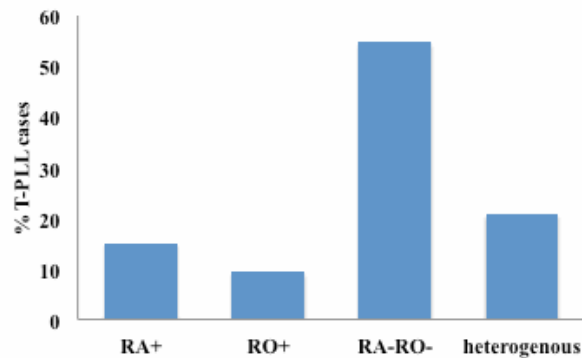
Figure III.4.1-1: The majority of T-PLL cases could not be unequivocally asigned to the „classic" CD45RA and CD45RO single positive naïve and T-cell memory populations. CD45 isoform expression was measured by flow cytometry on 53 T-PLL samples. Samples that contained >70% of T-cells staining positive for either CD45RA or CD45RO, or neither were assigned the following categories: RA+: CD45RA+ CD45RO-, RO+: CD45RA- CD45RO+, RA- RO-: CD45RA- CD45RO-. Double positivity for CD45RA and CD45RO in >70% of T-cells was never observed. Samples containing subpopulations of all categories were scored as „heterogeneous".

III.4.2. Conventional memory T-cell categories did not sufficiently describe the expression patterns observed in T-PLL peripheral blood samples

Due to the high incidence of non-conventional expression patterns of the CD45 isoforms RA and RO as well as of CCR7 and CD62L, the destinction of naïve, T_{EM}, T_{CM}, T_{EMRA} was deemed insufficient to describe the entire T-PLL patient cohort. Therefore, the additional categories of transitional memory T-cells (trans), naïve-CD62L-, T_{EM}-like, T_{CM}-like, and transitional T-cell memory (trans)-like were defined here for the first time based on the surface marker combinations given in Table III.4-1. Using theses more refined categories, the CD45RA/CD45RO double negative T-PLL cases were classified as T_{CM}-like, T_{EM}-like, and transitional memory-like based on their expression of CD62L and CCR7. No differentiation was made for CD45RA/CD45RO double negative cases based on their pan-CD45 expression.

Based on the categories outlined in Table III.4-1, 29 T-PLL cases could be classified according to the expression of a specific marker combination on >70% of T-PLL T-cells (Figure III.4.2-1).

Table III.4-1: Occurence of naive and memory T-cell phenotypes in T-PLL

		CD45RA	CD45RO	CCR7	CD62L	T-PLL cases	
						n=	%
naive		+	-	+	+	0/53	0%
effector		-	+	-	-	0/53	0%
memory	EM	-	+	-	-	2/53	4%
	CM	-	+	+	+	0/53	0%
	EMRA	+	-	-	-	5/53	9%
transitional		-	+	+	-	0/53	0%
naive-CD62L		+	-	+	-	3/53	6%
EM-like		-	-	-	-	11/53	21%
CM-like		-	-	+	+	1/53	2%
Trans-like		-	-	+	-	7/53	13%
mixed		n/a	n/a	n/a	n/a	24/53	45%

CM = central memory T-cells T_{CM}, EM = effector memory T-cells T_{EM}, EMRA = T_{EMRA}.
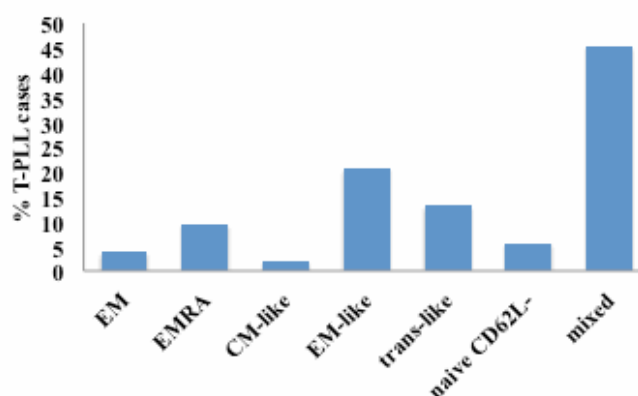
Figure III.4.2-1: Distribution of memory phenotypes across T-PLL samples. Memory phenotypes were assigned to T-PLL cases where >70% of T-PLL T-cells belonged to one memory subset, all remaining cases were scored as „mixed". CM = central memory T-cells T_{CM}, EM = effector memory T-cells T_{EMRA}.

When possible, i.e. based on an aberrant expression of T-cell lineage markers, only cells belonging to the T-PLL clone were taken into account. As outlined above (III.2.1.2), TCL1 expression was not an unequivocal marker for T-PLL cells, as subpopulations were observed within the presumed malignant clone ranging from TCL1-negative over varying degrees of expression intensity. Therefore, TCL1 negativity was not sufficient to rule out a malignant nature of a subpopulation and these cells were also taken into consideration for the assessment of the memory phenotype.
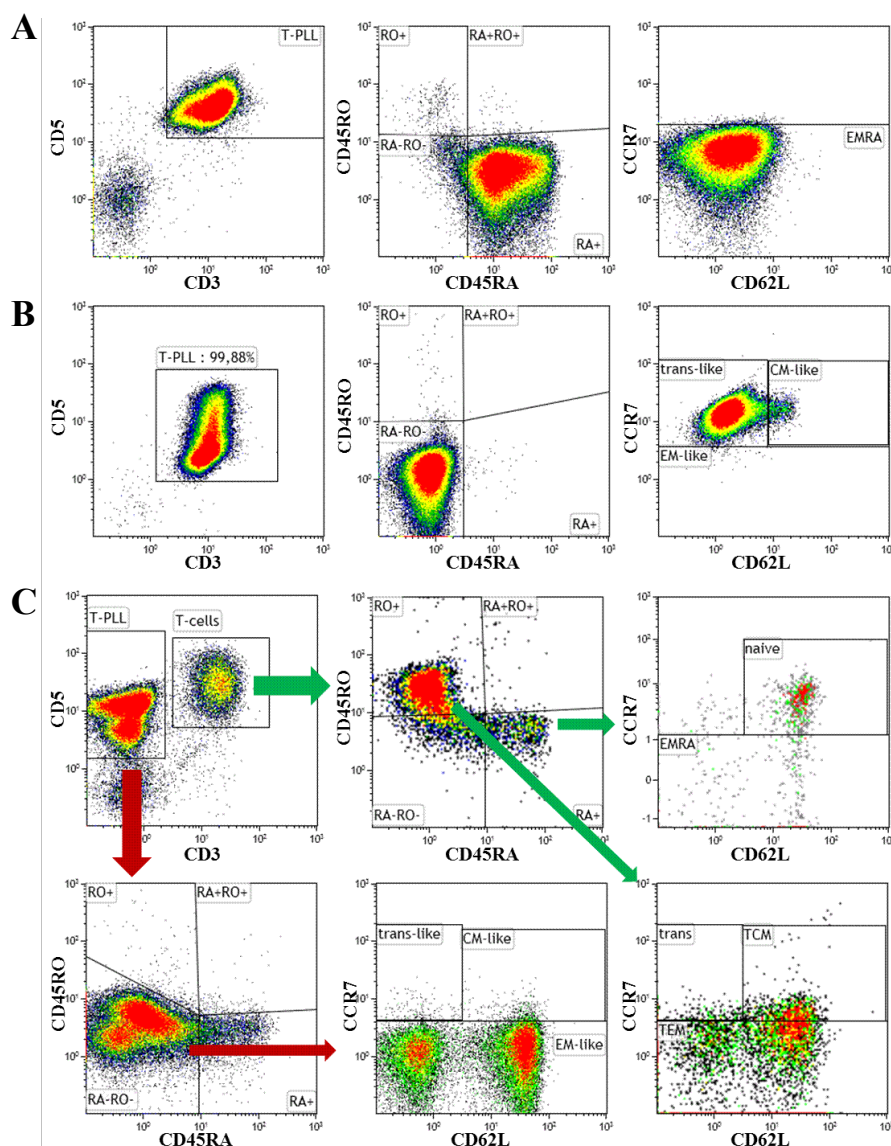
Figure III.4.2-2: T-PLL cases memory phenotypes were comparable to several T-cell memory subsets. Memory marker expression was analyzed by flow cytometry on peripheral blood samples of T-PLL patients. (A) A T-PLL case with the phenotype CD3+ CD5+ CD45RA+ CD45RO- CCR7- CD62L+ resembled T_{EMRA} cells. (B) Shown is a T-PLL case with the immunophenotype CD3+ CD5+ CD45RA- CD45RO- CCR7+ CD62L-. The CD45RA/RO expression does not equal conventional memory T-cells. Based on the positivity for CCR7 and absence of CD62L the case was classified as „transitional-like". (C) The T-PLL population in the case shown in C is CD3 negative. The T-PLL clone (red arrows) is CD45RA- CD45RO- and based on CCR7 expression and absence of CD62L classified as „transitional-like". The residual T-cells (green arrows) show both naive and effector memory (TEM) T-cells with the immunophenotypes of CD45RA+ CD45RO- CCR7+ CD62L+ and CD45RA- CD45RO+ CCR7- CD62L variable, respectively.

In summary of III.4.1, a memory (like) immunophenotype was the most prevalent seen in this T-PLL series. Naive or effector profiles were not observed. There were unconventional phenotypes and a high incidence of T-PLL cases with the coexistence of more than one sizable memory subpopulation (see also next chapter). The most

commonly encountered single memory phenotypes (one predominant clone) included T_{EM}-like (CD45RA- CD45RO- CCR7- CD62L-) in 20% of T-PLL cases, transitional memory T-cell like (CD45RA- CD45RO- CCR7+ CD62L-) in 13% of cases, and T_{EMRA} (CD45RA+ CD43RO- CCR7- CD62L-) in 10% of cases (Figure III.4.2-1). Examples for these phenotypes are shown in Figure III.4.2-2. In some surface CD3-negative T-PLL cases it was possible to distinguish healthy and malignant T-cells based on sCD3 positivity (Figure III.4.2-2 C). Expression patterns of memory markers and TCL1 positivity allowed in approx. 36% of T-PLL cases comparisons between subpopulations differing in their T-cell lineage marker expression pattern.

III.4.2.1. A significant proportion of T-PLL cases contained two or more different memory subpopulations

Within the T-PLL sample collection, 24 T-PLL cases out of 53 cases were composed of a mixed memory population. They could be characterized as memory T-cells, but there was a co-existence of two or three T-cell memory subpopulations. These subpopulations individually accounted for 13% to 67% of T-PLL T-lymphocytes within one sample. Subpopulations were recognized as such either if two subpopulations of comparable size were present (n=11, 21% of T-PLL cases analyzed) or if the main population did not exceed 70% of T-PLL lymphocytes (n=13, 25% of T-PLL cases analyzed). The population size was considered comparable if the difference was <10% of the total T-PLL T-cell population. In the latter case, the second largest population present within the peripheral blood sample was also taken into account and for cases where two or more populations of similar size co-existed with the main population, these memory populations were also considered for analysis.

Out of the 11 T-PLL cases with two memory populations that made up at least 10% of T-cells individually and did not differ in more than 10%, 7 cases displayed a CD45RA-CD45RO- phenotype (Table III.4-2). The most common phenotype observed in this patient subset was CD45RA- CD45RO- CCR7+ CD62L+ (T_{CM}-like) (n=4, 7.5 % of T-PLL cases analyzed), with either the co-existence of an transitional memory T-cell like phenotype (CD45RA- CD45RO- CCR7+ CD62L-) or a T_{EM}-like phenotype (CD45RA-CD45RO- CCR7- CD62L variable).

Table III.4-2: Incidence of co-existing memory population in T-PLL cases with two populations of similar size.

n=	CM-like	EM-like	trans-like	trans	TCM	EMRA	naive 62L-
CM-like	-	2	2	0	0	0	0
EM-like		-	3	0	0	1	0
trans-like			-	0	0	0	1
trans				-	2	0	0
TCM					-	0	0
EMRA						-	0
naive 62L-							-

In 7 T-PLL cases the main memory population comprised 49-65% of all T-PLL T-lymphocytes and co-existed with one smaller population making up between 20 and 35% of T-PLL T-cells. The most common memory phenotype observed in this patient subset was an T_{EM}-like expression pattern (CD45RA- CD45RO- CCR7- CD62var), that was detected as a subpopulation in two cases where the main population showed a T_{EM} phenotype (CD45RA- CD45RO+ CCR7- CD62L var) and two cases where the main population displayed CD45RA- CD45RO- CCR7+ CD62L- (transitional-like memory T-cells) (Table III.4-3).

Table III.4-3: T-PLL cases showing one main memory population and coexistence of another memory population

main	T_{EM}	trans-like	CM-like	EM-like	T_{EMRA}
additional					
T_{EM}					1
trans-like			1		
CM-like					
EM-like	2	2			
T_{EMRA}				1	

The remaining 6 T-PLL cases contained 3 (n=5) or 4 (n=1) subpopulations. In two of these cases, the T-PLL T-cell population was uniformely TCL1 positive. Therefore, at least for these two cases proof was given for the memory subpopulatotions to be a part of the T-PLL clone (Figure III.4.2-3). Interestingly, 5 of the 6 remaining cases contained a T-PLL T-cell population with naive T-cell phonotype (CD45RA+

CD45RO- CCR7+ CD62L+), a phenotype not observed in any of the othe T-PLL patient subsets (Figure III.4.2-4).
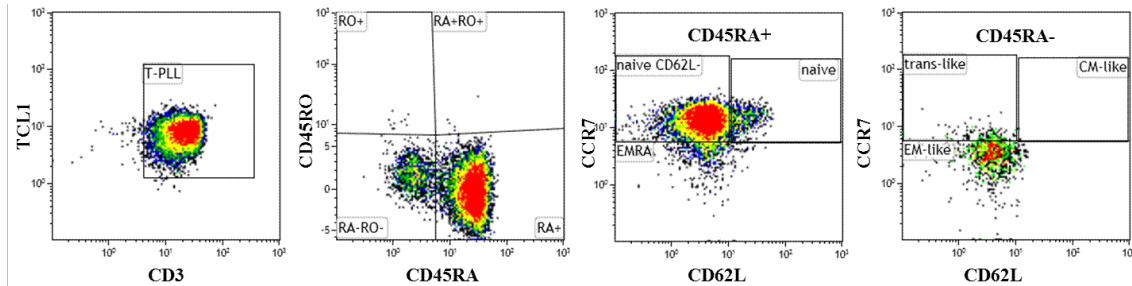
Figure III.4.2-3: A TCL1 positive T-PLL case showed memory T-cell subpopulations within the TCL1 positive T-cell population. A peripheral blood sample of a T-PLL patient was stained for the indicated markers and analyzed by flow cytometry.
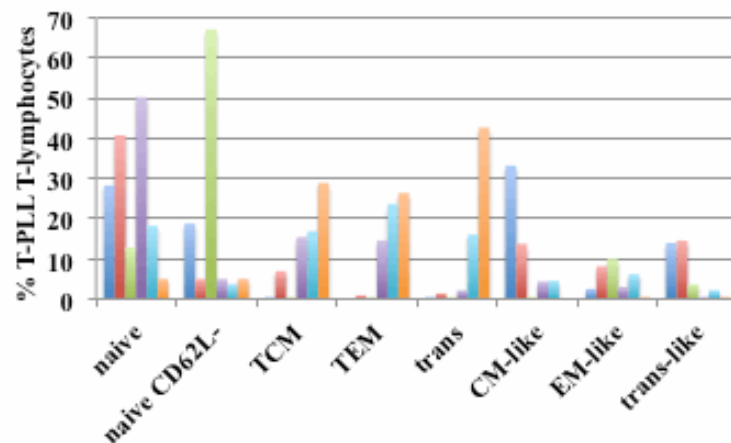
Figure III.4.2-4: Distribution of memory phenotypes in T-PLL samples with various subpopulations. A panel of memory makers was stained on 6 T-PLL pb samples and analyzed by flow cytometry. The frequency of the indicated memory categories was plotted.

III.4.2.2. The frequency of T_{EMRA}-cells in T-PLL sampels was inversely correlated with CD28 and CD95 expression

When comparing the overall frequencies of immunophenotypic marker expression on T-PLL cells within individual T-PLL peripheral blood samples, an increased percentage of T_{CM} cells within a T-PLL sample correlates with increased numbers of CCR5 and CD40L expressing cells (rho=0.29 and P=0.04, and rho=0.31 and P=0.03, respectively). T-PLL samples with lower numbers of transitional memory T-cells generally showed lower CXCR3 (rho=-0.30 and P=0.04) positivity and increased numbers of CD95 (rho=0.30 and P=0.03) and CD40L (rho=0.40 and P=0.004) expressing cells. A high

frequency of T_{EMRA} cells correlated with absence of CD28 (rho=-0.34 and *P*=0.03) and CD95 (rho=-0.33 and *P*=0.02). Of note, T-PLL samples containing higher frequencies of TCL1 positive and CD25 positive cells also contained larger T_{CM}-like populations (rho=0.41 with *P*=0.003, and rho=0.35 with *P*=003, respectively). T-PLL samples with high numbers of T_{CM}-like cells also showed increased frequencies of CXCR4 expression and lower numbers of CD95 positive cells (rho=-0.49 with *P*=-0.049, and rho=0.35 with *P*=003, respectively) (Table III.4-4).

No associations of memory subpopulations in T-PLL with T_H1 or T_H2 characteristics could be shown. T-PLL cases in general did not show the interleukin secretion patterns (III.9.5) or the patterns of chemokine receptor coexpression that are characteristic for T_H1 or T_H2 subsets (III.5.2).

Table III.4-4: Correlations between memory phenotypes and other marker profiles in T-PLL

		CD45RA	CD45RO	CCR7	CD62L	Statistically significant correlations
memory	EM	-	+	-	-	-
	CM	-	+	+	+	CCR5, CD40L
	EMRA	+	-	-	-	absence of CD28, absence of CD95
transitional		-	+	+	-	CXCR3, CD40L, CD95
EM-like		-	-	-	-	-
CM-like		-	-	+	+	TCL1, CD25, CXCR4, absence of CD95
Trans-like		-	-	+	-	-

III.4.2.3. Unsupervised hierarchical clustering groups T-PLL samples into 3 categories based on the percentages of T-PLL cells showing distinct memory marker expression patterns: T_{EMRA}, T_{EM}-like, and transitional/mixed

Due to the high number of T-PLL cases containing several memory subsets, manual assignment of the T-PLL cases to certain memory classes by itself seemed insufficient. In order to classify the T-PLL cases described above in an unbiased manner based on their complex expression patterns of memory markers, a hierarchical clustering was performed on n=53 T-PLL samples. All memory subsets as outlined in Table III.4-1 were included in the analysis as percentage of T-cells per T-PLL case. The T-PLL sampels clustered into 3 classes based on Eukledian distances, which were found to be defined by a T_{EM}-like phenotype (class I), a T_{EMRA} phenotype (class II). The third class

encompassed all T-PLL cases that either showed a predominant transitional memory phenotype or a mixed immunophenotype composed of several memory populations (Figure III.4.2-5). The major difference of this way of analyzing category asignments as opposed to he classifications based on the manual assignment to certain categories according to arbitraty cut-offs (section III.4.2) is that hierarchical clustering does not rely on pre-defined cut-offs and takes into account all cells within a T-PLL samples. This second analysis allowed for an unbiased classification of even heterogeneous T-PLL samples that contained 3 or more subpopulations. The samples were not categorized based on the predominance of single T-cell memory subpopulations but were clustered in an unbiased way based on similarities of the relative content of all T-cell memory subpopulations within individual T-PLL samples.

Cluster analysis was applied in order to sort the T-PLL cases into groups of similar cases, so called clusters. Clusters are groups of patient samples that show a higher similarity and smaller distance to one another than to samples of other clusters. In the process of agglomerative clustering each sample forms a single cluster at the begining of the analysis. In the present work, each T-PLL case was defined as a single cluster at the start of the analysis. The most similar clusters were then merged in iterative steps until all objects or samples belong to a larger cluster. Samples, once merged to a cluster, were not divided again but further samples may be added („agglomerative" clustering). The distance function that is used to calculate the distance between two clusters depends on the method applied. In the present work Ward's method was used as it tends to result in clusters of comparable size. The metric chosen as measure of distance between sample pairs in this case was the Eucledian distance, which is commonly used for the analysis of data that was measured on an interval scale (metric data). After grouping of the samples according to their similarity, cluster centers that can be viewed as the defining characteristic of the clusters, were calculated mathematically.

For all T-PLL cases, the content of every T-cell memory subpopulation (T_{CM}, T_{EM}, transitional memory, T_{EMRA}, T_{CM}-like, T_{EM}-like, and transitional-like) was included as percentage of all T-PLL cells in that case. T-PLL samples containing two or more subpopulations were treated the same way. The Eucledian distance between all T-PLL

cases based on their relative content of T-cell memory subpopulations was then calculated and the most similar T-PLL cases were merged together into clusters.
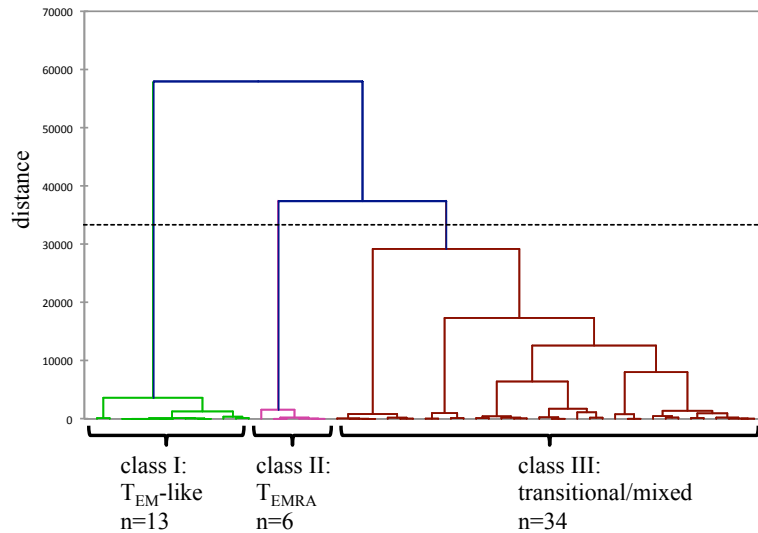
Figure III.4.2-5: T-PLL cases clustered into 3 groups based on memory phenotype. Agglomerative hierarchical clustering was performed based on Eucledian distances using Ward's method. At each step, pairs of clusters are combined in a way to minimize the increase in within-cluster variance after merging.

In in the first part of this chapter, the T_{EMRA} and T_{EM}-like were identified to be among the most commonly observed memory phenotypes in the T-PLL cases analyzed (Figure III.4.2-1). This finding was repeated by this more unbiased clustering method that brought up T_{EMRA} and T_{EM}-like phenotypes as the cluster centers of the two T-PLL subsets clustering apart from the majority of cases constituting the „mixed" class. This third class contained all transitional memory T-PLL cases, all remaining memory phenotypes and all T-PLL cases containing more than one memory phenotype. T-PLL cases, that contained several memory subpopulations were more similar to transitional memory T-PLL cases than to T_{EM} or T_{EMRA} cases and therefore clustered together with the transitional memory T-PLL cases in class III.

Traditional analysis of flow cytometric data is guided by assumptions on the data and is therefore rather biased. Principal component analysis (PCA) can reduce the complexity of data by identifying combinations of variables that adequately explain the overall observed variation within a flow cytometric data set in an unbiased manner. In addition, a depiction of flow cytometric data based on a PCA offers an unbiased view that is not

limited by a subjective choice of markers plotted against each other in a put-and-look strategy. PCA can be used to determine the length and direction of vectors in a two-dimensional field in order to identify the optimal view point for a data set.

Using the T-PLL cases that were the „central objects" of the clusters, the most representative case for each class, as examples, a principal component analysis was performed. Included were all T-PLL cells per sample that matched the following criteria: SSC/FSC low, CD5+ CD3+ (all three exemplary cases expressed surface CD3). For the T-PLL cells identified based on these markers the expression of CD45RA, CD45RO, CCR7 and CD62L was included in the PCA, as these surface markers were used to define the memory phenotypes. The principal components, a set of values of linearly uncorrelated variables, were calculated based on the possibly correlated observations of CD45RA, CD45RO, CCR7 and CD62L positive cells for each of the three T-PLL cases. The principal components can be described using „Eigenvectors". The contribution of every memory marker to the first two principal components was determined. Based on this information the angle and length of the axed for a depiction of all memory markers in an n-parametric radar plot in a two-dimensional space was determined.

Using this angle and length for CD45RA, CD45RO, CCR7 and CD62L it was possible view the data sets from the most informative viewpoint (Figure III.4.2-6).

The memory subsets found to be predominant by manual analysis were also identified in an unbiased statistical approach to be the main subpopulations within the three exemplary cases analyzed by PCA.
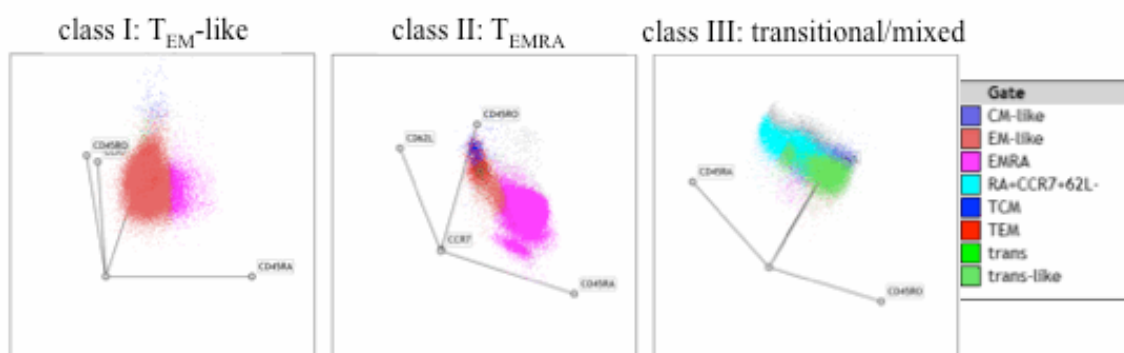
Figure III.4.2-6: Exemplary depiction of the principal components of the three T-PLL memory classes. Principal component analysis was performed on multi color flow cytometric data compensated for fluorescence overspill of CD5+ CD3+ lymphocytes for the predefined memory markers CD45RA, CD45RO, CCR7 and CD62L. The expression data was plotted according to the determined length and angle based on the contribution of the analyzed memory markers to the „Eigenvectors" best describing the T-PLL cases.

III.4.2.4. The class I T$_{EM}$ subset of T-PLL cases showed increased CD28 expression and a lower frequency of CXCR4 positive cells

No statistically significant bias of CD4 or CD8 expressing T-PLL cases towards certain memory phenotypes could be detected (data not shown).

Table III.4-5: Frequency of CD4/CD8 immunophenotype in the different memory classes in T-PLL

	class I: T$_{EM}$-like 13/53		class II: T$_{EMRA}$ 6/53		class III: transitional/mixed 34/53	
CD4+ CD8-	9/13	70%	2/6	33%	23/34	68%
CD4- CD8+	2/13	15%	4/6	67%	5/34	15%
CD4+ CD8+	2/13	15%	0/6	0%	6/34	17%

However, when the CD4/CD8 expression patterns on T-PLL peripheral blood samples were compared to the memory classes defined by hierarchical clustering, CD8 single positive T-PLL cases seemed to show a trend towards the T$_{EMRA}$ dominated class II. This observation did not reach statistical significance (Table III.4-5, Figure III.4.2-7).
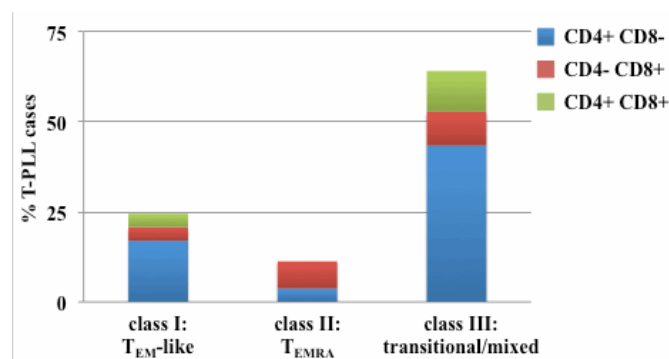
Figure III.4.2-7: CD8 single positive T-PLL cases showed a trend towards higher frequencies in the T$_{EMRA}$ memory class II.

Further comparison of marker expressions in the memory classes defined by cluster analysis of the expression patterns of CD45RA, CD45RO, CCR7 and CD62L (III.4.2.3) revealed a trend towards lower CD95 expression in class II T$_{EMRA}$ T-PLL cases.

In the same class BCL2 seemed to be expressed at lower frquencies than in the TEM-like and T$_{EMRA}$ T-PLL memory classes. CD95L showed an increase in class III transitional/mixed (data not shown). CD28 was found statistically significant less often in T-PLL cases clustering with the T$_{EMRA}$ memory class. The chemokine receptor

CXCR4 on the other hand appeared more frequently in T-PLL cases associated with the transitional/mixed memory class (Figure III.4.2-8).
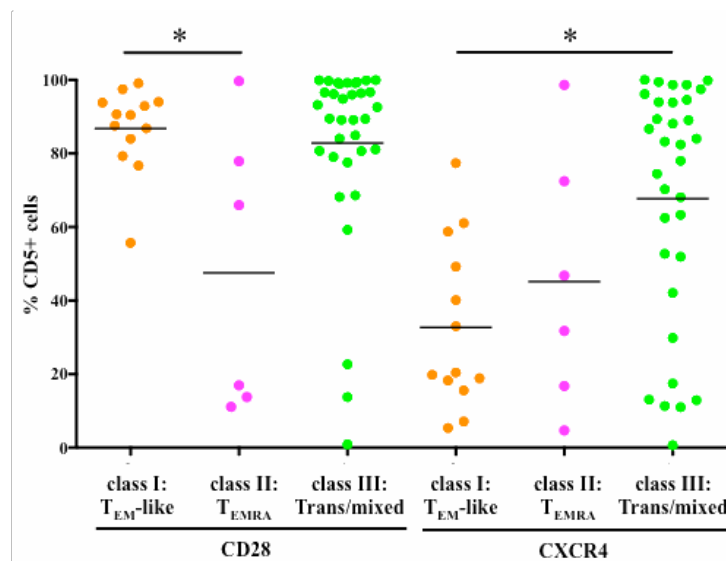
Figure III.4.2-8: T$_{EMRA}$ T-PLL cases showed less frequent CD28 expression while CXCR4 was observed more frequently in transitional/mixed cases. Marker expression was determined by flow cytometry. T-PLL cases were clustered into memory categories by hierarchical agglomerative clustering. Expression frequencies were compared between the three memory classes using a one-way Anova test with a Tukey test for repeated comparisons for CD28 (*P*=0.0039) and a Kruskall-Wallis test with Dunn's post test for CXCR4 (*P*=0.0068), as chemokine receptors did not follow a normal distribution in T-PLL.

In summary of III.4, the high proportion of various memory phenotype cells in virtually all T-PLL peripheral blood samples and the lack of T-PLL cases with a predominant naïve phenotype argue against the long held belief of T-PLL being a disease of early thymic emigrant T-cells. The early thymic emmigrant populations consists of antigen-inexperienced cells that have only been circulating in the body for a short amount of time. The memory phenotype of T-PLL cells, in contrast, is indicative of either prior antigenic stimulation or homeostatic proliferation associated with a prolonged circulation time since thymic exit. The memory phenotype most commonly observed in this T-PLL patient cohort was CD45RA- CD45RO- CD62L- CCR7-/+ (T$_{EM}$ like).However, when looking at the coexistence of several memory phenotypes, which was observed in 45% of T-PLL cases, occurence of T$_{CM}$ and transitional memory T-cells at the same time in the same T-PLL patient sample was the most frequently observed combination (*P*=8.3x10^{-23}) and accounted for 9% of such memory composite T-PLL and for 4% of all T-PLL cases in this study. In an unbiased hierarchical

clustering of immunoprofiles, T_{EM} and T_{EMRA} signatures were identified to most clearly separate 2 groups of tumor cell immunophenotypes .

III.5. Chemokine and cytokine receptor expression in T-PLL

The expression patterns of chemokine and cytokine receptors reveal details about the functional characteristics of a T-cell, what factors might influence the cell, what homing capacity it might have. Therefore these receptors were analyzed on T-PLL cells in the peripheral blood to gather information an possible effector functions of these cells.

III.5.1. Cytokine and chemokine receptor expression showed a much broader range in T-PLL cells from the peripheral blood than in T-cells from healthy donors

When comparing cytokine receptor expression in the T-cell compartment in the peripheral blood between patients with T-PLL and healthy donors, the frequency of positive staining T-cells in healthy controls was not donor dependent. In T-PLL patients, however, the variability was dramatically increased (Figure III.5.1-1).
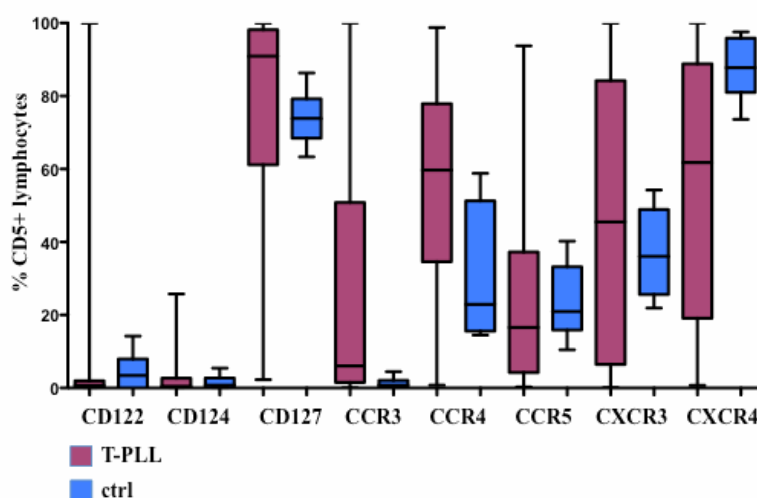
Figure III.5.1-1: Cytokine and chemokine receptor expression shows a higher variability in T-PLL T-cells than in the T-cell compartment of healthy donors. Shown are median, lower and upper quartile, minimum and maximum for CD122, CD124, CD127, CCR3, CCR4, CCR5, CXCR3 and CXCR4 for T-PLL cases (red, n=52, CCR4 n=50) and healthy donors (blue, n=50).

This was especially true for CD127. The mean percentages of CD127 expressing T-cells is comparable with 62.78% in T-PLL and 73.55% for healthy controls. The standard deviatation, however, was 38.85 in T-PLL with a range from 3.73 to 99.61% and a

standard deviation of 4.983 in healthy controls with a range from 68.28 to 78.45%. With respect to chemokine receptor expression, again healthy controls show a very tight spectrum of expression. Within the T-PLL samples, expression for each receptor varied between 0% and over 75% of T-cells staining positive (Figure III.5.1-1).

III.5.2. Expression patterns of cytokine receptors on T-PLL cells in the peripheral blood mimic those of antigen-inexperienced T-cells

Data on the chemokine receptor CCR7 was presented in the previous chapter. Here the expression pattern of other chemokine and cytokine receptors on peripheral blood T-cells in T-PLL patients will be presented. With respect to cytokine receptors, the IL-2 receptor α chain CD122, the IL-4 receptor β chain CD124 and IL-7 receptor β chain CD127 were assessed (Figure III.5.2-1).

For most T-PLL cases (42/50, 84% of all T-PLL cases analyzed) cytokine receptor expression did not differ significantly from the pattern observed on T-cells from healthy donors. Cytokine receptor chain expression in general was either present or absent on T-PLL peripheral blood samples (>50% of T-PLL cells either staining positive for the analyzed marker or lacking its expression). Subpopulations differing from the majority of cells with regard to their receptor expression pattern were rarely observed.
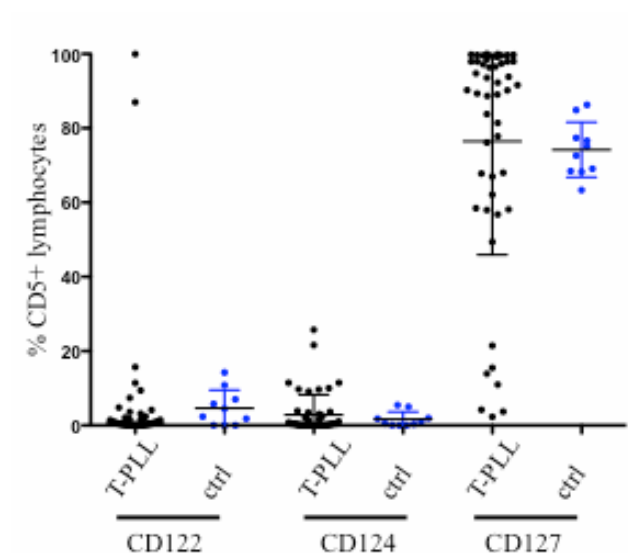
Figure III.5.2-1: **Cytokine receptor expression in T-PLL peripheral blood and bone marrow compared to peripheral blood from healthy donors.** Positivity for cytokine receptor expression was determined independently for every molecule on CD5+ lymphocytes for n= 52 T-PLL samples, and n=10 pB samples from healthy donors (ctrl).
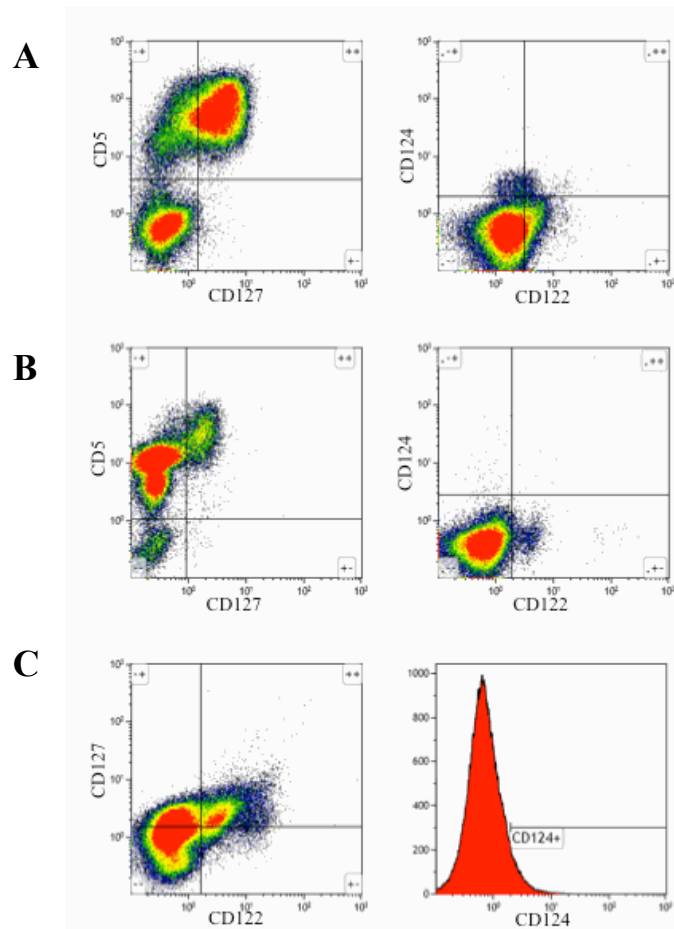
Figure III.5.2-2: **Cytokine receptor expression in peripheral blood T-lymphocytes of T-PLL patients.** Shown are plots from 3 exemplary T-PLL cases. All density plots containing CD5 on the y-axis are gated on lymphocytes, plot not depicting CD5 are gated on CD5+ lymphocytes. **(A)** Over 60% of CD5+ lymphocytes show positivity for CD127. A small CD124+ population can be distinguished (1,4% CD5+ cells). CD122 is expressed dimly on approx. 10% of cells. **(B)** Only lymphocytes with high CD5 expression stain positive for CD127 (10% of lymphocytes). CD122 is found on 2,7% of CD5+ cells while CD124 is virtually not detectable. **(C)** In this case the majority of CD5+ cells shows (dim) CD127 positivity with 12% of cells co-expressing CD122. CD124 was detected on 7% of CD5+ cells.

Positivity for CD122 or CD124 as judged by expression of the cytokine receptor on >10% of CD5 positive lymphocytes was detected in 2 T-PLL samples each. The CD122 positive T-PLL cases did not show any other common characteristics. The frequency of CD122 positive cells also correlated with CD45RO (rho=0.6, P=3.0x10^{-6}) and CCR7 (rho=0.3 , P=0.034). Of note, both CD124 positive T-PLL cases showed a decreased frequency of CD127 expression with only around 60% of CD5 positive lymphocytes staining positive for CD127. In striking contrast, CD127 was present on >49% of T-lymphocytes in 43 out of 50 cases (86%) (Figure III.5.2-2). In addition, higher frequencies of CD124 correlated with less frequent CD7 expression (rho=-0.38 ,

P=0.007), increased CD45RO positive cells (rho=0.4 , P=0.004) and more frequent CCR7 expression (rho=0.57 , P=1,8x10^{-5}).

Seven T-PLL cases contained only between 2-21% of CD127 expressing cells. An increased content of CD127 positive cells correlated with higher numbers of cells expressing TCL1 and CD28 (Table III.7-1). The most striking attribute of the CD127 negative T-PLL patient subset was that 42% of these cases (3/7) displayed a T_{EMRA} memory phenotype (CD45RA+ CD45RO- CCR7- CD62L-). CD127 negative T-PLL also contained at higher frequencies cells expressing CCR5 and CD95L (Table III.7-1).

III.5.3. Chemokine receptor expression was variable in T-PLL blood samples

The expression pattern of chemokine receptors showed a higher degree of heterogeneity (Figure III.5.3-1, Figure III.5.3-2) than the cytokine receptor expression patterns in T-PLL samples.
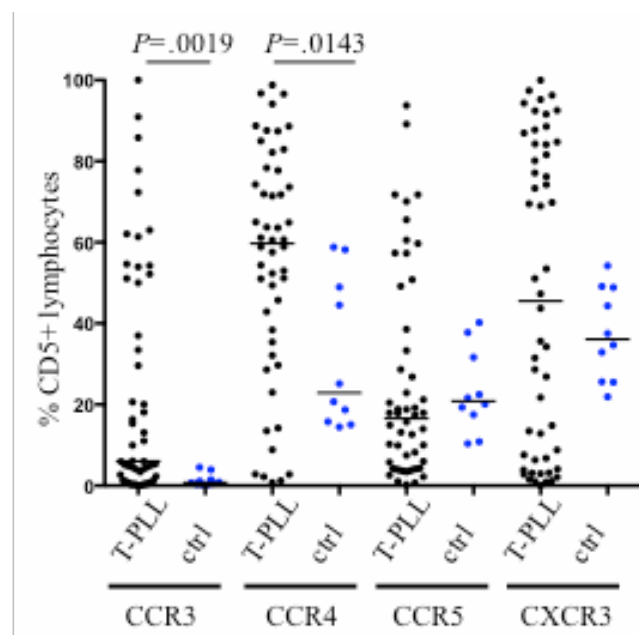
Figure III.5.3-1: **Comparison of chemokine receptor expression in T-PLL and healthy donor T-lymphocytes.** Positivity for chemokine receptor expression was determined independently for every molecule on CD5+ lymphocytes for n= 52 (CCR4 n=50) T-PLL pB samples, and n=10 pB samples from healthy donors.

The 2 most commonly expressed chemokine receptors in T-PLL samples were CXCR4, found in 60% of cases, and CCR4, detected on the majority of T-PLL cells in 64% of cases. For CCR4, the expression frequency was significantly increased in T-PLL

samples as compared to T-cells from healthy donors (P=0.143), while the portion of CXCR4 expressing cells was significantly decreased in T-PLL samples compared to T-cells from healthy donors (P=0.0118). Also, CCR4 showed a negative correlation with CD45RA (rho=-0.42, P=0.003). Higher numbers of CXCR4 positive T-PLL cells correlated with higher frequencies of cells staining positive for CD122 and CD124 (rho=0.33, P=0.018 and rho=0.29, P=0.044, respectively) (Table III.7-1). Also, increased numbers of CD45RO and CCR7 positive cells were observed in T-PLL cases with an increased frequency of CXCR4 positive cells (rho=0.66, P=9.7x10^{-8} and rho=0.35 , P=0.011, respectively).
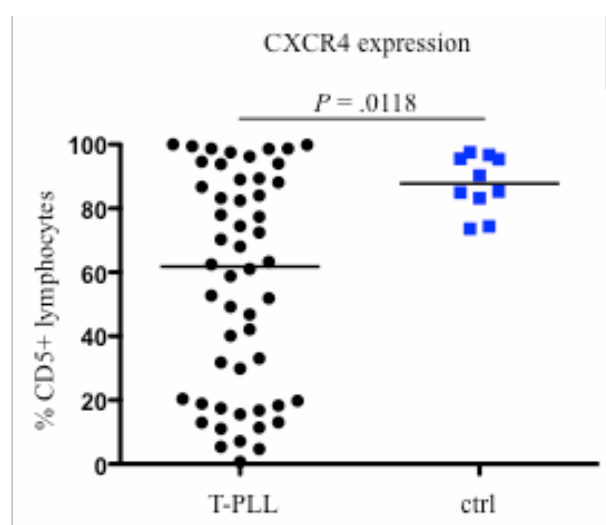
Figure III.5.3-2: **Comparison of CXCR4 expression in T-lymphocytes from T-PLL patients and healthy donors.** Positivity for CXCR4 was determined by flow cytometry on CD5+ lymphocytes for n= 52 T-PLL pB samples, and n=10 pB samples from healthy donors.

CCR3 was also detected more often in T-PLL samples than in blood samples of healthy adults (P=0.0019) but was still only found on the majority of T-PLL cells in 27% (14/52) of the T-PLL cases analyzed. T-PLL samples with high proportions of CCR3 positive T-PLL cells also contained increased numbers of cells expressing CD40L and CD122 (rho=0.45, P=0.0007 and rho=0.31 and P=0.021) (Table III.7 1). In addition, positive correlations were also found between CCR3 and CD45RO (rho=0.31, P=0.02) and a negative correlation between CCR3 and CD7 (rho=-0.3, P=0.01).

CXCR3 was expressed in 48% of T-PLL samples on more than half of the T-PLL T-lymphocyte population. Interestingly, both the CXCR3 positive and the CXCR3 negative T-PLL cases differed significantly from healthy donors with respect to the frequency of CXCR3 expressing cells (P<0.0001 and P=0.0004, respectively). CXCR3

121

expression did not correlate with the expression of other chemokine receptors, T-cell lineage markers or TCL1. Interestingly, CXCR3 expression showed a strong positive correlation with the anti-apoptotic molecule BCL2 and at the same time was strongly negatively correlated with the pro-apoptotic receptor CD95 (rho=0.47, P=0.0008 and rho=-0.39, P=0.007) (Table III.7 1).

For CCR5 no differences were detected between T-PLL cases and healthy donors with respect to the mean frequency of positive staining cells. Within the T-PLL patient cohort, however, higher number of CCR5 positive cells were detected in samples that lacked CD3 expression (rho=0.29, P=0.045) and cases with decreased CD28 expression (rho=0.35, P=0.012). Higher numbers of CCR5 positive cells in T-PLL peripheral blood samples also correlated with a higher frequency of CD40L positive and CD95L expressing cells (rho=0.30, P=0.029 and rho=0.32, P=0.030) (Table III.7 1).

Chemokine receptor co-expression patterns characteristic of T_H1 (CCR5+ CXCR3+) or T_H2 (CCR3+ CCR4+) were not observed in the T-PLL sample collection. Only one T-PLL case showed a co-expression of CCR3 and CCR4 indicative of a T_H2 phenotype, however, this case was CD4 negative and showed a cytotoxic T-cell phenotype. No co-expression patterns typical for T-PLL could be discerned and also no corellation with CD4 or CD8 expression could be detected.

III.5.4. A case study showed comparable chemokine and cytokine receptor expression in T-PLL cells from bone marrow vs peripheral blood

For one T-PLL patient samples of peripheral blood and bone marrow were available. When comparing cytokine and chemokine receptor expression in T-PLL T-lymphoid cells from both sites, no significant differences were observed for the expression of cytokine receptors. However, a slightly higher expression of CCR5 on CCR5 positive cells was found in the bone marrow sample (16% in BM, 19% in pB). In addition, the percentage of CCR3 positive T-cells was increased in the bone marrow. No differences were observed with regard to CCR4 expression. Strong differences were found with regard for the expression intensity of CXCR4, which was significantly higher expressed on CXCR4 positive cells in the peripheral blood than on bone marrow derived T-cells (Figure III.5.4-1).
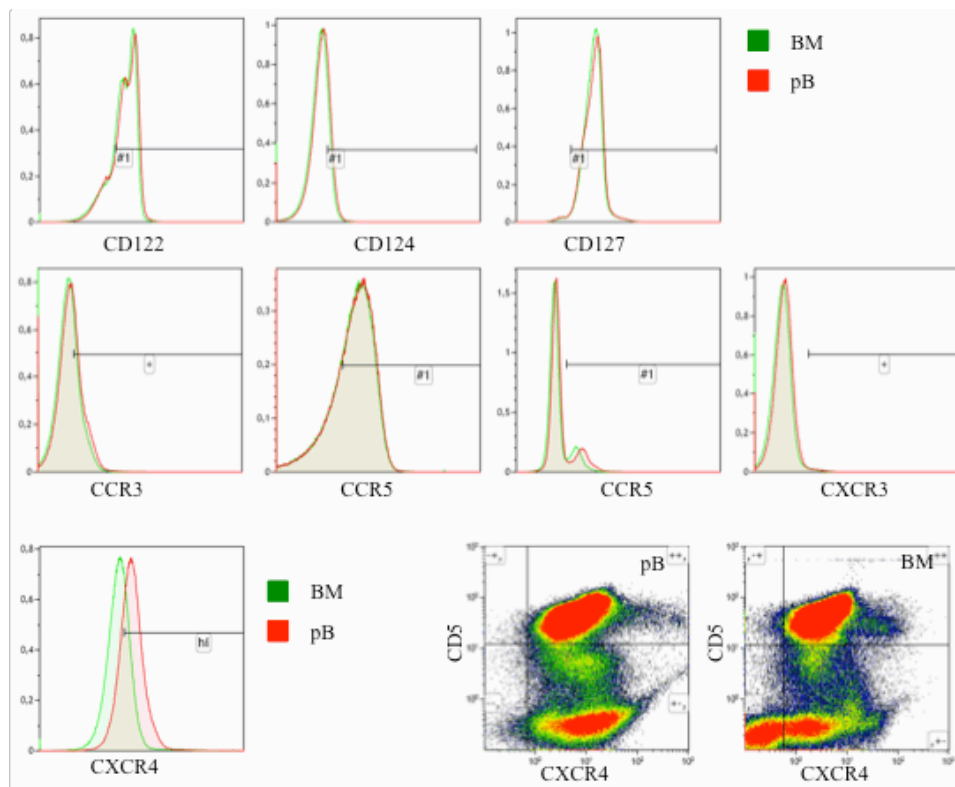
Figure III.5.4-1: **Comparison of cytokine and chemokine receptor expression in peripheral blood and bone marrow from a patient suffering from T-PLL.** The histograms show a comparison of receptor expression on CD5+ lymphocytes from BM (green) and pB (red). No differences are found except for CXCR4 (lower panels). The percentage of CXCR4hi cells is more than 2-fold higher in CD5+ cells from peripheral blood.

In summary of III.5, CD127 and CXCR4 were commonly expressed on T-PLL cells in the peripheral blood but the frequency of these cells varied. T-PLL cells in this patient cohort were characterized by a high incidence of CD127 expression and frequent positivity for CXCR4 and CCR4. T_H1 or T_H2-like expression patterns were never observed (compare also to III.4.1). The high variability among T-PLL patients with respect to the expression of single receptors might provide a possibility to further subdivide the patient cohort based on functional characteristics of the T-PLL cells and might correlate with clinical aspects.

III.6. The expression of activation and proliferation markers, as well as pro- and anti-apoptotic molecules on T-PLL cells showed distinct alterations

Expression patterns of lineage-, and memory markers or cytokine receptors might allow one to draw conclusions about the histogenesis of T-PLL. Information about the recent fate of a cell might be gathered for example from activation markers. In addition, the

expression of molecules involved in apoptotic and pro-survival pathways can give further information on the cellular function of T-PLL cells.

III.6.1. A subset of T-PLL patients presented with a high frequency of T-PLL cells staining positive for so-called activation markers in the peripheral blood

Both CD25 and CD69 are up-regulated shortly and transiently after the stimulation of mature T-cells. The frequency of T-PLL cells expressing these activation markers was assessed in n=37 T-PLL samples for CD69 and in n=49 T-PLL samples for CD25. In most T-PLL cases only few cells expressed a marker for early activation. For CD25 expressing T-PLL cases the mean percentage of positive T-cells was similar in T-PLL samples to that observed in healthy controls (Figure III.6.1-1). Interestingly, a subgroup of T-PLL samples showed a significantly higher percentage of CD25 positive T-cells. These 15 samples (15/49, 31%) contained a minimum of 20% of CD25 positive T-cells, the mean percentage was 53%. The mean percentage of CD25 positive T-cells in the CD25 low T-PLL samples was 5% ($P < 0.0001$).
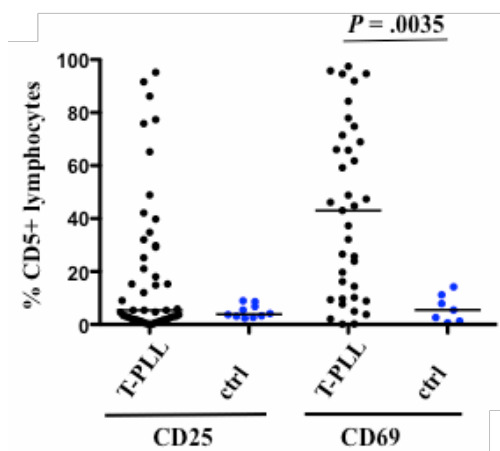
Figure III.6.1-1: **The frequency of CD69 expressing T-lymphocytes was significantly increased in T-PLL.** The percentage of CD25 and CD69 positive cells among CD5+ T-lymphocytes in the peripheral blood of T-PLL patients (CD25 n=49, CD69 n=37) and healthy donors (n=10 for CD25, n=7 for CD69) was compared. No significant differences were found between the T-PLL and the control group with regard to CD25 expression. However, a subset of patients showed a significantly higher proportion of CD25 positive cells than the remaining subset of T-PLL cases and healthy controls (n=15, >20% CD25+, $P < 0.0001$).

Higher numbers of CD25 positive cells were detected in T-PLL cases that were CD4 single positive or contained increased numbers of cells expressing TCL1 (rho=0.35, P=0.014 and rho=0.43, P=0.002, respectively). In addition, T-PLL cases with a high frequency of CD25 positive cells also showed higher proportions of CD28 and CXCR4

positive cells (rho=0.28, *P*=0.047 and rho=0.28, *P*=0.0049, respectively). CD122 expression was also found to correlate positively with CD25 (rho=0.29, *P*=0.049) (Table III.7-1). Interestingly, increased frequency of CD25 positive cells correlated with the central memory T-cell markers CD45RO, CCR7 and CD62L (rho=0.3, *P*=0.012; rho=0.3, *P*=0.02; rho=0.3, *P*=0.04, respectively).

The frequency of CD69 positive T-cells was significantly increased in T-PLL samples as compared to the T-cell pools from healthy donors (*P*=0.0035), with a mean percentage of 43% of cells staining positive for CD69 in the T-PLL samples and only 6% in the samples from healthy donors. The data is shown in Figure III.6.1-1.
In T-PLL cases lacking the surface expression of the CD3-TCR complex, cells expressing the activation marker CD69 were less frequent, indicating a physiological regulation of CD69 in T-PLL and functional TCR signaling (rho=-0.35, *P*=0.036). A decreased frequency of CD69 positive cells also correlated with higher numbers of CD122 and CD95L positive T-PLL cells (rho=-0.43, *P*=0.008 and rho=-0.35, *P*=0.033 respectively). A negative correlation was also observed between CD69 and CD45RO (rho=-0.3 and *P*=0.04) (Table III.7-1).

III.6.2. CD40L was expressed at a significantly increased frequency in T-PLL peripheral blood samples

CD40L is a marker for immediate early activation of T-cells and functions as a co-receptor for TCR stimulation. In peripheral blood samples from n=53 T-PLL patients, CD40L was detected on a mean of 15% of cells, while only 2% of T-cells expressed CD40L in the peripheral blood of healthy donors (Figure III.6.2-1).
The increased frequency of CD40L expression in T-PLL correlated strongly with a higher number of CCR3 and CD95L expressing cells (rho=0.45, *P*= 0.0007 and rho=0.4, *P*=0.005, respectively) (Table III.7-1). Other markers more frequently found in T-PLL samples with a higher content of CD40L expressing cells include CCR5, CCR7 and Ki67 (rho=0.30, *P*= 0.029; rho=0.32, *P*=0.02 and rho=0.38, *P*=0.008, respectively) (Table III.7-1).

125
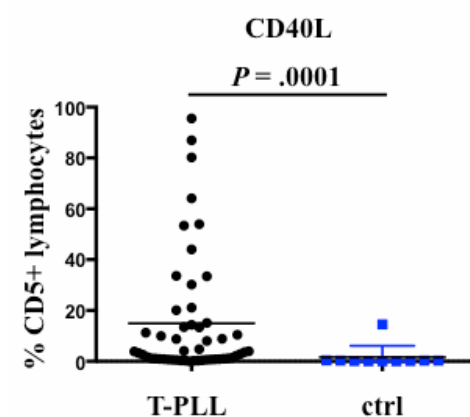
Figure III.6.2-1: CD40L expression is significantly increased in the peripheral blood of T-PLL patients in comparison to healthy donors. The CD40L expression in the blood of n=53 T-PLL patients and n=10 healthy donors was analyzed by flow cytometry.

III.6.3. T-PLL patients displayed a higher frequency of Ki67 and BCL2 expressing peripheral blood T-cells than healthy donors

Ki67 is a nuclear marker widely used in the diagnostic workup of lymphomas to detect proliferating cells. Ki67 was virtually absent from T-cells in the peripheral blood of healthy donors (mean percentage of Ki67 positive T-cells 2%).

T-PLL samples showed a significant increase in the frequency of Ki67 positive cells in the T-cell compartment in the peripheral blood (P=0.022) (Figure III.6.3-1). In the 47 analyzed T-PLL samples a mean of 12% of cells stained positive for Ki67.
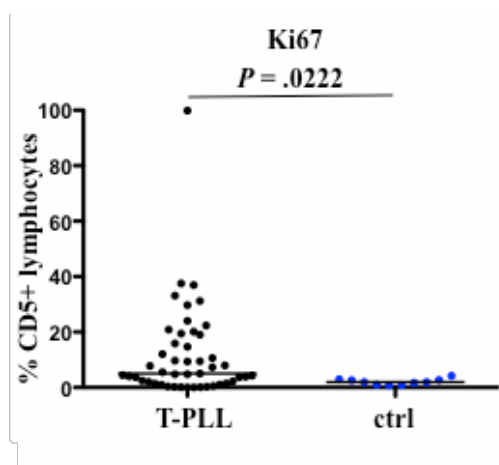
Figure III.6.3-1: **The frequency of Ki67 expressing cells was significantly increased in peripheral blood derived T-PLL compared to healthy donor T-cells.** The percentage of Ki67 expressing cells among CD5+ T-lymphocytes in the peripheral blood of T-PLL patients (n=47) and healthy donors (n=10) was compared.

A similar observation was made for BCL2, an important mediator of protection from programmed cell death. Under the given experimental settings, BCL2 was virtually absent from T-cells in the peripheral blood of healthy donors (n=10). The 47 T-PLL samples analzyed showed a much broader range of expression from 0.0% to 99.9% of CD5 positive T-lymphoid cells in comparison to healthy controls, which varied between 0.88% and 21.15%.
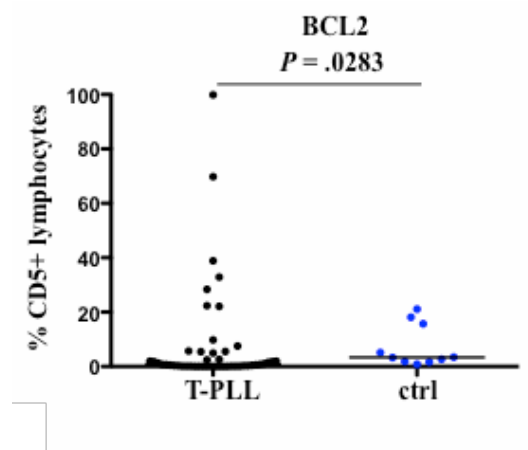
Figure III.6.3-2: Frequency of BCL2+ cells was increased in T-PLL cells in the peripheral blood compared to healthy donor T-cells. The percentage of BCL2 expressing cells among CD5+ T-lymphocytes in the peripheral blood of T-PLL patients (n=47) and healthy donors (n=10) was compared.

In total, the frequency of BCL2 positive T-cells was significantly increased in T-PLL samples (P=0.0283) (Figure III.6.3-2). As described above, there was a strong correlation between increased rates of BCL2 and CXCR3 expressing cells and decreased numbers of CD95 positive cells in T-PLL peripheral blood samples (III.5.2), indicating an anti-apoptotic phenotype in a T-PLL subset.

III.6.4. The CD95-CD95L axis showed complex aberrations in peripheral blood derived T-PLL cells

The CD95-CD95L axis plays a major role in the protection of homeostasis in the immune system by inducing cell death in T-lymphocytes. The expression of both CD95 and especially CD95L on T-cells is tightly regulated. In the peripheral blood of 10 healthy donors approximately 50% of T-cells stained positive for CD95, whereas only few CD95L expressing cells could be detected (<20% of T-cells).
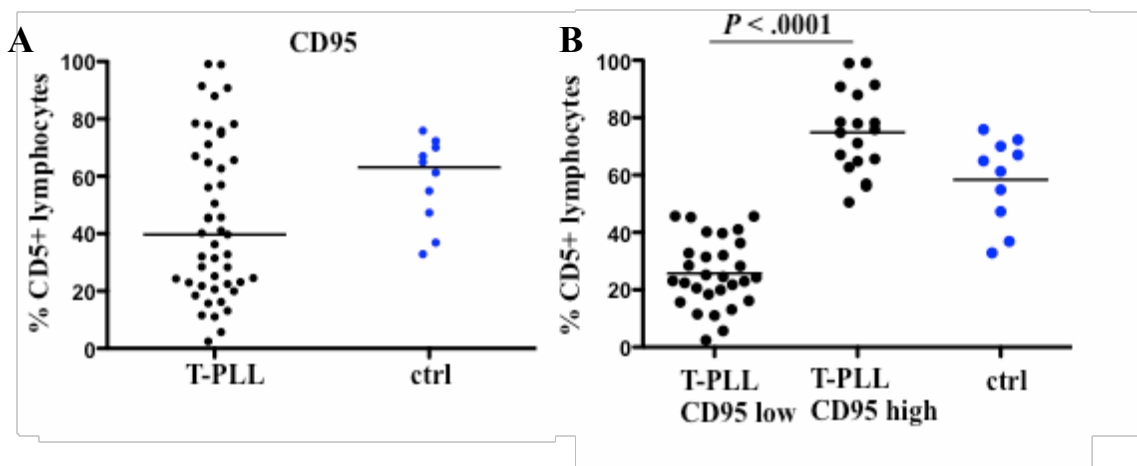
Figure III.6.4-1: **CD95 expression in T-PLL vs. healthy donor CD5+ lymphocytes in the peripheral blood. (A)** The percentage of CD95 expressing cells among CD5+ T-lymphocytes in the peripheral blood of T-PLL patients (n=47) and healthy donors (n=10) was determined by flow cytometry. No significant differences were found between the T-PLL and the control group. **(B)** T-PLL cases were subdivided into T-PLL CD95 low if the percentage of CD95+ cells was <50% and T-PLL CD95 high if positivity for CD95 was >50%. The frequency of CD95 expression differed significantly between both groups and the control group (CD95 low vs. ctrl: *P*<.0001; CD95 high vs. ctrl: *P*=.0176).

The 47 T-PLL cases analyzed for CD95 expression could be subdivided into two groups based on the frequency of CD95 expressing T-cells. 29 cases were judged as „CD95 low" with CD95 expression detectable on less than 50% of T-cells. The second group consisted of 18 cases that showed CD95 expression on >50% of CD5 positive cells „CD95 high") (Figure III.6.4-1 B).

Of note, the percentage of CD95 expressing cells was found to be extremely variable between T-PLL cases, reaching from virtually absent expression to almost 100% positivity. Higher numbers of CD95 positive cells were detected in T-PLL samples also containing increased numbers of the TCR co-receptor CD28 (rho=0.4, *P*=0.06) and CD40L (rho=0.34, *P*=0.02). In accordance with its role as key player in apoptosis, CD95 showed a strong negative correlation with BCL2 expression (rho=-0.54, *P*=0.00008) (Table III.7-1).

The mean frequency of CD95L expressing T-cells in the blood of 10 healthy donors was 14.4%. For 47 T-PLL cases the frequency of CD95L positive T-cells and T-PLL cells was determined. In the T-PLL patient cohort this frequency was significantly reduced to 4.9% (Figure III.6.4-2). Again, in the T-PLL cases a high variability was observed ranging from 0.01 to 49% of CD5 positive cells expressing CD95L.

Figure III.6.4-2: The frequency of CD95L expressing cells was significantly reduced in T-PLL in comparison to T-cells in the peripheral blood of healthy donors. The percentage of CD95L expressing cells among CD5+ T-lymphocytes in the peripheral blood of T-PLL patients (n=47) and healthy donors (n=10) was determined by flow cytometry and compared.

T-PLL samples that contained higher numbers of cells expressing CD95L, a mediator of programmed cell death showed decreased frequencies of the activation marker CD69 and the homeostatis receptor CD127 (rho=-0.35, P=0.0 and rho=-0.4, P=0.0, respectively). In contrast, CCR5, CD40L and CD124 were found on higher proportions of cells in T-PLL peripheral blood samples with frequent CD95L expression (Table III.7-1). Also, CD45RO showed a positive correlation with CD95L (rho=0.3, P=0.02).

In summary of chapters III.6.1.-4, T-PLL cells in the peripheral blood showed distinct signs of proliferative activity and protection from cell death. The T-PLL sample collection showed increased frequencies of CD95 and Ki67 expressing cells, while the markers BCL1 and CD95L associated with survival and apoptosis were expressed with a significantly decreased frequency. For CD25 and CD95 patient subsets within the T-PLL patient cohort were described that showed an increased frequency of CD25 expressing T-cells and patient subsets showing both increased and decreased frequencies of CD95 positive cells. Interestingly, expression of the activation marker CD69 did not correlate with expression of other activation-related markers like CD25 or Ki67 (Figure III.6.4-3).

Figure III.6.4-3: Comparison of markers for activation, proliferation and anti-apoptotic potential in T-PLL peripheral blood T-lymphocytes. Depicted is marker expression vs. CD5 expression in density plots gated on lymphocytes. Percentages are given as % of lymphocytes. **(A)** The case shown here shows high CD69 expression that co-incides with an above average Ki67 positivity and a large subset of CD25+ cells. **(B)** In this case two CD5+ population differing in expression intensity can be distinguished. The majority of T-lymphocytes expresses CD69 with a slight increase in the CD5 high population. Ki67 is expressed in almost 40% and virtually all T-lymphocytes stain positive for CD95. **(C)** This case shows a high proportion of CD69 and Ki67 positive cells. 9% of lymphocytes stain dimly positive for BCL2.

III.7. Comprehensive correlations of immunophenotypic markers in T-PLL

To generate a more comprehensive view on the immunophenotype of T-PLL cells in the peripheral blood the correlations between the expression frequencies of the analyzed markers were assessed. Correlations between single markers were given when expression patterns and comparisions between T-PLL samples and healthy donors were described in the text. The comprehensive correlation matrix is shown in Figure III.7.1-1.

III.7.1. TCL1 expression correlated strongly with CD25 and CD127 expression

The dendrogram of marker correlations in T-PLL shows three groups of markers clustering together (Figure III.7.1-1 as indicated by the red line, Table III.7-1).

Most noteworthy, the cluster depeicted in the lower part of the figure shows that the expression of the T-PLL oncogene TCL1 was strongly correlated with the expression of the IL7 receptor α chain CD127 (rho=0.316 and P=0.027). Other markers showing a strong correlation within this group include the pro-apoptotic receptor CD95 (correlation with TCL1 rho=-0.28 and P=0.058). The TCR co-receptor CD28 also clustered within this group (correlation with CD95 rho=0.4 and P=0.006, correlation with CD127 rho=0.284 and P=0.00008).
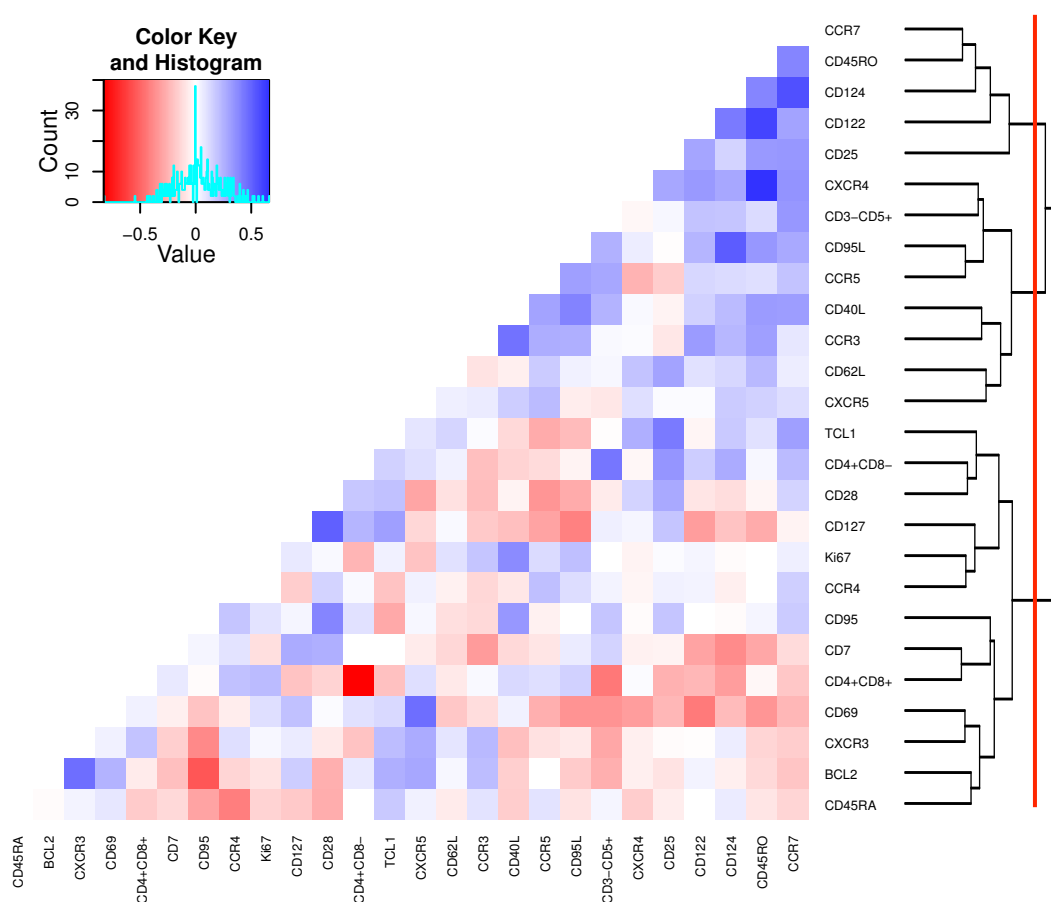
Figure III.7.1-1: Heat map of correlations between the expression frequencies of immunophenotypic markers in peripheral blood T-PLL cells. Spearman correlations were calculated based on continuous expression values (% T-cells). Clustering and heat map display courtesy of Giuliano Crispatzu (Herling lab). Shown are the values per marker pair of the Spearman correlation coefficient. *P* values are not represented. Statistically significant correlations are listed in Table III.7-1.

Table III.7-1: Summary of the immunophenotypic features of the analyzed T-PLL patient cohort

Parameter	cut off >% positive T-cells	Distribution	Statistically significant correlations
TCL1+	>5%	35/52 (67%)	CD25+ (P=0.002), CD127+ (P=0.027), CCR7+ (P=0.02)
sTCR+/sCD3+		41/51 (80%)	CD69+ (P=0.036), CCR7+ (P=0.02) sCD3- correlated with CD4+ (P=0.001), CXCR3+ (P=0.041)
CD4+ CD8-		34/52 (65%)	sCD3- (P=0.001), CD25+ (P=0.014)
CD4- CD8+		8/52 (15%)	-
CD4+ CD8+		10/52 (20%)	CD124- (P=0.026)
CD7+	>50%	41/44 (93%)	CD45RO- (P=0.04), CCR3- (P=0.02), CD124- (P=0.007), CD122- (P=0.03)
CD25+	>20%	15/49 (31%)	CD4+CD8- (P=0.014), TCL1+ (P=0.002), CD28+ (P=0.05), CXCR4+ (P=0.05), CD122+ (P=0.05), CD45RO+ (P=0.02), CCR7+ (P=0.02), CD62L+ (P=0.04)
CD69+	>40%	19/37 (51%)	CXCR5+ (P=0.027), CD45RO- (P=0.04) CD122- (P=0.009), CD95L- (P=0.033)
CD28+		47/53 (87%)	CD25+ (P=0.047), CD127+ (P=0.0001), CD95+ (P=0.006), CCR5- (P=0.012)
CD122+		2/50 (4%)	CD25+ (P=0.05), CD69- (P=0.009), CXCR4+ (P=0.018), CD124+ (P=0.002), CD7- (P=0.03), CD45RO+ (P=3.0*10^{-6}$), CCR7+ ($P$=0.03)
CD124+	>21%	2/50 (4%)	CD122+ (P=0.002), CD95L+ (P=0.0001), CD124- (P=0.007), CD45RO+ (P=0.004), CCR7+ (P=1.8*10^{-5}$) CD124- correlated with CD4+CD8+ (P=0.026)
CD127+		43/50 (86%)	TCL1+ (P=0.027), CD28+ (P=0.0001), CCR5- (P=0.034), CD122- (P=0.025), CD95L- (P=0.004)
CCR3+		14/52 (27%)	CD40L+ (P=0.0007), CD122+ (P=0.021), CD7- (P=0.02), CD45RO+ (P=0.02)
CCR4+		32/50 (64%)	CD45RA- (P=0.003)
CCR5+	>50%	11/52 (21%)	sCD3- (P=0.045), CD28- (P=0.012), CD40L+ (P=0.029), CD95L+ (P=0.031)
CXCR3+		25/52 (48%)	BCL2+ (P=0.0008), CD95- (P=0.007)
CXCR4+		30/52 (58%)	CD122+ (P=0.018), CD124+ (P=0.045), CD45RO+ (P=9.7*10^{-8}$), CCR7+ ($P$=0.01)
Ki67+	>40%	16/47 (34%)	CD40L+ (P=0.008)
BCL2+	>10%	8/47 (17%)	CXCR3+ (P=0.0008), CD95- (P=0.000007)
CD95+	>50%	18/47 (38%)	CD28+ (P=0.006), CD40L+ (P=0.02), BLC2- (P=0.00007), CD45RA- (P=0.04)
CD95L+	>5%	12/47 (26%)	CCR5+ (P=0.030), CD40L+ (P=0.005), CD124+ (P=0.0001), CD69- (P=0.034), CD127- (P=0.004), CD45RO+ (P=0.02)
CD40L+	>5%	22/52 (42)	CCR3+ (P=0.0007), CCR5+ (P=0.029), CD95L+ (P=0.005), Ki67+ (P=0.008), CCR7+ (P=0.02)

On the other end, a cluster of markers was defined by the correlation of the co-stimulatory CD40L, the pro-apoptotic CD95L (rho=0.4 and *P*=0.005). Of note, at this end of the spectrum also the chemokine receptor CCR3 (rho=0.45 and *P*=0.0007) was found which was also significantly up-regulated in T-PLL as compared to healthy donor peripheral blood samples. The third cluster contained the T-cell memory marker CD45RO as well as the activation marker CD25 (rho=0.3 and *P*=0.02). The cytokine receptors CD122 and CD124, although only rarely expressed in T-PLL, also were found in this cluster.

In order to fully summarize the immunophenotypic data collected as part of the present study a density plot of the expression data matrix (heatmap) was generated (Figure III.7.1-2).
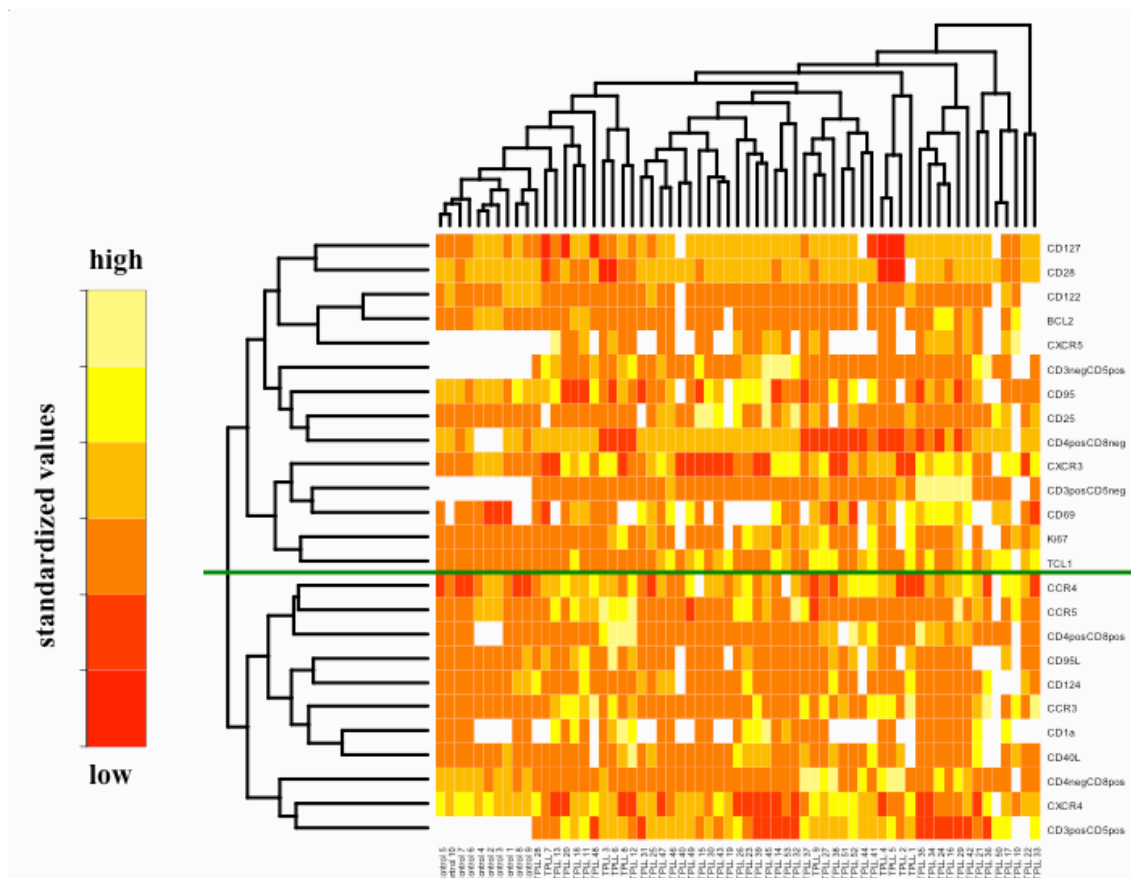
Figure III.7.1-2 Expression frequencies of immunological markers in peripheral blood samples of T-PLL patients and healthy donors. Hierarchical clustering was performed on both samples (T-PLL n=53, ctrl n=10, x-axis) and markers analyzed by flow cytometry (y-axis). Higher standardized values are represented in lighter colors (yellow) while lower standardized values are depicted in darker colors (red). The green line devides two clusters based on expression of immunologic markers.

A complete linkage analysis based on Eukledian distances of all n=53 T-PLL cases and n=10 healthy donor controls based on expression frequencies of immunological markers is displayed in Figure III.7.1-2. The heatmap displayed the expression of immunological markers measured by flow cytometry as percentage of T-PLL cells or T-cells. To avoid extreme results both the top and bottom 1 percent of values were trimmed. Normalization was performed for each marker by subtracting the mean and dividing by the standard deviation. The values were then represented on a 6-step equidistant scale.

Interestingly, the T-PLL patient cohort segregated in a number of clusters, representing the observed heterogeneity of the cohort. When looking at the clustering of the immunological markers, again the two classes also described by the correlation studies above segregate from one another. One class of markers comprising amongst others TCL1, CD69, CD25 and the proliferation marker Ki67 are clearly up-regulated in T-PLL in comparison to healthy donor (above the green line). The second class (below the green line) again comprises CD40L and other chemokine and cytokine receptors that were found only rarely at high frequencies in T-PLL.

III.8. Aberrant chemokine levels in the plasma of T-PLL patients show a bias towards an immunosuppressive profile

III.8.1. Only few chemokines reached the detection level in T-PLL plasma samples

A characteristic feature of T-PLL is the presence of extremly high and exponentially increasing numbers of malignant T-cells in the peripheral blood of patients. This might affect the cytokine and chemokine millieu either by direct production or consumption by the T-PLL cells or by influencing other chemokine producing cell types and thus influence the patient's immune system. Therefore, cytokines that are mainly produced by T-cells (IL-2, IL-4, IL-10, and IFN- γ) were assessd. In addition, important pro-inflammatory factors (TNF-α, RANTES and PDGF-BB) were analyzed. Also, IL-1RA as important mediator of immunosuppression was measured. In order to assess whether increased numbers of circulating T-PLL cells coincided with changes to serum cytokine levels in these patients, a number of cytokines were measured in plasma from 32 patients with T-PLL. Most cytokines assessed were below the detection limit of the assay applied (IL-1β, IL-2, IL-4, IL-10, IFN-γ, TNF-α). An exemplary data set is shown for IL-2 in Figure III.8.1-1.
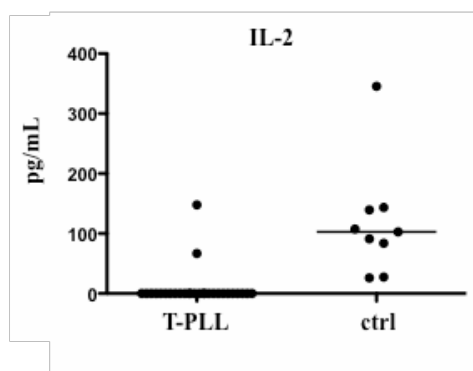
Figure III.8.1-1: IL-2 was undetectable in 93% of T-PLL plasma samples. Plasma from n=32 T-PLL patients and serum from n=9 healthy donors were analyzed using a bead-based multiplex immunoassay (P=0.0026).

III.8.2. Pro-inflammatory chemokines RANTES and PDGF-BB were found at lower levels in the blood of T-PLL patients

Both RANTES and PDGF-BB were significantly reduced in the plasma of T-PLL patients (Figure III.8.2-1 and Figure III.8.2-2), whereas IL-1RA showed a trend towards higher levels than in the serum of healthy donors (Figure III.8.2-3).
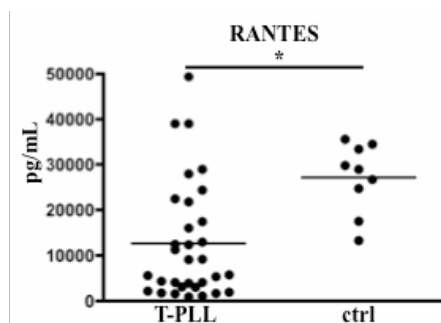
Figure III.8.2-1: RANTES levels were significantly reduced in the serum of patients suffering from T-PLL. Plasma from n=32 T-PLL patients and serum from n=9 healthy donors were analyzed using a bead-based multiplex immunoassay ($P = 0.0026$).

Of the few chemokines detectable in the T-PLL samples, RANTES and PDGF-BB have a pro-inflammatory function and were found at lower levels in T-PLL patients. IL-1RA counteracts the pro-inflammatory effects of other IL-1 family members. Taken together, the chemokine levels in the peripheral blood of T-PLL patients hint at a possible suppressive effect on the immune system.

135
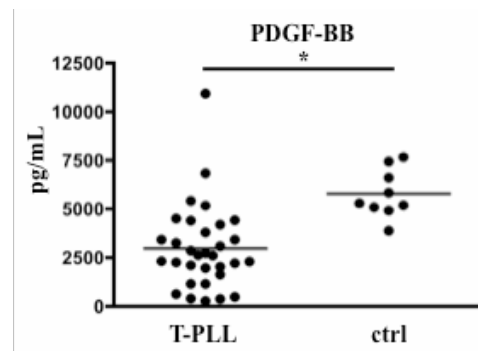
Figure III.8.2-2: **PDGF-BB levels were significantly reduced in the serum of patients suffering from T-PLL.** Plasma from n=32 T-PLL patients and serum from n=9 healthy donors were analyzed using a bead-based multiplex immunoassay ($P = 0.0007$).
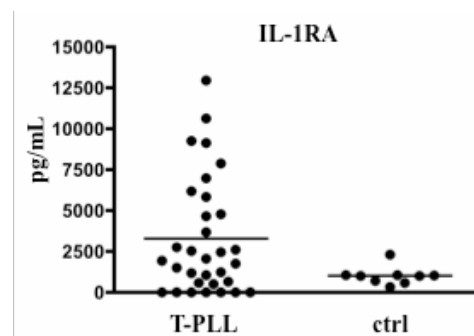
Figure III.8.2-3: IL-1RA levels were slightly increased in the serum of patients suffering from T-PLL. Plasma from n=32 T-PLL patients and serum from n=9 healthy donors were analyzed using a bead-based multiplex immunoassay ($P = 0.0674$).

III.9. The response to stimulation of the T-cell receptor complex in primary T-PLL lymphocytes

To better understand the biological characteristics of T-PLL and to potentially identify signaling pathways that could be targeted by therapeutic intervention, the relevance of aberrant TCR signaling in the malignant cells in T-PLL was interrogated by defining the response of T-PLL cells to cross-linking of the TCR complex. In the first part of this chapter, special emphasis is placed on intracellular mechanisms of signal transduction that are a direct result of activation of the TCR signaling cascade, before phenotypic changes induced by stimulation will be described. Finally, the functional characteristics, i.e. cytokine production, proliferation and sensitivity towards AICD were investigated and will be reported. The response to CD3 and CD28 cross-linking was only investigated in sCD3 and CD28 positive T-PLL cases.

III.9.1. Second messenger generation as part of the T-cell receptor proximal signaling pathway was enhanced in T-PLL cells

III.9.1.1. T-PLL cells showed a more pronounced increase in intracellular Ca^{2+} levels after TCR stimulation than did healthy donor T-cells

Intracellular Ca^{2+} levels increase strongly after cross-linking of the TCR complex and this effect can be mediated by additional co-receptor stimulation. Under the chosen experimental conditions, however, in T-cells from healthy donors only a 20-fold relative increase in fluorescence intensity could be detected after antibody-induced stimulation of the TCR complex. A similar relative increase between 10 and 20-fold was observed in T-PLL lymphocytes after stimulation with a cross-linking αCD3 antibody alone. Cross-linking of the stimulating αCD3 antibody with αIgG induced a 100 to 150-fold relative increase of Ca^{2+} in T-PLL lymphocytes. This might indicate a lower stimulation threshold or a higher propensity for Ca^{2+} flux in T-PLL cells as compared to T-cells from healthy donors. Alterations to the kinetics of the response can be ruled out, as intracellular Ca^{2+} was continuously measured for a period of 10min.
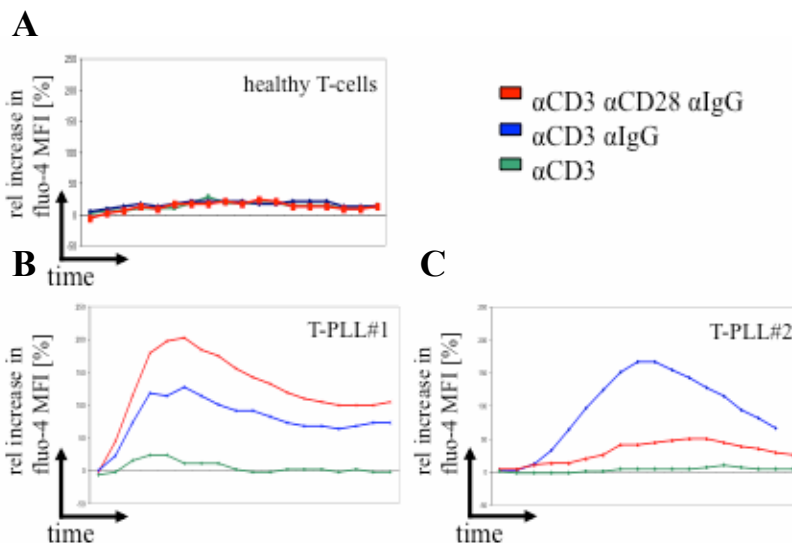
Figure III.9.1-1: T-PLL cells displayed a higher increase in Ca2+ levels after stimulation than healthy T-cells. Isolated lymphocytes loaded with the Ca^{2+} indicator dye fluo-4 were stimulated as indicated with either 10µg/mL soluble αCD3 antibody (OKT3), 20µg/mL αCD28 antibody (15E8) or 10µg/mL αIgG antibody at t=0 and changes in intracellular Ca^{2+} levels were measured over time on a single cell level. Plotted is the percentual increase as compared to baseline. **(A)** Under the given experimental conditions virtually no increase in Ca^{2+} was observed in T-cells from healthy donors (n=4). **(B)** A representative T-PLL case is shown. **(C)** In this T-PLL case CD28 costimulation abrogated the increase in intracellular Ca^{2+} levels.

In T-cells from healthy donors physiologic costimulation by CD28 ligation or as in our studies by *in vitro* cross-linking showed a synergistic effect to CD3 cross-linking. In

70% of T-PLL cases an enhanced Ca^{2+} response was observed in the presence of additional CD28 costimulation over strong CD3 cross-linking alone. Interestingly, a CD28-mediated abrogation of Ca^{2+} flux in response to CD3 cross-linking was observed in one third of T-PLL cases (Figure III.9.1-1, Table III.9-1). No discernable associations with expression patterns of immunologic markers or functional characteristics could be detected for this group of T-PLL cases.

Table III.9-1: Overview on the effect of CD28 costimulation on intracellular Ca^{2+} levels in T-PLL

effect of CD28 co-stimulation			
activating		inhibitory	
9/13	70%	4/13	30%

III.9.1.2. T-PLL cells showed increased ROS generation after TCR cross-linking

The generation of ROS has been recognized in recent years as an important mediator in TCR proximal signal transduction comparable to Ca^{2+} [93].
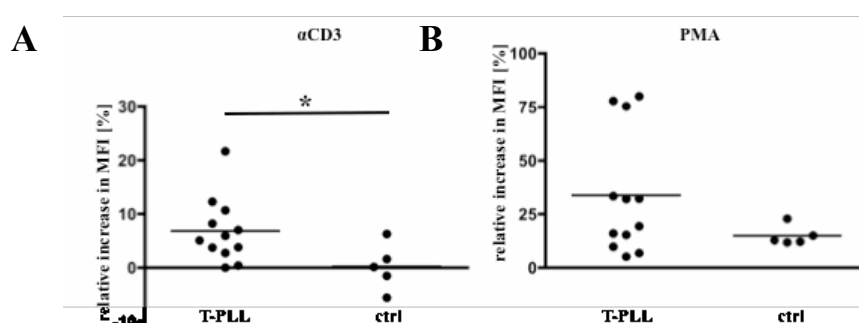
Figure III.9.1-2: **T-PLL cells showed increased ROS generation after TCR cross-linking.** Isolated lymphocytes from patients with T-PLL (n=12) and healthy donors (n=5) loaded with the ROS indicator dye H_2DCFDA were stimulated as indicated with either 10μg/mL plate bound αCD3 antibody (OKT3) or 100ng/mL PMA for 20min and ROS content was assessed on a single cell level. Plotted is the percentual increase as compared to unstimulated cells. **(A)** Stimulation with αCD3 induces an significantly higher increase of ROS in T-PLL cells as compared to lymphocytes from healthy donors ($P = 0.0424$). **(B)** After PMA stimulation few T-PLL cases respond strongly, in total there is no significant difference to healthy donor lymphocytes.

Cross-linking of the TCR by plate bound αCD3 antibody induced a minor increase in ROS in T-cells from healthy donors. T-PLL cells in contrast showed a significantly higher ROS induction with a mean relative increase of 6.8% compared to healthy T-cells with a mean increase of 0.2% (P=0.0424). Stimulation of lymphocytes using

PMA, a substance known to induce a PKC-dependent increase in ROS [65], was used both as a positive control for the assay and to interrogate the effects elicited when the TCR proximal signaling cascade was circumvented. Baseline ROS levels could not be compared as dye loading and instrument setup were not sufficiently standardized.

PMA induced a measurable increase in ROS levels in both T-cells from patients with T-PLL (mean relative increase: 33.67%) and healthy donors (mean relative increase: 14.98%). Interestingly, a subset of T-PLL cases (3/12) showed a very pronounced increase in ROS (>75%) while the majority of cases displayed a response comparable to T-cells from healthy donors (Figure III.9.1-2).

In summary, T-PLL cells show significantly increased levels of the second messengers Ca^{2+} and ROS after activation of the TCR signaling cascade.

In summary of chapter III.9, in T-PLL cells activation of the TCR signaling cascade resulted in a dramatic increase of both intracellular messengers, ROS and Ca^{2+}, that surpassed the reaction observed in T-cells of healthy donors. Both Ca^{2+} and ROS are important intracellular mediators downstream of the TCR complex. Taken together, this set of data indirectly shows that the TCR proximal signaling cascade is functional and indicates that the activation threshold in T-PLL cells might be lowered or not as tightly regulated compared to healthy T-cells. Interestingly, CD28 costimulation did not show the expected activating effect in 30% of T-PLL cases where it abrogated the increase in intracellular Ca^{2+}.

III.9.2. T-PLL cells were partially resistant to activation-induced cell death

T-PLL patients suffer from an accumulation of malignant T-cells. This might be caused by a failure of these cells to undergo cell death and to be eliminated from the organism. Induction of apoptosis by AICD in previously expanded T-lymphocyte populations is a crucial mechanism in the maintenance of homeostasis in the immune system and its deregulation can lead to malignant transformantion and auto-immune effects. The ability of T-PLL cells to undergo AICD was assessed and directly compared to T-cells from healthy donors.
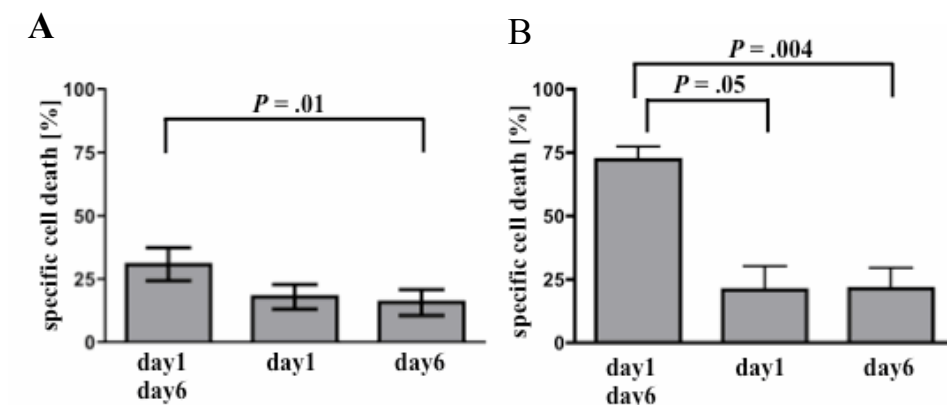
Figure III.9.2-1: **T-PLL cells were more resistant to AICD than healthy donor T-cells.** Isolated lymphocytes cultured in the presence of 10U/mL IL-2 were stimulated on the indicated timepoints with PHA (1µg/mL). Viability was measured by Annexin V/7AAD negativity on day 7. **(A)** Lymphocytes from n=8 T-PLL patients show a small but significant increase in cell death after repeated stimulation. **(B)** Lymphocytes from healthy donors (n=3) show a 3-fold higher degree of cell death induction after re-stimulation than after single stimulation.

In a PHA restimulation model, T-cells from healthy donors showed a significant induction of specific cell death after restimulation about 3-times over single stimulations on either day 1 or 6. Cell death induction in response to restimulation was not completely abrogated in T-PLL cells as shown by a small 1.8-fold but significant increase over stimulation on day 6 alone (P = 0.01) (Figure III.9.2-1).
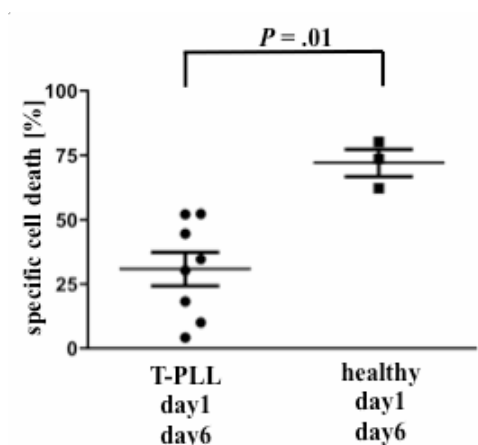
Figure III.9.2-2: **AICD was significantly reduced in T-PLL lymphocytes compared to T-cells from healthy donors.** Isolated lymphocytes cultured in the presence of 10U/mL IL-2 were stimulated on the indicated timepoints with PHA (1µg/mL). Viability was measured by Annexin V/7AAD negativity on day 7.

Direct comparison on the cell death rates elicited by restimulation in lymphocytes from T-PLL patients and healthy donors shows significant resistance in the T-PLL cases with a 2.3-fold higher induction of cell death in healthy T-cells ($P = 0.01$) (Figure III.9.2-2).
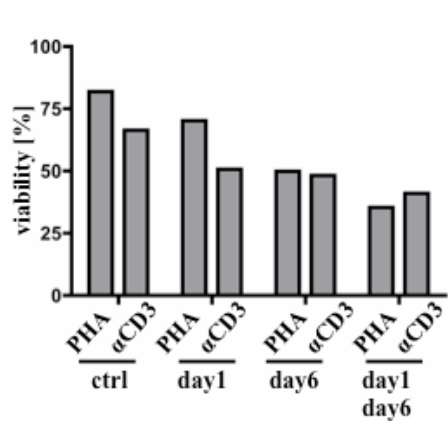
Figure III.9.2-3: **PHA and αCD3 induced a comparable loss in viability after re-stimulation in a T-PLL case.** Isolated lymphocytes cultured in the presence of 10U/mL IL-2 were stimulated on the indicated timepoints with PHA (1µg/mL) or plate bound αCD3 (OKT3, 10µg/mL). Viability was measured by Annexin V/7AAD negativity on day 7.

To ensure that PHA stimulation had comparable effects to direct activation of the TCR pathway, PHA and αCD3 stimulation were compared in one T-PLL case. Both stimuli induced a comparable loss of viability in response to restimulation (Figure III.9.2-3). Two cases were analyzed for their response to repeated αCD3 only. Of note, these two T-PLL cases showed complete resistance towards AICD induction (Figure III.9.2-4).
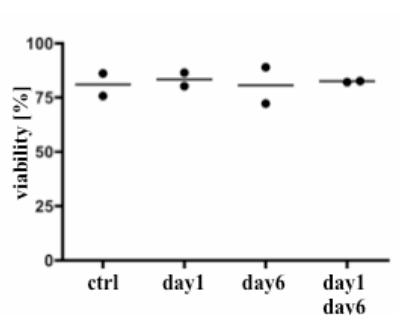
Figure III.9.2-4: **Two T-PLL cases displayed complete resistance against αCD3 induced loss of viability.** Isolated lymphocytes cultured in the presence of 10U/mL IL-2 were stimulated on the indicated timepoints with plate bound αCD3 (OKT3, 10µg/mL). Viability was measured by Annexin V/7AAD negativity on day 7.

III.9.3. T-PLL lymphocytes proliferated in response to activation of the TCR cascade

To help discerning whether T-PLL at its clinically overt leukemic stage shows rather accumulative pro-survival (via decreased death rates) vs proliferative growth kinetics, the effect of stimulation of TCR signaling on the proliferative response in T-PLL cells was examined as well. T-PLL T-cells from three independent donors readily up-

regulated Ki67, a marker for mitotically active cells, after single cross-linking of either the TCR complex or the CD28 coreceptor. After efficient stimulation by combining the two stimuli or PMA/ionomycin treatment, Ki67 positive cells were significantly increased over untreated cultures (P = 0.0347 αnd P = 0.0368, respectively) (Figure III.9.3-1).
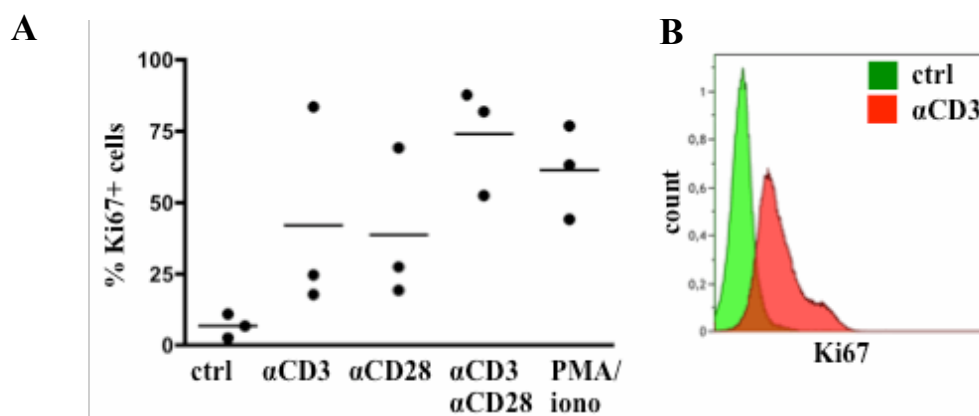
Figure III.9.3-1: **T-PLL cells readily up-regulated Ki67 in response to TCR and co-receptor cross-linking.** Expression of activation markers was assessed flow cytometrically after 48h stimulation with the indicated combinations of αCD3 (OKT3, 10μg/mL), αCD28 (15E8, 20μg/mL), PMA (100ng/mL) and ionomycin (1mM). **(A)** The percentage of Ki67+ cells is significantly increased upon stimulation with αCD37/αCD28 (P = 0.0347), αnd PMA/iono (P = 0.0368) in n=3 T-PLL samples. **(B)** αCD3 cross-linking alone induces marked up-regulation of Ki67.
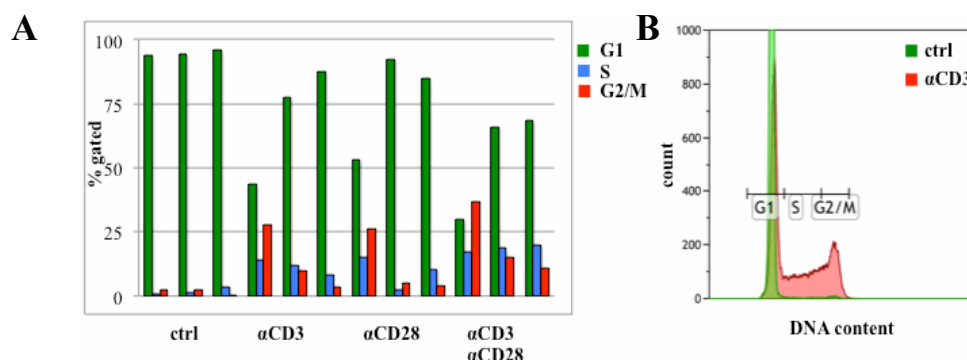
Figure III.9.3-2: Progress through the cell cycle was induced in T-PLL lymphocytes upon activation of the TCR signaling cascade. DNA content of T-PLL PBMC (n=3) was assessed following activation for 48 with αCD3 (OKT3, 10μg/mL) and αCD28 (15E8, 20μg/mL) as indicated. **(A)** An exemplary dataset is shown. A shift from G1 to S and G2/M phases of the cell cycle can be observed after stimulation. **(B)** This exemplary data shows a decrease of cells in G1 and an accumulation in S and G2/M after αCD3 stimulation.

T-PLL cells showed a decreased likelihood to undergo apoptosis in response to TCR restimulation. In addition, they readily displayed signs of proliferation like up-regulation of Ki67 expression and cell cycle entry. Taken together, in conjunction with

their high degree of cell death resistance a marked proliferative response to TCR stimuli might account for the extremely high WBC and their exponential rise seen in T-PLL patients.

III.9.4. Activation-induced phenotypic changes in T-PLL cells *in vitro*

After the recognition of their specific antigen presented in the context of MHC molecules, T-cells undergo characteristic functional changes that are reflected by their immunophenotype. A number of molecules that are specifically up-regulated with characteristic kinetics after T-cell stimulation are often referred to as „activation markers". These molecules include CD25, CD38, and CD69. Co-receptor stimulation is able to modulate these changes. The same effects can also be observed after *in vitro* stimulation.
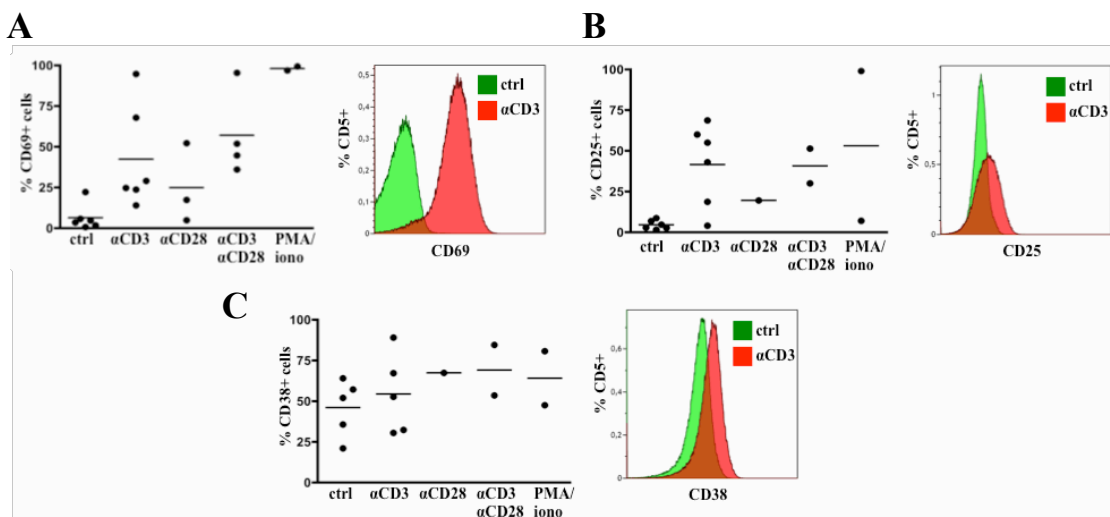
Figure III.9.4-1: T-PLL cells readily up-regulated activation markers in response to TCR and co-receptor cross-linking. Expression of activation markers was assessed flow cytometrically after 24-48h stimulation with the indicated combinations of αCD3 (OKT3, 10µg/mL), αCD28 (15E8, 20µg/mL), PMA (100ng/mL) and ionomycin (1mM). **(A)** The percentage of CD69+ cells is significantly increased upon stimulation with αCD3 (αCD3 $P = 0.0312$, αCD3 αCD28 $P = 0.0095$). **(B)** CD25 expression is induced in a large proportion of cells in response to the tested stimuli. Statistical significance, however, was not reached. **(C)** CD38 expression further increases above baseline in response to every stimulus tested.

Overall, a pronounced increase was observed for every one of these molecules after cross-linking of the TCR complex with plate bound αCD3 antibodies or treatment with PMA/ionomycin, a strong stimulus circumventing the TCR proximal signaling cascade. Of note, CD28 ligation by itself caused a slight increase in expression of the three markers analyzed and further enhanced the effect of CD3 cross-linking, as was to be

inferred from the reported effect of costimulation on healthy T-cells (Figure III.9.4-1). A direct comparison of T-PLL T-cells and T-cells from healthy donors was not performed.

The percentage of CD69 positive T-lymphoid cells increased 6.5-fold after CD3 cross-linking, an effect that was further enhanced to 8.8-fold when CD28 costimulation was present. A 4-fold increase was caused by CD28 cross-linking alone. CD25 positive cells increased approx. 10-fold in response to CD3 cross-linking alone and combined CD3/CD28 stimulation. CD28 cross-linking alone also caused an 4-fold increase in CD25 positive cells. CD38 was already expressed by 46% of resting cells which slightly increased to 54.45% after CD3 stimulation. CD28 cross-linking alone caused an 1.5-fold increase in CD38 positive T-PLL cells, this increase remained unaffected when CD3 was cross-linked at the same time (Figure III.9.4-2).

A   **B**   **C**
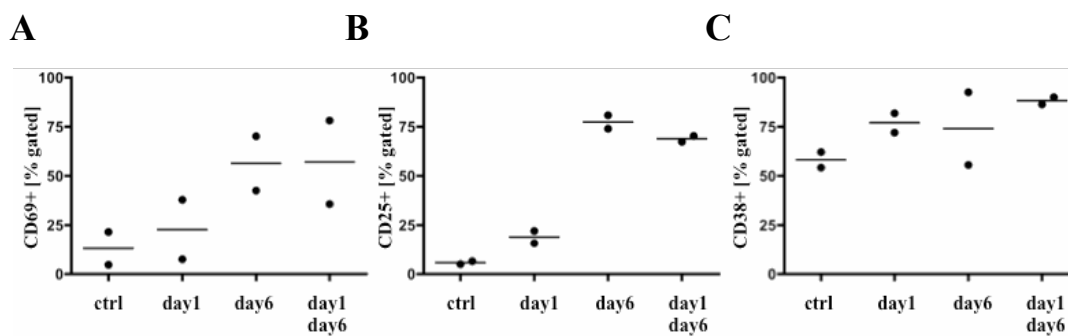
Figure III.9.4-2: The proportion of CD69 and CD25 increased short term after stimulation while CD38 remains elevated on T-PLL lymphocytes. Isolated lymphocytes cultured in the presence of 10U/mL IL-2 were stimulated on the indicated timepoints with PHA (1µg/mL). Activation marker exression was measured by flow cytometry on day 7. **(A)** Shown are CD69+ cells as percentage of T-PLL T-cells. **(B)** CD25 positive cells are plotted. **(C)** Shown are CD38+ cells as percentage of T-PLL T-cells.

Before it was shown that T-PLL cells are resistant to AICD (III.9.2). This could be caused by a failure of the T-PLL cells to respond to restimulation. To assess the effect of single and repeated stimulations over time, T-PLL lymphocytes were stimulated either on day 1, day 6 or day 1 and day 6 with the potent lymphocyte mitogen phytohemagglutinin (PHA) and activation marker expression was analyzed on day 7. While on the first day after treatment all markers were strongly induced, 6 days after stimulation both CD69 and CD25 were only slightly elevated above baseline. CD38 expression, however, seemed to be sustained over time. Re-stimulation recapitulated the outcome of short term stimulation for all markers analyzed (Figure III.9.4-2). Therefore,

T-PLL cells were still sensitive to restimulation, ruling out a stimulation refractory phenotype as a pathogenic mechanism.

CD40L is a molecule crucially implicated in the induction of an efficient immune response by stimulating B-cells. On T-PLL T-lymphoid cells CD40L expression was induced by cross-linking of the TCR complex. Interestingly, up-regulation in response to PMA/ionomycin was less pronounced. CD28 co-stimulation alone elicited a slightly stronger response than TCR cross-linking via CD3 alone. Again, combined stimulation via CD3 and CD28 showed enhanced CD40L expression as compared to single agent treatment (Figure III.9.4-3).
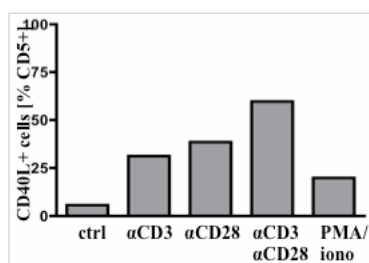
Figure III.9.4-3: **CD40L expression increases on T-PLL cells in response to stimulation.** Expression of CD40L was assessed flow cytometrically for one patient sample after 24h stimulation with the indicated combinations of αCD3 (OKT3, 10μg/mL), αCD28 (15E8, 20μg/mL), PMA (100ng/mL) and ionomycin (1mM).
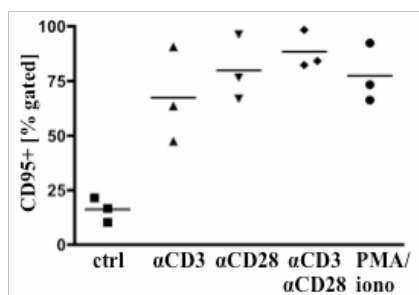
Figure III.9.4-4: **CD95 was significantly up-regulated on T-PLL cells in response to stimulation.** CD95 expression was assessed flow cytometrically after 24h stimulation with the indicated combinations of αCD3 (OKT3, 10μg/mL), αCD28 (15E8, 20μg/mL), PMA (100ng/mL) and ionomycin (1mM). $P = 0.0006$ (1 way anova).

The function of the adaptive immune system is crucially linked to the regulation of cell death induction in the T-cell compartment. Accordingly, molecules critical for survival and programmed cell death in T-lymphocytes are tightly regulated in response to stimulation via the TCR. The expression pattern of the pro-apoptotic molecules CD95 and CD95L was measured on T-PLL cells after T-cell stimulation to assess whether

deregulation of these molecules might be implicated in the natural history of the disease and the observed defect in AICD induction. The anti-apoptotic molecule BCL2 was investigated in parallel.

CD95 was up-regulated significantly after TCR complex cross-linking as well as CD28 costimulation alone from a baseline expression in 16% of cells to 67% and 80% after CD3 or CD28 cross-linking, respectively. The combination of both stimuli slightly enhanced this effect to CD95 positivity in 88% of T-PLL cells. PMA/ionomycin stimulation was sufficient to induce CD95 expression (Figure III.9.4-4).
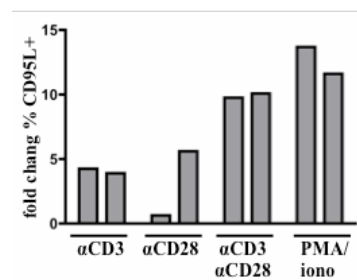
Figure III.9.4-5: **The percentage of CD95L expressing cells strongly increased in response to efficient activation of the TCR pathway**. CD95L expression was assessed flow cytometrically on T-PLL lymphocytes from two indepedent patient samples after 24h of continued stimulation with the indicated combinations of αCD3 (OKT3, 10μg/mL), αCD28 (15E8, 20μg/mL), PMA (100ng/mL) and ionomycin (1mM) and plotted as fold change in comparison to untreated T-PLL cells.

Single stimulation via the TCR complex or the co-receptor CD28 had only a modest effect on CD95L expression and resulted in a 3.75-fold increase. Both signals combined or strong stimulation by PMA/ionomycin induced a robust 10- and 12-fold increase of CD95L expression on primary T-PLL cells, respectively (Figure III.9.4-5).
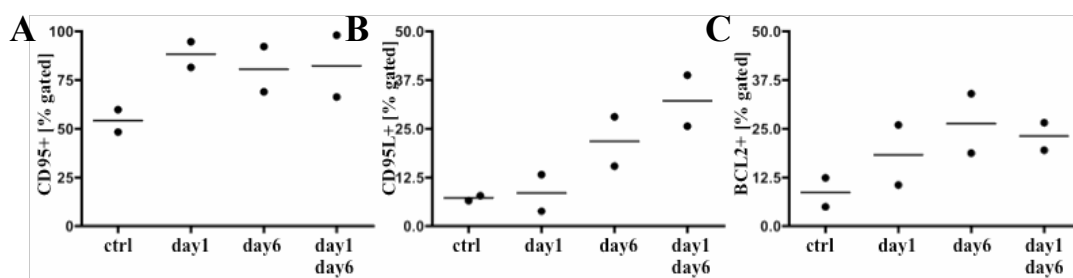
Figure III.9.4-6: **Restimulated T-PLL cells up-regulated both pro- and anti-apoptotic molecules.** Isolated lymphocytes form n=2 T-PLL pB samples cultured in the presence of 10U/mL IL-2 were stimulated on the indicated timepoints with PHA (1μg/mL). Marker expression was analyzed by flow cytometry on day 7. **(A)** The proportion of CD95+ cells increased after stimulation and stayed high over time. **(B)** CD95L expression increased transiently after stimulation and was further induced after restimulation. **(C)** The number of BCL2 positive cells showed a prolonged increase after stimulation.

The extrinsic pathway of apoptosis is especially important in the context of AICD. Therefore, the expression of CD95 and CD95L was assessed not only directly after stimulation but also after a prolonged time and in response to restimulation.

CD95 expression was increased after stimulation and was still elevated 6 days later. Restimulation did not cause a further increase as the vast majority of cells already expressed CD95. CD95L, in contrast, showed a 3-fold increase immediately after stimulation but expression levels returned to baseline after one week. Restimulation, however, elicited a response even more pronounced than single stimulation. BCL2 positive cells increased 3-fold directly after stimulation and only went down to 70%. Restimulation recapitulated the effect of single short term stimulation (Figure III.9.4-6).

T-PLL cells readily undergo activation-associated immunophenotypic changes and up-regulate markers of early activation. This effect is also observed after re-stimulation, showing there is no refractory period that might account for the defect in AICD induction. Also CD95 and CD95L are up-regulated in response to stimulation, indicating that any defect in the CD95/CD95L axis impairing cell death induction in T-PLL would have to be downstream of CD95. Even after stimulation BCL2 was only expressed in around 25% of T-PLL cells and therefore is unlikely to play a major role in protection against AICD.

III.9.5. Cytokine production of T-PLL cells in response to stimulation

Many important functions of T-cells are mediated by the cytokines they produce in response to a specific stimulus. The potential of T-PLL cells to produce cytokines was assessed to gain insights into their functional features. When freshly isolated T-PLL PBMC were stimulated *ex vivo* 21% of T-PLL cells were able to produce IL-2. In contrast, only 6% could produce IL-4 and only 2% IFN-γ producing cells were detected (Figure III.9.5-1).

When T-PLL cells were cultured over a longer period of time allowing for differentiation of the cells *in vitro* strong stimulation like PMA/ionomycin and TCR complex cross-linking in presence of co-receptor stimulation lead to production of IL-2 in the majority of cells (66% and 46%, respectively). Of note, CD28 cross-linking by itself induced an effect comparable to TCR cross-linking by αCD3 (28% and 34%, respectively). In addition, CD28 also induced an increase in IL-4 producing cells

comparable to PMA/ionomycin (42% and 30%, respectively), whereas IL-4 production was affected neither by CD3 cross-linking or αCD3 in combination with αCD28. Regardless of the stimulus applied only <5% of T-LL cells producing IFN-γ could be detected (Figure III.9.5-2).
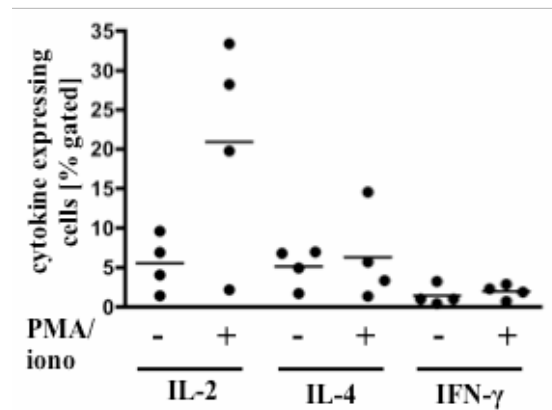
Figure III.9.5-1: **Short term stimulation of T-PLL lymphocytes *ex vivo* revealed the propensity for IL-2 production.** Freshly isolated T-PLL PBMC isolated from n=4 peripheral blood samples were stimulated with PMA (100ng/mL) and ionomycin (1mM) for 4h in presence of Brefeldin A followed by intracellular staining for cytokines and flow cytometric analysis.
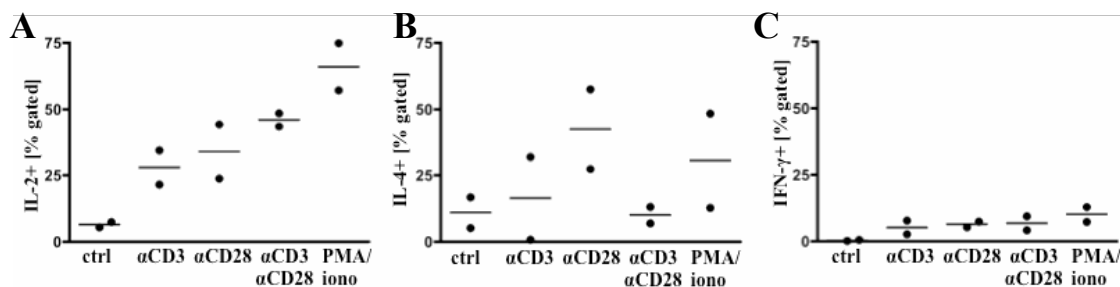
Figure III.9.5-2: **Prolonged activation of the TCR pathway allowed for the differentiation of IL-2 and IL-4 producing T-PLL T-lymphocytes.** Isolated T-PLL PBMC from n=2 pB samples were cultured for 48h in the presence of the indicated stimuli (plate bound αCD3 (OKT3, 10μg/mL), plate bound αCD28 (15E8, 20μg/mL), PMA (100ng/mL) and ionomycin (1mM)). The cells were treated with Brefeldin A followed by intracellular staining for cytokines and flow cytometric analysis. **(A)** Shown are IL-2 producing lymphocytes that increase in percentage with increasing stimulation intensity. **(B)** Shown are IL-4 producing lymphocytes. **(C)** Given is the percentage of IFN-γ producing lymphocytes.

When assessing the production of all three cytokines on the single cell level, a considerable number of cells expressed two or more cytokines (Figure III.9.5-3). Two T-PLL cases were analyzed after 48h stimulation with αCD3 αCD28 for co-expression of cytokines. In both cases double-producing populations were detected for IL-2 and IL-4 as well as IL-2 and IFN-γ with both populations making up for about 6% of total cells.

A small (2% of viable cells) triple-producing population staining positive for IL-2, IL-4 and IFN-γ was also detected after prolonged stimulation and possibly differentiation under non-skewing culture conditions.
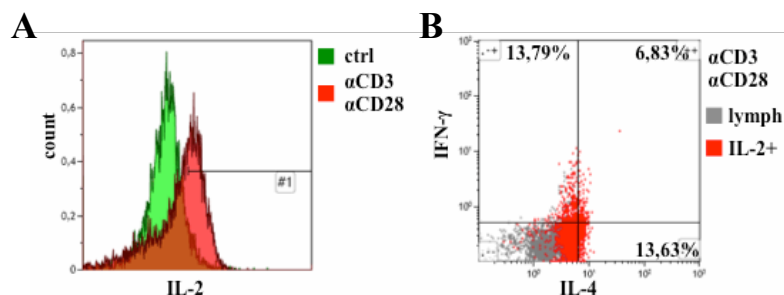
Figure III.9.5-3: **Stimulated T-PLL lymphocyte cultures contained populations co-expressing IL-2, IL-4 and IFN-γ.** Isolated T-PLL PBMC were cultured for 48h in the presence of the plate bound αCD3 (OKT3, 10µg/mL) and plate bound αCD28 (15E8, 20µg/mL). The cells were treated with Brefeldin A followed by intracellular staining for cytokines and flow cytometric analysis. **(A)** IL-2 positivity is compared in unstimulated cells (ctrl, green) to stimulated cells (αCD3 αCD28, red). **(B)** Shown is the expression of IL-4 and IFN-γ after stimulation of lymphocytes. IL-2 producing cells are marked in red.

IL-2 production was only transient and the numbers of IL-2 producing cells returned to baseline one week after stimulation with PHA. Interestingly, PHA stimulation elicited short term IL-4 production in 25% of T-lymphoid cells in 2 T-PLL cases analyzed. Repeated stimulation with PHA did not result in IL-4 or IFN-γ production. In addition, the proportion of IL-2 producing cells was slightly lower than the initial response in re-stimulated T-PLL cultures (Figure III.9.5-4).
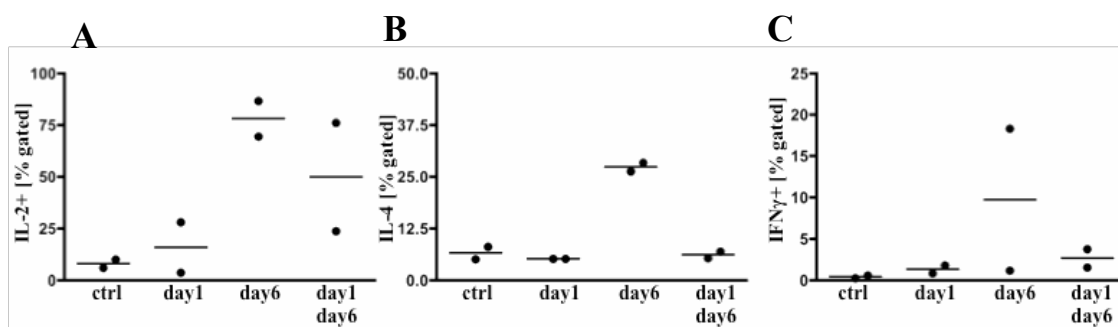
Figure III.9.5-4: **IL-2 was transiently expressed by >75% of T-PLL cells after short-term stimulation.** Isolated lymphocytes from n=2 T-PLL pB samples cultured in the presence of 10U/mL IL-2 were stimulated on the indicated timepoints with PHA (1µg/mL). Cytokine expression was measured after short term Brefeldin A treatment by flow cytometry on day 7. **(A)** IL-2 production is transiently induced after stimulation (day 6) and partially recovered after restimulation. **(B)** The number of IL-4 producing cells transiently increases after stimulation (day 6). Restimulation is not able to recapitulate this effect. **(C)** A modest and transient increase in IFN-γ producing cells was only observed in one case.

In summary, approx. 20% of T-cells in the peripheral blood of T-PLL patients had the ability to produce IL-2 in response to stimulation *ex vivo*. After prolonged stimulation or *in vitro* culture, which might be caused by the presence of FBS that also confers a stimulus to the cells, the percentage of T-PLL cells able to produce IL-2 increased to approx. 70%. Together with the up-regulation of the high affinity IL-2 receptor chain CD25 this might form a protective autokrine loop. IL-4 is only produced after prolonged times in culture and co-receptor stimulation or stimuli like PMA/iono that do not activate TCR proximal signaling. IFN- γ expression was only observed in one T-PLL case in 20% of cells in response to stimulation after prolonged *in vitro* culture.

III.9.6.   Expression patterns of cytokine and chemokine receptors on stimulated T-PLL cells

Cytokines and chemokines play a major role in controlling lymphocyte function, especially in the context of stimulation. T-PLL cells were shown to express high levels of the receptor for the homeostatic cytokine IL-7, CD127. Physiologically, CD127 is down-regulated in response to T-cell activation. To asssess, whether IL-7 might aberrrantly act as pro-survival factor also on activated T-PLL cells, CD127 expression was measured after stimulation of both the TCR cascade using PMA/ionomycin and a cytokine cocktail containing IL-7, because cytokine receptors are physiologically internalized after ligand binding. Both stimuli resulted in a virtually complete loss of CD127 surface expression (Figure III.9.6-1).
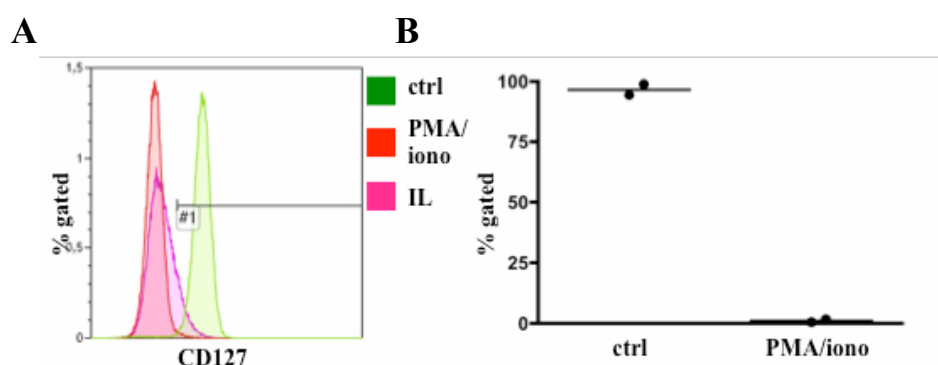
Figure III.9.6-1: **T-PLL cells lost CD127 expression upon stimulation.** Isolated T-PLL PBMC were stimulated for 48h with either 100ng/mL PMA plus 1mM ionomycin (PMA/iono) or IL-2, IL-4 and IL-7 (100U/mL each) and CD127 expression was measured by flow cytometry. **(A)** The overlay shows a comparison of CD127 expressing cells as percentage of CD5+ lymphocytes. **(B)** The quantification of CD127 after PMA/iono stimulation of two T-PLL cases shows a virtually complete loss in comparison to untreated (ctrl) cells.

Chemokine receptor expression is a major determinant of T-cell homing. After efficient activation of T-PLL cells by either TCR complex and co-receptor cross-linking or PMA/ionomycin both CCR3 and CCR4 showed a trend towards a higher percentage of positive cells. CCR5 was significantly induced by these stimuli (P = 0.0282). CXCR3 expression was elicited by TCR cross-linking by itself and further increased in the presence of CD28 coreceptor stimulation to statistical significance (P = 0.0044) (Figure III.9.6-2).

Analysis of stimulation-induced chemokine receptor expression on the single cell levels revealed co-expression of the chemokine receptors analyzed on T-PLL cells. Two T-PLL cases were analyzed for this and exemplary data is shown in Figure III.9.6-3. After a combination of TCR complex and co-receptor cross-linking, a 7-fold increase of CCR4 positive T-PLL cells was detected in the case depicted. 97% of the CCR4+ T-PLL cells co-expressed CCR3 (data not shown). The CCR3/CCR4 double positive population also contains virtually all CCR5 and CXCR3 double positive cells present in the culture after stimulation (Figure III.9.6-3).
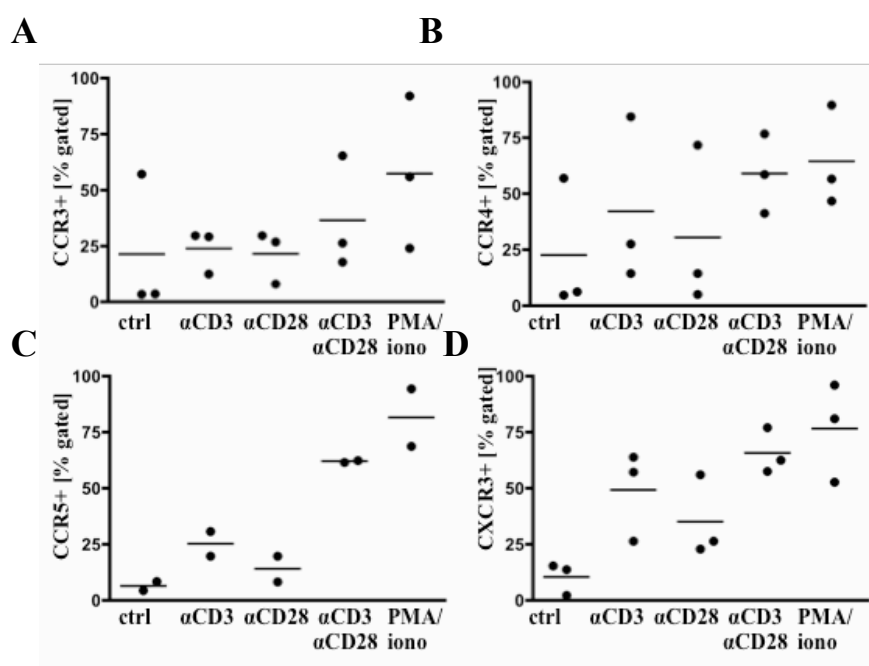
Figure III.9.6-2: **CCR3, CCR4, CCR5 and CXCR3 were up-regulated on T-PLL cells after activation of the TCR signaling pathway.** Isolated T-PLL PBMC were cultured for 48h in the presence of the indicated stimuli (plate bound αCD3 (OKT3, 10μg/mL), plate bound αCD28 (15E8, 20μg/mL), PMA (100ng/mL) and ionomycin (1mM)) and analyzed for receptor expression by flow cytometry. **(A)** CCR3 expression increases slightly after activation (n=3). **(B)** CCR4 shows a trend towards higher expression after stimulation (PMA/iono P = 0.017, n=3). **(C)** CCR5 expression increased in response to αCD3/ αCD28 treatment (P = 0.0282, n=2). **(D)** CXCR3 expression increased significantly after stimulation with αCD3/ αCD28 and PMA/iono treatment (P = 0.0044 and P = 0.0186, n=3, respectively).

151
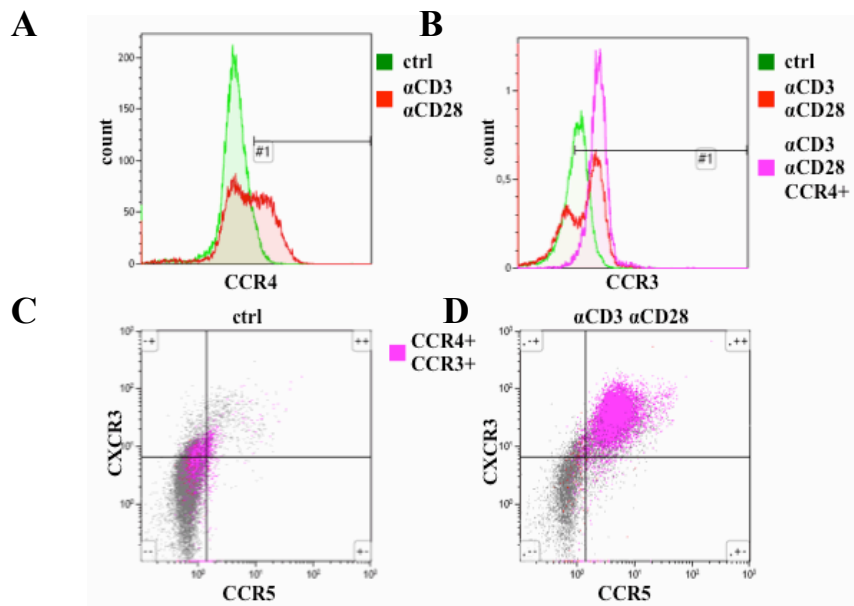
Figure III.9.6-3: **CCR4, CCR3, CCR5 and CXCR3 were co-expressed on T-PLL cells after αCD3/ αCD28 cross-linking.** Isolated T-PLL PBMC were cultured for 48h in the presence of plate bound αCD3 (OKT3, 10µg/mL) and αCD28 (15E8, 20µg/mL) and analyzed for receptor expression by flow cytometry. **(A)** The overlay shows an increased number of CCR4 expressing T-lymphocytes after stimulation. **(B)** Shown is a comparison of CCR3 positive cells after stimulation gated on CD5+ lymphocytes (red) and CCR4 positive T-lymphocytes (purple). **(C)** CCR5 and CXCR3 expression on untreated lymphocytes with CCR3+CCR4+ T-cells in depicted in purple. **(D)** After stimulation expression of CCR5 and CXCR3 is induced on cells also staining positive for CCR3+CCR4+ T-cells depicted in purple.

Homing to and exit from secondary lymphoid organs are crucial factors for efficient immune responses and are based on the tight regulation of homing receptor expression in response to T-cell activation. Previously, complex patterns of homing marker expression were shown on *ex vivo* T-PLL T-cells (III.4). Restimulation experiments showed that these expression patterns are not fixed but are dynamically regulated. CD44, which mediates homing to the bone marrow and has been utilized as an activation marker, showed a transient 5-fold increase in response to PHA stimulation. One week after activation, CD44 expression was back to baseline levels of CD44 high positivity in 8% of cells. Restimulation induced an 8-fold increase to 87% of highly expressing CD44 than over-night stimulation alone. CCR7 was expressed on virtually all T-PLL cells in the cases analyzed and seemed to be decreased slightly over a longer period of time after stimulation. CD62L was down-regulated from 91% positivity to 52% in response to stimulation and increased again to 75% CD62L positive T-PLL cells once the stimulus was removed. Taken together, the pattern of homing receptor expression observed after restimulation of T-PLL lymphocytes resembles that seen on effector memory T-cells (Figure III.9.6-4) [181].

A   **B**   **C**
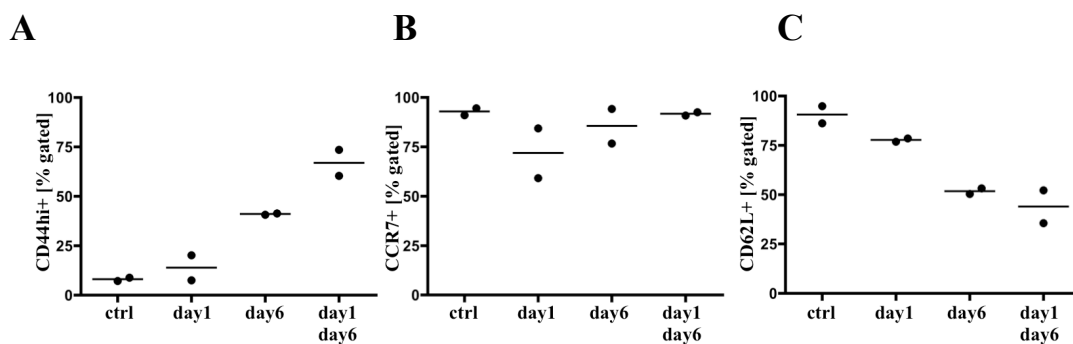
Figure III.9.6-4: The expression pattern of lymph node homing markers on T-PLL cells after repeated stimulation resembled that of effector memory T-cells. Isolated lymphocytes from n=2 T-PLL peripheral blood samples cultured in the presence of 10U/mL IL-2 were stimulated on the indicated timepoints with PHA (1µg/mL). Homing markers expression was analyzed by flow cytometry on day 7. **(A)** The percentage of cell expressing high levels of CD44 (CD44hi) increases transiently after stimulation and is further increased by restimulation. **(B)** CCR7 expression remains largely unaffected by repeated stimulation. **(C)** The proportion of CD62L expressing cells strongly decreases with repeated stimulation.

To establish the effect of T-cell stimulation on memory marker expression in comparison to homing receptor modulation in T-PLL, CD45RA and CD45RO expression intensity was measured in 2 T-PLL cases after repeated stimulation with PHA. Interestingly, CD45RO expression was unaffected by T-cell activation in T-PLL cells. CD45RA, on the other hand, was up-regulated on previously CD45RO single positive cells one week after primary activation and more so after restimulation, shifting the immunophenotype towards an unconventional CD45RA/CD45RO double positive phenotype (Figure III.9.6-5). The memory phenotype as judged by the expression of surface markers seems to retain at least some level of plasticity in T-PLL cells.
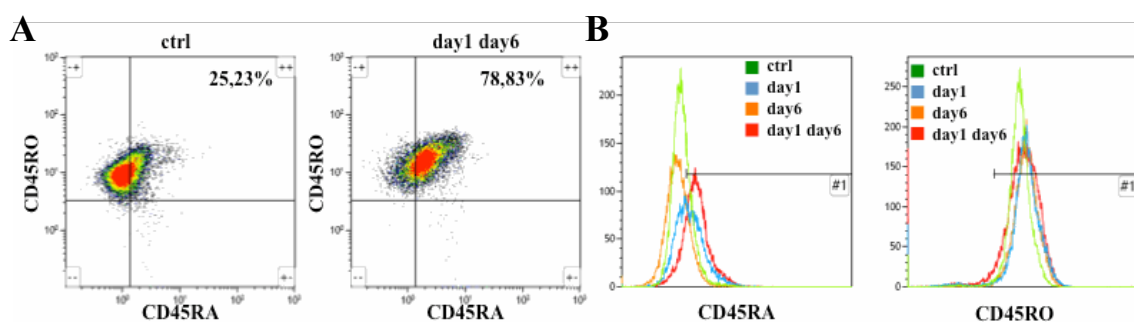
Figure III.9.6-5: CD45RA expression increased slightly after repeated stimulation of T-PLL cells. Isolated lymphocytes from n=2 T-PLL pB samples cultured in the presence of 10U/mL IL-2 were stimulated on the indicated timepoints with PHA (1µg/mL). CD45 isoform expression was analyzed by flow cytometry on day 7. **(A)** The proportion of CD45RA+ RO+ double positive cells increases 3-fold after repeated stimulation. **(B)** Direct comparison shows CD45RO levels to remain unaffected by stimulation, while CD45RA expression intensity increases over time after stimulation with an especially pronounced shift after repeated stimulation.

III.9.7. AKT and ERK kinase pathways were active in T-PLL cells after TCR stimulation

ERK is a known mediator of TCR-induced signals. AKT has also been implicated in T-cell activation and was shown to be influenced by TCL1 [72]. The standard method to detect phosphorylation as a sign of kinase activation is Western blotting. Unfortunately, this only allows for the analysis of cell populations. In order to assess if subpopulations seen in individual T-PLL samples show differential activation of the kinase pathways, a readout on the single cell level is necessary. This can be done by flow cytometry [106]. Therefore, the feasibility of detecting AKT and ERK phosphorylation by flow cytometry in primary T-PLL cells was investigated. Lymphocytes were isolated from one T-PLL peripheral blood sample and stimulated as described previously (Figure I.6.5-1). Phosphorylation of both AKT and ERK could be detected in response to stimulation. High ERK phosphorylation was sustained even a week after stimulation. Interestingly, upon restimulation of T-PLL cells over 20% of T-cells activated the pro-survival AKT pathway as judged by phosphorylation of AKT. Virtually all pAKT positive cells also showed ERK phosphorylation. Also, total ERK phosphorylation was increased more than 3-fold in comparison to the single stimulation conditions and more than two fold when looking at pERK single positive cells (Figure III.9.7-1). The analysis of subpopulations within the T-PLL population was impaired by stimulation induced changes to TCL1 protein expression (see chapter III.10.1).
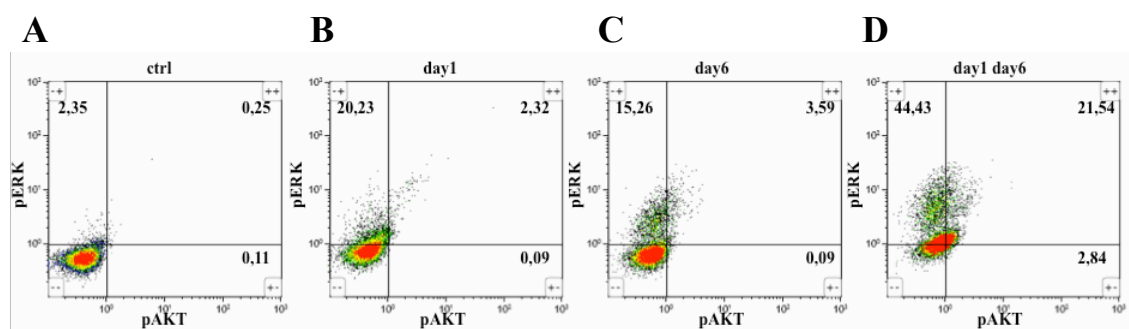
Figure III.9.7-1: Both AKT and MAPK signaling pathways were active after restimulation of T-PLL cells. Isolated lymphocytes from n=1 T-PLL pB samples cultured in the presence of 10U/mL IL-2 were stimulated on the indicated timepoints with PHA (1µg/mL). Phosphorylation status was analyzed by flow cytometry on day 7. **(A)** Shown are untreated T-PLL cells on day 7 of culture. **(B)** T-PLL cells were stimulated on day 1 and the stimulus removed after 24h. Protein phosphorylation was determined on day 7. **(C)** T-PLL cells were cultured for 6 days and then stimulated for 24h before determination of kinase phosphorylation. **(D)** The T-PLL cells were stimulated twice for 24h on day 1 and day 6. Flow cytometric analysis was performed on day 7.

In summary of III.9, T-PLL cells showed enhanced generation of the 2nd signaling messengers Ca^{2+} and ROS in response to TCR stimulation in comparison to T-cells from healthy donors. The activation markers CD25, CD38, CD44, and CD69 were upregulated after stimulation and T-PLL cells also showed signs of proliferation such as Ki67 expression and cell cycle progression. Stimulation of T-PLL cells *in vitro* induced the expression of both pro-survival and pro-apoptotic molecules (CD40L, BCL2, CD95, CD95L). The expression of the chemokine receptors CCR3, CCR4, CCR5 and CXCR3 increased in response to stimulation. Both CD127 and CD62L surface expression was reduced after stimulation of T-PLL cells. Production of IL-2 was observed in a subset of freshly isolated T-PLL cells after PMA/ionomycin treatment. IL-4 and IFN-γ could only be obseved after prolonged *in vitro* stimulation. T-PLL cells were more resistant to AICD after restimulation. The activation of the AKT and ERK pathways in response to PHA treatment could be measured by flow cytometry in primary T-PLL cells.

III.10. Dysregulation of TCL1 and the outcomes of TCR stimulation
III.10.1. TCL1 expression was dynamically regulated in T-PLL cells

Physiologically, TCL1 is silenced in peripheral T-cells by promoter hypermethylation [206]. In the majority of T-PLL cases TCL1 is constitutively expressed in T-PLL cells in the peripheral blood due to chromosomal aberrations bringing the TCL1 gene under the control of strong TCR α chain regulatory loci. For the analysis of TCL1 protein expression in T-PLL see chapter III.2. TCL1 expression levels were found to be modulated in T-PLL cells in response to activation of the TCR signaling cascade. Three T-PLL cases with comparatively uniform and high baseline TCL1 expression were analyzed in this respect. Two cases showed a strong and uniform up-regulation of TCL1 that was detected 24h after stimulation and decreased again slightly after 48h (data not shown). Stimulation resulted in homogenous up-regulation of activation markers, eg. CD69, in these cases (Figure III.10.1-1). The remaining T-PLL case showed a more complex pattern of TCL1 expression in response to stimulation (Figure III.10.1-1 B).

Overall, the expression intensity as judged by mean fluorescence intensity (MFI) in TCL1 decreased after TCR cross-linking in this T-PLL case. Expression analysis of CD69 revealed two populations after stimulation. 60% of lymphocytes showed an induction of CD69 with an accumulation of TCL1 high cells within this population. Virtually all CD69 negative cells showed a reduction in TCL1 expression intensity as

compared to untreated T-PLL cells. Taken together, activated T-PLL cells showed altered TCL1 protein expression.
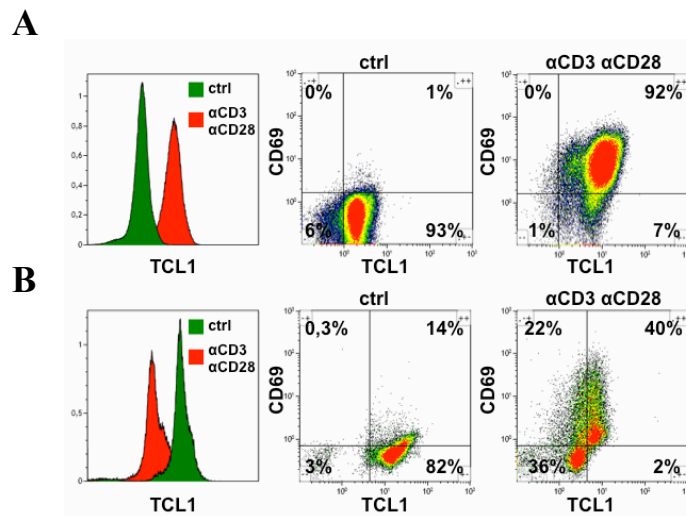
Figure III.10.1-1: **TCL1 expression was dynamically regulated in activated T-PLL cells upon TCR stimulation.** Isolated PBMC of n=3 T-PLL patients were stimulated for 24h with plate bound αCD3 (OKT3, 10µg/mL) and αCD28 (15E8, 20µg/mL) and analyzed for the expression of TCL1 and CD69 by flow cytometry. Plotted are the proportions of lymphocytes. **(A)** Exemplary measurement from two T-PLL cases showing strong and uniform increase in TCL1 expression upon stimulation. **(B)** One case displayed an overall loss in TCL1 expression intensity after stimulation. Analysis on the single cell level reveals two subpopulations, an activated population with high TCL1 expression and positive for CD69 and an population lacking CD69 and reduced TCL1 levels.

III.10.2. Effect of experimentally reduced TCL1 protein expression on primary T-PLL cells

III.10.2.1. Nucleofection was an efficient method to introduce siRNAs into primary T-PLL cells

To elucidate the functional effects of TCL1 expression in primary T-PLL cells in the peripheral blood, a siRNA-mediated knockdown strategy was applied. In a screening experiment 3 different siRNA sequences were introduced into T-PLL PBMC using the nucleofection technology comparing 2 different nucleofection programs. Already after 24h T-PLL cells transfected with each siTCL1 showed a reduction in the number of TCL1 positive T-PLL cells. The most efficienct program dependet on the siRNA sequence used, in the T-PLL case in Figure III.10.2-1 siTCL1-3 and program U were the most effective combination.
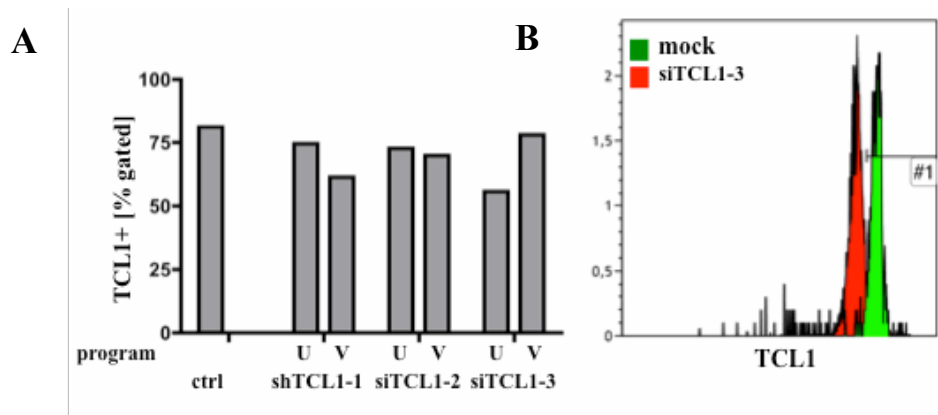
Figure III.10.2-1: Nucleofection of anti-sense RNAs targeting TCL1 lead to reduced TCL1 protein expression. Isolated T-PLL PBMC were transfected with siRNA targeting TCL1 or siRNA with a scrambled sequence. After 24h culture TCL1 expression levels were assessed by flow cytometry. **(A)** Depicted are cells gated as TCL1 positive. Cells were nucleofected with the different constructs and comparing 2 different nucleofection programms. Knockdown efficiency varied depending on construct and programm. **(B)** Comparison of TCL1 expression levels between mock transfected cells and cells transfected with siTCL1-3 using programm U shows a marked loss in fluorescence intensity after knockdown.

TCL1 knockdown in T-PLL PBMC from a second patient revealed that also the most efficient sequence is strongly donor-dependent. In this case, transfection with siTCL1-2 resulted in a loss of TCL1 positivity in about 50% of cells after 24h (Figure III.10.2-2).
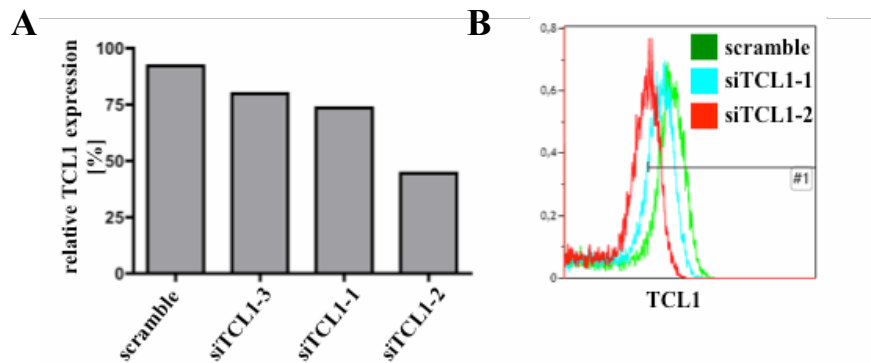
Figure III.10.2-2: **TCL1 protein expression intensity decreased up to 50% 24h after siRNA transfection.** Isolated T-PLL PBMC were transfected with either siRNA targeting TCL1 (see II.12 for details) or siRNA with a scrambled sequence. After 24h culture TCL1 expression levels were assessed by flow cytometry. **(A)** Relative TCL1 protein expression was calculated with reference to untransfected control T-PLL cells. Transfection with siTCL1-2 resulted in a marked decrease in fluorescence intensity. **(B)** Comparison of TCL1 expression intensity after transfection with siTCL1-1 or siTCL1-2 shows a marked loss of TCL1 especially after transfection with siTCL1-2.

This sample was used directly for further analysis, whereas the remaining samples were analyzed for TCL1 expression again 48h after transfection. After 48h efficient knockdown was observed also for the remaining two sequences (Figure III.10.2-3). Due to the high variability between cases, no standard knockdown procedure could be

157

established. Therefore, when available cell numbers allowed, all three siTCL1 sequences were transfected individually, TCL1 expression assessed at 24h and 48h after transfection and the T-PLL cells with the lowest remaining TCL1 expression levels were used for further analysis.
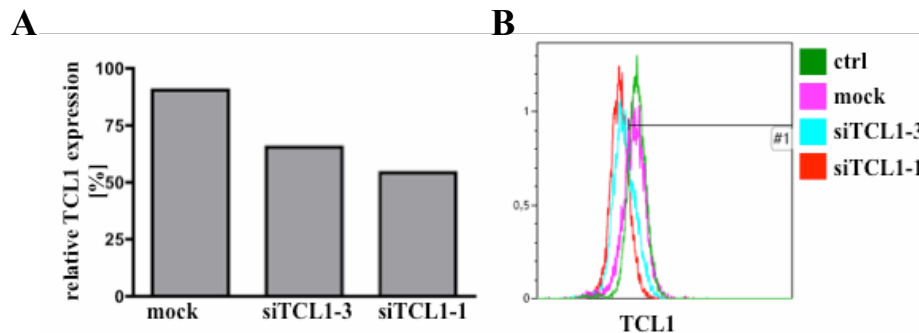
Figure III.10.2-3: **TCL1 protein expression intensity decreased further 48h after siRNA transfection.** Isolated T-PLL PBMC were transfected with either siRNA targetting TCL1 or mock transfected without siRNA. After 48h of culture TCL1 expression levels were assessed by flow cytometry. **(A)** Relative TCL1 protein expression was calculated with reference to untransfected control cells. Transfection with duplex siRNA with sequence 1 (duplex1) resulted in a marked decrease in fluorescence intensity. **(B)** Comparison of TCL1 expression intensity after transfection with either a duplex siRNA with scrambled sequence or two different sequences targetting TCL1 shows a marked loss of TCL1 after transfection with both siRNAs.

III.10.3. Modified TCL1 expression influenced 2nd messenger generation in T-PLL

The generation of second messengers in response to activation of the TCR signaling cascade was found to be altered in T-PLL cells as compared to healthy T-cells. To analyze the effect of TCL1 on TCR proximal signaling, the induction of Ca^{2+} flux in response to TCR cross-linking was measured in primary T-PLL cells 24h after TCL1 knockdown.

Modulation of TCL1 expression did not alter the response to unspecific lymphocyte stimuli like ionomycin, a Ca^{2+} ionophore used as positive control (data not shown), or PHA. Direct activation of the TCR signaling cascade by CD3 cross-linking resulted in an extensive increase in intracellular Ca^{2+} levels in mock transfected cells. In T-PLL cells with reduced TCL1 levels the Ca^{2+} response to TCR activation showed kinetics comparable to mock transfected T-PLL cells, the amplitude of the increase in intracellular Ca^{2+} levels, however, was reduced (Figure III.10.3-1).

A   **B**
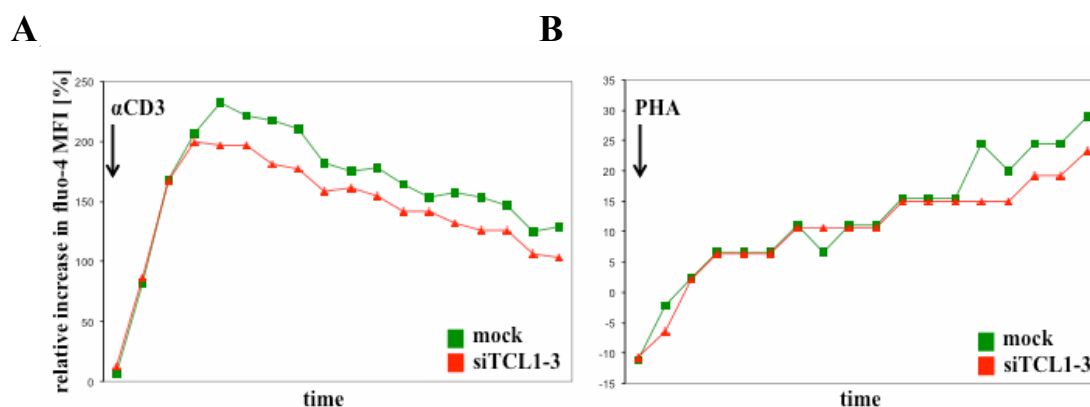
Figure III.10.3-1: TCR induced Ca^{2+} flux was reduced after TCL1 knockdown. TCL1 was knocked down by nucleofection and intracellular Ca^{2+} levels were measured flow cytometrically 24h later using fluo-4. Arrows demarcate the timepoint of stimulus addition. Shown are representative data from n=2 patient samples. **(A)** T-PLL lymphocytes show a strong increase in intracellular Ca^{2+} after TCR cross-linking with αCD3 (OKT3 10μg/mL). In cells with reduced TCL1 levels (siTCL1-2) the amplitude of the response is slightly lower. Shown is a representative measurement of the T-PLL case shown in Figure III.10.1-2. **(B)** No differences in response are observed after stimulation with PHA (1μg/mL).

When ROS generation was assessed after T-lymphocyte stimulation in T-PLL cells after down-modulation of TCL1 expression, no differences between mock transfected and TCL1 knockdown T-PLL cells were detected. Of note, baseline levels of ROS were increased about 2-fold in resting T-PLL cells after TCL1 knockdown (Figure III.10.3-2).

A   **B**
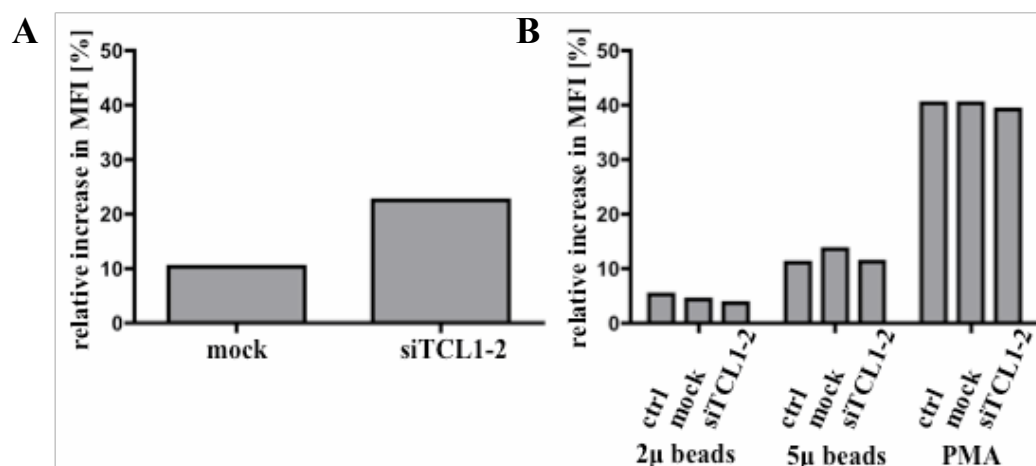
Figure III.10.3-2: **Steady state ROS levels increased after TCL1 knockdown whereas ROS generation in response to stimulation was unaffected.** 24h after TCL1 knockdown T-PLL lymphocytes (n=1) were loaded with the ROS indicator dye H$_2$DCFDA and stimulated as indicated with bead bound αCD2 αCD3 αCD28 or 100ng/mL PMA for 20min and ROS content was assessed on a single cell level. **(A)** Mean fluorescence intensity of H$_2$DCFDA is markedly increased after TCL1 knockdown. **(B)** Plotted is the percentual increase as compared to unstimulated cells. No differences were observed between untransfected cells (ctrl), cells transfected without siRNA (mock) and cells transfected with siRNA targetting TCL1 (siTCL1-2).

In summary, TCL1 expression levels affected the increase in intracellular Ca^{2+} levels after TCR stimulation, but not ROS generation. However, TCL1 expression mediated some effect on baseline ROS levels, as baseline ROS levels increased upon loss of TCL1 expression.

III.10.4. TCL1 targeting siRNA partially counteracted the effect of TCR stimulation on TCL1 expression levels

TCL1 expression was shown to be regulated in response to antigen receptor stimulation (III.10.1). To further analyze the effect of TCL1 down-regulation in the context of T-cell stimulation, first the effect of stimulation on TCL1 levels in both mock- and siRNA transfected cells was compared.

CD3 cross-linking by itself and also in combination with CD28 costimulation resulted in distinct up-regulation of TCL1 protein expression levels. Transfection with siRNAs targeting TCL1 counteracted this effect to about 50% after CD3 single stimulation but could not efficiently block up-regulation after αCD3/ αCD28 stimulation. Interestingly, PMA/ionomycin stimulation led to a marked loss of TCL1 in untreated control T-PLL cells. After knockdown-induced down-regulation of TCL1 expression levels, PMA/ionomycin caused a marked up-regulation in TCL1 again, contrary to the effect observed in untransfected control T-PLL cells (Figure III.10.4-1).
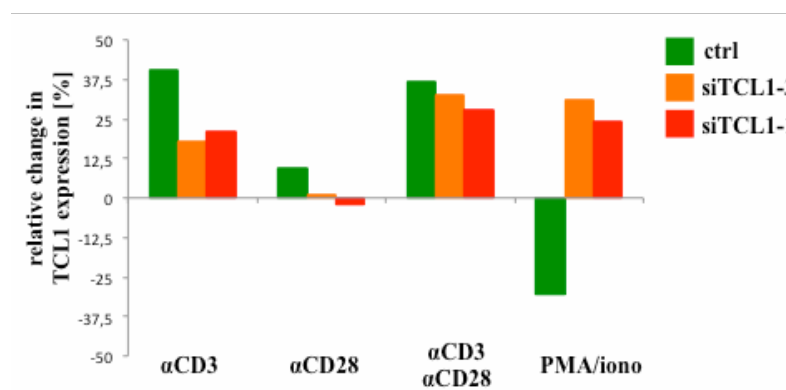
Figure III.10.4-1: Down regulation of TCL1 after knockdown was counteracted by T-cell stimulation. Isolated T-PLL PBMC (n=1) were transfected with siRNA targetting TCL1. Cells were stimulated 24h after transfection with the indicated combinations of αCD3 (OKT3, 10μg/mL), αCD28 (15E8, 20μg/mL), PMA (100ng/mL) and ionomycin (1mM). TCL1 expression was assessed by flow cytometry 24h after stimulation and 48h after knockdown. Up-regulation of TCL1 after TCR cross-linking with αCD3 is diminished after siRNA transfection. Costimulation with αCD28 in addition to αCD3 rescues TCL1 up-regulation. Strong TCR signaling induced by PMA/iono results in decreased endogenous TCL1 levels (ctrl), while TCL1 expression shows a marked increase in the knockdown samples.

III.10.5. Stress-induced down-regulation of Ki67 was counteracted by TCL1 knockdown

Nucleofection of T-PLL cells even under optimized culture conditions subjects the cells to a considerable amount of stress resulting in a loss of viability and an altered response to stimulation.
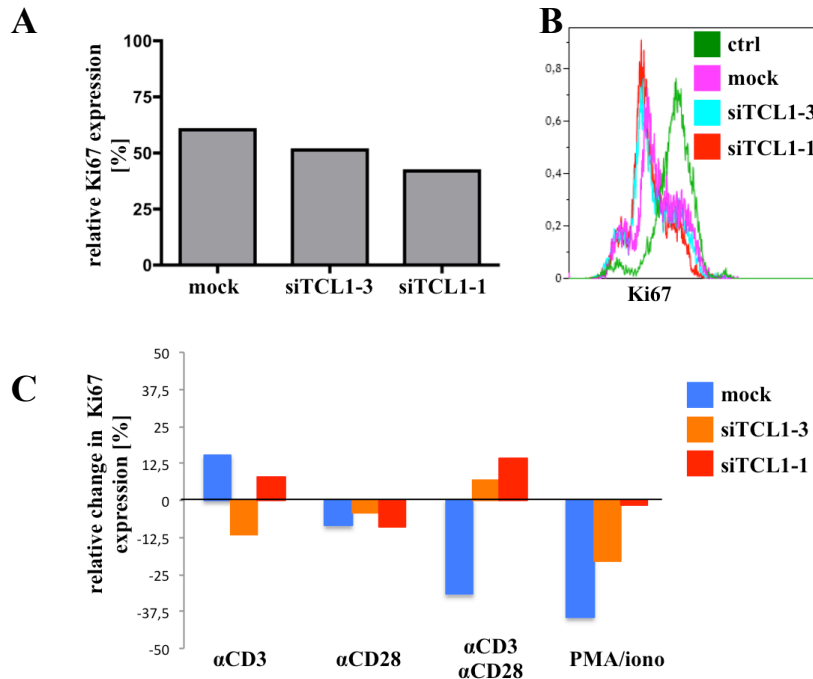
Figure III.10.5-1: Nucleofection-induced loss of Ki67 expression was prevented by experimental TCL1 down-regulation. Isolated T-PLL PBMC (n=1) were transfected with either siRNA targeting TCL1 or mock transfected without siRNA. Cells were stimulated 24h after transfection with the indicated combinations of αCD3 (OKT3, 10μg/mL), αCD28 (15E8, 20μg/mL), PMA (100ng/mL) and ionomycin (1mM). Ki67 expression was assessed by flow cytometry 24h after stimulation and 48h after knockdown. **(A)** Mean fluorescence intensities were compared and the Ki67 expression on unstimulated untransfected T-PLL cells was set to 100%. **(B)** T-PLL T-cells were gated based on CD45 and CD5 expression and Ki67 expression levels for untransfected (ctrl, green), mock transfected (mock, purple), siTCL1-3 (turquoise) and siTCL1-1 (red) without stimulation. **(C)** Changes in MFI for Ki67 compared to unstimulated untransfected T-PLL cells (ctrl) were compared.

Baseline expression of Ki67 showed a 60% reduction after mock nucleofection alone. In T-PLL cells with reduced TCL1 expression Ki67 reached only 50% of the expression intensity of untreated T-PLL cells (Figure III.10.5-1). Interestingly, after nucleofection cross-linking of the TCR complex only induced a modest 1.15-fold induction of Ki67. Stimulation of mock transfected cells with αCD3/ αCD28 and PMA/ionomycin resulted in Ki67 levels of 68% and 60% of untreated T-PLL cells, respectively. TCL1 knockdown counteracted this Ki67 loss. T-PLL cells nucleofected with TCL1 siRNA

showed a 1.14-fold increase in Ki67 expression levels. When taking into account that TCL1 levels were actually increased in the knockdown samples in response to αCD3/αCD28 stimulation, TCL1 could in this case confer a protective effect.

III.10.6. TCL1 knockdown enhanced activation marker expression after stimulation

To further assess the response to stimulation of T-PLL cells after reduction of TCL1 expression levels activation marker expression was measured 48h after siRNA transfection and 24h after stimulation. Of note, neither CD25 nor CD38 did show the expected pattern of up-regulation in response to TCR activation after nucleofection and were therefore excluded from this analysis (data not shown).

CD69 expression was virtually absent after nucleofection. Activation of the TCR cascade by either cross-linking of CD3 or PMA/ionomycin treatment induced CD69 expression in over 50% of cells. CD28 costimulation did not influence CD69 positivity. TCL1 knockdown enhanced the CD69 up-regulation in resonse to TCR activation, resulting in 77% CD69+ cells after αCD3/αCD28 stimulation (Figure III.10.6-1).
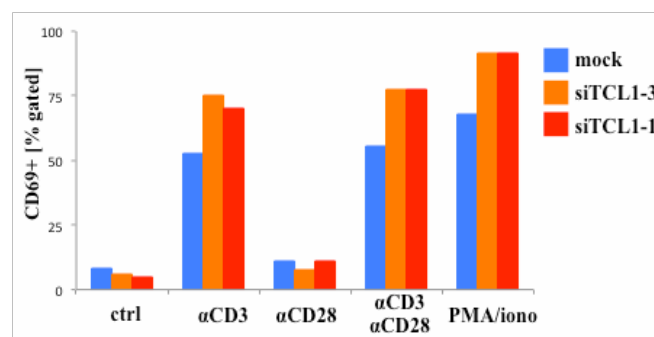
Figure III.10.6-1: The stimulation-dependent increase of CD69 positive cells was enhanced by TCL1 knockdown. Isolated T-PLL PBMC (n=1) were transfected with either siRNA targetting TCL1 or mock transfected without siRNA. Cells were stimulated 24h after transfection with the indicated combinations of αCD3 (OKT3, 10μg/mL), αCD28 (15E8, 20μg/mL), PMA (100ng/mL) and ionomycin (1mM). CD69 expression was assessed by flow cytometry 24h after stimulation and 48h after knockdown. Shown are CD69+ cells as percentage of CD5+ T-PLL cells.

Homing receptors are dynamically regulated in response to T-cell activation and showed distinct expression patterns in T-PLL. CD44 regulates both immune cell migration and memory T-cell function and has been used as an activation marker. Upon TCL1 down-regulation CD44 showed a trend towards lower expression levels. In mock transfected cells CD44 expression remained unaffected by stimulation. After TCL1

knockdown activation of the TCR signaling pathways induced a very distinct up-regulation of CD44. As CD3 cross-linking and PMA/ionomycin stimulation had a comparable effect, again TCR proximal signaling seems to be dispensable for the effects on CD44 expression by modulated TCL1 expression levels (Figure III.10.6-2).
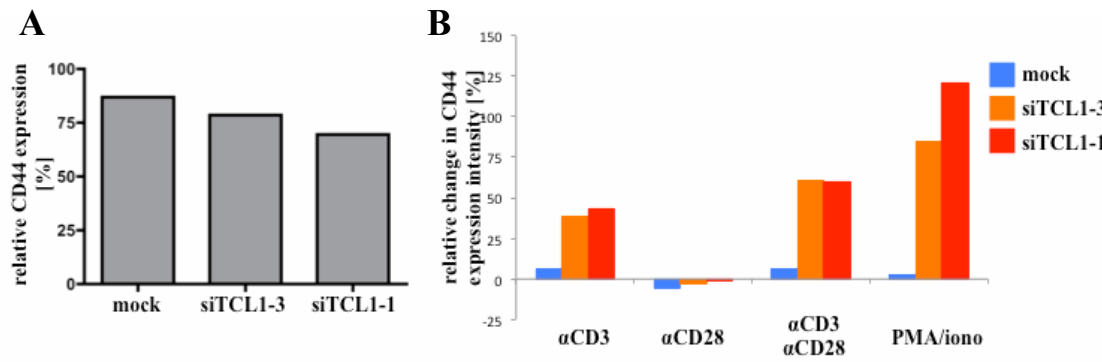
Figure III.10.6-2: The αCD3/ αCD28 induced CD44 up-regulation was enhanced after TCL1 knockdown. Isolated T-PLL PBMC (n=1) were transfected with either siRNA targetting TCL1 or mock transfected without siRNA. Cells were stimulated 24h after transfection with the indicated combinations of αCD3 (OKT3, 10µg/mL), αCD28 (15E8, 20µg/mL), PMA (100ng/mL) and ionomycin (1mM). CD44 expression was assessed by flow cytometry 24h after stimulation and 48h after knockdown. **(A)** Mean fluorescence intensities were compared and the CD44 expression on unstimulated untransfected T-PLL cells was set to 100%. **(B)** Shown are CD44+ cells as percentage of CD5+ T-PLL cells for the stimulation and transfection conditions indicated.

In summary of chapter III.10, primary TCL1 positive T-PLL cells showed altered TCL1 protein expression after stimulation by TCR and co-receptor cross-linking. Whether stimulation resulted in an up- or down-regulation of TCL1 protein levels was donor-dependent. The efficiency of experimental down-regulation of TCL1 protein expression by nucleofection of siRNA into primary T-PLL cells derived from the peripheral blood was also strongly donor dependent with respect to optimal siRNA sequence and nucleofection conditions. Nevertheless, a 50% reduction of TCL1 protein expression could be reached. TCL1 knockdown could only partially abrogate the stimulation-induced increase in TCL1 protein expression. TCL1 down-regulation led to an reduced Ca^{2+} flux after TCR cross-linking and resulted in increased steady-state ROS levels in the T-PLL cells. Nucleofection prevented T-PLL cells from up-regulating activation and proliferation markers in response to stimulation. The presence of siRNAs targeting TCL1 rescued expression of CD44 and CD69 at least in part. Experimental down-regulation of TCL1 is feasible and hints at a role for TCL1 in regulating the cellular response to TCR pathway activation.

III.11. Main novel findings of the present work

- Loss of the pan-leukocyte marker CD45 was frequently observed in T-PLL

- Loss of sCD3 expression on T-PLL cells was accompanied by more frequent CD4 expression

- Although infrequent, oligo-clonality exists in clinical samples of T-PLL

- The detection of TCL1 expression on a single cell level by multi color flow cytometry is feasible

- TCL1 protein expression showed variability within individual T-PLL samples

- TCL1 protein expression was dynamically up- and down-regulated in primary T-PLL cells in response to stimulation in a donor-dependent manner

- TCL1 oncogene expression correlated strongly with surface expression of CD25 and CD127

- T-PLL cells of individual donors showed heterogeneous T-memory cell marker expression

- The most common pattern of memory marker expression was the unconventional T_{EM}-like CD45RA- CD45RO- CD62L- CCR7-/+ phenotype

- T-PLL cases clustered into three classes based on memory phenotype: I) T_{EMRA},II) T_{EM}-like, and III) transitional/mixed

- CD4/CD8 expression did not show statistically significant correlations with memory or functional features of the T-PLL cases analyzed

- No T_H1 or T_H2 phenotype could be assigned to T-PLL cells as no typical chemokine receptor expression patterns nor production of IL-4 or IFNγ could be observed directly *ex vivo*. In few cases prolonged *in vitro* culture and stimulation under non-skewing (no differentiation) conditions induced IL-4 production

- T-PLL cells readily responded to T-cell receptor stimulation by second messenger generation, IL-2 production, and proliferation

- T-PLL cells were (partially) resistant to AICD

- Experimental down-modulation of TCL1 levels reduced Ca^{2+} flux after TCR stimulation

IV. Discussion:

IV.1. TCL1 flow cytometry facilitates diagnosic approaches to T-PLL

IV.1.1. Diagnostic relevance of flow cytometry and challenges of T-PLL diagnosis

The WHO classification of haematopoietic malignancies firmly established immunophenotyping and molecular genetics as important aspects in the diagnostic workup of lymphoid neoplasms in addition to morphological analysis [198]. Multi color flow cytometry is of particular importance not only for initial diagnosis but also for disease monitoring and detection of minimal residual disease (MRD) [34]. The subclassification of PTCL/L by flow cytometry, however, is hindered by a lack of disease-specific markers. Also, PTCL/L do not show the characteristic immunophenotypic profiles found in B-cell neoplasias but are more often characterized by a loss of certain T-cell specific markers. Therefore, the identification of disease specific markers or marker combinations would greatly facilitate the subclassification of PTCL/L [34].

This is especially true for T-PLL. Like most other mature T-cell neoplasias, T-PLL is predominantly CD4 positive and shows no distinctive features that are captured by current routine flow cytometry. Especially the distinction between T-PLL and SS is difficult to accomplish by flow cytometry alone as shown for example by the Euroflow initiative [210]. In addition, the morphological appearence of T-PLL cells often closely resembles Sézary cells and also the clinical features show a significant overlap. On the other hand, a considerable overlap of presenting features has also been shown for CD8 positive T-PLL and T-LGL [71].

The scope of the present work was to utilize 10-colour flow cytometry to define a characteristic T-PLL immunophenotype and to investigate the feasibility of flow cytometric analysis of the T-PLL associated marker TCL1.

IV.1.2. Flow cytometric detection of TCL1 significantly aids in T-PLL diagnostics

In the present study, TCL1 was detected for the first time in T-PLL whole blood samples by multi color flow cytometry. A directly labelled TCL1 antibody was included into a panel of markers routinely used also in diagnostic panels. Sample preparation was performed using a protocol that is also used routinely for diagnostic panels (eg. detection of ZAP-70 in CLL samples). Taken together, direct TCL1 staining as part of a

diagnostic multi color flow cytometry panel is feasible and might aid in the diagnostics of T-PLL and blastic plasmacytoid dendritic cell neoplasm (BPDCN) and risk-stratification of CLL.

TCL1 expression was detected by flow cytometry in 67% of T-PLL cases (III.2). Matutes et al. detected chromosomal aberrations involving the TCL1 gene locus in 76% of patients [135]; however, they did not interrogate TCL1 protein levels. In a study by Herling et al. TCL1 was detected on a three-tier score by immunohistochemistry. Dim or high TCL1 expression was found in >75% of cases [72]. It would be interesting to assess whether the TCL1-negative T-PLL cases in the present study carry aberations of chromosome 14 or express TCL1 mRNA. There is evidence of a loss of TCL1 protein expression in a T-PLL case with a chromosomal translocation t(14;14) aberration in the TPLL1 study (data not shown, Hopfinger et al. [78]). A loss of TCL1 protein expression over the course of the disease or a t(14;14) without TCL1 protein expression might explain the comparatively low proportion of TCL1 positive T-PLL cases in this work.

TCL1 expression in T-PLL was expected to be consistently high and stable in T-PLL, as TCRα regulatory loci have been shown to overrule physiological silencing of the TCL1 gene [80]. Interestingly, TCL1 expression levels varied greatly between T-PLL patients and carried prognostic information as T-PLL patients with lower TCL1 levels showed a significantly longer progression-free survival in response to FMC-A (III.2.2). In addition, data presented in this study shows that TCL1 can be dynamically regulated in T-PLL cells in response to stimulation, again suggesting an additional level of regulation (III.10.1).

Most interestingly, in a substantial proportion of T-PLL cases TCL1 levels displayed distinct intratumoral variation. Often populations differing in TCL1 expression also showed differential expression of at least one T-cell associated marker. Usually, however, these populations moved along an expression continuum of the markers and shared distinct functional features like activation marker expression or cytokine production.

In summary, the detection of TCL1 by flow cytometry was feasible and sensitive, but by itself not sufficient to identify all T-PLL cases. However, detection of TCL1 expression might aid in therapeutic decisions.

In the patient cohort analyzed in the present study, in 32% of T-PLL cases the T-PLL cells showed decreased CD45 expression intensity (III.1.2). This has been reported previously as a common sign of malignant T-cells and has also been described in a few T-PLL/T-CLL cases [61]. Also, a reduction in CD45 expression intensity has been shown to occur in acute large cell lymphoma and both up- and down-regulation of CD45 expression was reported in peripheral T-cell lymphoma [85, 98].

CD45 has been implicated in the regulation of signal transduction downstream of the TCR [225]. CD45 contains an intracellular phosphatase domain that removes inibitory phosphate residues from Srk family kinases, thus enabling their activation [75]. Additional reports have also shown lck activity to be elevated in the absence of CD45 [23]. In a mouse model generated by Baker et al. the authors conclusively show how a loss of CD45 expression contributes to the development of leukemia by further enhancing the activity of a constitutively active Lck^{F505}, which by itself is not sufficient for oncogenic transformation [9]. Accordingly, the observed loss of CD45 expression on primary T-PLL cells might be a mechnism to enhance signaling by the TCR and to lower the activation threshold in these cells.

In addition, 4% of T-PLL cases showed a loss of CD5 surface expression (III.1.3). Aberrant expression of CD5 is a common feature of T-LGL [127] but with the exception of one isolated CD5 negative T-PLL case, this phenomenon has not been shown in a larger T-PLL patient cohort yet.

In the present study 80% of cases were found to be surface CD3 positive and 93% showed strong expression of CD7 (III.1.3). These results fit well with the published data of two large cohorts of T-PLL patients from Matutes et al. [135] (78 patients) and Herling et al. (57 patients) [71] that was later on extended further to 86 patients [72]. Of note, CD7 is also described to be highly expressed in T-PLL [60] in near 100% of cases [71] and to be lost only in rare cases [53]. Even though in the prestent study CD7 expression levels could not be quantified due to technical limitations of the experimental setup, several subpopulations differing in CD7 expression levels were identified within the malignant populations as judged by TCL1 positivity in at least 4 cases. This indicates that CD7 is not as uniformly highly expressed as previously thought and might even be dynamically regulated over the course of disease.

Loss of CD7 was previously shown to occur at a late stage of T-cell memory differentiation [168]. These cells have a high activation threshold and are sensitive to AICD, both funtional features that are not shared by T-PLL cells.

With regard to CD4 and CD8 T-cell subset markers, 65% of cases were single positive for CD4, 15% stained single positive for CD8. Co-expression of CD4 and CD8 was found in 20% of cases (III.1.4). This fits very well with data published by Matutes et al. and Herling et al. [135, 71]. Both Matutes and Herling report the incidence of CD4 single positivity to be around 60%. The T-PLL patient cohort presented here is comparable to the patient collective described by Matutes et al., where 13% of cases were CD8 single positive, while in the cohort described by Herling et al. this group only amounted to 4% of cases. The same holds true for CD4/CD8 double positive T-PLL cases (Matutes et al. CD4+CD8+: 21%, Herling et al. CD4+CD8+: 35%).

The typical T-PLL immunophenotype previously reported is CD3+/- CD5+ CD7+ CD4+/- CD8 -/+. In the present work, loss of CD45 expression was shown as additional common feature of T-PLL. TCL1 was previously known as a specific marker for T-PLL when detected in mature T-cells. However, this is the first study showing TCL1 detection by flow cytometry in a large patient cohort. In this way, TCL1 expression can be assessed in the same sample tube as the T-PLL marker panel described above, thus streamlining the diagnostic procedure.

IV.2. T-PLL cells showed an unconventional and novel memory phenotype
IV.2.1. T-cell leukemias can be assigned to certain stages of T-cell development based on surface marker expression

It was shown previously that nodal peripheral T-cell lymphomas correlate with physiolgical subsets of mature T-cells [177]. Detection of both, markers for T-cell differentiation but also activation markers by immunohistochemistry, was applied before to analyze cases of AITL, ALCL and peripheral T-cell lymphoma not otherwise specified (PTCL-nos) [59]. It was shown that AITL and ALCL correspond to the effector T-cell subset (CD45RA+ CD45RO- CD27-), whereas a subgroup of PTCL-nos corresponds to T_{CM} (CD45RA- CD45RO+ CD27+). In previous work by Lee et al. AITL had already been described as a disease of CD2+ CD3+ CD4+ CD5+ CD7- mature helper T-cells [117]. Recent work also shows that cutaneous T-cell lymphomas

are derived from distinct T-cell subsets. For a leukemic presentation of CTCL, Sézary syndrome, a typical phenotype corresponding to T_{CM} characterized by CCR7 positivity and CD27 expression was detected. Mycosis fungoides cells in contrast do not express the lymph node homing markers CD62L and CCR7, instead they stain positive for the skin homing markers CCR4 and CLA, a phenotype correlating to T_{EM} [25]. With regard to mature T-cell leukemias T-LGL is the best characterized entity with regard to immunophenotype [144]. T-LGL carries a phenotype of CD45RA+ CD45RO- CD27- CD28- CCR7-, which equals the appearance of effector T-cells and is common for all large granular leukemias. CD62L expression is absent in this entity [121].

IV.2.2. The memory phenotype of T-PLL was variable with the largest patient subset displaying a CD45RA- C45RO- CD62L- CCR7-/+ (transitional memory-like) phenotype

For T-PLL, a memory phenotype (CD45RA- CD29+ CD45RO+) has been described by Matutes et al. in 41% of analyzed T-PLL cases [135]. Herling et al. found 60% of their T-PLL cohort to express CD45RO [72]. Of note, the less frequent naïve CD45RA phenotype was reported by others associated with an improved prognosis over memory phenotype T-PLL [170, 53]. All previously described T-PLL patient cohorts describe a proportion of cases that cannot be ascribed to the traditional CD45RA single positive naïve and CD45RO single positive memory classification. Not even the analysis of additional markers like CD29 could solve this conundrum [135]. Therefore, in the present study a more elaborate panel of markers identified to be differentially expressed according to T-cell memory subgroups was applied (II.7.3.3). Surprisingly, 54% of the T-PLL cases in this study expressed neither CD45RA nor CD45RO. This finding accompanies the loss of CD45 expression detected in >30% of T-PLL peripheral blood samples analyzed.

A lack of CD62L expression and only infrequent positivity for CCR7 on the T-PLL cases in this cohort point towards a restricted ability to home to draining lymph nodes. CCR7 was shown to be up-regulated on antigen-experienced effector memory T-cells in response to TCR stimulation [179]. Taken together, this indicates a similarity between T-PLL cells and effector memory T-cells.

In the cases that did express CD45 isoforms and that showed a homegenous expression of memory markes, a T_{EMRA} phenotype was the most commonly observed (CD45RA+

CD45RO- CCR7- CD62L-. For the T-PLL cases that could not be categorized along the conventional memory subsets due to a loss of CD45, surrogate categories were introduced (Table III.4-1). The most common of these phenotypes were T_{EM}-like (CD45RA- CD45RO- CCR7- CD62L-) and transitional T-cell-like (CD45RA- CD45RO- CCR7+ CD62L-). Further cluster analysis of all T-PLL cases within the present study revealed these three memory subsets described above to best define the three memory classes the T-PLL cases clustered into (III.4.2.3). The T_{EMRA} class characterized in this study by single positivity for CD45RA probably corresponds to the CD45RA supposedly naïve T-PLL cases described by Matutes et al. and Herling et al. [72, 136, 170]. The T_{EMRA} memory T-cell subset is distinguished from naïve T-cells by the absence of CD62L and CCR7 expression. Both markers were assessed on T-PLL cells for the first time in this study. Based on these results, no real "naïve" T-PLL cells could be identified, firmly establishing T-PLL as a disease of memory T-cells.

IV.2.3. T-PLL cells did not show functional characteristics of T_H1 or T_H2 cells

Functionally, the present study showed for the first time that a large proportion of T-PLL cells were able to produce IL-2 but not IL-4 or IFN-γ after *ex vivo* stimulation. Continuous stimulation over 48h increased the number of IL-2 producing cell to virtually 100% and also induced T_H2 like T-cell subsets co-expressing IL-4. These features recapitulate the cytokine producing capabilities of memory T-cells in that these cells are readily able to produce IL-2 but need time to differentiate in order to produce IL-4 or IFN-γ. The production of IL-4 and IFN-γ are usually thought to be mutually exclusive. In T-PLL, co-expression of both T_H1 and T_H2-type cytokines indicates that T-PLL cells might not be permanently primed towards one helper T-cell fate.

Among the chemokine receptors investigated besides CCR7, CCR4 and CXCR4 were the only ones consistently expressed on significant proportions of the T-PLL population. In comparison to T-cells from healthy donors, however, CXCR4 expression was markedly reduced. CCR3, CCR5 and CXCR3 were found only rarely on small subsets of T-PLL cells. The high incidence of CCR4 positive T-PLL cases together with the ability to produce IL-4 but not IFN-γ might indicate a bias towards T_H2 priming in T-PLL [173]. Monoclonal antibodies targeting CCR4 have found their way into the clinic for the treatment of CCR4 positive lymphoma via direct killing [88, 111, 83].

Given the high penetrance of CCR4 positivity in T-PLL, these agents might be a feasible opportunity for the treatment of chemotherapy-refractory T-PLL.

CCR4 is expressed on a major proportion of memory T-cells in the peripheral blood, thus underscoring the memory character of T-PLL cells. Recent work by Rivino et al. identified CCR4 positive memory cells as a distinct non-polarized subset among central memory T-cells with the propensity to produce low levels of IL-4 [173]. T-PLL cells might well reflect this central memory subset.

CXCR4 is widely expressed in the immune system and in the mature T-cell compartment. It shows high expression on naïve cells, intermediate but generally positive expression in the central memory subset and is down-regulated in effector memory cells [64]. The decreased frequency of CXCR4 positive T-cells in peripheral blood samples fits well with the concept of a effector memory nature of T-PLL cells. CXCR4 has been established as therapeutic target for example in CLL, where the receptor seems to play a role in mobilizing cancer cells from their protective niche [22]. Given the high and constitutive expression of CXCR4 on a subset of T-PLL cases, treatment with CXCR4 antagonists might be a promising approach to support treatment by debulking nodal tumor manifestations in the liver, spleen or lymph nodes. By "flushing out" the tumor cells into the peripheral blood, T-PLL cells might become more amenable for treatment with conventional multi-agent chemotherapy.

Analysis of expression patterns of CCR3, CCR5 and CXCR3 in PTCL/L revealed a certain degree of heterogeneity within tumor entities [112, 88] which is also observed for T-PLL in the work presented here. Re-evaluation of the data generated and presented here using comprehensive bioinformatic data extraction methods might yield information on how the subsets of CCR3, CCR5 and CXCR3 positive T-PLL cases differ functionally and immunophenotypically.

Further proof, however, that the fate of T-PLL cells is not entirely fixed and that they are still capable of differentiating *in vitro* is based on the the observation, that chemokine receptors not expressed in the resting state are up-regulated in response to TCR cross linking. This holds true for CCR3, CCR4, CCR5 and CXCR3. Interestingly, these receptors are co-expressed after activation of T-PLL cells. On naïve T-cells CXCR3 is not expressed but quickly up-regulated in response to stimulation. In contrast, CCR4 and CCR5 are only acquired over a prolonged period of time on proliferating T-cells, especially CCR3 is usually only expressed after prolonged

proliferation of T-cells under T_H2 skewing conditions [179, 112]. While CCR3, CCR4, CCR5 and CXCR3 are expressed on memory T-cells depending on their prior polarization, after stimulation memory T-cells rapidly down-regulate CCR3, CCR5, and CXCR3 [223, 179]. These complex regulation patterns are not reflected in stimulated T-PLL cells where control of chemokine receptor expression appears less finely tuned. The broad up-regulation of chemokine receptors might provide a means for T-PLL cells to gather pro-survival signals from the microenvironment to sustain activation-induced proliferation.

IV.2.4. The pattern of cytokine receptor expression on T-PLL cells recapitulates that seen on resting T-cells

The prevalent cytokine receptor expression pattern on primary T-PLL cells observed in this study was CD122- CD124- CD127+. This reflects the most frequently detected pattern of cytokine receptor chain expression in the T-cell compartment of healthy donors. Physiologically, CD127 is highly expressed on resting naïve and peripheral memory T-cells and was recently implicated as a marker of long living memory T-cells [81]. In response to T-cell activation CD127 is down-regulated while CD122 and CD124 are up-regulated in turn [174]. CD124 expression, while high in double positive thymocytes, is low but positive on recent thymic emmigrants, providing more evidence that T-PLL cells are not comparable to late thymic T-cell subsets [202].

The loss of CD127 on the surface of T-PLL cells was observed accordingly after stimulation. Together with the absence of CD62L, the positivity of T-PLL cells for CD127 indicates that primary T-PLL cells in the peripheral blood are phenotypically similar to resting effector memory T-cells. The functional down-regulation of CD127 on T-PLL cells in response to stimulation rules out an aberrant protective role of IL-7 receptor expression as contributing factor in T-PLL pathogenesis. However, the physiologic shut down of IL-7 signaling in T-PLL remains to be investigated. Of note, double positive thymocytes are CD127-, thus the cytokine receptor pattern observed on T-PLL cells is not indicative of a late actual thymic origin. Interestingly, the percentage of CD127 positive cells displayed a broader distribution among T-PLL cases compared to healthy donors [156]. This suggests that T-PLL cells might undergo stimulation by self-peptide MHC complexes or gamma family cytokines *in vivo*. CD127 expression levels regulate IL-7 consumption and IL-7 availability in turn affects CD127 expression

levels [138]. In a future study both a direct comparison of CD127 expression levels on T-PLL cells and T-cells from healthy donors as well as an analysis of serum IL-7 levels in T-PLL patients should be performed to further characterize the role of IL-7 in T-PLL.

The data presented in this work indicate that T-PLL is a disease of often CD45 low or negative memory T-cells. At least a small subset of T-PLL cases seem to be primed towards an IL-4 producing T_H2 type. Functionally, the prolonged period of *in vitro* stimulation these cells require for IL-4 production is more indicative of a central memory character. Nevertheless, T-PLL cells do not easily fit into the conventional classification scheme of healthy T-cells.

IV.2.5. T-PLL cases with an activated phenotype formed a distinct T-PLL subset

One subset of T-PLL cases was characterized by a high proportion of T-PLL cells expressing markers of early activation such as CD25 or CD69. In addition, subsets of patients with increased numbers of Ki67 positive mitotically active cells and BCL2 positive cells in the peripheral blood T-lymphoid compartment were identified. Delgado et al. describe two T-PLL cases differing in activation status and show a much higher sensitivity to purine analogues in a T-PLL case with an activated phenotype [39]. Herling et al. on the other hand found no clear correlation between expression of activation markers and aggressive disease features [72].

Of note, a high frequency of CD69 positive cells in a T-PLL sample correlated with sCD3 and TCR expression, therefore indicating that the activation status of T-PLL cells is dependent on TCR mediated signaling processes. CD25 expression strongly correlated with TCL1 expression, indicating that TCL1 might enhance these signaling processes (Table III.7-1). CD25 positivity is common in the CD4 positive HTLV-induced AITL [34] and has also been observed in CTCL cells of skin and peripheral blood [89]. The frequency of 31% and the medium-high incidence of CD25 positive cells (CD25 expression intensity per cell was not determined as part of this work) with which CD25 was shown to be expressed in T-PLL in this work puts the use of CD25 as a "specific" marker for AITL into perspective and highlights the need for comprehensive marker panels for flow cytometry in this context. It also justifies the experimental study of the CD25 directed immunotoxin denileukin diftitox (ONTAK) in T-PLL.

173

The data presented here provide evidence of an activated phenotype in 37% of T-PLL cases. These patients could easily be identified by routine flow cytometry and might benefit more than the general T-PLL patient population from treatment with purine analogues as first line treatment.

IV.2.6. The sCD3 negative T-PLL cells expressed CD4

As the surface expression of CD3 and the TCR heterodimer are directly linked [66] one can assume that sCD3- cases do not express a TCR on the cell surface, either, although experimental proof has not been given in T-PLL. CD5 might be down-regulated in these cells to make up for the loss of upstream signals by lowering the activation threshold. In the present study sCD3 negative T-PLL cases were all exclusively CD4 positive. As CD4 lineage commitment is generally believed to depend on a stronger TCR induced signal than CD8 expression, CD3 loss might be a secondary event happening after CD4 lineage commitment. Given the fact that CD8 expression is more variable and seems more dynamically regulated, it stands to reason that also sCD3- CD4/CD8 double positive T-PLL cases develop from initially CD4 single positive cells. However, three CD/CD8 double positive T-PLL cases reported by Mizuki et al. strengthen the possibility of a late thymic origin from double positive thymocytes. The authors found T-PLL cells to display CD4+ CD8 αβ, an immunophenotype characteristic for thymic cells. Taken together with negativity for TdT, CD1a and recombination activating gene-1 (RAG-1) the authors claim a late thymic origin of the disease [146]. In case reports the existence of two or more malignant populations differing in their immunophenotype has been described in T-PLL. Dührsen et al. present the case of a patient with A-T [43]. The leukemic cells in the peripheral blood of this patient were heterogeneous in that one third displayed a CD4-CD8+ cytotoxic phenotype and the majority showed double positivity for CD4 and CD8. The tumor subsets did not differ on the chromosomal level and showed similar responsiveness to stimulation. Furthermore, the ratio of the two populations stayed constant even in face of changing WBCs and responded comparably to chemotherapy. Therefore, the authors argue in favor of the retained capacity of the malignant clone for further differentiation.

However, as molecules such as CD5 are known to modulate signal transduction of the TCR cascade and CD4 positive T-cells show differential reactions to stimulation

compared to CD8 positive T-cells, further studies investigating the activation response in these CD3+/- and CD4+ vs. CD8+ T-PLL subsets are of great interest.

IV.3. Overt T-PLL is a clonal disease with striking intratumoral heterogeneity

IV.3.1. Both TCL1 and memory marker expression were heterogenous within individual T-PLL cases

The work presented here shows for the first time an analysis of TCL1 expression on the single cell level in the peripheral blood of T-PLL patients. This revealed differences in TCL1 protein expression levels between T-PLL subpopulations within individual samples. In addition, data presented in this study shows that TCL1 can be dynamically altered in T-PLL cells in response to stimulation, again suggesting an additional level of regulation. These complex patterns of TCL1 expression in T-PLL indicate the need to perform further functional studies using appropriate experimental models to investigate the functional role of TCL1 in T-PLL. The work presented here for example showed the feasibility of siRNA-mediated down-regulation of TCL1 protein levels in primary T-PLL cells.

This so called intratumoral heterogeneity became also very obvious with respect to the epression of T-cell memory markers in T-PLL. In 45% of T-PLL cases in this study two or more T-cell memory subpopulations coexist within the T-PLL cell population. This might be an indication of T-PLL cells not experiencing any developmental block and hints at their ability to further differentiate, an idea already brought up in earlier case studies [43]. However, it also raised the question of the clonality of the T-PLL cells in general. For other T-cell lymphoma / leukemia entities phenomena such as the preferential use of certain TCR chains as well as a phenotypic drift with regards to TCR Vβ chain expression or a skewing of the TCR repertoire in the parallel normal T-cell compartment has been described [220].

Earlier work on this topic in T-PLL showed monoclonality without exception in a collective of 11 cases of chronic lymphocytic leukemias of the T-cell lineage that were classified into T-CLL and T-PLL based on aggressiveness [50]. In a second publication two additional T-cell CLL cases, one CD4- CD8+, one CD4 CD8 double negative were analyzed for intratumoral heterogeneity of TCR Vβ chain expression. The leukemic

clones showed expression of only one Vβ chain, Vβ 8.1 and Vβ 6.9 respectively, without any additional mutations [162].

The work presented here drastically increased the number of T-PLL cases reported to be analyzed for clonality based on protein expression of TCR Vβ families. In 34% of analyzed T-PLL cases a clonal expansion of T-PLL cells was proven, with Vβ2 and Vβ12 being the Vβ families most often detected. Further studies are needed to elaborate if this slight bias in TCR Vβ family usage might point towards a bias of TCR specificities in T-PLL. For CLL the identification of recurrent BCR specificities was highly useful to evaluate the contribution of BCR signaling to disease development [207]. Preferential use of certain Vβ chains has been previously described in T-LGL as well as a phenotypic drift over the course of disease [31]. A skewing of the TCR repertoire was observed in CTCL [220]. Taken together, these findings indicate a certain plasticity in TCR Vβ chain expression and the existence of specific (auto)antigens or self-MHC as drivers of disease.

Interestingly, in 34% of T-PLL cases the T-PLL cells did not react with any of the Vβ antibodies available. This is taken as a sign of clonality. The lack of detectable TCR Vβ expression coincides with a lack of CD3 surface expression. However, the available Vβ antibody repertoire covers only approx. 70% of TCR Vβ families. Therefore, the high incidence of T-PLL clones that failed to react might also be indicative of a skewing of Vβ family usage toward a Vβ family not tested for. Analysing TCR Vβ usage by methods of molecular genetics to assign these T-PLL cases to a certain Vβ family would be highly interesting.

Two noteworthy cases were described in the present T-PLL patient cohort. In one case two TCR Vβ families could be detected within the T-PLL cell population. Malignant derivation of the T-cell was shown by aberrant expression of CD4 and CD8. It can be assumed that in this T-PLL case the disease either developed from two independent T-cell clones or that there is an *in vivo* shift with regard to TCR Vβ usage. This kind of phenotypic shift has already been described for T-LGL [31]. The authors described that in a cohort of 71 T-LGL patients, 37% of cases showed a change in the dominant Vβ chain. In these cases, the dominant malignant clone shrank in size, while a second clone with differing Vβ specificity took over.

For T-PLL the presented findings indicate that T-PLL might be a disease affecting the whole T-cell repertoire. The chromosomal aberrations causing a dysregulation of TCL1

expression might occur in early precursor T-cells, accounting for the variability and retention of plasticity observed in T-PLL, while secondary events are necessary for full leukemic development. It would be highly informative to perform longitudinal studies in such a case in order to observe how these clones develop further.

The second noteworthy observation with regard to clonality in T-PLL was an unvonventional case where the T-PLL clone stained positive for two independent Vβ families, Vβ1 and Vβ16. Usually, allelic exclusion at the Vβ loci ensures that only a single Vβ chain is expressed on any given T-cell [212]. Failures of this process resulting in the expression of two different Vβ chain in a single T-cell have been reported previously [155, 37]. Little is known about the functional consequences of dual TCR expression for T-cell signaling and also for the immune response.

In the presented T-PLL patient cohort no predominance of certain Vβ families could be detected. However, the presence of two Vβ specificities in a single T-PLL case hints towards either an oligoclonal nature of the disease or a phenotypic drift over the course of the disease. Future studies following TCR Vβ utilization in T-PLL patients are needed to explain the observed phenomenon.

IV.4. The TCR cascade and the outcome of its activation in T-PLL is skewed to promote cell survival

IV.4.1. T-PLL showed hyperactive 2nd messenger generation after TCR stimulation

TCR signaling has been implicated as driving pathogenic force in the development of T-cell malignancies. Only recently, defective TCR proximal signaling and a block in 2nd messenger generation has been shown to prevent apoptosis in cutaneous T-cell lymphoma (CTCL) cells [101]. Therefore, 2nd messenger generation in response to TCR cross-linking on T-PLL cells was investigated. In striking contrast to CTCL cells, that show impaired Ca^{2+} release and reduced generation of ROS upon TCR stimulation [101], both 2nd messengers are significantly increased in T-PLL cells after activation. Based on this it is fair to assume that the TCR proximal signaling pathway leading to PLCγ activation in T-PLL cells is functional and once induced is highly active. The data presented here also show that TCL1 expression directly correlates with intracellular Ca^{2+} levels after TCR cross-linking (III.10.2). In previous work Herling et al. showed an recruitment of TCL1 into membrane bound activation induced TCR-kinase complexes

177

[72]. This hints towards a role for TCL1 as an enhancer of TCR proximal signaling strength for example by inhibiting negative regulatory effects or by stabilizing kinase complexes.

While ROS generation in response to TCR activation was significantly higher in T-PLL cells than in T-cells from healthy donors, alteration of TCL1 levels had no effect on this. Experimentally reduced TCL1 expression levels did, however, correlate with higher steady state ROS levels, thus implicating TCL1 in the control of the intracellular redox equilibrium.

IV.4.2. In a subset of T-PLL CD28 costimulation had a unique inhibitory effect

To date an inhibitory effect of CD28 costimulation on 2nd messenger generation in response to TCR activation has not been reported. In about one third of T-PLL cases analyzed, CD28 cross-linking in addition to CD3 ligation resulted in lower intracellular Ca^{2+} levels than CD3 cross-linking alone. In single T-PLL cases a decrease in intracellular ROS levels was observed if the TCR was stimulated in presence of CD28 costimulation. However, regulation of Ca^{2+} influx and ROS generation by CD28 seemed to rely on independent mechanisms, as cases were observed in which CD28 had an inhibitory effect on Ca^{2+} levels but not ROS generation. It is conceivable that perturbations of the activation threshold or kinase activity by TCL1 might affect also the consequences of CD28 costimulation. Due to the low number of T-PLL cases available for functional studies, no conclusions about the interrelation between TCL1 and CD28 can be drawn based on the data presented here. Future studies should address this question for example by overexpressing TCL1 in Jurkat T-cells, a cell line where both the signaling cascade induced by TCR cross-linking as well as the CD28 dependent signaling events have been characterized in detail.

IV.4.3. T-PLL cells were activated in response to TCR stimulation implying interference with this pathway as a potential therapeutic approach

Previous studies on the response of T-PLL or T-CLL cells to TCR activation have been anecdotal in nature by usually only reporting on one or two patients and contradictory in their findings [125, 102]. The present study showed consistent up-regulation of the activation markers CD25, CD38, CD69 within 24h after CD3 cross-linking in 6 patient samples. CD25 and CD69 were lost within a week after stimulation while CD38 was

increased over the whole 7d period of observation. In addition, an increase in mitotic activity as judged by Ki67 positivity was found as well as cell cycle progression in all three samples analyzed. Taken together, this study provides compelling evidence that the TCR signaling cascade in T-PLL cells is intact and able to transduce pro-proliferative signals. Even though the anti-apoptotic protein BCL-2 was increased after stimulation, CD95 and CD95L were also induced and might counteract the positive effects of TCR cross-linking. Loss of viability might also be a consequence of a lack of supportive factors that are provided *in vivo* by the microenvironment.

Further analysis is needed to identify which of these factors are crucial for survival and proliferation of T-PLL cells. Nevertheless, seeing that the TCR signaling cascade is functional and highly active after stimulation interference with the TCR signaling cascade looks like a promising treatment approach. The TCR signaling cascade is highly dependent on tyrosine kinases, making interference with this class of enzymes a promising therapeutic approach. The tyrosine kinase inhibitor Dasatinib, an Imatinib derivative, shows a strong efficacy in inhibiting Src kinases and the therapeutic efficacy is being tested in PTCL/L [116]. Other downstream kinases under investigation are cyclin-dependent kinases (flavopiridol) and PKCβ (enzastaurin) [166]. Proteasome inhibition has been shown to efficiently down-modulate NF-kappa B activity. The proteasome inhibitor Bortezomib shows considerable activity in hematologic malignancies and the strong dependence of PTCL/L on the NF-kappa B pathway makes Bortezomib an interesting candidate in T-PLL. Limited data are already available showing promising results [154].

IV.4.4. Defective AICD induction as a possible underlying pathogenic mechanism in T-PLL

The CD95 axis is of special importance in the regulation of AICD. In T-LGL a resistance to CD95 mediated apoptosis was identified as a pathologic mechanism [111]. CD95 was found to be widely expressed on primary T-PLL cells. This corresponds to physiological CD95 expression in the T-cell compartment which is high on CD45RO positive memory T-cells and virtually absent on CD45RA positive unprimed cells [111, 67]. CD95L was only rarely and dimly expressed on T-PLL cells. The expression of both molecules increases upon stimulation and especially the increased expression of CD95 is stable and protracted. While repeated stimulation was able to induce cell death

in T-PLL cells, the observed apoptosis rate was significantly lower than in T-cells from healthy donors. Increased viability after repeated stimulation of T-PLL cells might be a central mechanism contributing to the accumulation of tumor cells.

The distinct proliferative response and resistance to AICD correlate with a marked increase in phosphorylation of ERK, a major player in the mitogenic MAP kinase pathway, directly after T-PLL cell stimulation. After restimulation of T-PLL cells we observed the activation of the anti-apoptotic kinase AKT in addition to ERK, which might confer protection against AICD on the molecular level.

The high proportion of T-PLL cells that readily produce IL-2 implicates a role for autocrine IL-2 signaling for the survival and proliferation of T-PLL cells *in vivo*. In addition, IL-2 is indispensable for AICD. A lack of IL-2 is, therefore, unlikely to be the cause of the reduced propensity to undergo AICD observed in T-PLL cells.

Therefore, increased AICD resistance seems to be a central pathological mechanism in T-PLL. In order to exploit this knowledge for therapeutic intervention, further functional studies are needed to define the mechanism responsible for the pro-survival phenotype of T-PLL cells.

IV.5. Summary and Outlook

In this work, the flow cytometric detection of TCL1 in peripheral blood samples was shown to be feasible. In future clinical studies it would be interesting to see, if the existence of subpopulations differing in TCL1 levels in individual T-PLL samples changes over time and if this contains prognostic information.

With respect to the existence of two T-PLL clones as judged by TCR Vβ chain expression observed in one T-PLL case in this study, expanding this analysis to a greater sample number and to repeated measurements per sample would provide insights, whether T-PLL is indeed of oligoclonal origin or whether there is a clonal drift over the course of disease or after cytoreductive treatment. Aligment with molecular (PCR-based) data on the TCR Vβ repertoire is additionally usefull in this [224].

The majority of T-PLL cases in this work could not be assigned to conventional T-cell memory categories. However, for the two subsets of T-PLL cases characterized by a T_{EM} and a T_{EMRA} immunophenotype, respectively, it would be of great interest to assess if these groups also show characteristic clinical features.

The data presented here indicate a role of TCR-mediated activation and a reduced susceptibility to AICD in the pathogenesis of T-PLL. However, further functional studies also in a murine T-PLL model are needed to fully understand the biological and clinical relevance of this finding.

Zusammenfassung

Die T-Zell prolymphozytische Leukämie (T-PLL) ist eine seltene, aber sehr aggressiv verlaufende Erkrankung, deren pathobiologischer Hintergrund bislang nur unzureichend verstanden wird. Die aberrante Expression des Onkogens T-cell leukemia 1 (TCL1) wird als Auslöser angesehen. Ziel dieser Arbeit war es, eine gesunde T-Zellpopulation zu definieren, die immunphänotypisch malignen T-PLL Zellen entspricht. Darüberhinaus sollten funktionelle Charakteristika der T-PLL Zelle identifiziert werden. Dazu wurde eine umfassende Immunphänotypisierung von n=53 T-PLL Blutproben durchgeführt. Rückschlüsse auf die Stimulierbarkeit der T-PLL Zellen durch Aktivierung des T-Zellrezeptors (TZR) wurden anhand von Messungen sekundärer Botenstoffe und der Expressionsanalyse von Aktivierungsmarkern gezogen. Außerdem wurden der durch Stimulation ausgelöste Zelltod und die Zellteilung untersucht. Um die funktionelle Relevanz der TCL1 Expression in primären T-PLL Zellen zu testen, wurde die TCL1 Expression mittels siRNA unterdrückt. Eine deutliche Heterogenität der TCL1 Expression wurde innerhalb von Blutproben einzelner Patienten beobachtet. In 32% der untersuchten Fälle entsprach auch die Expression von CD45 nicht dem physiologischen Muster. Auffällig war die Existenz einer bisher nicht beschriebenen CD45RA- C45RO- CD62L- CCR7-/+ Population in 52% der Fälle. Die Klonalität der T-PLL Population konnte in 68% der Fälle durch die durchflusszytometrische Bestimmung der Vβ Expression bestätigt werden. Ein Patient zeigte eine oligoklonale T-PLL Population und in einem weiteren Fall exprimierten die T-PLL Zellen zwei unterschiedliche TZR Vβ Ketten. Die Bildung reaktiver Sauerstoffradikale sowie der Anstieg der intrazellulären Ca^{2+} Konzentration nach T-Zell Aktivierung war stärker in T-PLL als in gesunden T-Zellen. Wurde die TCL1 Expression jedoch experimentell verringert, so wurde auch der Stimulations-abhängige Anstieg der Ca^{2+} Konzentration abgemildert. T-PLL Zellen zeigten eine rasche und robuste Expression von Aktivierungsmarkern nach Stimulation. Außerdem traten diese Zellen schnell in den Zellzyklus ein und waren in der Lage, Interleukin-2 zu produzieren. Darüberhinaus waren T-PLL Zellen deutlich weniger sensitiv gegenüber aktivierungsinduziertem Zelltod als gesunde T-Zellen. Diese Eigenschaften repräsentieren möglicherweise einen zentralen pathophysiologischen Mechansimus bei der Entstehung der T-PLL.

Summary

T-cell prolymphocytic leukemia (T-PLL) is a rare and understudied mature T-cell tumor with an aggressive clinical course. Aberrant expression of the T-cell leukemia 1 (TCL1) oncogene is thought to play a causative role. In order to elucidate the underlying pathogenic mechanisms in T-PLL it was aimed to assign a "normal counterpart" and to discern functional features, especially in the context of T-cell receptor (TCR) signalling, distinguishing T-PLL cells from healthy T-cells. To this end, extensive immunophenotyping of peripheral blood samples of up to n=53patients with T-PLL, including also functional readouts, was performed. Responsiveness to TCR cross-linking was judged with respect to second messenger generation, up-regulation of activation markers as well as induction of proliferation and apoptosis. To assess the functional impact of TCL1 expression in primary T-PLL cells, siRNA-mediated knockdown experiments were performed. We observed a distinct intra-tumoral heterogeneity with regard to TCL1 expression. In addition, TCL1 levels were altered in response to TCR- and co- receptor stimulation. In 32% of the analyzed cases CD45 expression was found to be dysregulated. The immunophenotype of T-PLL was very heterogeneous. Nevertheless over 52% of T-PLL samples contained subpopulations displaying a novel and unconventional CD45RA- C45RO- CD62L- CCR7-/+ phenotype. Clonality was proven based on Vβ chain usage in 68% of T-PLL cases. Interstingly, one T-PLL case turned out to be oligoclonal, while another case expressed two different Vβ chains on the T-PLL cells. Generation of reactive oxygen species and increase in intracellular Ca^{2+} levels in response to TCR cross-linking were enhanced in T-PLL cells as compared to T-cells from healthy donors. The increase in intracellular Ca^{2+} induced by TCR cross-linking was blunted upon TCL1 siRNA-mediated knockdown, implicating a role of TCL1 in TCR proximal signaling. Up-regulation of activation markers was fast and robust in T-PLL cells. Following stimulation T-PLL cells readily entered the cell cycle and were able to produce IL-2. In addition T-PLL cells were found to be only weakly susceptible to activation-induced cell death, possibly hinting at a central pathogenetic mechanism. Overall, T-PLL cells appeared phenotypically similar to memory T-cells, a subset known for its high sensitivity towards stimulation. In addition, the activating TCR signalling cascade was shown to be highly active. The presented data also support a role of TCR-induced proliferation and a block in cell death induction as a central pathogenetic mechanism in T-PLL.

V.   References

1.   Aifantis I, Raetz E, Buonamici S (2008) Molecular pathogenesis of T-cell leukaemia and lymphoma. Nat Rev Immunol 8(5):380–390

2.   Alves NL, van Leeuwen EMM, Derks IAM, van Lier RAW (2008) Differential regulation of human IL-7 receptor alpha expression by IL-7 and TCR signaling. J Immunol 180(8):5201–5210

3.   Andrew DP, Ruffing N, Kim CH, Miao W, Heath H, Li Y, Murphy K, Campbell JJ, Butcher EC, Wu L (2001) C-C chemokine receptor 4 expression defines a major subset of circulating nonintestinal memory T cells of both Th1 and Th2 potential. J Immunol 166(1):103–111

4.   Andrian von UH, Mempel TR (2003) Homing and cellular traffic in lymph nodes. Nat Rev Immunol 3(11):867–878

5.   Anikeeva N, Sykulev Y (2011) Mechanisms controlling granule-mediated cytolytic activity of cytotoxic T lymphocytes. Immunol Res 51(2-3):183–194

6.   Arrol HP, Church LD, Bacon PA, Young SP (2008) Intracellular calcium signalling patterns reflect the differentiation status of human T cells. Clin Exp Immunol 153(1):86–95

7.   Baaten BJG, Li C-R, Deiro MF, Lin MM, Linton PJ, Bradley LM (2010) CD44 regulates survival and memory development in Th1 cells. Immunity 32(1):104–115

8.   Baggiolini M (1998) Chemokines and leukocyte traffic. Nature 392(6676):565–568

9.   Baker M, Gamble J, Tooze R, Higgins D, Yang FT, O'Brien PC, Coleman N, Pingel S, Turner M, Alexander DR (2000) Development of T-leukaemias in CD45 tyrosine phosphatase-deficient mutant lck mice. EMBO J 19(17):4644–4654

10.   Barlage S, Rothe G, Knuechel R, Schmitz G (1999) Flow cytometric immunophenotyping of mature lymphatic neoplasias using knowledge guided cluster analysis. Anal Cell Pathol 19(2):81–90

11.   Beach DD, Gonen RR, Bogin YY, Reischl IGI, Yablonski DD (2007) Dual role of SLP-76 in mediating T cell receptor-induced activation of phospholipase C-gamma1. J Biol Chem 282(5):2937–2946

12.   Boise LH, Minn AJ, Noel PJ, June CH, Accavitti MA, Lindsten T, Thompson CB (2010) CD28 costimulation can promote T cell survival by enhancing the expression of Bcl-xL. Immunity. 1995. 3: 87-98. J Immunol 185(7):3788–3799

13.   Bonecchi R, Bianchi G, Bordignon PP, D D'Ambrosio, R Lang, A Borsatti, S Sozzani, P Allavena, P A Gray, A Mantovani, and F Sinigaglia (1998) Differential expression of chemokine receptors and chemotactic responsiveness

of type 1 T helper cells (Th1s) and Th2s. J Exp Med 187(1):129–134

14. Boothby M, Mora AL, Aronica MA, Youn J, Sheller JR, Goenka S, Stephenson L (2001) IL-4 signaling, gene transcription regulation, and the control of effector T cells. Immunol Res 23(2-3):179–191

15. Borst J, Coligan JE, Oettgen H, Pessano S, Malin R, Terhorst C (1984) The delta- and epsilon-chains of the human T3/T-cell receptor complex are distinct polypeptides. Nature 312(5993):455–458

16. Boyman O, Létourneau S, Krieg C, Sprent J (2009) Homeostatic proliferation and survival of naïve and memory T cells. Eur J Immunol 39(8):2088–2094

17. Boyton RJ, Altmann DM (2002) Is selection for TCR affinity a factor in cytokine polarization? Trends in Immunology 23(11):526–529

18. Brandt VL, Roth DB (2009) Recent insights into the formation of RAG-induced chromosomal translocations. Adv Exp Med Biol 650:32–45

19. Brito-Babapulle V, Catovsky D (1991) Inversions and tandem translocations involving chromosome 14q11 and 14q32 in T-prolymphocytic leukemia and T-cell leukemias in patients with ataxia telangiectasia. Cancer Genetics and Cytogenetics 55(1):1–9

20. Brito-Babapulle V, Maljaie SH, Matutes E, Hedges M, Yuille M, Catovsky D (1997) Relationship of T leukaemias with cerebriform nuclei to T-prolymphocytic leukaemia: a cytogenetic analysis with in situ hybridization. Br J Haematol 96(4):724–732

21. Brunning RD (1991) T-prolymphocytic leukemia. Blood 78(12):3111–3113

22. Burger JA (2010) Chemokines and chemokine receptors in chronic lymphocytic leukemia (CLL): from understanding the basics towards therapeutic targeting. Semin Cancer Biol 20(6):424–430

23. Burns CM, Sakaguchi K, Appella E, Ashwell JD (1994) CD45 regulation of tyrosine phosphorylation and enzyme activity of src family kinases. J Biol Chem 269(18):13594–13600

24. Campbell JJ, Murphy KE, Kunkel EJ, Brightling CE, Soler D, Shen Z, Boisvert J, Greenberg HB, Vierra MA, Goodman SB, Genovese MC, Wardlaw AJ, Butcher EC, Wu L (2001) CCR7 expression and memory T cell diversity in humans. J Immunol 166(2):877–884

25. Campbell JJ, Clark RA, Watanabe R, Kupper TS (2010) Sezary syndrome and mycosis fungoides arise from distinct T-cell subsets: a biologic rationale for their distinct clinical behaviors. Blood 116(5):767–771

26. Cao TM, Coutre SE (2003) T-cell prolymphocytic leukemia: update and focus on alemtuzumab (Campath-1H). Hematology 8(1):1–6

27.   Carpenter AC, Bosselut R (2010) Decision checkpoints in the thymus. Nat Immunol 11(8):666–673

28.   Chan A, Iwashima M, Turck C, Weiss A (1992) ZAP-70: a 70 kd protein-tyrosine kinase that associates with the TCR [zeta] chain. Cell 71:649–662

29.   Chao CC, Jensen R, Dailey MO (1997) Mechanisms of L-selectin regulation by activated T cells. J Immunol 159(4):1686–1694

30.   Chiarle R, Voena C, Ambrogio C, Piva R, Inghirami G (2008) The anaplastic lymphoma kinase in the pathogenesis of cancer. Nat Rev Cancer 8(1):11–23

31.   Clemente MJ, Wlodarski MW, Makishima H, Viny AD, Bretschneider I, Shaik M, Bejanyan N, Lichtin AE, Hsi ED, Paquette RL, Loughran TP, Maciejewski JP (2011) Clonal drift demonstrates unexpected dynamics of the T-cell repertoire in T-large granular lymphocyte leukemia. Blood 118(16):4384–4393

32.   Cools J, Vandenberghe P (2009) New flow cytometry in hematologic malignancies. Haematologica 94(12):1639–1641

33.   Costa D, Queralt R, Aymerich M, Carrió A, Rozman M, Vallespí T, Colomer D, Nomdedeu B, Montserrat E, Campo E (2003) High levels of chromosomal imbalances in typical and small-cell variants of T-cell prolymphocytic leukemia. Cancer Genetics and Cytogenetics 147(1):36–43

34.   Craig FE, Foon KA (2008) Flow cytometric immunophenotyping for hematologic neoplasms. Blood 111(8):3941–3967

35.   Crispín JC, Tsokos GC (2009) Transcriptional regulation of IL-2 in health and autoimmunity. Autoimmun Rev 8(3):190–195

36.   Darzynkiewicz Z, Huang X (2001) Analysis of Cellular DNA Content by Flow Cytometry. onlinelibrarywileycom. doi: 10.1002/0471142735.im0507s60

37.   Davodeau F, Peyrat MA, Romagné F, Necker A, Hallet MM, Vié H, Bonneville M (1995) Dual T cell receptor beta chain expression on human T lymphocytes. J Exp Med 181(4):1391–1398

38.   De Rosa SC, Herzenberg LA, Herzenberg LA, Roederer M (2001) 11-color, 13-parameter flow cytometry: identification of human naive T cells by phenotype, function, and T-cell receptor diversity. Nat Med 7(2):245–248

39.   Delgado J, Bustos JG, Jimenez MC, Quevedo E, Hernandez-Navarro F (2002) Are Activation Markers (CD25, CD38 and CD103) Predictive of Sensitivity to Purine Analogues in Patients with T-cell Prolymphocytic Leukemia and other Lymphoproliferative Disorders? Leuk Lymphoma 43(12):2331–2334

40.   Dembic Z, Haas W, Weiss S, McCubrey J, Kiefer H, Boehmer von H, Steinmetz M (1986) Transfer of specificity by murine α and β T-cell receptor genes. Nature 320(6059):232–238

41. Dong C (2008) TH17 cells in development: an updated view of their molecular identity and genetic programming. Nat Rev Immunol 8(5):337–348

42. Dungarwalla M, Matutes E, Dearden CE (2008) Prolymphocytic leukaemia of B- and T-cell subtype: a state-of-the-art paper. Eur J Haematol 80(6):469–476

43. Dührsen U, Uppenkamp M, Uppenkamp I, Becher R, Engelhard M, König E, Meusers P, Meuer S, Brittinger G (1986) Chronic T cell leukemia with unusual cellular characteristics in ataxia telangiectasia. Blood 68(2):577–585

44. Dürig J, Bug S, Klein-Hitpass L, Boes T, Jöns T, Martin-Subero JI, Harder L, Baudis M, Dührsen U, Siebert R (2007) Combined single nucleotide polymorphism-based genomic mapping and global gene expression profiling identifies novel chromosomal imbalances, mechanisms and candidate genes important in the pathogenesis of T-cell prolymphocytic leukemia with inv(14)(q11q32). Leukemia 21(10):2153–2163

45. Fazilleau N, Mark L, McHeyzer-Williams LJ, McHeyzer-Williams MG (2009) Follicular Helper T Cells: Lineage and Location. Immunity 30(3):324–335

46. Feng B, Jorgensen JL, Hu Y, Medeiros LJ, Wang SA (2010) TCR-V flow cytometric analysis of peripheral blood for assessing clonality and disease burden in patients with T cell large granular lymphocyte leukaemia. J Clin Pathol 63(2):141–146

47. Feng Y, Broder CC, Kennedy PE, Berger EA (1996) HIV-1 entry cofactor: functional cDNA cloning of a seven-transmembrane, G protein-coupled receptor. Science 272(5263):872–877

48. Feuerer M, Hill JA, Mathis D, Benoist C (2009) Foxp3+ regulatory T cells: differentiation, specification, subphenotypes. Nat Immunol 10(7):689–695

49. Fiorentino DF, Bond MW, Mosmann TR (1989) Two types of mouse T helper cell. IV. Th2 clones secrete a factor that inhibits cytokine production by Th1 clones. J Exp Med 170(6):2081–2095

50. Foa R, Pelicci PG, Migone N, Lauria F, Pizzolo G, Flug F, Knowles DM, Dalla-Favera R (1986) Analysis of T-cell receptor beta chain (T beta) gene rearrangements demonstrates the monoclonal nature of T-cell chronic lymphoproliferative disorders. Blood 67(1):247–250

51. Foster TJ (2005) Immune evasion by staphylococci. Nat Rev Micro 3(12):948–958

52. French SW, Malone CS, Shen RR, Renard M, Henson SE, Miner MD, Wall R, Teitell MA (2003) Sp1 transactivation of the TCL1 oncogene. J Biol Chem 278(2):948–955

53. Garand R, Goasguen J, Brizard A, Buisine, Charpentier A, Claisse JF, Duchayne E, Lagrange M, Segonds C, Troussard X, Flandrin G (1998) Indolent course as a relatively frequent presentation in T-prolymphocytic leukaemia.

Groupe Français d'Hématologie Cellulaire. Br J Haematol 103(2):488–494

54. Garderet L, Bittencourt H, Kaliski A, Daniel M, Ribaud P, Socié G, Gluckman E (2001) Treatment of T-prolymphocytic leukemia with nonmyeloablative allogeneic stem cell transplantation. Eur J Haematol 66(2):137–139

55. Garding A, Bhattacharya N, Haebe S, Müller F, Weichenhan D, Idler I, Ickstadt K, Stilgenbauer S, Mertens D (2013) TCL1A and ATM are co-expressed in chronic lymphocytic leukemia cells without deletion of 11q. Haematologica 98(2):269–273

56. Gascoigne NR, Palmer E (2011) Signaling in thymic selection. Curr Opin Immunol 23(2):207–212

57. Gaudio E, Spizzo R, Paduano F, Luo Z, Efanov A, Palamarchuk A, Leber AS, Kaou M, Zanesi Z, Bottoni A, Costinean S, Rassenti LZ, Nakamura T, Kipps TJ, Aqeilan RI, Pekarsky Y, Trapasso F, Croce CM (2012) Tcl1 interacts with Atm and enhances NF-κB activation in hematologic malignancies. Blood 119(1):180–187

58. Geginat J, Lanzavecchia A, Sallusto F (2003) Proliferation and differentiation potential of human CD8+ memory T-cell subsets in response to antigen or homeostatic cytokines. Blood 101(11):4260–4266

59. Geissinger E, Bonzheim I, Krenács L, Roth S, Reimer P, Wilhelm M, Müller-Hermelink HK, Rüdiger T (2006) Nodal peripheral T-cell lymphomas correspond to distinct mature T-cell populations. J Pathol 210(2):172–180

60. Ginaldi L, Matutes E, Farahat N, De Martinis M, Morilla R, Catovsky D (1996) Differential expression of CD3 and CD7 in T-cell malignancies: a quantitative study by flow cytometry. Br J Haematol 93(4):921–927

61. Gorczyca W, Weisberger J, Liu Z, Tsang P, Hossein M, Wu CD, Dong H, Wong JYL, Tugulea S, Dee S, Melamed MR, Darzynkiewicz Z (2002) An approach to diagnosis of T-cell lymphoproliferative disorders by flow cytometry. Cytometry 50(3):177–190

62. Gritti C, Dastot H, Soulier J, Janin A, Daniel MT, Madani A, Grimber G, Briand P, Sigaux F, Stern MH (1998) Transgenic mice for MTCP1 develop T-cell prolymphocytic leukemia. Blood 92(2):368–373

63. Groom JR, Luster AD (2011) CXCR3 in T cell function. Experimental Cell Research 317(5):620–631

64. Groot F, van Capel TMM, Schuitemaker J, Berkhout B, de Jong EC (2006) Differential susceptibility of naïve, central memory and effector memory T cells to dendritic cell-mediated HIV-1 transmission. Retrovirology 3:52

65. Gülow K, Kaminski M, Darvas K, Süss D, Li-Weber M, Krammer PH (2005) HIV-1 trans-activator of transcription substitutes for oxidative signaling in activation-induced T cell death. J Immunol 174(9):5249–5260

66. Hall C, Berkhout B, Alarcon B, Sancho J, Wileman T, Terhorst C (1991) Requirements for cell surface expression of the human TCR/CD3 complex in non-T cells. International Immunology 3(4):359–368

67. Hamann D, Baars PA, Hooibrink B, van Lier RW (1996) Heterogeneity of the human CD4+ T-cell population: two distinct CD4+ T-cell subsets characterized by coexpression of CD45RA and CD45RO isoforms. Blood 88(9):3513–3521

68. Hayday AC, Pennington DJ (2007) Key factors in the organized chaos of early T cell development. Nat Immunol 8(2):137–144

69. Herling M, Patel KA, Khalili J, Schlette E, Kobayashi R, Medeiros LJ, Jones D (2006) TCL1 shows a regulated expression pattern in chronic lymphocytic leukemia that correlates with molecular subtypes and proliferative state. Leukemia 20(2):280–285

70. Herling M, Valbuena JR, Jones D, Medeiros LJ (2007) Skin involvement in T-cell prolymphocytic leukemia. J Am Acad Dermatol 57(3):533–534

71. Herling M, Khoury JD, Washington LT, Duvic M, Keating MJ, Jones D (2004) A systematic approach to diagnosis of mature T-cell leukemias reveals heterogeneity among WHO categories. Blood 104(2):328–335

72. Herling M, Patel KA, Teitell MA, Konopleva M, Ravandi F, Kobayashi R, Jones D (2008) High TCL1 expression and intact T-cell receptor signaling define a hyperproliferative subset of T-cell prolymphocytic leukemia. Blood 111(1):328–337

73. Herling M, Patel KA, Weit N, Lilienthal N, Hallek M, Keating MJ, Jones D (2009) High TCL1 levels are a marker of B-cell receptor pathway responsiveness and adverse outcome in chronic lymphocytic leukemia. Blood 114(21):4675–4686

74. Herling M, Teitell MA, Shen RR, Medeiros LJ, Jones D (2003) TCL1 expression in plasmacytoid dendritic cells (DC2s) and the related CD4+ CD56+ blastic tumors of skin. Blood 101(12):5007–5009

75. Hermiston ML, Zikherman J, Tan AL, Lam VC, Cresalia NM, Oksenberg N, Goren N, Brassat D, Oksenberg JR, Weiss A (2009) Differential impact of the CD45 juxtamembrane wedge on central and peripheral T cell receptor responses. Proc Natl Acad Sci USA 106(2):546–551

76. Hoh F, Yang YS, Guignard L, Padilla A, Stern MH, Lhoste JM, Tilbeurgh H (1998) Crystal structure of p14TCL1, an oncogene product involved in T-cell prolymphocytic leukemia, reveals a novel [beta]-barrel topology. Structure 6(2):147–155

77. Hopfinger G, Herling M (2009) Mature T-cell malignancies: a diagnostic and therapeutic challenge. memo 2(3):134–141

78. Hopfinger G, Busch R, Pflug N, Weit N, Westermann A, Fink AM, Cramer P,

Reinart N, Winkler D, Fingerle-Rowson G, Stilgenbauer S, Döhner H, Kandler G, Eichhorst B, Hallek M, Herling M (2013) Sequential chemoimmunotherapy of fludarabine, mitoxantrone, and cyclophosphamide induction followed by alemtuzumab consolidation is effective in T-cell prolymphocytic leukemia. Cancer 119(12):2258–2267

79.   Hoyer JD, Ross CW, Li CY, Witzig TE, Gascoyne RD, Dewald GW, Hanson CA (1995) True T-cell chronic lymphocytic leukemia: a morphologic and immunophenotypic study of 25 cases. Blood 86(3):1163–1169

80.   Hoyer KK, Herling M, Bagrintseva K, Dawson DW, French SW, Renard M, Weinger JG, Jones D, Teitell MA (2005) T cell leukemia-1 modulates TCR signal strength and IFN-gamma levels through phosphatidylinositol 3-kinase and protein kinase C pathway activation. J Immunol 175(2):864–873

81.   Huster KM, Busch V, Schiemann M, Linkemann K, Kerksiek KM, Wagner H, Busch DH (2004) Selective expression of IL-7 receptor on memory T cells identifies early CD40L-dependent generation of distinct CD8+ memory T cell subsets. Proc Natl Acad Sci USA 101(15):5610–5615

82.   Ichikawa K, Noguchi M, Imai H, Sekiguchi Y, Wakabayashi M, Sawada T, Komatsu N (2011) A case of T cell prolymphocytic leukemia involving blast transformation. Int J Hematol 93(5):667–672

83.   Ishida T, Ueda R (2011) Immunopathogenesis of lymphoma: focus on CCR4. Cancer Sci 102(1):44–50

84.   Jaffe ES, Krenács L, Raffeld M (1997) Classification of T-cell and NK-cell neoplasms based on the REAL classification. Ann Oncol 8 Suppl 2:17–24

85.   Jamal S, Picker LJ, Aquino DB, McKenna RW, Dawson DB, Kroft SH (2001) Immunophenotypic analysis of peripheral T-cell neoplasms. A multiparameter flow cytometric approach. Am J Clin Pathol 116(4):512–526

86.   Jameson SC, Masopust D (2009) Diversity in T cell memory: an embarrassment of riches. Immunity 31(6):859–871

87.   Jiang L, Yuan CM, Hubacheck J, Janik JE, Wilson W, Morris JC, Jasper GA, Stetler-Stevenson M (2009) Variable CD52 expression in mature T cell and NK cell malignancies: implications for alemtuzumab therapy. Br J Haematol 145(2):173–179

88.   Jones D, Dang NH, Duvic M, Washington LT, Huh YO (2001) Absence of CD26 expression is a useful marker for diagnosis of T-cell lymphoma in peripheral blood. Am J Clin Pathol 115(6):885–892

89.   Jones D, Ibrahim S, Patel K, Luthra R, Duvic M, Medeiros LJ (2004) Degree of CD25 expression in T-cell lymphoma is dependent on tissue site: implications for targeted therapy. Clin Cancer Res 10(16):5587–5594

90.   Jones K, Maguire J, Davenport A (2011) Chemokine receptor CCR5: from

AIDS to atherosclerosis. British Journal of Pharmacology 162(7):1453–1469

91.   Jourdan P, Abbal C, Nora N, Hori T, Uchiyama T, Vedrell J, Bouscet J, Taylor N, Péne J, Yssel H (1998) Cutting edge: IL-4 induces functional cell-surface expression of CXCR4 on human T cells. The Journal of Immunology (160):4153–4157

92.   Kaech SM, Wherry EJ, Ahmed R (2002) Effector and memory T-cell differentiation: implications for vaccine development. Nat Rev Immunol 2(4):251–262

93.   Kaminski M, Sauer SW, Klemke C-D, Süss D, Okun JG, Krammer PH, Gülow K (2010) Mitochondrial reactive oxygen species control T cell activation by regulating IL-2 and IL-4 expression: mechanism of ciprofloxacin-mediated immunosuppression. The Journal of Immunology 184(9):4827–4841

94.   Kaminski M, Kiessling M, Süss D, Krammer PH, Gülow K (2007) Novel Role for Mitochondria: Protein Kinase C{theta}-Dependent Oxidative Signaling Organelles in Activation-Induced T-Cell Death. Molecular and Cellular Biology 27(10):3625

95.   Kang S-M, Narducci MG, Lazzeri C, Mongiovì AM, Caprini E, Bresin A, Martelli F, Rothstein J, Croce CM, Cooper MD, Russo G (2005) Impaired T- and B-cell development in Tcl1-deficient mice. Blood 105(3):1288–1294

96.   Kao J, Harootunian AT, Tsien RY (1989) Photochemically generated cytosolic calcium pulses and their detection by fluo-3. J Biol Chem 264(14):8179–8184

97.   Karin N (2010) The multiple faces of CXCL12 (SDF-1alpha) in the regulation of immunity during health and disease. Journal of Leukocyte Biology 88(3):463–473

98.   Kesler MV, Paranjape GS, Asplund SL, McKenna RW, Jamal S, Kroft SH (2007) Anaplastic large cell lymphoma: a flow cytometric analysis of 29 cases. Am J Clin Pathol 128(2):314–322

99.   Khot A, Dearden C (2009) T-cell prolymphocytic leukemia. Expert Rev Anticancer Ther 9(3):365–371

100.   Klas C, Debatin KM, Jonker RR, Krammer PH (1993) Activation interferes with the APO-1 pathway in mature human T cells. International Immunology 5(6):625–630

101.   Klemke CD, Brenner D, Weiss EM, Schmidt M, Leverkus M, Gulow K, Krammer PH (2009) Lack of T-Cell Receptor-Induced Signaling Is Crucial for CD95 Ligand Up-regulation and Protects Cutaneous T-Cell Lymphoma Cells from Activation-Induced Cell Death. Cancer Res 69(10):4175–4183

102.   Kluin Nelemans HC, Gmelig Meyling FHJ, Kootte AMM, Ottolander Den GJ, Termijtelen A, Kluin PM, Beverstock GC, Brand A (1987) T-cell prolymphocytic leukemia with an unusual phenotype CD4+ CD8. Cancer

60(4):794–803

103.   Krammer PH (2000) CD95's deadly mission in the immune system. Nature 407(6805):789–795

104.   Krammer PH, Arnold R, Lavrik IN (2007) Life and death in peripheral T cells. Nat Rev Immunol 7(7):532–542

105.   Krishnan B, Else M, Tjonnfjord GE, Cazin B, Carney D, Carter J, Ketterer N, Catovsky D, Ethell M, Matutes E, Dearden CE (2010) Stem cell transplantation after alemtuzumab in T-cell prolymphocytic leukaemia results in longer survival than after alemtuzumab alone: a multicentre retrospective study. Br J Haematol 149(6):907–910

106.   Krutzik PO, Nolan GP (2003) Intracellular phospho-protein staining techniques for flow cytometry: monitoring single cell signaling events. Cytometry A 55(2):61–70

107.   Kumar A, Humphreys TD, Kremer KN, Bramati PS, Bradfield L, Edgar CE, Hedin KE (2006) CXCR4 physically associates with the T cell receptor to signal in T cells. Immunity 25(2):213–224

108.   Kumar L, Pivniouk V, la Fuente de MA, Laouini D, Geha RS (2002) Differential role of SLP-76 domains in T cell development and function. Proc Natl Acad Sci USA 99(2):884–889

109.   Kussick SJ, Wood BL, Sabath DE (2002) Mature T cell leukemias which cannot be adequately classified under the new WHO classification of lymphoid neoplasms. Leukemia 16(12):2457–2458

110.   Laine J, Künstle G, Obata T, Sha M, Noguchi M (2000) The protooncogene TCL1 is an Akt kinase coactivator. Mol Cell 6(2):395–407

111.   Lamy T, Loughran TP (1999) Current concepts: large granular lymphocyte leukemia. Blood Rev 13(4):230–240

112.   Langenkamp A, Nagata K, Murphy K, Wu L, Lanzavecchia A, Sallusto F (2003) Kinetics and expression patterns of chemokine receptors in human CD4+ T lymphocytes primed by myeloid or plasmacytoid dendritic cells. Eur J Immunol 33(2):474–482

113.   Langerak AW, van Den Beemd R, Wolvers-Tettero IL, Boor PP, van Lochem EG, Hooijkaas H, van Dongen JJ (2001) Molecular and flow cytometric analysis of the Vbeta repertoire for clonality assessment in mature TCRalphabeta T-cell proliferations. Blood 98(1):165–173

114.   Lanzavecchia A, Sallusto F (2005) Understanding the generation and function of memory T cell subsets. Curr Opin Immunol 17(3):326–332

115.   Lavin MF (2008) Ataxia-telangiectasia: from a rare disorder to a paradigm for cell signalling and cancer. Nat Rev Mol Cell Biol 9(10):759–769

116. Lee KC, Ouwehand I, Giannini AL, Thomas NS, Dibb NJ, Bijlmakers MJ (2010) Lck is a key target of imatinib and dasatinib in T-cell activation. Leukemia 24(4):896–900

117. Lee S-S, Rüdiger T, Odenwald T, Roth S, Starostik P, Müller-Hermelink HK (2003) Angioimmunoblastic T cell lymphoma is derived from mature T-helper cells with varying expression and loss of detectable CD4. Int J Cancer 103(1):12–20

118. Lennert K (1975) Morphology and classification of malignant lymphomas and so-called reticuloses. Acta neuropathologica Supplementum (Suppl 6):1–16

119. Létourneau S, Krieg C, Pantaleo G, Boyman O (2009) IL-2- and CD25-dependent immunoregulatory mechanisms in the homeostasis of T-cell subsets. J Allergy Clin Immunol 123(4):758–762

120. Lim TS, Mortellaro A, Lim CT, Hammerling GJ, Ricciardi-Castagnoli P (2011) Mechanical interactions between dendritic cells and T cells correlate with T cell responsiveness. J Immunol 187(1):258–265

121. Lima M, Almeida J, dos Anjos Teixeira M, del Carmen Alguero M, Santos AH, Balanzategui A, Queirós AL, Bárcena P, Izarra A, Fonseca S, Bueno C, Justiça B, Gonzalez M, San Miguel JF, Orfao A (2003) TCRαβ+/CD4+ Large Granular Lymphocytosis. Am J Pathol 163(2):763–771

122. Liu HF, Ma J, Winter C, Bayer R (2010) Recovery and purification process development for monoclonal antibody production. MAbs 2(5):480–499

123. Loetscher M, Geiser T, O'Reilly T, Zwahlen R, Baggiolini M, Moser B (1994) Cloning of a human seven-transmembrane domain receptor, LESTR, that is highly expressed in leukocytes. J Biol Chem 269(1):232–237

124. Loetscher P, Uguccioni M, Bordoli L, Baggiolini M, Moser B, Chizzolini C, Dayer JM (1998) CCR5 is characteristic of Th1 lymphocytes. Nature 391(6665):344–345

125. Lohmeyer J, Hadam M, Ho A, Hesse A, Pralle H (1987) T-cell prolymphocytic leukemia (T-PLL) with unique surface phenotype. Blut 54(4):223–229

126. Lukes RJ, Collins RD (1974) Immunologic characterization of human malignant lymphomas. Cancer 34(4 Suppl):suppl:1488–503

127. Lundell R, Hartung L, Hill S, Perkins SL, Bahler DW (2005) T-cell large granular lymphocyte leukemias have multiple phenotypic abnormalities involving pan–T-cell antigens and receptors for MHC molecules. Am J Clin Pathol 124(6):937–946

128. Luster AD (1998) Chemokines—chemotactic cytokines that mediate inflammation. New England Journal of Medicine 338(7):436–445

129. Macallan DC, Wallace D, Zhang Y, De Lara C, Worth AT, Ghattas H, Griffin

GE, Beverley PCL, Tough DF (2004) Rapid turnover of effector-memory CD4(+) T cells in healthy humans. J Exp Med 200(2):255–260

130. Mackall CL, Fry TJ, Gress RE (2011) Harnessing the biology of IL-7 for therapeutic application. Nat Rev Immunol 11(5):330–342

131. Mahnke YD, Roederer M (2010) OMIP-001: Quality and phenotype of Ag-responsive human T-cells. Cytometry A 77(9):819–820

132. Malek TR, Castro I (2010) Interleukin-2 receptor signaling: at the interface between tolerance and immunity. Immunity 33(2):153–165

133. Malljaie S, Brito-Babapulle V, Matutes E, Horns L, De Schouwer P, Catovsky D (1995) Expression of c-myc oncoprotein in chronic T cell leukemias. Leukemia 9(10):1694–16949

134. Marafiot T, Pozzobon M, Hansmann M-L, Ventura R, Pileri SA, Roberton H, Gesk S, Gaulard P, Barth TFE, Du MQ, Leoncini L, Moller P, Natkunam Y, Siebert R, Mason DY (2005) The NFATc1 transcription factor is widely expressed in white cells and translocates from the cytoplasm to the nucleus in a subset of human lymphomas. Br J Haematol 128(3):333–342

135. Matutes E, Brito-Babapulle V, Swansbury J, Ellis J, Morilla R, Dearden C, Sempere A, Catovsky D (1991) Clinical and laboratory features of 78 cases of T-prolymphocytic leukemia. Blood 78(12):3269–3274

136. Matutes E, Brito-Babapulle V, Swansbury J, Ellis J, Morilla R, Dearden C, Sempere A, Catovsky D (1991) Clinical and laboratory features of 78 cases of T-prolymphocytic leukemia. Blood 78(12):3269–3274

137. Matutes E, Talavera JG, O'Brien M, Catovsky D (1986) The morphological spectrum of T-prolymphocytic leukaemia. Br J Haematol 64(1):111–124

138. Mazzucchelli R, Durum SK (2007) Interleukin-7 receptor expression: intelligent design. Nat Rev Immunol 7(2):144–154

139. McManus MT, Sharp PA (2002) Gene silencing in mammals by small interfering RNAs. Nat Rev Genet 3(10):737–747

140. Mercieca J, Matutes E, Dearden C, MacLennan K, Catovsky D (1994) The role of pentostatin in the treatment of T-cell malignancies: analysis of response rate in 145 patients according to disease subtype. J Clin Oncol 12(12):2588–2593

141. Merkenschlager M, Terry L, Edwards R, Beverley P (1988) Limiting Dilution Analysis of Proliferative Responses in Human-Lymphocyte Populations Defined by the Monoclonal-Antibody Uchl1 - Implications for Differential Cd45 Expression in T-Cell Memory Formation. Eur J Immunol 18(11):1653–1661

142. Messi M, Giacchetto I, Nagata K, Lanzavecchia A, Natoli G, Sallusto F (2002) Memory and flexibility of cytokine gene expression as separable properties of

human TH1 and TH2 lymphocytes. Nat Immunol 4(1):78–86

143.   Minta A, Kao J, Tsien R (1989) Fluorescent indicators for cytosolic sodium. Journal of Biological Chemistry 264(32):19449–19457

144.   Mitsui T, Maekawa I, Yamane A, Ishikawa T, Koiso H, Yokohama A, Handa H, Matsushima T, Tsukamoto N, Murakami H, Nojima Y, Karasawa M (2004) Characteristic expansion of CD45RA CD27 CD28 CCR7 lymphocytes with stable natural killer (NK) receptor expression in NK- and T-cell type lymphoproliferative disease of granular lymphocytes. Br J Haematol 126(1):55–62

145.   Miyagaki T, Sugaya M, Fujita H, Ohmatsu H, Kakinuma T, Kadono T, Tamaki K, Sato S (2010) Eotaxins and CCR3 interaction regulates the Th2 environment of cutaneous T-cell lymphoma. J Investig Dermatol 130(9):2304–2311

146.   Mizuki M, Tagawa S, Machii T, Shibano M, Tatsumi E, Tsubaki K, Tako H, Yokohama A, Satou S, Nojima J, Hirota T, Kitani T (1998) Phenotypical heterogeneity of CD4+CD8+ double-positive chronic T lymphoid leukemia. Leukemia 12(4):499–504

147.   Murphy KM, Stockinger B (2010) Effector T cell plasticity: flexibility in the face of changing circumstances. Nat Immunol 11(8):674–680

148.   Nagata K, Tanaka K, Ogawa K, Kemmotsu K, Imai T, Yoshie O, Abe H, Tada K, Nakamura M, Sugamura K, Takano S (1999) Selective expression of a novel surface molecule by human Th2 cells in vivo. J Immunol 162(3):1278–1286

149.   Narducci MG, Fiorenza MT, Kang S-M, Bevilacqua A, Di Giacomo M, Remotti D, Picchio MC, Fidanza V, Cooper MD, Croce CM, Mangia F, Russo G (2002) TCL1 participates in early embryonic development and is overexpressed in human seminomas. Proc Natl Acad Sci USA 99(18):11712–11717

150.   Newrzela S, Cornils K, Li Z, Baum C, Brugman MH, Hartmann M, Meyer J, Hartmann S, Hansmann M-L, Fehse B, Von Laer D (2008) Resistance of mature T cells to oncogene transformation. Blood 112(6):2278–2286

151.   Oh-hora M (2009) Calcium signaling in the development and function of T-lineage cells. Immunol Rev 231(1):210–224

152.   Omilusik K, Priatel JJ, Chen X, Wang YT, Xu H, Choi KB, Gopaul R, McIntyre-Smith A, Teh H-S, Tan R, Bech-Hansen NT, Waterfield D, Fedida D, Hunt SV, Jefferies WA (2011) The Ca(v)1.4 calcium channel is a critical regulator of T cell receptor signaling and naive T cell homeostasis. Immunity 35(3):349–360

153.   Osipovich O, Oltz EM (2010) Regulation of antigen receptor gene assembly by genetic–epigenetic crosstalk. Seminars in Immunology 22(6):313–322

154.   Ozpuyan F, Meyer P, Ni H, Al-Masri H, Alkan S (2007) Bortezomib induces

apoptosis in T-cell prolymphocytic leukemia (T-PLL). Leuk Lymphoma 48(11):2247–2250

155. Padovan E, Giachino C, Cella M, Valitutti S, Acuto O, Lanzavecchia A (1995) Normal T lymphocytes can express two different T cell receptor beta chains: implications for the mechanism of allelic exclusion. J Exp Med 181(4):1587–1591

156. Park J-H, Adoro S, Lucas PJ, Sarafova SD, Alag AS, Doan LL, Erman B, Liu X, Ellmeier W, Bosselut R, Feigenbaum L, Singer A (2007) "Coreceptor tuning": cytokine signals transcriptionally tailor CD8 coreceptor expression to the self-specificity of the TCR. Nat Immunol 8(10):1049–1059

157. Patrussi L, Baldari CT (2008) Intracellular mediators of CXCR4-dependent signaling in T cells. Immunology Letters 115(2):75–82

158. Pekarsky Y, Hallas C, Croce CM (2001) Molecular basis of mature T-cell leukemia. JAMA 286(18):2308–2314

159. Pekarsky Y, Koval A, Hallas C, Bichi R, Tresini M, Malstrom S, Russo G, Tsichlis P, Croce CM (2000) Tcl1 enhances Akt kinase activity and mediates its nuclear translocation. Proc Natl Acad Sci USA 97(7):3028–3033

160. Pekarsky Y, Palamarchuk A, Maximov V, Efanov A, Nazaryan N, Santanam U, Rassenti L, Kipps T, Croce CM (2008) Tcl1 functions as a transcriptional regulator and is directly involved in the pathogenesis of CLL. Proceedings of the National Academy of Sciences 105(50):19643–19648

161. Pepper M, Jenkins MK (2011) Origins of CD4(+) effector and central memory T cells. Nat Immunol 131(6):467–471

162. Picard F, Martin T, Legras F, Lioure B, Pasquali JL (1993) Molecular analysis of T-cell receptor V beta chains of human T-cell chronic lymphocytic leukemia does not show intraclonal variability: implications for immunotherapy. Blood 82(7):2152–2156

163. Ploner A Heatplus. In: R package version 2.6.0. http://www.bioconductor.org/packages/2.12/bioc/vignettes/Heatplus/inst/doc/annHeatmap.pdf. Accessed 6 Aug 2013

164. Popescu NC, Zimonjic DB (2002) Chromosome-mediated alterations of the MYC gene in human cancer. J Cell Mol Med 6(2):151–159

165. Prussin C, Yin Y, Upadhyaya B (2010) T(H)2 heterogeneity: Does function follow form? J Allergy Clin Immunol 126(6):1094–1098

166. Querfeld C, Rizvi MA, Kuzel TM, Guitart J, Rademaker A, Sabharwal SS, Krett NL, Rosen ST (2006) The Selective Protein Kinase C β Inhibitor Enzastaurin Induces Apoptosis in Cutaneous T-Cell Lymphoma Cell Lines through the AKT Pathway. J Investig Dermatol 126(7):1641–1647

167. Rabinovitch PSP, June CHC, Grossmann AA, Ledbetter JAJ (1986) Heterogeneity among T cells in intracellular free calcium responses after mitogen stimulation with PHA or anti-CD3. Simultaneous use of indo-1 and immunofluorescence with flow cytometry. J Immunol 137(3):952–961

168. Rappl G, Schrama D, Hombach A, Meuer EK, Schmidt A, Becker JC, Abken H (2008) CD7 −T Cells are Late Memory Cells Generated from CD7 +T Cells. Rejuvenation Research 11(3):543–556

169. Ravandi F, Aribi A, O'brien S, Faderl S, Jones D, Ferrajoli A, Huang X, York S, Pierce S, Wierda W, Kontoyiannis D, Verstovsek S, Pro B, Fayad L, Keating M, Kantarjian H (2009) Phase II Study of Alemtuzumab in Combination With Pentostatin in Patients With T-Cell Neoplasms. Journal of Clinical Oncology 27(32):5425–5430

170. Ravandi F, O'Brien S, Jones D, Lerner S, Faderl S, Ferrajoli A, Wierda W, Garcia-Manero G, Thomas D, Koller C, Verstovsek S, Giles F, Cortes J, Herling M, Kantarjian H, Keating M (2005) T-cell prolymphocytic leukemia: a single-institution experience. Clin Lymphoma Myeloma 6(3):234–239

171. Reth M (1989) Antigen receptor tail clue. Nature 338(6214):383–384

172. Ries L, Melbert D, Krapcho M, Stinchcomb D (2008) SEER Cancer Statistics Review, 1975–2005. National Cancer Institute; Bethesda, MD: 2008. Springer Verlag

173. Rivino L, Messi M, Jarrossay D, Lanzavecchia A, Sallusto F, Geginat J (2004) Chemokine receptor expression identifies Pre-T helper (Th)1, Pre-Th2, and nonpolarized cells among human CD4+ central memory T cells. J Exp Med 200(6):725–735

174. Rochman Y, Spolski R, Leonard WJ (2009) New insights into the regulation of T cells by γc family cytokines. Nat Rev Immunol 9(7):480–490

175. Ropars V, Despouy G, Stern M-H, Benichou S, Roumestand C, Arold ST (2009) The TCL1A Oncoprotein Interacts Directly with the NF-κB Inhibitor IκB. PLoS ONE 4(8):e6567

176. Rowen L, Koop BF, L H (1996) The complete 685-kilobase DNA sequence of the human β T cell receptor locus. Science (272):1755–1762

177. Rüdiger T, Geissinger E, Müller-Hermelink HK (2006) "Normal counterparts" of nodal peripheral T-cell lymphoma. Hematol Oncol 24(4):175–180

178. Saito T, Germain RN (1987) Predictable acquisition of a new MHC recognition specificity following expression of a transfected T-cell receptor β-chain gene. Nature 329(6136):256–259

179. Sallusto F, Kremmer E, Palermo B, Hoy A, Ponath P, Qin S, Förster R, Lipp M, Lanzavecchia A (1999) Switch in chemokine receptor expression upon TCR stimulation reveals novel homing potential for recently activated T cells. Eur J

Immunol 29(6):2037–2045

180. Sallusto F, Mackay CR, Lanzavecchia A (1997) Selective expression of the eotaxin receptor CCR3 by human T helper 2 cells. Science 277(5334):2005–2007

181. Sallusto F, Geginat J, Lanzavecchia A (2004) Central memory and effector memory T cell subsets: function, generation, and maintenance. Annu Rev Immunol 22:745–763

182. Sallusto F, Lenig D, Förster R, Lipp M, Lanzavecchia A (1999) Two subsets of memory T lymphocytes with distinct homing potentials and effector functions. Nature 401(6754):708–712

183. Salmon M, Pilling D, Borthwick NJ, Viner N, Janossy G, Bacon PA, Akbar AN (1994) The progressive differentiation of primed T cells is associated with an increasing susceptibility to apoptosis. Eur J Immunol 24(4):892–899

184. Schmitz I, Krueger A, Baumann S, Schulze-Bergkamen H, Krammer PH, Kirchhoff S (2003) An IL-2-dependent switch between CD95 signaling pathways sensitizes primary human T cells toward CD95-mediated activation-induced cell death. J Immunol 171(6):2930–2936

185. Secchiero P, Zella D, Curreli S, Mirandola P, Capitani S, Gallo RC, Zauli G (2000) Engagement of CD28 modulates CXC chemokine receptor 4 surface expression in both resting and CD3-stimulated CD4+ T cells. J Immunol 164(8):4018–4024

186. Seki I, Suzuki M, Miyasaka N, Kohsaka H (2010) Expression of CD45 isoforms correlates with differential proliferative responses of peripheral CD4+ and CD8+ T cells. Immunology Letters 129(1):39–46

187. Shapiro HM (2003) Practical Flow Cytometry, 4 ed. Wiley-Liss

188. Sherrington PD, Fisch P, Taylor AM, Rabbitts TH (1994) Clonal evolution of malignant and non-malignant T cells carrying t(14;14) and t(X;14) in patients with ataxia telangiectasia. Oncogene 9(8):2377–2381

189. Smith-Garvin JE, Koretzky GA, Jordan MS (2009) T cell activation. Annu Rev Immunol 27:591–619

190. Son NH, Murray S, Yanovski J, Hodes RJ, Weng N (2000) Lineage-specific telomere shortening and unaltered capacity for telomerase expression in human T and B lymphocytes with age. J Immunol 165(3):1191–1196

191. Spits H (2002) Development of αβ t cells in the human thymus. Nat Rev Immunol 2(10):760–772

192. Sprent J, Surh CD (2011) Normal T cell homeostasis: the conversion of naive cells into memory-phenotype cells. Nat Immunol 131(6):478–484

193. Stern M, Soulier J, Rosenzwaig M, Nakahara K, Canki-Klain N, Aurias A, Sigaux F, Kirsch I (1993) MTCP-1: a novel gene on the human chromosome Xq28 translocated to the T cell receptor alpha/delta locus in mature T cell proliferations. Oncogene 8(9):2475–2483

194. Stilgenbauer S, Schaffner C, Litterst A, Liebisch P, Gilad S, Bar-Shira A, James MR, Lichter P, Döhner H (1997) Biallelic mutations in the ATM gene in T-prolymphocytic leukemia. Nat Med 3(10):1155–1159

195. Sugimoto J, Hatakeyama T, Narducci MG, Russo G, Isobe M (1999) Identification of the TCL1/MTCP1-like 1 (TML1) gene from the region next to the TCL1 locus. Cancer Res 59(10):2313–2317

196. Surh CD, Sprent J (2008) Homeostasis of Naive and Memory T Cells. Immunity 29(6):848–862

197. Suzuki G, Nakata Y, Dan Y, Uzawa A, Nakagawa K, Saito T, Mita K, Shirasawa T (1998) Loss of SDF-1 receptor expression during positive selection in the thymus. International Immunology 10(8):1049–1056

198. Swerdlow S, Campo E, Lee Harris N, Jaffe ES, Pileri SA, Stein H, Thiele J, Vardiman JW (2008) WHO Classification of Tumours of Haematopoietic and Lymphoid Tissue (IARC WHO Classification of Tumours), Fourth Edition. World Health Organization

199. Sykulev Y (2010) T cell receptor signaling kinetics takes the stage. Sci Signal 3(153):pe50

200. Syrbe U, Siveke J, Hamann A (1999) Th1/Th2 subsets: distinct differences in homing and chemokine receptor expression? Springer Semin Immunopathol 21(3):263–285

201. Takada K, Jameson SC (2009) Naive T cell homeostasis: from awareness of space to a sense of place. Nat Rev Immunol 9(12):823–832

202. Tan C, Taylor AA, Coburn MZ, Marino JH, Van De Wiele CJ, Teague TK (2011) Ten-color flow cytometry reveals distinct patterns of expression of CD124 and CD126 by developing thymocytes. BMC Immunol 12:36

203. Tashiro K, Tada H, Heilker R, Shirozu M, Nakano T, Honjo T (1993) Signal sequence trap: a cloning strategy for secreted proteins and type I membrane proteins. Science 261(5121):600–603

204. Teachey DT, Seif AE, Grupp SA (2010) Advances in the management and understanding of autoimmune lymphoproliferative syndrome (ALPS). Br J Haematol 148(2):205–216

205. Team RC R: A Language and Environment for Statistical Computing. In: R Foundation for Statistical Computing. http://www.r-project.org/. Accessed 6 Aug 2013

206. Teitell MA (2005) The TCL1 family of oncoproteins: co-activators of transformation. Nat Rev Cancer 5(8):640–648

207. Tobin G (2007) The immunoglobulin genes: Structure and specificity in chronic lymphocytic leukemia. Leuk Lymphoma 48(6):1081–1086

208. Toldi G, Kaposi A, Zsembery Á, Treszl A, Tulassay T, Vásárhelyi B (2011) Human Th1 and Th2 lymphocytes are distinguished by calcium flux regulation during the first 10min of lymphocyte activation. Immunobiology 217(1):7–7

209. Valbuena JR, Herling M, Admirand JH, Padula A, Jones D, Medeiros LJ (2005) T-cell prolymphocytic leukemia involving extramedullary sites. Am J Clin Pathol 123(3):456–464

210. van Dongen JJM, Lhermitte L, Böttcher S, Almeida J, van der Velden V H J, Flores-Montero J, Rawstron A, Asnafi V, Lécrevisse Q, Lucio P, Mejstrikova E, Szczepański T, Kalina T, de Tute R, Brüggemann M, Sedek L, Cullen M, Langerak A W, Mendonça, Macintyre E, Martin-Ayuso M, Hrusak O, Vidriales M B, Orfao A (2012) EuroFlow antibody panels for standardized n-dimensional flow cytometric immunophenotyping of normal, reactive and malignant leukocytes. Leukemia 26(9):1908–1975

211. van Genderen H, Kenis H, Lux P, Ungeth L, Maassen C, Deckers N, Narula J, Hofstra L, Reutelingsperger C (2006) In vitro measurement of cell death with the annexin A5 affinity assay. Nat Protoc 1(1):363–367

212. van Meerwijk JPM, Romagnoli P, Iglesias A, Bluethmann H, Steinmetz M (1991) Allelic exclusion at DNA rearrangement level is required to prevent coexpression of two distinct T cell receptor beta genes. J Exp Med 174(4):815–819

213. Vandenberghe PA, Ceuppens JL (1990) Flow cytometric measurement of cytoplasmic free calcium in human peripheral blood T lymphocytes with fluo-3, a new fluorescent calcium indicator. J Immunol Methods 127(2):197–205

214. Veiga-Fernandes H, Walter U, Bourgeois C, McLean A, Rocha B (2000) Response of naïve and memory CD8+ T cells to antigen stimulation in vivo. Nat Immunol 1(1):47–53

215. Vig M, Kinet J-P (2009) Calcium signaling in immune cells. Nat Immunol 10(1):21–27

216. Virgilio L, Isobe M, Narducci MG, Carotenuto P, Camerini B, Kurosawa N, Croce CM, Russo G (1993) Chromosome walking on the TCL1 locus involved in T-cell neoplasia. Proc Natl Acad Sci USA 90(20):9275

217. Virgilio L, Lazzeri C, Bichi R, Nibu K, Narducci MG, Russo G, Rothstein JL, Croce CM (1998) Deregulated expression of TCL1 causes T cell leukemia in mice. Proc Natl Acad Sci USA 95(7):3885–3889

218. Virgilio L, Narducci MG, Isobe M, Billips LG, Cooper MD, Croce CM, Russo

G (1994) Identification of the TCL1 gene involved in T-cell malignancies. Proc Natl Acad Sci USA 91(26):12530–12534

219. Vudattu NK, Kuhlmann-Berenzon S, Khademi M, Seyfert V, Olsson T, Maeurer MJ, Unutmaz D (2008) Increased numbers of IL-7 receptor molecules on CD4+CD25-CD107a+ T-cells in patients with autoimmune diseases affecting the central nervous system. PLoS ONE 4(8):e6534–e6534

220. Warner K, Weit N, Crispatzu G, Admirand JH, Jone D, Herling M (2013) T-Cell Receptor Signaling in Peripheral T-Cell Lymphoma – A Review of Patterns of Alterations in a Central Growth Regulatory Pathway. Current Hematologic Malignancy Reports 1–15

221. Wiktor-Jedrzejczak W, Dearden C, de Wreede L, van Biezen A, Brinch L, Leblond V, Brune M, Volin L, Kazmi M, Nagler A, Schetelig J, de Witte T, Dreger PP (2012) Hematopoietic stem cell transplantation in T-prolymphocytic leukemia: a retrospective study from the European Group for Blood and Marrow Transplantation and the Royal Marsden Consortium. Leukemia 26(5):972–976

222. Wlodkowic D, Telford W, Skommer J, Darzynkiewicz Z (2010) Apoptosis and Beyond: Cytometry in Studies of Programmed Cell Death. Methods Cell Biol 103:44–44

223. Yang J, Liu X, Nyland SB, Zhang R, Ryland LK, Broeg K, Baab KT, Jarbadan NR, Irby R, Loughran TP (2010) Platelet-derived growth factor mediates survival of leukemic large granular lymphocytes via an autocrine regulatory pathway. Blood 115(1):51–60

224. Sandberg Y, van Gastel-Mol EJ, Verhaaf B, Lam KH, van Dongen JJM, Langerak AW (2005) BIOMED-2 Multiplex Immunoglobulin/T-Cell Receptor Polymerase Chain Reaction Protocols Can Reliably Replace Southern Blot Analysis in Routine Clonality Diagnostics. The Journal of molecular diagnostics : JMD 7(4):495

225. Zamoyska R (2007) Immunity - Why Is There so Much CD45 on T Cells? Immunity 27(3):421–423

226. Zhang C (2012) Hybridoma Technology for the Generation of Monoclonal Antibodies. Methods Mol Biol 901:117–135

227. Zhang W, Sloan-Lancaster J, Kitchen J, Trible RP, Samelson LE (1998) LAT: the ZAP-70 tyrosine kinase substrate that links T cell receptor to cellular activation. Cell 92(1):83–92

228. Zhu J, Yamane H, Paul WE (2010) Differentiation of effector CD4 T cell populations (*). Annu Rev Immunol 28:445–489

VI. Preliminary Publications

Hopfinger G, Busch R, Pflug N, **Weit N**, Westermann A, Fink AM, Cramer P, Reinart N, Winkler D, Fingerle-Rowson G, Stilgenbauer S, Döhner H, Kandler G, Eichhorst B, Hallek M, Herling M. Sequential chemo-immunotherapy of fludarabine, mitoxantrone, and cyclo-phosphamide induction followed by alemtuzumab consolidation is effective in T-cell prolymphocytic leukemia Cancer. 2013 Jun 15;119(12):2258-67. doi: 10.1002/cncr.27972. Epub 2013 Mar 19.

VII. Appendix

VII.1. Index of figures

VII.2. Index of tables

VIII. Lebenslauf

Nicole Yvonne Weit
Elsa-Brandström Weg 27
89075 Ulm
Germany
phone: +49 176 61903246
email: weit.nicole@gmail.com

date of birth: 17.09.1982
place of birth: Langenau, Germany
parents: Ernst and Cornelia Weit

Education and Professional Experience:

04/2012 until present	application specialist for flow cytometry, Beckman Coulter GmbH, Krefeld
03/2008 - 03/2012	graduate student, Department of Internal Medicine I, University Hospital of Cologne
03/2002 – 09/2007	Diploma in Human Biology, Philipps University Marburg, Germany, overall grade 1.3
09/1993 – 06/2002	Abitur at the Robert-Bosch grammar school, Langenau, Germany, overall grade 1.1

Grants and Awards:

- German José Carreras Leukmia Foundation grant 10/01 "Molecular correlates of disease initiation and progression in T-PLL" awarded to Herling M, **Weit N**, Hallek M
- Nolting Stiftung "Mechanism of T-cell leukemia 1-mediated oncogenic transformation in T-cell prolymphocytic leukemia" awarded to **Weit N**, Herling M

Original Publications:

- Hopfinger G, Busch R, Pflug N, **Weit N**, Westermann A, Fink AM, Cramer P, Reinart N, Winkler D, Fingerle-Rowson G, Stilgenbauer S, Döhner H, Kandler G, Eichhorst B, Hallek M, Herling M. Sequential chemoimmunotherapy of fludarabine, mitoxantrone, and cyclophosphamide induction followed by

alemtuzumab consolidation is effective in T-cell prolymphocytic leukemia. Cancer. 2013 Jun 15;119(12):2258-67. doi: 10.1002/cncr.27972. Epub 2013 Mar 19.

- Myhrinder AL, Hellqvist E, Bergh AC, Jansson M, Nilsson K, Hultman P, Jonasson J, Buhl AM, Pedersen LB, Jurlander J, Klein E, **Weit N**, Herling M, Rosenquist R, Rosén A. Molecular characterization of neoplastic and normal 'sister' lymphoblastoid B-cell lines from chronic lymphocytic leukemia. Leuk Lymphoma. 2013 Aug;54(8):1769-79. doi: 10.3109/10428194.2013.764418. Epub 2013 Feb 25.

- Brechmann M, Mock T, Nickles D, Kiessling M, **Weit N,** Breuer R, Müller W, Wabnitz G, Frey F, Nicolay JP, Booken N, Samstag Y, Klemke CD, Herling M, Boutros M, Krammer PH, Arnold R. A PP4 Holoenzyme balances physiological and oncogenic nuclear factor-kappa B signaling in T lymphocytes. Immunity. 2012 Oct 19;37(4):697-708. doi: 10.1016/j.immuni.2012.07.014.

- Herling M, Patel KA, **Weit N**, Lilienthal N, Hallek M, Keating MJ, Jones D. High TCL1 levels are a marker of B-cell receptor pathway responsiveness and therapy resistance in chronic lymphocytic leukemia. Blood. 2009 Nov 19;114(21):4675-86. doi: 10.1182/blood-2009-03-208256. Epub 2009 Sep 21.

Oral Presentations:
- „Functional T-cell receptor competence but resistance toward cell death induction in T-cell prolymphocytic leukemia" **Weit N** at the XXVII Congress of the International Society for Advancement of Cytometry, 2012
- „Update on TCL1 – marker, oncogene and potential target" **Weit N** at the Freiburg Scientific Meeting of Experimental CLL Research Molecular Hematology, 2011
- "Towards better molecular understanding and treatment options in T-PLL - initial data from a new joint laboratory and clinical research pipeline at the GCLLSG" **Weit N**, Pflug N at the Vth Young Investigators Meeting on CLL, 2010

Poster Presentations:

- **Weit N**, Hopfinger G, Pflug N, Beckert H, Gleim C, Lilienthal N, Hallek M, Herling M "High expression and functional signalling implicate CXCR4 in T-PLL biology" at the DGHO Jahrestagung, Basel 2011

- **Weit N**, Hopfinger G, Pflug N, Beckert H, Hallek M, Herling M "Towards better molecular understanding and treatment options in T-PLL - initial data from a new joint laboratory and clinical research pipeline " at the T-cell lymphoma Forum, San Francisco 2011

- **Weit N,** Herling M "The role of TCL1 in the malignant transformation of T-cells" at the Spring School on Immunology by the German Society for Immunology 2009

Reviews:

- Warner K, Crispatzu G, Al-Ghaili N, **Weit N**, Florou V, You JM, Newrzela S, Herling M. Models for mature T-cell lymphomas – A critical appraisal of experimental systems and their contribution to current T-cell tumorigenic concepts. <u>Crit Rev Oncol Hematol.</u> [in press]

- Warner K, **Weit N**, Crispatzu G, Admirand JH, Jones D, Herling M. T-Cell Receptor Signaling in Peripheral T-Cell Lymphoma – A Review of Patterns of Alterations in a Central Growth Regulatory Pathway. <u>Curr Hematol Malig Rep</u>. 2013 Jul 27. [Epub ahead of print]

- Hopfinger G, **Weit N**, Herling M. Recent developments in the treatment of peripheral T-cell lymphoma. <u>Memo.</u> 2010;3:73–6

- Hopfinger G, **Weit N**, Herling M. Diagnostische Schritte und Therapieoptionen bei peripheren T-Zell-Neoplasien. <u>Wien Klin Wochenschr.</u> 2009;4:165-76

Köln, September 1st 2013